

الجمهورية الجزائرية الديمقراطية الشعبية
وزارة التعليم العالي والبحث العلمي

UNIVERSITÉ BADJI MOKHTAR - ANNABA
BADJI MOKHTAR – ANNABA UNIVERSITY



جامعة باجي مختار – عنابة

Faculté : TECHNOLOGIE

Département : Génie civil

Domaine : SCIENCES ET TECHNOLOGIES

Filière : Génie civil

Spécialité : structures

Mémoire

Présenté en vue de l'obtention du Diplôme de Master

Thème :

**Seismic vulnerability and reinforcement analysis of
historical masonry school in Annaba city – Algeria**

Présenté par : *GRAIRIA Saad*

Encadrant : Mr ATHMANI Allaeddine MC-A Université BADJI MOKHTAR-ANNABA

Jury de Soutenance :

| | | | |
|--------------------|------------|----------------------|-----------|
| DJEGHABA Kamel | Professeur | Badji Mokhtar-Annaba | Président |
| ATHMANI Allaeddine | MC-A | Badji Mokhtar-Annaba | Encadrant |
| MEZIGHECHE Nawel | MA-A | Université | Examineur |

Année Universitaire : 2022/2023

DEDICATION



With deep gratitude and sincere appreciation, i dedicate this thesis to the exceptional teachers at the university of Annaba. Their guidance and patience have shaped my education profoundly. I am grateful to the university administration, library staff, and esteemed jury for their invaluable support. To my dear friends and family, your unwavering encouragement has meant the world to me. Thank you for your contributions, and may your futures be filled with happiness and success.



THE ACKNOWLEDGEMENT



I would like to begin by expressing my heartfelt gratitude to my dear mom and dad. Your unwavering love, support, and encouragement have been the driving force behind my achievements. I am forever grateful for the sacrifices you have made and the belief you have instilled in me.

Next, I extend my appreciation to myself for the hard work, dedication, and perseverance I have demonstrated throughout this journey. It is through my own determination and relentless efforts that I have reached this significant milestone. I take pride in the personal growth and accomplishments I have achieved.

I am immensely grateful to Mr. Athmani allaeddine for his guidance and support as my supervisor. His expertise, insights, and overwhelming belief in my abilities have been invaluable in shaping this research. I am also grateful to Mr. Hatem seboui for his continuous assistance and help throughout this process. His dedication and availability have made a significant impact on the progress of this work.

I would like to extend my sincere thanks to all the teachers who have imparted their knowledge and expertise during my academic journey. Your passion for teaching and commitment to our education have greatly influenced my intellectual growth.

To my friends and classmates, I express my heartfelt gratitude for your support and camaraderie throughout this journey. Your presence has made the challenges more manageable and the successes more meaningful.

Lastly, I want to thank my old friends, who have been with me through thick and thin. Your unwavering support, sincere friendship, and understanding have meant the world to me. I eagerly look forward to reuniting with you soon and creating new memories together.

To all those mentioned above, and to anyone else who has contributed to my academic and personal growth, I extend my deepest appreciation. Your presence, support, and belief in me have been instrumental in my success, and I am forever grateful for your impact in my life.



ABSTRACT

Unreinforced masonry buildings (URM) in Annaba, Algeria, face significant seismic vulnerability due to their construction before the implementation of seismic codes. This study focuses on evaluating the seismic vulnerability of URM structures by selecting a prototype made of stones from Old Annaba. Using the macro-element approach and 3D modelling in the software 3Muri©, the prototype's behaviour under seismic loads is analysed considering bending, shearing, and diagonal traction.

The research compares the test results of the unreinforced masonry building with a reinforced counterpart to assess the extent of damages and the effectiveness of reinforcement strategies. Fragility curves with a log-normal distribution are developed, incorporating displacement-based damage data from the modelling. These curves aid in understanding the seismic vulnerability of URM structures and guide retrofitting efforts and seismic design guidelines.

This study contributes to the knowledge of URM buildings' seismic behaviour in Annaba, supporting the assessment and enhancement of their resilience. The findings inform the preservation and rehabilitation of historic URM structures, ensuring their safety and sustainability in earthquake-prone regions.

Keywords: unreinforced masonry, seismic vulnerability, Annaba, macro-element approach, 3D modelling, seismic behaviour, fragility curves, displacement-based damage, retrofitting, seismic design, historic buildings, preservation, rehabilitation.

RESUMÉ

Les bâtiments en maçonnerie non armée (URM) à Annaba, en Algérie, sont confrontés à une vulnérabilité sismique importante en raison de leur construction avant la mise en œuvre des codes sismiques. Cette étude porte sur l'évaluation de la vulnérabilité sismique des structures de l'URM en sélectionnant un prototype en pierres du Vieux Annaba. À l'aide de l'approche macro-éléments et de la modélisation 3D dans le logiciel 3Muri©, le comportement du prototype sous charges sismiques est analysé en tenant compte de la flexion, du cisaillement et de la traction diagonale.

La recherche compare les résultats des tests du bâtiment en maçonnerie non renforcée avec un bâtiment de contrepartie renforcée pour évaluer l'étendue des dommages et l'efficacité des stratégies de renforcement. Des courbes de fragilité avec une distribution log-normale sont développées, incorporant des données de dommages basées sur le déplacement issues de la modélisation. Ces

courbes aident à comprendre la vulnérabilité sismique des structures URM et guident les efforts de modernisation et les directives de conception sismique.

Cette étude contribue à la connaissance du comportement sismique des bâtiments de l'URM à Annaba, soutenant l'évaluation et l'amélioration de leur résilience. Les résultats éclairent la préservation et la réhabilitation des structures historiques de l'URM, garantissant leur sécurité et leur durabilité dans les régions sujettes aux tremblements de terre.

Mots clés : maçonnerie non armée, vulnérabilité sismique, Annaba, approche macro-élémentaire, modélisation 3D, comportement sismique, courbes de fragilité, endommagement par déplacement, réhabilitation, conception parasismique, bâtiments historiques, préservation, réhabilitation.

خلاصة

تواجه مباني البناء غير المدعمة (URM) في عنابة ، الجزائر ، ضعفاً زلزالياً كبيراً بسبب بنائها قبل تطبيق الرموز الزلزالية. تركز هذه الدراسة على تقييم الضعف الزلزالي لهياكل URM من خلال اختيار نموذج أولي مصنوع من الحجارة من عنابة القديمة. باستخدام نهج العناصر الكلية والنمذجة ثلاثية الأبعاد في برنامج Muri © 3، يتم تحليل سلوك النموذج الأولي تحت الأحمال الزلزالية مع الأخذ في الاعتبار الانحناء والقص والجر القطر.

يقارن البحث نتائج الاختبار لمبنى البناء غير المدعم بنظير مقوى لتقييم مدى الأضرار وفعالية استراتيجيات التعزيز. تم تطوير منحنيات الهشاشة مع التوزيع اللوغاريتمي الطبيعي ، بدمج بيانات الضرر القائم على الإزاحة من النمذجة. تساعد هذه المنحنيات في فهم الضعف الزلزالي لهياكل URM وتوجيه جهود التعديل التحديثي وإرشادات التصميم الزلزالي.

تساهم هذه الدراسة في معرفة السلوك الزلزالي لمباني URM في عنابة ، ودعم تقييم وتعزيز مرونتها. تشير النتائج إلى الحفاظ على هياكل URM التاريخية وإعادة تأهيلها ، مما يضمن سلامتها واستدامتها في المناطق المعرضة للزلازل.

الكلمات المفتاحية: البناء غير المدعم ، الضعف الزلزالي ، عنابة ، نهج العنصر الكلي ، النمذجة ثلاثية الأبعاد ، السلوك الزلزالي ، منحنيات الهشاشة ، الضرر الناجم عن الإزاحة ، التعديل التحديثي ، التصميم الزلزالي ، المباني التاريخية ، الحفظ ، إعادة التأهيل.

TABLE OF CONTENTS

| | |
|---|----|
| GENERAL INTRODUCTION | 1 |
| CHAPTER I REVUE ON HISTORICAL MASONRY BUILDINGS | 3 |
| I.1 Introduction | 4 |
| I.2 Material properties of masonry | 4 |
| I.2.1 The units | 4 |
| I.2.2 The mortar | 11 |
| I.3 Assembly of mortar and masonry | 16 |
| I.3.1 External mechanical deterioration | 16 |
| I.3.2 Internal mechanical deterioration | 16 |
| I.3.3 Chemical deterioration..... | 17 |
| I.3.4 Biodeterioration | 17 |
| I.4 Estimation of the mechanical properties of masonry | 17 |
| I.4.1 The Italian code NTC 18 | 17 |
| I.5 Masonry building behaviours..... | 21 |
| I.5.1 Domain of vulnerability modelling..... | 21 |
| I.5.2 The seismic behaviour mechanisms..... | 21 |
| I.6 Seismic analysis ‘pushover’ | 23 |
| I.6.1 Why is pushover analysis used? | 24 |
| I.6.2 A brief overview of the technique: | 24 |
| I.7 The strengthening..... | 33 |
| I.7.1 Surface treatment | 33 |
| I.7.2 External reinforcement | 35 |
| I.8 Conclusion | 40 |
| CHAPTER II TREMURI MODELLING | 41 |
| II.1 Introduction:..... | 42 |
| II.2 Macro-element modelling: | 42 |
| II.2.1 Macro-element approach: | 43 |
| II.2.2 Equivalent frame..... | 44 |
| II.2.3 Structural element behaviour | 46 |
| II.2.4 The structure's three-dimensional assembly | 47 |
| II.3 Modelling masonry piers and spandrels..... | 48 |
| II.4 Strength and failure criteria for urm panels implemented in tremuri program..... | 50 |
| II.4.1 The failure modes | 50 |
| II.4.1.1 Bending ultimate moment | 50 |
| II.4.1.2 Shear turnšek and cačovic criteria..... | 51 |

| | | |
|--------------------------------------|--|----|
| II.4.2 | Strength criteria | 52 |
| II.5 | Wall modelling..... | 55 |
| II.6 | Spatial modelling | 57 |
| II.7 | The structure after modelling | 61 |
| II.8 | Conclusion | 62 |
| CHAPTER III CASE STUDY | | 63 |
| III.1 | Introduction..... | 64 |
| III.2 | Study case | 65 |
| III.2.1 | Presentation of the asla hocine primary school | 65 |
| III.2.2 | Urban study | 66 |
| III.2.3 | Architectural study | 67 |
| III.3 | Study case and diagnosis..... | 71 |
| III.3.1 | Constructive and structural analysis | 71 |
| III.4 | Reference codes | 76 |
| III.5 | Actions | 77 |
| III.5.1 | Description of actions..... | 77 |
| III.5.2 | Permanent and variable loads..... | 77 |
| III.5.3 | General evaluation of the actions | 78 |
| III.6 | The loads | 79 |
| III.7 | The mechanical characteristics..... | 80 |
| III.7.1 | Masonry..... | 80 |
| III.7.2 | Timber | 80 |
| III.7.3 | Steel..... | 81 |
| III.7.4 | Floors..... | 81 |
| III.7.5 | Roof elements..... | 82 |
| III.8 | Conclusion | 82 |
| CHAPTER IV STATIC VERIFICATION | | 83 |
| IV.1 | Introduction..... | 84 |
| IV.2 | Reference code..... | 84 |
| IV.3 | analysis method..... | 85 |
| IV.3.1 | Type of analysis performed | 85 |
| IV.4 | Model description | 86 |
| IV.4.1 | materials | 86 |
| IV.4.1.1 | Mechanical behaviour of the masonry | 86 |
| IV.4.1.2 | Wall with shear mechanism | 87 |
| IV.4.1.3 | Wall with bending mechanism..... | 88 |
| IV.4.1.4 | In the absence of residual resistance | 89 |
| IV.5 | Loads..... | 89 |
| IV.5.1 | Seismic load: | 89 |
| IV.5.2 | Static Load: | 90 |
| IV.6 | Global static verification | 90 |

| | | |
|---|---|-----|
| IV.6.1 | Slenderness of the masonry | 90 |
| IV.6.2 | Load eccentricity | 91 |
| IV.6.3 | Verification at vertical loads | 91 |
| IV.6.4 | the results..... | 92 |
| IV.6.4.1 | Wall: 1..... | 86 |
| IV.6.4.2 | Wall: 3..... | 86 |
| IV.6.4.3 | Wall: 6..... | 88 |
| IV.6.4.4 | Wall: 7..... | 89 |
| IV.6.4.5 | Wall: 8..... | 90 |
| IV.6.4.6 | Wall: 9..... | 92 |
| IV.6.4.7 | Wall: 10..... | 92 |
| IV.7 | Finds..... | 94 |
| IV.8 | Conclusion | 95 |
| CHAPTE V SEISMIC PERFORMANCE ANALYSIS | | 96 |
| V.1 | Introduction..... | 97 |
| V.2 | Seismic spectrum assessment..... | 97 |
| V.2.1 | Site selection..... | 98 |
| V.2.2 | Reconnaissance and soil studies | 98 |
| V.2.3 | Modelling and calculation methods | 98 |
| V.2.4 | Seismic zone classification | 98 |
| V.2.5 | Classification Of Works According to Their Importance | 99 |
| V.2.6 | Site classification | 100 |
| V.2.7 | Calculation response Spectrum..... | 100 |
| V.2.8 | Observance of Algerian seismic regulations..... | 102 |
| V.3 | Pushover analysis description | 104 |
| V.4 | Data validation | 105 |
| V.4.1 | Domain resistance calculation | 105 |
| V.5 | Results..... | 109 |
| V.5.1 | Result details..... | 110 |
| V.5.2 | Results legend..... | 111 |
| V.5.3 | Seismic analysis no. 4 Direction X | 112 |
| V.5.4 | Seismic analysis no. 5 Direction Y | 119 |
| V.6 | Assessment of the performance point (x direction)..... | 123 |
| V.6.1 | Graphical ‘‘using excel table’’: | 123 |
| V.6.2 | Numerical: | 125 |
| V.6.3 | Finds | 126 |
| V.7 | Assessment of the performance point (Y direction)..... | 126 |
| V.7.1 | Graphical ‘‘using excel table’’..... | 126 |
| V.7.2 | Numerical | 128 |
| V.7.3 | Finds: | 129 |
| V.8 | Vulnirability analysis: | 129 |

| | | |
|--|--|-----|
| V.8.1 | Fragility and vulnerability functions..... | 129 |
| V.8.1 | Finds | 134 |
| V.9 | Conclusion | 134 |
| CHAPTER VI REINFORCEMEN ANALYSIS | | 136 |
| VI.1 | Introduction..... | 137 |
| VI.2 | Types of reinforcement used..... | 138 |
| VI.2.1 | Wall frames | 138 |
| VI.2.2 | Frcm systems..... | 138 |
| VI.3 | Reinforcement type characteristics | 139 |
| VI.3.1 | Reinforcements frcm (walls) | 139 |
| VI.3.2 | Reinforcements wall (Steel frames) | 140 |
| VI.3.3 | Reinforcements horizontal elements (Steel frame “tie rod “)..... | 140 |
| VI.4 | Masonry with FRCM reinforcement | 141 |
| VI.4.1 | Compression bending | 141 |
| VI.4.2 | Shear..... | 142 |
| VI.5 | Static reinforcement verifications | 143 |
| VI.5.1 | Wall: 1 | 143 |
| VI.5.2 | Wall: 6 | 144 |
| VI.5.3 | Wall: 7 | 146 |
| VI.5.4 | Wall: 10..... | 148 |
| VI.6 | Seismic vulnerability analysis..... | 149 |
| VI.6.1 | Results | 150 |
| VI.7 | Assessment of the performance point (x direction)..... | 162 |
| VI.7.1 | Graphical ‘using excel table’ | 162 |
| VI.7.2 | Numerical | 162 |
| VI.8 | Assessment of the performance point (Y direction)..... | 163 |
| VI.8.1 | Graphical ‘using excel table’ | 163 |
| VI.8.2 | Numerical | 163 |
| VI.9 | Vulnerability analysis..... | 164 |
| VI.9.1 | Analytical functions for fragility curve | 164 |
| V.1.1 | Damage distribution of the studied structure | 165 |
| VI.9.2 | Finds | 166 |
| VI.10 | Conclusion | 166 |
| GENERAL CONCLUSION | | 168 |

LIST OF FIGURES

| | |
|---|----|
| FIGURE I 1 DIFFERENT TYPES OF MORTAR AND THEIR CLASSIFICATIONS "1" | 12 |
| FIGURE I 2. DIFFERENT TYPES OF MORTAR AND THEIR CLASSIFICATIONS "2" | 13 |
| FIGURE I 3. MASONRY CONSTRUCTION COMPONENTS | 15 |
| FIGURE I 4. DIFFERENT SHEAR MODES OF URM WALL | 22 |
| FIGURE I 5. IN-PLANE AND OUT-OF-PLANE FORCES | 23 |
| FIGURE I 6. STRUCTURE CAPACITY CURVE | 24 |
| FIGURE I 7. GLOBAL RESPONSE AND PERFORMANCE | 25 |
| FIGURE I 8. DEVELOPMENT OF THE CAPACITY CURVE..... | 26 |
| FIGURE I 9. THE DIFFERENT METHODS UTILIZED TO DISTINGUISH THE PERFORMANCE POINT | 27 |
| FIGURE I 10 CONVERSION TO ADRS SPECTRA (ATC 40) | 28 |
| FIGURE I 11 SCHEMATIC REPRESENTATION OF CAPACITY SPECTRUM METHOD (ATC 40) | 29 |
| FIGURE I 12.DETERMINATION OF HYSTERETIC..... | 30 |
| FIGURE I 13. REDUCTION OF DEMAND SPECTRUM..... | 31 |
| FIGURE I 14 INTERSECTION POINT OF DEMAND AND CAPACITY SPECTRUMS WITHIN ACCEPTABLE TOLERANCE (ATC 40)..... | 32 |
| FIGURE I 15 THE CONCEPT FOR A "SAWTOOTH" CAPACITY SPECTRUM (ATC 40)..... | 32 |
| FIGURE I 16 STRENGTHENING OF MASONRY WALLS BY APPLICATION OF SINGLE AND DOUBLE SIDED REINFORCED CONCRETE (RC) JACKETS..... | 34 |
| FIGURE I 17 STRENGTHENING OF MASONRY WALLS USING FRP STRUCTURAL REPOINTING..... | 34 |
| FIGURE I 18 FABRIC REINFORCED CEMENTITIOUS MATRIX (FRMC) | 35 |
| FIGURE I 19. POST-TENSIONING STRENGTHENING SYSTEM..... | 36 |
| FIGURE I 20. STEEL RING-FRAME STRENGTHENING TECHNIQUE | 37 |
| FIGURE I 21. THE REINFORCED CORE TECHNIQUE..... | 38 |
| FIGURE I 22. TIE BARS MADE OF IRON TENSION MEMBERS | 38 |
| FIGURE I 23. THE RETROFITTING TECHNIQUES | 39 |
| FIGURE II 1. MEF AND THE EFM..... | 43 |
| FIGURE II 2. SHEMA OF MACROELEMENTS TAKEN FROM LAGOMARSINO ET AL (2008B)..... | 44 |
| FIGURE II 3. STRUCTURE EQUIVALENT FRAME IDENTIFICATION | 45 |
| FIGURE II 4. ILLUSTRATION OF EFFECTIVE HEIGHT IDENTIFICATION METHOD TAKEN FROM DOLCE (1991)..... | 45 |
| FIGURE II 5. IDENTIFICATION OF FAILURE MODES FOR A MICROELEMENT TAKEN FROM (SERGIO LAGOMARSINO, 2013)..... | 47 |
| FIGURE II 6. 3D ASSEMBLING OF MASONRY WALLS: CLASSIFICATION OF 3D AND 2D RIGID NODES AND OUT-OF- PLANE MASS SHARING. (SERGIO LAGOMARSINO, 2013)..... | 48 |
| FIGURE II 7. ELEMENT BEHAVIOUR CURVE..... | 49 |
| FIGURE II 8.DIFFERENT TYPES OF FAILURES (RAFFAELLO, 2012) | 50 |

| | |
|---|--|
| FIGURE II 9. STRENGTH CRITERION IN BENDING-ROCKING | 51 |
| FIGURE II 10. TURNŠEK AND CAČOVIC SHEAR STRENGTH AND STRENGTH CRITERIA COMPARISON | 52 |
| FIGURE II 11. THE DIVISIONS OF WALL FRAME | 55 |
| FIGURE II 12. WALL MODEL NODES AND THE ECCENTRICITIES | 56 |
| FIGURE II 13. COMPONENTS DISPLACEMENTS ACCORDING TO DOF | 58 |
| FIGURE II 14. THE FORCES TRANSMITTED BY THE MACRO-ELEMENTS..... | 59 |
| FIGURE II 15. THE REFERENCE ELEMENT | 60 |
| FIGURE II 16 3D VIEW OF THE BUILDING AFTER MODELLING AND THE MACROELEMENTS STRUCTURE MECH ... | 61 |
| FIGURE III 1. MAIN FACADE | 65 |
| FIGURE III 2 MASS GROUNDING PLAN | 66 |
| FIGURE III 3 SITUATION PLAN | 66 |
| FIGURE III 4 GROUND FLOOR PLAN AND BLOCKS DIVISIONS | 69 |
| FIGURE III 5 ARCHITECTURAL PLAN CUT AA' | 70 |
| FIGURE III 6 ARCHITECTURAL PLAN CUT BB' | 70 |
| FIGURE III 7 ARCHITECTURAL PLAN CUT CC' | 71 |
| FIGURE III 8 MATERIALS AND ARCHITECTURE PLAN FIRST FLOOR | 73 |
| FIGURE III 9 MATERIAL PLAN 1ST FLOOR AND 2ND FLOOR..... | 73 |
| FIGURE III 10.RDC SURVEY PLAN | 74 |
| FIGURE III 11 1ST FLOOR PLAN VIEW | 75 |
| FIGURE III 12 ROOF PLAN VIEW | 76 |
| FIGURE III 13 FLOOR CONCEPT | 81 |
| FIGURE IV 1 3D VIEW OF THE STRUCTURE MODEL..... | 84 |
| FIGURE IV 2 | WALL BEHAVIOUR CURVE WITH SHEAR MECHANISM |
| | 87 |
| FIGURE IV 3 WALL BEHAVIOUR CURVE WITH BENDING MECHANISM | 88 |
| FIGURE IV 4 WALL BEHAVIOUR CURVE IN CASE OF ABSENCE OF RESIDENTIAL RESISTANCE..... | 89 |
| FIGURE IV 5 THE STRUCTURE WALLS NUMBERS..... | 92 |
| FIGURE IV 6 WALL 1 ELEMENT VERIFICATION | 86 |
| FIGURE IV 7 WALL 3 ELEMENT VERIFICATION | 86 |
| FIGURE IV 8 WALL 6 ELEMENT VERIFICATION | 88 |
| FIGURE IV 9 WALL 7 ELEMENT VERIFICATION | 89 |
| FIGURE IV 10 WALL 8 ELEMENT VERIFICATION | 90 |
| FIGURE IV 11 WALL 9 ELEMENT VERIFICATION | 92 |
| FIGURE IV 12 WALL 10 ELEMENT VERIFICATION | 92 |
| FIGURE V 1 RISK RASSESSMENT FORMWORK..... | 97 |
| FIGURE V 2 THE ELASTIC RESPONSE SPECTRUM FOR A= 0.2 | 103 |
| FIGURE V 3 WALL 10 DEFORMATIONS RESULT FOR X DIRECTION | 112 |
| FIGURE V 4 WALL 10 RESISTANCE DOMAIN DIAGRAM..... | 114 |

| | |
|--|-----|
| FIGURE V 5 WALL 7 DEFORMATIONS RESULT FOR X DIRECTION | 114 |
| FIGURE V 6 WALL 7 RESISTANCE DOMAIN DIAGRAM..... | 117 |
| FIGURE V 7 PLAN DEFORMED SHAPE FOR X DIRECTION | 118 |
| FIGURE V 8 PUSHOVER CURVES FOR X DIRECTION..... | 118 |
| FIGURE V 9 WALL 8 RESISTANCE DOMAIN DIAGRAM..... | 119 |
| FIGURE V 10 WALL 8 RESISTANCE DOMAIN DIAGRAM..... | 121 |
| FIGURE V 11 PLAN DEFORMED SHAPE Y DIRECTION | 122 |
| FIGURE V 12 PUSHOVER CURVES Y DIRECTION | 122 |
| FIGURE V 13 MDOF CAPACITY CURVE FOR X DIRECTION | 123 |
| FIGURE V 14 SDOF CAPACITY CURVE FOR X DIRECTION | 124 |
| FIGURE V 15 BI-LINEAR EQUIVALENT CAPACITY CURVE X DIRECTION..... | 124 |
| FIGURE V 16 INTERSECTION OF THE CAPACITY CURVE AND THE DEMAND X DIRECTION..... | 125 |
| FIGURE V 17 MDOF CAPACITY CURVE Y DIRECTION | 127 |
| FIGURE V 18 SDOF CAPACITY CURVE Y DIRECTION..... | 127 |
| FIGURE V 19 BI-LINEAR EQUIVALENT CAPACITY CURVE Y DIRECTION..... | 127 |
| FIGURE V 20 INTERSECTION OF THE CAPACITY CURVE AND THE DEMAND Y DIRECTION..... | 128 |
| FIGURE V 21 FRAGILITY CURVES STAGES..... | 130 |
| FIGURE V 22 FRAGILITY CURVE (X DIRECTION)..... | 132 |
| FIGURE V 23 FRAGILITY CURVE (Y DIRECTION)..... | 132 |
| FIGURE V 24 DAMAGE HISTOGRAM (X DIRECTION)..... | 133 |
| FIGURE V 25 VULNERABILITY HISTOGRAM (Y DIRECTION)..... | 134 |
| FIGURE VI 1 3D VIEW AFTER REINFORCEMENT | 137 |
| FIGURE VI 2 WALL 10 RESISTANCE DOMAIN DIAGRAM AFTER REINFORCEMENT..... | 153 |
| FIGURE VI 3 WALL 7 RESISTANCE DOMAIN DIAGRAM AFTER REINFORCEMENT..... | 156 |
| FIGURE VI 4 PLAN DEFORMED SHAPE FOR X DIRECTION AFTER REINFORCEMENT | 157 |
| FIGURE VI 5 PUSHOVER CURVES FOR X DIRECTION BEFORE AND AFTER REINFORCEMENT | 157 |
| FIGURE VI 6 WALL 8 RESISTANCE DOMAIN DIAGRAM..... | 160 |
| FIGURE VI 7 PLAN DEFORMED SHAPE FOR Y DIRECTION AFTER REINFORCEMENT | 161 |
| FIGURE VI 8 PUSHOVER CURVES FOR Y DIRECTION BEFORE AND AFTER REINFORCEMENT..... | 161 |
| FIGURE VI 9 INTERSECTION OF THE CAPACITY CURVE AND THE DEMAND X DIRECTION AFTER REINFORCEMENT | 162 |
| FIGURE VI 10 INTERSECTION OF THE CAPACITY CURVE AND THE DEMAND Y DIRECTION AFTER REINFORCEMENT | 163 |
| FIGURE VI 11 FRAGILITY CURVE FOR X DIRECTION AFTER REINFORCEMENT | 164 |
| FIGURE VI 12 FRAGILITY CURVE FOR Y DIRECTION AFTER REINFORCEMENT | 164 |
| FIGURE VI 13 DAMAGE HISTOGRAM AFTER REINFORCEMENT (X DIRECTION) | 165 |
| FIGURE VI 14 DAMAGE HISTOGRAM AFTER REINFORCEMENT (Y DIRECTION) | 165 |

LIST OF TABLES

| | |
|---|----|
| TABLE I 1. TYPES OF MASONRY UNITS (MASONRY- ROOF - FLOOR CONSTRUCTION, 2020) | 5 |
| TABLE I 2. REFERENCE RANGES FOR DIFFERENT MASONRY MATERIAL PARAMETERS (SEBOUI HATEM, 2022)..... | 18 |
| TABLE I 3. CORRECTION FACTORS FOR DIFFERENT PARAMETERS OF MASONRY TYPES (SEBOUI HATEM, 2022) | 19 |
| TABLE I 4. KNOWLEDGE LEVELS ARE BASED ON AVAILABLE INFORMATION AND CORRESPONDING VALUES OF THE CONFIDENCE FACTORS FOR MASONRY BUILDINGS (SEBOUI HATEM, 2022) | 19 |
| TABLE II 1. STRENGTH CRITERIA FOR URM PANELS IMPLEMENTED IN TREMURI PROGRAM (SERGIO LAGOMARSINO, 2013)..... | 52 |
| TABLE II 2. THE MECHANICAL CHARACTERISTICS OF STEEL FRAMES IMPLEMENTED IN TREMURI PROGRAM..... | 54 |
| TABLE II 3. THE MECHANICAL CHARACTERISTICS OF WALL PANEL IMPLEMENTED IN TREMURI PROGRAM | 54 |
| TABLE III 1 BUILDING BLOCK DIVISIONS | 67 |
| TABLE III 2 . DIVISIONS DIMENSIONS AND OPENINGS | 68 |
| TABLE III 3. THE STRUCTURE ELEMENTS..... | 72 |
| TABLE III 4. THE USED MATERIAL TABLES | 74 |
| TABLE III 5 . SOME MATERIALS PROPRE WEIGHTS | 78 |
| TABLE III 6. FLOOR LOADS..... | 79 |
| TABLE III 7 . BALCONY LOADS | 79 |
| TABLE III 8. ROOF SLOPE LOADS | 79 |
| TABLE III 9. MASONRY ELEMENT MECHANICAL CHARACTERISTICS | 80 |
| TABLE III 10. MATERIALS COEFFICIENTS..... | 80 |
| TABLE III 11. TIMBER MECHANICAL CHARACTERISTICS | 80 |
| TABLE III 12 STRUCTURAL STEEL MECHANICAL CHARACTERISTICS | 81 |
| TABLE III 13 FLOOR DIMENSIONS | 81 |
| TABLE III 14 LOOR MECHANICAL CHARACTERISTICS..... | 81 |
| TABLE III 15 ROOF MATERIALS | 82 |
| TABLE III 16 THE RESISTANCE DIRECTION OF THE FLOOR..... | 82 |
| TABLE IV 1 THE BEHAVIOUR OF THE MASONRY IN SHEAR AND THE RELATED LEVEL OF DAMAGE | 87 |
| TABLE IV 2 THE BEHAVIOUR OF THE MASONRY IN BENDING MECHANISM AND THE RELATED LEVEL OF DAMAGE | 88 |
| TABLE IV 3 THE LEGEND TABLE FOR VERIFICATION OF ELEMENT STATUS..... | 92 |
| TABLE IV 4 SLENDERNESS AND ECCENTRICITY VERIFICATION FOR WALL 1..... | 86 |
| TABLE IV 5 VERTICAL LOAD BEARING RESISTANCE VERIFICATION FOR WALL 1..... | 86 |
| TABLE IV 6 SLENDERNESS AND ECCENTRICITY VERIFICATION FOR WALL 3..... | 87 |
| TABLE IV 7 VERTICAL LOAD BEARING RESISTANCE VERIFICATION FOR WALL 3..... | 87 |
| TABLE IV 8 SLENDERNESS AND ECCENTRICITY VERIFICATION FOR WALL 6..... | 88 |
| TABLE IV 9 VERTICAL LOAD BEARING RESISTANCE VERIFICATION FOR WALL 6..... | 88 |
| TABLE IV 10 SLENDERNESS AND ECCENTRICITY VERIFICATION FOR WALL 7..... | 89 |
| TABLE IV 11 VERTICAL LOAD BEARING RESISTANCE VERIFICATION FOR WALL 7..... | 90 |

| | |
|--|-----|
| TABLE IV 12 SLENDERNESS AND ECCENTRICITY VERIFICATION FOR WALL 8..... | 90 |
| TABLE IV 13 VERTICAL LOAD BEARING RESISTANCE VERIFICATION FOR WALL 8..... | 91 |
| TABLE IV 14 SLENDERNESS AND ECCENTRICITY VERIFICATION FOR WALL 9..... | 92 |
| TABLE IV 15 VERTICAL LOAD BEARING RESISTANCE VERIFICATION FOR WALL 9..... | 92 |
| TABLE IV 16 SLENDERNESS AND ECCENTRICITY VERIFICATION FOR WALL 10..... | 93 |
| TABLE IV 17 VERTICAL LOAD BEARING RESISTANCE VERIFICATION FOR WALL 10..... | 93 |
| TABLE V 1. THE SITES CLASSIFICATIONS | 100 |
| TABLE V 2. THE ZONES ACCELERATION | 100 |
| TABLE V 3. SITES PERIODS | 101 |
| TABLE V 4. QUALITY FACTORS INDEX..... | 101 |
| TABLE V 5. WEIGHTING COEFFICIENT | 102 |
| TABLE V 6 DIRECTION OF THE EARTHQUAKE | 105 |
| TABLE V 7 SUMMARY OF VERIFICATION EQUATIONS FOR MASONRY WALL..... | 109 |
| TABLE V 8 VERIFICATION OF THE CRITICAL DIRECTION OF THE EARTHQUAKE | 110 |
| TABLE V 9 PUSHOVER CRITICAL DIRECTION OF THE EARTHQUAKE | 110 |
| TABLE V 10 COLOURS LEGEND | 111 |
| TABLE V 11 WALL 10 ANALYSIS DAMAGE RESULTS X DIRECTION | 112 |
| TABLE V 12 WALL 10 INPUT CONDITIONS | 113 |
| TABLE V 13 WALL 10 GEOMETRY | 113 |
| TABLE V 14 WALL 10 MECHANICAL CHARACTERISTICS | 113 |
| TABLE V 15 WALL 10 APPLIED FORCES FOR X DIRECTION | 113 |
| TABLE V 16 WALL 10 RESISTANCE FORCES VERIFICATIONS FOR X DIRECTION | 114 |
| TABLE V 17 WALL 7 ANALYSIS DAMAGE RESULTS X DIRECTION | 115 |
| TABLE V 18 WALL 7 INPUT CONDITIONS | 115 |
| TABLE V 19 WALL 7 GEOMETRY | 116 |
| TABLE V 20 WALL 7 MECHANICAL CHARACTERISTICS | 116 |
| TABLE V 21 WALL 7 APPLIED FORCES FOR X DIRECTION | 116 |
| TABLE V 22 WALL 7 RESISTANCE FORCES VERIFICATIONS FOR X DIRECTION | 116 |
| TABLE V 23 WALL 8 DEFORMATIONS RESULT FOR Y DIRECTION | 119 |
| TABLE V 24 WALL 8 INPUT CONDITIONS | 119 |
| TABLE V 25 WALL 8 GEOMETRY | 120 |
| TABLE V 26 WALL 8 MECHANICAL CHARACTERISTICS | 120 |
| TABLE V 27 WALL 8 APPLIED FORCES FOR Y DIRECTION | 120 |
| TABLE V 28 WALL 8 RESISTANCE FORCES VERIFICATIONS FOR Y DIRECTION | 120 |
| TABLE V 29 PERFORMANCE POINT X DIRECTION NUMERICAL METHOD DATA..... | 126 |
| TABLE V 30 PERFORMANCE POINT Y DIRECTION NUMERICAL METHOD DATA | 129 |
| TABLE V 31. CORRESPONDENCE BETWEEN DAMAGE LEVEL D_{sk} AND DAMAGE GRADES D_k RELATED TO STRUCTURAL AND NON-STRUCTURAL DAMAGE, (SERGIO LAGOMARSINO, ET AL,2006)..... | 133 |
| TABLE VI 1 BLOCK MECHANICAL CHARACTERISTICS | 139 |
| TABLE VI 2 PIERS ELEMENT TYPE OF REINFORCEMENT | 139 |

| | |
|--|-----|
| TABLE VI 3 PIERS FRCM GEOMETRICS | 139 |
| TABLE VI 4 FRCM ON PIERS MECHANICAL CHARACTERISTICS | 139 |
| TABLE VI 5 SPANDREL ELEMENT TYPE OF REINFORCEMENT | 140 |
| TABLE VI 6 SPANDREL FRCM GEOMETRICS | 140 |
| TABLE VI 7 FRCM ON SPANDREL MECHANICAL CHARACTERISTICS | 140 |
| TABLE VI 8 WALL FRAME REINFORCEMENT CHARACTERISTICS FOR WALLS | 140 |
| TABLE VI 9 TIE ROD REINFORCEMENT CHARACTERISTICS FOR HORIZONTAL ELEMENTS | 140 |
| TABLE VI 10 WALL 1 STATIC STATE AFTER REINFORCEMENT | 143 |
| TABLE VI 11 WALL 1 SLANDERNESS AND ECCENTRECITY VERIFICATION AFTER REINFORCEMENT | 144 |
| TABLE VI 12 WALL 1 VERTICAL LOAD BEARING VERIFICATION AFTER REINFORCEMENT | 144 |
| TABLE VI 13 WALL 6 STATIC STATE AFTER REINFORCEMENT | 144 |
| TABLE VI 14 WALL 6 SLANDERNESS AND ECCENTRECITY VERIFICATION AFTER REINFORCEMENT | 144 |
| TABLE VI 15 WALL 6 VERTICAL LOAD BEARING VERIFICATION AFTER REINFORCEMENT | 145 |
| TABLE VI 16 WALL 7 STATIC STATE AFTER REINFORCEMENT | 146 |
| TABLE VI 17 WALL 7 SLANDERNESS AND ECCENTRECITY VERIFICATION AFTER REINFORCEMENT | 146 |
| TABLE VI 18 WALL 7 VERTICAL LOAD BEARING VERIFICATION AFTER REINFORCEMENT | 147 |
| TABLE VI 19 WALL 10 STATIC STATE AFTER REINFORCEMENT | 148 |
| TABLE VI 20 WALL 10 SLANDERNESS AND ECCENTRECITY VERIFICATION AFTER REINFORCEMENT | 148 |
| TABLE VI 21 WALL 10 VERTICAL LOAD BEARING VERIFICATION AFTER REINFORCEMENT | 148 |
| TABLE VI 22 VERIFICATION OF THE CRITICAL DIRECTION OF THE EARTHQUAKE AFTER REINFORCEMENT | 150 |
| TABLE VI 23 PUSHOVER CRITICAL DIRECTION OF THE EARTHQUAKE AFTER REINFORCEMENT | 150 |
| TABLE VI 24 WALL 10 DYNAMIC STATE AFTER REINFORCEMENT | 151 |
| TABLE VI 25 WALL 10 ANALYSIS DAMAGE RESULTS X DIRECTION AFTER REINFORCEMENT | 151 |
| TABLE VI 26 WALL 10 INPUT CONDITIONS | 151 |
| TABLE VI 27 WALL 10 GEOMETRY | 152 |
| TABLE VI 28 WALL 10 MECHANICAL CHARACTERISTICS | 152 |
| TABLE VI 29 WALL 10 REINFORCEMENT TYPOLOGY APPLIED | 152 |
| TABLE VI 30 WALL 10 APPLIED FORCES FOR X DIRECTION AFTER REINFORCEMENT | 152 |
| TABLE VI 31 WALL 10 RESISTANCE FORCES VERIFICATIONS FOR X DIRECTION AFTER REINFORCEMENT | 153 |
| TABLE VI 32 WALL 7 DYNAMIC STATE AFTER REINFORCEMENT | 154 |
| TABLE VI 33 WALL 7 ANALYSIS DAMAGE RESULTS X DIRECTION AFTER REINFORCEMENT | 154 |
| TABLE VI 34 WALL 7 INPUT CONDITIONS | 154 |
| TABLE VI 35 WALL 7 GEOMETRY | 155 |
| TABLE VI 36 WALL 7 MECHANICAL CHARACTERISTICS | 155 |
| TABLE VI 37 WALL 7 REINFORCEMENT TYPOLOGY APPLIED | 155 |
| TABLE VI 38 WALL 7 APPLIED FORCES FOR X DIRECTION AFTER REINFORCEMENT | 155 |
| TABLE VI 39 WALL 7 RESISTANCE FORCES VERIFICATIONS FOR X DIRECTION AFTER REINFORCEMENT | 156 |
| TABLE VI 40 WALL 8 DYNAMIC STATE AFTER REINFORCEMENT | 158 |
| TABLE VI 41 WALL 8 ANALYSIS DAMAGE RESULTS Y DIRECTION AFTER REINFORCEMENT | 158 |
| TABLE VI 42 WALL 8 INPUT CONDITIONS | 158 |

| | |
|---|-----|
| TABLE VI 43 WALL 8 GEOMETRY | 159 |
| TABLE VI 44 WALL 8 MECHANICAL CHARACTERISTICS | 159 |
| TABLE VI 45 WALL 8 APPLIED FORCES FOR Y DIRECTION AFTER REINFORCEMENT | 159 |
| TABLE VI 46 WALL 8 RESISTANCE FORCES VERIFICATIONS FOR Y DIRECTION AFTER REINFORCEMENT | 159 |
| TABLE VI 47 PERFORMANCE POINT X DIRECTION NUMERICAL METHOD DATA AFTER REINFORCEMENT | 162 |
| TABLE VI 48 PERFORMANCE POINT Y DIRECTION NUMERICAL METHOD DATA AFTER REINFORCEMENT | 163 |
| TABLE VI 49. CORRESPONDENCE BETWEEN DAMAGE LEVEL D_{sk} AND DAMAGE GRADES D_k RELATED TO STRUCTURAL AND NON STRUCTURAL DAMAGE..... | 165 |
| TABLE VI 50 COMPARAISON OF THE DAMAGE HISTOGRAMS BEFORE AND AFTER REINFORCEMENT FOR BOTH SEISMIC DIRECTIONS | 166 |

THE LIST OF ABBREVIATIONS

l is the length of the panel

t is the thickness

σ_0 is the average compression tension

N is the axial compressive action (assumed positive in compression)

N_u is the maximum axial compressive action of the panel and it is equal to $0.85 f_m l t$ - f_m is the average resistance in compression of the masonry.

E Young's modulus

E_h Young's modulus horizontal

G Shear modulus

W load weight

f_m Mean compressive strength

f_{vm0} Mean shear strength

f_{vlim} shear strength (limit) (2.2 MPa)

f_k the characteristic values or the Characteristic strength

γ_M partial factor

$f_{m;a;m}$ Mean compressive strength

$f_{h;m}$ Mean compressive strength horizontal

f_b Mean compressive strength brick element

$f_{m;a;v;o;m}$ Mean initial shear strength

F_u masonry compressive strength

$\mu_{m;a;m}$ Bed-joint friction coefficient

M is the resistance to limb

H is the height of the frame

L is the length of the panel

T is the thickness

Σ_0 is the average compression tension

N is the axial compressive action (assumed positive in compression)

N_u is the maximum axial compressive action of the panel and it is equal to $0.85 f_m l t$

$H'p$ is assumed as the maximum value between the axial load n acting on spandrel and h_p

H_p is the minimum value between the tensile strength of elements coupled to the spandrel and $0.4f_{hu}dt$

c friction coefficient and cohesion of mortar joint

ϕ interlocking parameter

σ_s entity of compressive stresses acting at the end-sections of the spandrel)

l' length of compressed part of cross section

τ_0 masonry shear strength

b stress distribution factor as function of slenderness

J, w : modulus of inertia and modulus of resistance

GENERAL INTRODUCTION

Algeria, a nation steeped in a profound cultural legacy, boasts a remarkable abundance of masonry structures that bear witness to its historical and architectural heritage. From the ancient Berber civilizations to the Islamic influences and the French colonial period, Algeria's heritage reflects a tapestry of diverse cultural traditions. The architectural marvels scattered across the country serve as tangible embodiments of this captivating heritage, embodying the stories of the past and the enduring spirit of the Algerian people.

The masonry structures found throughout Algeria stand as enduring testaments to the nation's rich history. These structures, ranging from grand palaces and mosques to humble dwellings and fortifications, encapsulate the architectural prowess and craftsmanship of their respective eras. They symbolize the cultural identity of Algeria, preserving the narratives of its ancient civilizations, conquerors, and cultural interactions.

However, amidst the allure and historical significance of these masonry structures, concerns arise regarding their preservation and longevity. Algeria faces unique challenges in safeguarding its architectural heritage. The absence of dedicated research and limited efforts in reinforcing these structures have left them vulnerable to deterioration and potential loss. Furthermore, the lack of comprehensive codes or guidelines specific to the Algerian context adds complexity to the task of analyzing and rehabilitating masonry structures.

Analyzing masonry structures proves to be an intricate task due to the need for detailed modelling using methods like the element finite method, which can be time-consuming and labour-intensive. However, owing to the complex nature of the material and the dearth of standardized methodologies. In this thesis, we direct our attention to one such remarkable structure, the School of Asla Hocine in Annaba. This iconic building is a distinguished heritage masonry edifice in Algeria. The paramount objective of our study is to conduct a comprehensive seismic assessment and rehabilitation investigation of this venerable building. To achieve this goal, we employ the macroelement method "Equivalent Frame Method," an internationally recognized approach substantiated by the esteemed Italian

3muri software. The thesis is meticulously structured into six chapters, each dedicated to distinct facets of the assessment and rehabilitation process. Chapter 1 undertakes extensive bibliographic research, meticulously scrutinizing masonry structures, elucidating their constituent elements, appraising the mechanical characteristics of masonry walls, and probing dynamic analysis methods, including the renowned pushover analysis technique and viable reinforcement methodologies. Chapter 2 focuses intently on the modelling hypotheses and methodology that underpin our study, elucidating the advantages and rationale underpinning the adoption of the Equivalent Frame Method. Chapter 3 provides a comprehensive exposition of the School of Asla Hocine, encompassing its architectural and structural characteristics, constituting the indispensable foundation for subsequent analytical undertakings. Chapter 4 meticulously executes the static verification of the structure, meticulously scrutinizing its stability and ensuring compliance with rigorous safety standards. Progressing further, Chapter 5 delves extensively into seismic and vulnerability analyses, comprehensively scrutinizing the structure's response to seismic forces, identifying potential vulnerabilities, and discerning the fragility and extent of potential damage. Finally, Chapter 6 meticulously delineates an array of meticulous reinforcement strategies, propounding the proposed measures to fortify the structure's resilience, subsequently followed by a rerun of the static, seismic, and vulnerability analyses to ascertain the efficacy and impact of the reinforcement endeavours. This comprehensive study strives to contribute significantly to the preservation and safeguarding of Algeria's invaluable masonry heritage, furnishing valuable insights and recommendations to guide future undertakings in the assessment and rehabilitation of comparable structures.

**CHAPTER I
REVUE ON
HISTORICAL
MASONRY
BUILDINGS**

I.1 INTRODUCTION

Masonry structure material refers to the materials used to build a masonry construction, often employing blocks or bricks composed of concrete, clay, stone, or glass. The material attributes of the masonry construction, including the units, mortar, and assembly, determine the building's strength, durability, and overall performance.

Masonry buildings are recognized for their strength and durability, making them a popular choice for a variety of applications, including residential, commercial, and industrial development. The material features of the masonry construction can be adapted to specific uses, such as load-bearing capacity, resistance to weather conditions, and thermal performance.

Compressive strength, water absorption, thermal expansion, and resistance to weathering and erosion are all important material attributes of a masonry construction. The compressive strength of the masonry unit and mortar is crucial to the structure's load-bearing capability, while water absorption influences durability and weather resistance. Thermal expansion is vital to consider when constructing a structure to handle temperature fluctuations, and resistance to weathering and erosion influences the structure's lifetime and maintenance requirements.

Overall, a masonry building's material qualities are a significant concern in its design and construction, and careful material selection may assist to guarantee that the structure achieves the specified performance standards and has a long service life.







I.2 MATERIAL PROPERTIES OF MASONRY




Units in masonry construction are the building blocks used to create material properties of masonry structures, including the unit, mortar, and assembly. The unit refers to the building blocks used, while the mortar acts as the bonding agent. The masonry assembly involves arranging and bonding these components. Considering these properties is crucial for durable and robust masonry construction.




I.2.1 The Units




The structure. They can be made of materials such as bricks, concrete blocks, or stone blocks. The size, shape, and material of the units impact the design, strength, and aesthetic appeal of the masonry. Factors such as dimensions, compressive strength, and compatibility with mortar should be considered for structural integrity and durability. Adhering to building codes and standards is essential for successful masonry construction.



Table I 1.types of masonry units (MASONRY- ROOF - FLOOR CONSTRUCTION, 2020)




| | | |
|---|---|--|
| <p>Brick masonry construction</p> | <p>Sun-dried or unburnt clay bricks</p> <p>Un-dried or unburned bricks are less durable and are typically employed in temporary buildings. They are made in three stages: clay, molding, and drying. They are exposed to sunshine after molding and dried utilizing heat from the sun. These bricks are less resistant to water and fire, making them unsuitable for permanent buildings.</p> |  |
| <p>A "brick" is an artificial structural element that takes the shape of a rectangular block of clay. Bricks of any form or size may be made and there are various types.</p> | <p>Burnt clay bricks</p> <p>Burnt bricks are classified into four types: first class bricks, second class bricks, third class bricks, and fourth class bricks.</p> <p>Brick masonry construction makes use of first-class burnt clay bricks. For less important construction, third class bricks are used in masonry. Second class bricks are best for masonry construction that is plastered as it lacks finish compared with first class bricks.</p> <p>The overall tensile strength offered by the brick masonry is less and is irrespective of the class of brick chosen. Overall performance depends on the size, position, and number of openings provided to the masonry structure.</p> | <div style="display: flex; justify-content: space-around;"> <div data-bbox="810 987 1078 1216">  <p>First Class Bricks)</p> </div> <div data-bbox="1102 987 1372 1216">  <p>Second Class Bricks</p> </div> </div> <div style="display: flex; justify-content: space-around; margin-top: 20px;"> <div data-bbox="810 1317 1078 1541">  <p>Third Class Bricks</p> </div> <div data-bbox="1102 1317 1372 1541">  <p>Fourth Class Bricks</p> </div> </div> |
| | <p>Fly ash bricks</p> <p>Fly ash bricks are made from fly ash and water and have superior qualities than clay bricks. They are lightweight and resistant to freeze-thaw cycles, with good fire</p> |  |


| | |
|--|--|
| <p>insulation, high strength, consistent diameters, decreased water penetration, and no soaking required before use in masonry construction.</p> | |
| <p>Concrete bricks</p> <p>Concrete bricks are made from concrete that contains cement, sand, coarse particles, and water. They are used to create masonry and framed structures, facades, and fences, and they have an outstanding visual presence. Concrete bricks may be made on-site, reducing the amount of mortar required, and providing a variety of colors.</p> |  |
| <p>Engineering bricks</p> <p>Engineering bricks have a high compressive strength and are utilized in applications that need strength, frost resistance, acid resistance, low porosity, and damp proof courses.</p> |  |
| <p>Sand lime or calcium silicate bricks</p> <p>Calcium silicate bricks are often known as sand lime bricks because they are comprised of sand and lime. These bricks are used in the construction industry for a variety of applications, including decorative work in buildings, masonry work, and so on.</p> |  |

| | | | |
|---|---|--|--|
| <p>Stone masonry construction</p> <p>Stone is the most durable, strong and weather-resistant construction material compared with any others. These are less affected by daily wear and tear. Masonry structures made out of stone hence last for a longer period. It has a life period of 300 to 1000 plus years. Due to its numerous advantageous, it is widely used in masonry construction.</p> <p>Stone masonry has two main classifications: -rubble masonry -ashlar masonry</p> | <p>Rubble masonry is again classified into:</p> | <p>Random Rubble masonry</p> <p>Is rubble masonry that uses either undressed or hammer dressed stones. Furthermore, random rubble masonry is classified into two types:</p> <p>Coursed:</p> <p>The stones used in this form of brickwork are of varying sizes.</p> <p>This is the most basic and least expensive type of stone masonry. The masonry work in coursed random rubble masonry is done in courses such that the stones in each course are of identical height.</p> <p>Uncoursed:</p> <p>The stones used in this form of brickwork are of varying sizes. This is the most basic and least expensive type of stone masonry. The courses are not maintained on a regular basis in uncoursed random rubble masonry. The bigger stones are put first, with spalls or sneeks filling in the gaps between them</p> |  <p>Coursed random rubble masonry</p>  <p>uncoursed random rubble masonry</p> |
| | | <p>Uncoursed or Coursed Square Masonry</p> <p>The stone blocks of this style are hammered into roughly square shapes. In most cases, the facing stones are hammer-dressed. As quoins, large stones are utilized. The use of chips in bedding is avoided as much as possible.</p> |  <p>Coursed Square Masonry</p> |

| | | | |
|--|--|--|---|
| | | <p>Coursed: Straight bed and side stones are utilized in this form of construction. The stones are normally squared before being hammer dressed or straight cut. The work in coursed square rubble masonry is done in varied depth courses.</p> <p>Uncoursed: Stones with straight bed and sides are utilized in this form of construction. The stones are normally squared before being hammer dressed or straight cut.</p> <p>Different sizes of stones with straight edges and sides are put on face in many unusual patterns in uncoursed square rubble brickwork.</p> |  <p>Uncoursed Square Masonry</p> |
| | | <p>Flint rubble masonry</p> <p>This form of brickwork is prevalent in locations where flint is abundant.</p> <p>As indicated below, flint stones ranging in thickness from 8 to 15cm and length from 15 to 30cm are put in the facing in the shape of coursed or uncoursed masonry.</p> |  |
| | | <p>Polygonal Rubble Masonry</p> <p>The stones in this form of brickwork are crudely processed to an irregular polygonal shape. The stones should be set in such a way that lengthy vertical joints in face work are avoided and joints are broken as much as</p> |  |

| | | | |
|--|--|--|--|
| | | <p>feasible. Small stone chips, as seen in the image, should not be utilized to support the stones on the face.</p> | |
| | | <p>Dry Rubble Masonry</p> <p>In the form of random rubble masonry without cement, this type of construction is the cheapest, and this type of masonry is utilized in the building of retaining walls of earthen dams and canal slopes. As indicated below, the hallow areas left around and stones should be closely packed with smaller stone pieces.</p> |  |
| | <p>Ashlar Masonry</p> <p>It is well dressed (cut, worked) masonry, which can be either an individual stone that has been treated till squared or masonry made from such stone. It is the finest stone masonry unit, which is usually cuboid or trapezoidal. Is again classified into:</p> | <p>Ashlar Fine Masonry</p> <p>Ashlar masonry is a style of stonework in which finely cut and precisely shaped stones are laid in a uniform pattern to create a smooth and elegant surface. The type of stone used is typically a high-quality, finely-grained stone such as granite, limestone, or marble. The stones are cut to a specific size and shape and laid in rows with carefully controlled joints to create a clean, precise appearance.</p> |  <p style="text-align: center;">Ashlar Fine Masonry</p> |

| | | |
|--|--|---|
| | <p>Ashlar Block in Course</p> <p>Ashlar blocks in course construction are accurately cut and shaped and the bricks laid in a running bond pattern, with each block offset from the one below it. This creates a strong and stable wall that is able to withstand the forces of nature and the weight of the structure it supports.</p> |  <p>Ashlar Block in Course</p> |
| | <p>Ashlar Chamfered Masonry</p> <p>Durable and elegant finish that requires skilled craftsmen to create. The blocks are cut at a consistent angle and laid in horizontal courses with tightly controlled joints, creating a smooth and even surface. The result is a durable and elegant finished product that can withstand the test of time.</p> |  |
| | <p>Ashlar Rough Tooled Masonry</p> <p>Ashlar rough tooled masonry is a rustic and natural look for buildings in rural areas. It creates irregular marks and grooves on the surface of the stone, giving it a rustic and natural appearance. The rough tooling must be done with great care to ensure that the blocks fit together tightly and create a stable wall. It also gives the building a sense of age and character, while providing a durable and long-lasting surface.</p> |  |

| | | | |
|--|--|---|---|
| | | <p style="text-align: center;">Rock or Quarry Faced Masonry</p> <p>The rough surface of rectangular blocks of stone is obtained by chipping or carving the surface with a hammer and chisel or other hand tools. This is utilized in the construction of buildings that need to have a rough and natural appearance, such as country residences, lodges, or structures in rural or mountainous settings. The stone chipping or carving must be done with great care to ensure that the blocks fit firmly together and form a sturdy wall.</p> |  |
|--|--|---|---|

I.2.2 The Mortar

Sand, water, and a binder (such as cement or lime) are combined uniformly to form mortar, which has the proper consistency. It is employed to repair gaps, level races, and create consistent bedding. The first mortars were made of clay or clay-straw combinations, and they have developed through the years to become gypsum mortar and lime mortar. And so on.



Figure I 1 different types of motar and their classifications "1"

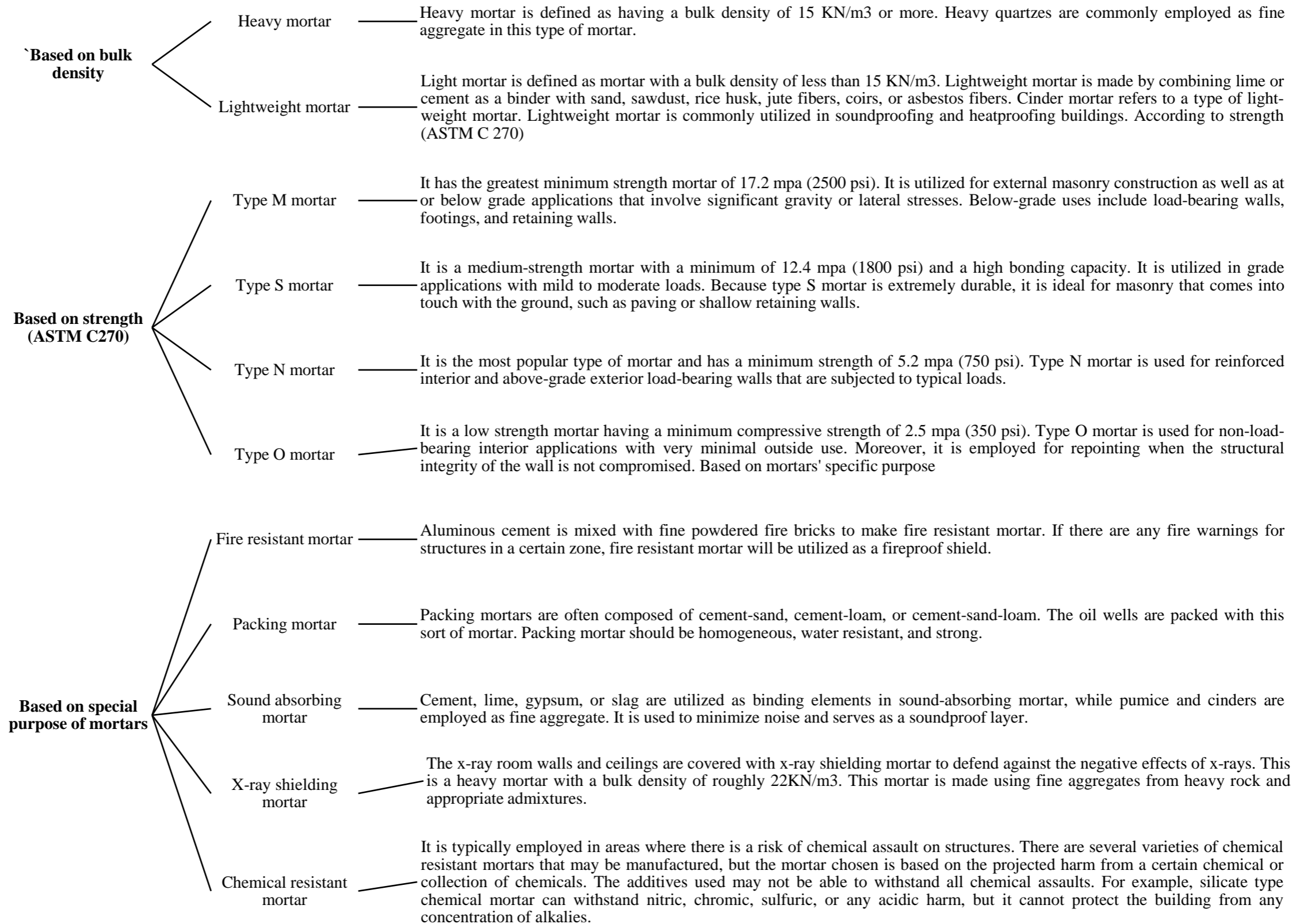


Figure 1 2 different types of motar and their classifications ‘‘2’’

An outline of the broad history of mortar is useful for context. Not all mortars are created equal. It was found thousands of years ago that burning certain clays and stones created compounds that were ideal for use as mortar binders. Cement was made by burning limestone with clay. Lime was created by burning purer limestone.

The success and performance of the cements and limes created varied greatly. Some of the variations were produced by the different compositions of the minerals burnt, while others were induced by the different procedures utilized. There are several variables in the process of producing cement or lime, as well as numerous variations in the rock or mineral resources utilized. It is a highly specialized study of industrial technology and chemistry.

For thousands of years, lime has been the primary binder in mortars throughout the Western world. Cements have been employed in certain places and for specific types of masonry, but they have been utilized less broadly. The reason for this is that excellent lime (produced by burning limestone in a certain method) works extremely well in masonry walls. It is quite robust (with the correct sand), incredibly flexible (it even cures its own cracks), and enables moisture to pass through readily (while repelling water on the exterior).

The best mortar limes are manufactured from exceptionally high-calcium limestone. Perhaps because high-calcium limestone is not widely available, and because it was not widely known before 1900 how to control all the variables in the process of making good lime, it was easily outsold by Portland cement, a scientifically formulated product that hardens quickly and can be made almost anywhere.

It's no surprise that, with the industrial revolution of the nineteenth century, Portland cement began to be mass-produced by a few and became widely relied on. This highly standardized substance was invented in the 1870s and had begun to replace lime as the primary binder for mortar by the 1920s and 1930s.

Masons had completely forgotten how to make or use lime as a binder in their mortars by the 1960s.

Lime mortar science and use has made a resurgence in recent years, owing mostly to the efforts of a few tradespeople. People are rediscovering the fundamentals of lime mortar, realizing that it is, in fact, the greatest mortar for human-scale construction and repair.

Finally, in order to improve systematic reading comprehension, we have summarized the text as follows:

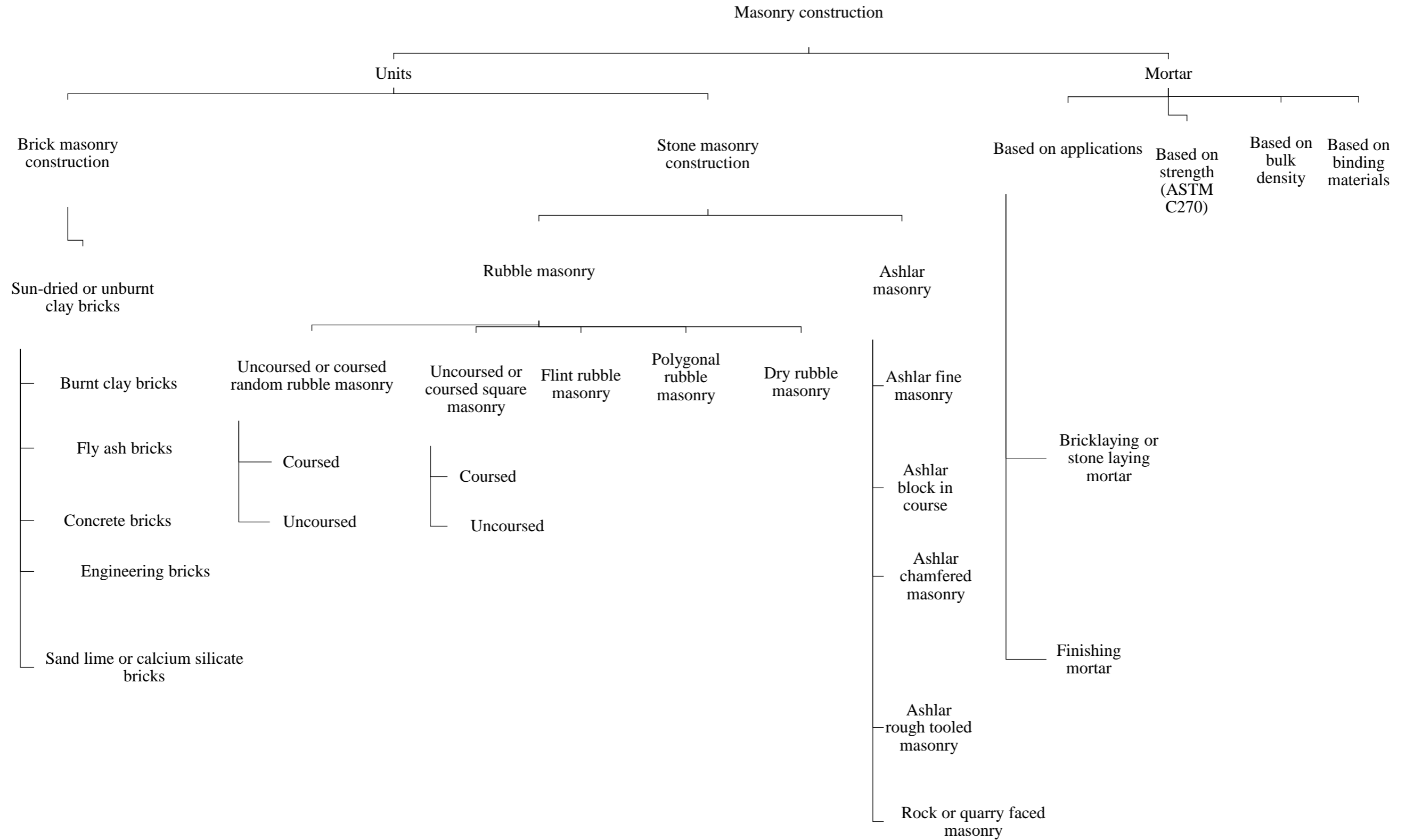


Figure 1.3 masonry construction component

I.3 ASSEMBLY OF MORTAR AND MASONRY

According to (Valek, 2003) the interaction between mortar and masonry is an effect between them which results in some physical or chemical change to one or both of them. It is as an evaluation of compatibility performance. Bad interaction means that incompatible materials or repair techniques were applied. It results in deterioration and accelerated weathering of masonry material. However, the use of an incompatible mortar or treatment does not mean bad interaction a priori, it merely brings about conditions favourable for deterioration. The deterioration itself happens through environmental agents. For example, a dense cement mortar containing salts used for repointing of porous sandstone masonry may not cause any bad interaction without the presence of moisture in very dry ageing conditions. Water or moisture is needed for a chemical and most physical deterioration processes to take place (Collepari 1990). Summarised by Amoroso & Fassina (1983), water is the main cause of degradation mechanisms for masonry materials.

A way of studying building materials from a conservation science point of view is to study their damage mechanisms and their deterioration (e.g. Torraca in Porous Building Materials, 1988). Possibly the best model for scientific studies of deterioration of masonry materials is based on a review of literature on deterioration of porous materials published by ICCROM in 1976 (Stambolov and van Asperen de Bore 1976). Torraca (1988) later on in 'Porous Building Materials' described material deterioration under the following categories:

I.3.1 External Mechanical Deterioration

This is caused by excess of stress with respect to the strength of the material (load, thermal expansion, stress caused by transport or working techniques, dynamic load and vibration). When excessive stress occurs, the material cracks and even small hair-cracks can lead, in combination with other deterioration factors, to accelerated deterioration.

I.3.2 Internal Mechanical Deterioration

This is sometimes called physical deterioration and is mostly due to a physical variation of water inside masonry like evaporation, capillary flow. A large stress can arise inside the pore structure when water freezes and crystals of ice or minerals are formed within the originally water filled pores damage caused by salt crystallisation and efflorescence or similar effects.

I.3.3 Chemical Deterioration

This is mostly connected with a reaction between sulphate and the other compounds in the masonry (Colleparidi 1990) Chemical coivosioll almost always requires the presence of water (Torraca 1988). Water can play two roles in chemical corrosion:

- (A) water in the form of liquid and vapour is chemically active
- (B) water in the form of liquid acts as a transport medium for other components

Water which has been in contact with other solid material of the same kind is not chemically active (rising damp) but it can still act as a transport medium for other deterioration agents, e.g. See physical deterioration. The danger of chemical corrosion increases with atmospheric pollution and acid rains (Charola 1986).

I.3.4 Biodeterioration

This can be caused by bacteria, algae and/or fungi which produce acid. Lichens can also penetrate into several millimetres of the surface of the material. Moss commonly grows on the surface of alkaline inaterials (lime mortar, torraca 1988). Roots of higher vegetation can penetrate deeply into joints and cause deterioration of the masonry.

I.4 ESTIMATION OF THE MECHANICAL PROPERTIES OF MASONRY

There are several methods for evaluating the mechanical properties of historic masonry buildings. There are two sorts of approaches: direct and indirect. In the first approach, mechanical properties are extracted directly from the material by in-situ or laboratory studies.

(Due to political and administrative constraints, a lack of testing instruments, and a lack of access to construction components, there is a lack of interest in research and restoration of historic masonry structures in Algeria. Access to building components is restricted to a few state agencies).

The attributes are retrieved indirectly in the second method through a correlation methodology from databases that provide comparable estimates or from component qualities. Which this approach is based on a visual examination as well as knowledge of the construction type and the morphology of the wall, in condition.

The Italian codentc18 is used for correlation processes.

I.4.1 The Italian Code Ntc 18

As (SEBOUI Hatem, 2022) said ,The main mechanical characteristics of various types of ancient masonry, whose mechanical attributes rely on knowledge levels, or KLS, are referenced in the Italian Code (NTC, 2018).

The reference values for the masonry qualities under the most typical situations in historic URM structures are shown in Table 1.

The multipliers mentioned in Table 2 should be used to adjust the design material specifications for masonry with superior characteristics.

Each knowledge level has a confidence factor (CF) value assigned to it, as shown in Table 3.

Table 1 2. Reference ranges for different masonry material parameters (SEBOUI Hatem, 2022).

| Masonry typology | Compression strength f_m (mpa) | Shear strength τ_0 (kpa) | Young modulus E_m (mpa) | Shear modulus G_m (mpa) | Weight density W_m (kN/m ³) |
|--|-------------------------------------|----------------------------------|------------------------------|---------------------------------|---|
| | Min – max | Min – max | Min – max | Min –max | |
| Irregular stone masonry (pebbles, erratic, irregular Stones) | 1.0 - 1.8 | 20 - 32 | 690 - 1050 | 230 - 350 | 19 |
| Uncut stone masonry with facing walls of limited Thickness | 2.0 - 3.0 | 35 - 51 | 1020 - 1440 | 340 - 480 | 20 |
| Cut stone with good bonding | 2.6 - 3.8 | 56 - 74 | 1500 - 1980 | 500 - 660 | 21 |
| Soft stone masonry such as tuff and limestone | 1.4 - 2.4 | 28 - 42 | 900 - 1260 | 300 - 420 | 16 |
| Dressed rectangular stone masonry | 6.0 - 8.0 | 90 - 120 | 2400 - 3200 | 780 - 940 | 22 |
| Solid brick masonry with lime mortar | 2.4 - 4.0 | 60 - 90 | 1200 - 1800 | 400 - 600 | 18 |

Table I3. Correction factors for different parameters of masonry types (SEBOUI Hatem, 2022)

| Masonry typology | Good mortar quality | Joint thickness <10 mm | Regular Courses of bricks | Transverse connection | Wide or poor internal core | Grout injection | Reinforced plaster |
|--|---------------------|------------------------|---------------------------|-----------------------|----------------------------|-----------------|--------------------|
| Irregular stone masonry(pebbles, erratic,...) | 1.5 | - | 1.3 | 1.5 | 0.9 | 2 | 2.5 |
| Uncut stone masonry with facing walls of limited thickness | 1.4 | 1.2 | 1.2 | 1.5 | 0.8 | 1.7 | 2 |
| Cut stone with good bonding | 1.3 | - | 1.1 | 1.3 | 0.8 | 1.5 | 1.5 |
| Soft stone masonry (tuff, limestone) | 1.5 | 1.5 | - | 1.5 | 0.9 | 1.7 | 2 |
| Dressed rectangular stone masonry | 1.2 | 1.2 | - | 1.2 | 0.7 | 1.2 | 1.2 |
| Solid brick masonry with lime mortar | 1.5 | 1.5 | - | 1.3 | 0.7 | 1.5 | 1.5 |

Table I4. Knowledge levels are based on available information and corresponding values of the confidence factors for masonry buildings (SEBOUI Hatem, 2022)

| Knowledge levels | Geometry | Constructive details | Material properties | Analysis methods | CF |
|------------------|---|----------------------------|---|------------------|------|
| KL1 | Geometric survey of masonry, masonry, floor, vaults, staircase. | Limited in-situ inspection | Limited in situ investigations: - Strength: minimum value from table 2. - Modulus of elasticity: average value of the interval of Table 2 | All methods | 1.35 |
| | Identification of the loads on each wall element, identification of the type of foundation. | | Extensive in situ investigations: | | |
| | Identification of cracks and | | | | |

| | | | | | |
|------------|---------------------|---|---|--|-------------|
| <p>KL2</p> | <p>deformation.</p> | <p>Extensive and comprehensive in-situ inspection</p> | <p>- Strength: average value from Table 2. - Modulus of elasticity: average value of the tests or the interval in Table 2.</p> | | <p>1.20</p> |
| <p>KL3</p> | | | <p>Comprehensive in situ investigations Case a) availability of at least three experimental values of the strength: - Strength: average experimental value. - Modulus of elasticity: average value of the tests or the interval in Table 2. Case b) availability of 2 experimental values of the strength: - Strength: if the average experimental value is within the range of Table 2, take the average value from the table; if the average experimental value is higher or lower than the range of Table 2, taking the experimental value, - Modulus of elasticity: same value as LK3 Case a. Case c) availability of a single experimental value of the strength: - Strength: if the average experimental value is within the range of Table 2 or higher, take the</p> | | <p>1.00</p> |

| | | | | | |
|--|--|--|---|--|--|
| | | | <p>average value of the table; if the average experimental value is lower than the range of table 2, it takes the minimum value of the table,</p> <p>- Modulus of elasticity: same value as LK3 Case c.</p> | | |
|--|--|--|---|--|--|

I.5 MASONRY BUILDING BEHAVIOURS

I.5.1 Domain Of Vulnerability Modelling

Under the domain of vulnerability modeling, many modeling methodologies for seismic capability of brick buildings have been presented. The goal of structural modeling is to generate seismic resistance characteristics for the MDOF (Multi-degree of freedom) or ESDOF (Equivalent single degree of freedom), such as strength, stiffness, and deformation capacity. These parameters are utilized as input to the structural demand analysis. The capacity curve, which defines the building's lateral force-deformation resistance, is a common result of structural modeling.

Vertical walls resist gravity loads, whereas horizontal parts (diaphragms) distribute gravity loads and transfer inertial seismic lateral forces to the walls.

I.5.2 The Seismic Behaviour Mechanisms

Masonry buildings often display three-dimensional reaction behavior when subjected to earthquake ground motion impacts. The primary processes that a masonry building shows when subjected to dynamic seismic stresses are classified as **in-plane** mechanisms and **out-of-plane** mechanisms. The building's three-dimensional reaction is comprised of an interplay between those two systems. Yet, because of the inherent challenges in investigating such complicated interactions, the difference between the two main processes is widely used to simplify the problem.

The walls that are parallel to the primary direction of ground shaking are referred to as in-plane walls. Because of their orientation, these walls offer the building's lateral load resistance and endure in-plane deformation and stresses. Windows and door apertures are generally perforated into in-plane walls. Seismic

damage to masonry walls, as well as laboratory testing, revealed that masonry walls subjected to in-plane loads can exhibit typical sorts of behaviors associated with multiple failure modes, flexural and shear failures, or a mix of both.

When the horizontal load causes tensile flexural cracking at the corners, the wall begins to act as a virtually rigid body rotating about the toe. Diagonal shear failure is commonly defined by the creation of a diagonal fracture that begins in the center of the wall and spreads to the corners. In the case of a regular brickwork design, the fracture usually travels through the mortar joints, although it can also move through the blocks. Another type of failure mode is sliding shear failure, which occurs when a horizontal bed joint plane fails, generally at one of the wall's extremities. Unfortunately, this failure is only conceivable for extremely squat walls.

The diagonal cracking shear failure is the most typically found in-plane failure mechanism in post-earthquake damage assessments, particularly in ancient brick and stone masonry buildings.

The development of various failure mechanisms is determined by multiple elements, including the geometry of the wall, boundary conditions, outgoing axial load, physical properties of the masonry constituents (compression and shear strength of masonry), and masonry geometrical properties (block aspect ratio, masonry pattern). It should be emphasized that distinguishing the presence of a certain kind of mechanism is difficult since two or more failure mechanisms may occur with interactions between them.

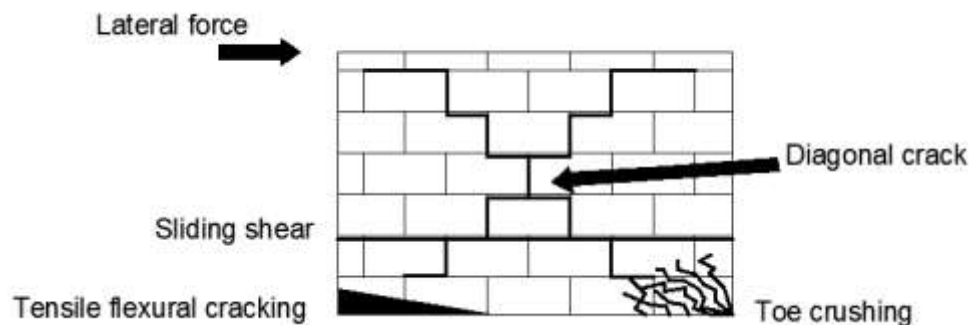


Figure I 4. Different shear modes of URM wall

Flexural failure Predominates in slender walls, while diagonal cracking predominates in intermediate slender walls over flexure and bed joint sliding as vertical stress increases. At rising degrees of vertical compression and increasing ratios Of mortar and block strengths, cracking via blocks continues to prevail to diagonal cracking propagating through mortar joints.

- (Shear failure mode emerges in constrained masonry structures owing to in-plane seismic loads (acting parallel to the plane of the wall), whereas flexural failure mode may develop due to either in-plane or out-of-plane loads (acting perpendicular to the plane of the wall).

- Horizontal cracking at the mortar bed joints on the tension side of the wall characterizes flexural failure induced by in-plane lateral stresses.)
- In unreinforced masonry walls, the out-of-plane shear failure mechanism a bending alone.
- According to the elastic theory of plates, the condition of primary stresses in a simply supported rectangular plate (panel) under an out-of-plane point load is tension-tension, with the largest tensile stress located at the center of the panel and on the tension side. As a result, cracking of the panel under out-of-plane stresses begins in the center and spreads to the supports.

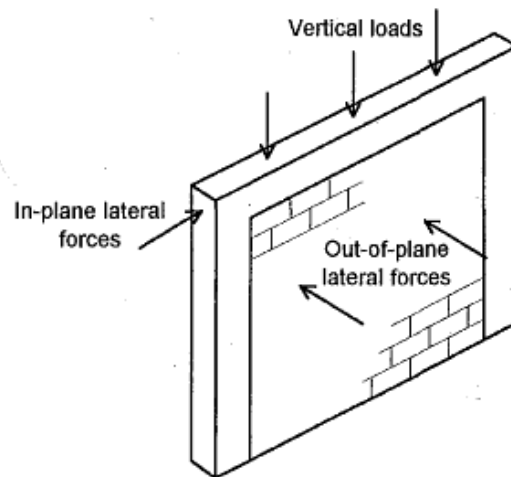


Figure I 5. in-plane and out-of-plane forces

I.6 SEISMIC ANALYSIS ‘PUSHOVER’

The nonlinear static pushover analysis method is an approximate method in which the structure is subjected to an increasing lateral load until a target displacement is reached.

The pushover analysis consists of a series of elastic analyses, superimposed to approximate a capacity curve or shear force curve at the base - displacement at the top.

The first step is to apply the gravitational and lateral force which results from a behavior law of the bilinear or trilinear type, the lateral load is increased in an iterative manner until reaching a first plastification of an element (appearance of plastic patella). By taking into account the new state of equilibrium due to the reduction of the stiffness, the process continues until having a limit displacement at the top of the structure or until an instability.

When the dominating response is that of the fundamental mode, the displacement of a system with numerous degrees of freedom can be nearly equal to that of a system with a single degree of freedom.

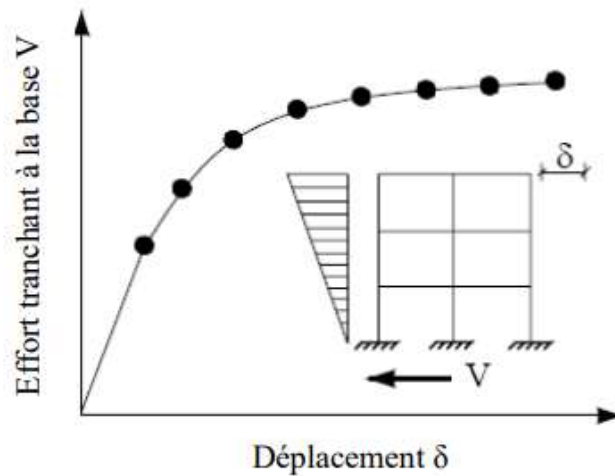


Figure I 6. structure capacity curve

I.6.1 Why Is Pushover Analysis Used

Reasonable estimates of inelastic deformation or damage in structures are required for performance-based methods.

Elastic Analysis is incapable of providing this data.

Nonlinear dynamic response history analysis can provide the necessary information, but it can be time-consuming.

I.6.2 A Brief Overview Of The Technique

A pushover analysis is divided into two sections. Initially, the "Capacity Curve" or pushover is computed by applying incremental static loads to an inelastic model of the structure. Second, this curve is used in conjunction with another "Demand" tool to calculate goal displacement.

I.6.2.1.1 The capacity curve

- 1) The Structural Analytical Model will include gravity loads, known sources of inelastic behaviour such as material constraints and plasticity effects, as well as P-Delta effects.
- 2) The modal properties such as periods and mode shapes, modal participation factors, and effective modal mass will also be computed.
- 3) The lateral inertial forces will be distributed according to the assumed distribution and a pushover curve generated:

The choice of the seismic force distributions is up to the designer, the available options are: · **uniform:** distribution of forces, deduced from a uniform trend of accelerations along the height of the construction;

Static forces: proportional distribution to static forces

$$F_i = F_h \cdot z_i \cdot \frac{W_i}{\sum z_j \cdot W_j}$$

Modal distribution: this distribution is an alternative to "static forces" and is calculated on the basis of the identified significant modes following the calculation of modal forms. At the bottom right side, a panel allows to select which distribution to use between static and modal forces.

- 4) The model allows for evaluation of the structure's behaviour under dynamic loading (Convert the Pushover Curve to the First Mode Capacity Curve for low and medium height's buildings).
- 5) Reduce the complexity of the capacity curve (Use bilinear approximation)

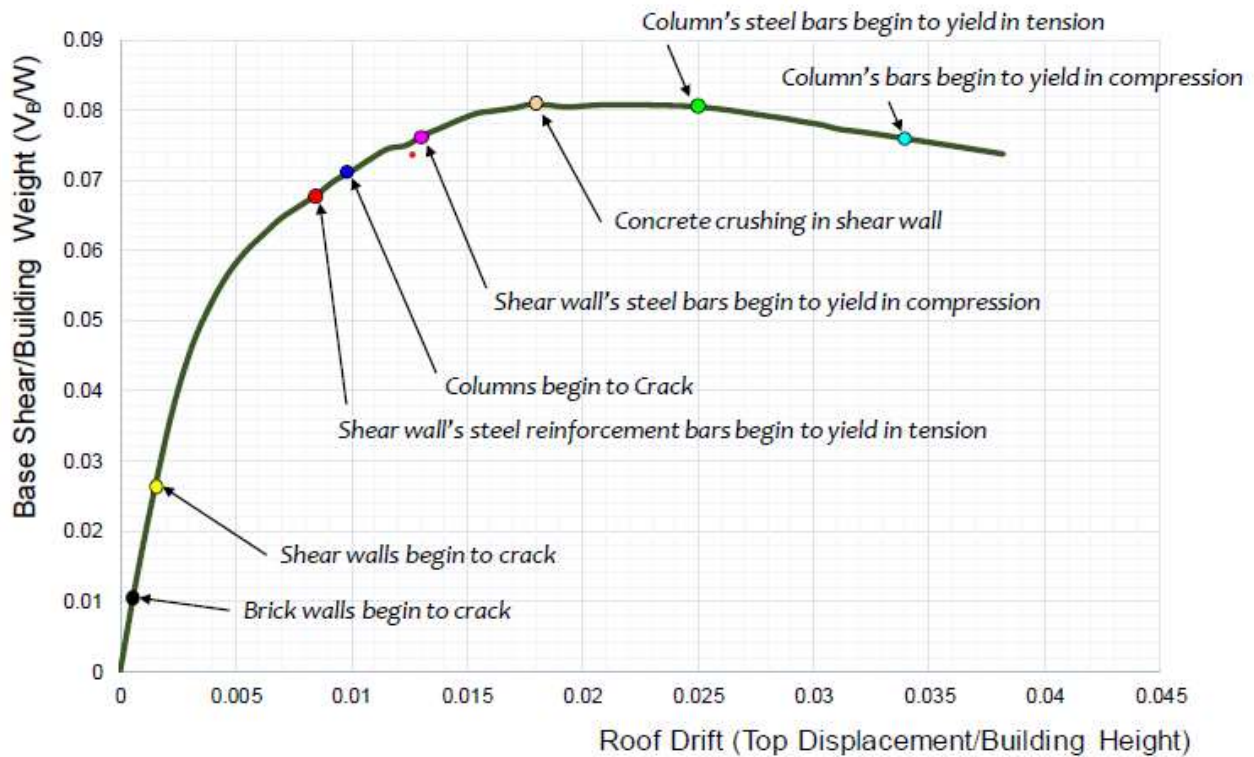


Figure I 7. Global Response and Performance

The structure's nonlinear static analysis yields a "pushover curve," as seen on the left. The sign above the curve shows that the lateral load pattern for this curve was upper triangular. Different pushover curves will be produced by various load patterns, such as uniform or proportional to first mode shape.

The pushover curve on the right is a simplified first mode bilinear variant. This curve is termed a "Capacity Curve", or "Capacity Spectrum". The values on the capacity curve's X and Y axes are modal acceleration and modal displacement.

Capacity Spectrum should transform to Another form of pushover curve (SA-SD form).

The first approach discussed is the so-called Demand Capacity Spectrum approach. This approach is detailed in the ATC 40 publication.

I.6.2.1.2 The demand curve

The output will be from;

A response spectrum in the form of displacement-acceleration, which reflects the seismic hazard level. And it will be a 5% damped ELASTIC spectrum modified for site effects, expected performance and equivalent damping. The displacement and associated acceleration will be graphed to represent the seismic loading on a structure.

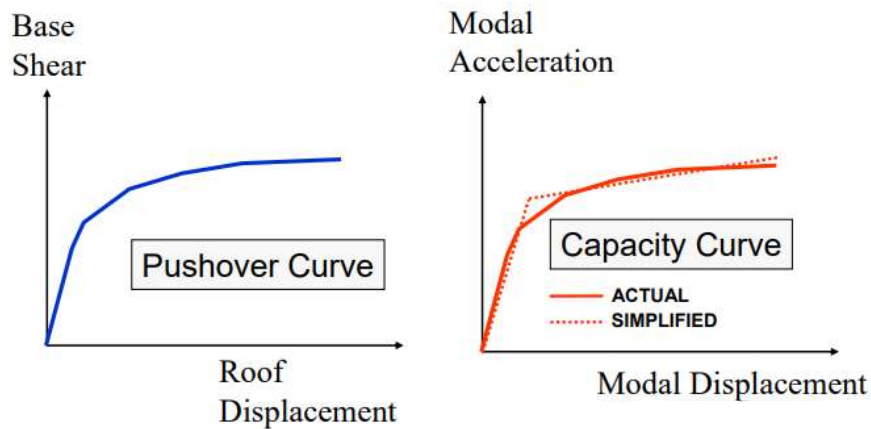


Figure I 8. Development of the Capacity Curve

Using the following equations, the Capacity Curve is transformed to a Capacity Spectrum relationship:

$$Sa = \frac{Vi}{\alpha m * w} \qquad Sd = \frac{u}{PF1 * \phi ij}$$

When M is the total mass of the building, ϕ_{ij} is the modal amplitude at storey level “i” for mode “j”, PF1 is a participation factor, and m is the modal mass coefficient, which are provided by:

$$PF1 = \frac{\{\phi\}^T [M] \{I\}}{\{\phi\}^T [M] \{\phi\}} \qquad \alpha_M = \frac{[\sum_{j=1}^N Mi * \phi_{ij}]^2}{\sum_{i=1}^N Mi \sum_{j=1}^N Mi * \phi^2_{ij}}$$

PF1 = modal participation factor for the first natural mode.

α_1 =Modal mass coefficient for the first natural mode.

M = mass assigned to level I .

ϕ_i = amplitude of mode 1 at level i.

V= base shear.

u= roof displacement (V and the associated u make up points on the capacity curve).

S_a =spectral acceleration.

S_d =spectral displacement (S_a and the associated S_d make up points on the capacity spectrum).

I.6.2.1.3 Target displacement using an elastic spectrum

Many methods have been known in that field as:

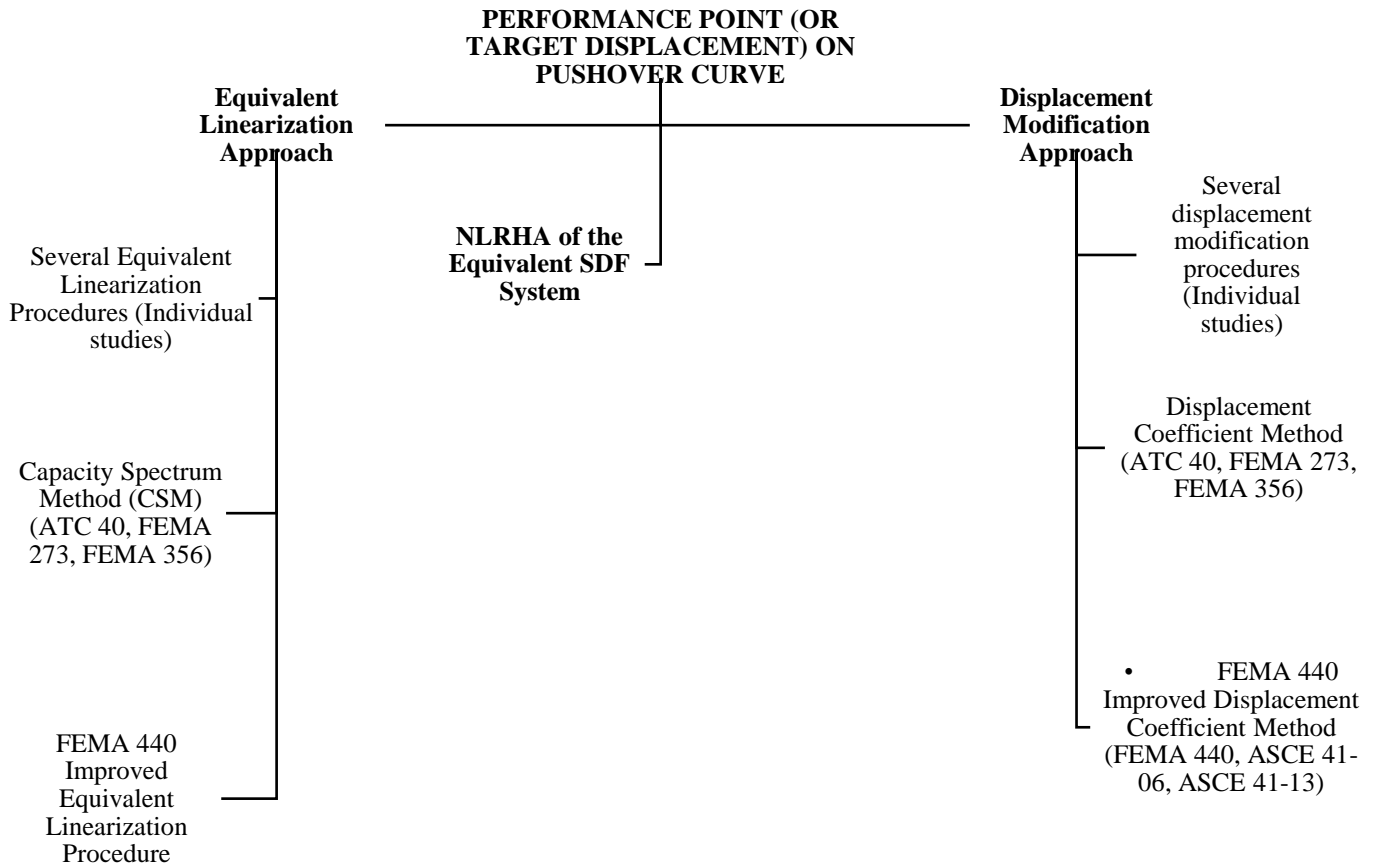


Figure I 9. the different methods utilized to distinguish the Performance Point

I.6.2.1.4 Method of equivalent linearization

Capacity spectrum approach (csm) (atc 40, fema 273, fema 356):

Conversion the Demand Spectrum to ADRS spectra

“Application of the Capacity-Spectrum technique requires that both the demand response spectra and structural capacity (or pushover) curves be plotted in the spectral acceleration vs. Spectral displacement domain. Spectra plotted in this format are known as Acceleration-Displacement Response Spectra (ADRS) after Mahaney et al., 1993.

Every point on a response spectrum curve has associated with it a unique spectral acceleration, S_a , spectral velocity, S_v , spectral displacement, s_d and period, T . To convert a spectrum. From the standard S_a vs T format found in the building code to ADRS format, it is necessary to determine the value of S_{di} for each point on the curve, S_{ai} , T_i . This can be done with the equation:

$$S_{di} = \frac{T_i^2}{4\pi^2} S_{ai} g$$

Tandard demand response spectra contain a range of constant spectral acceleration and a second range of constant spectral velocity. Spectral acceleration and displacement at period T_i are given by:

$$S_{ai} g = \frac{2\pi}{T_i} S_v \quad S_{di} = \frac{T_i}{2\pi} S_v \quad \text{“(ATC 40) “}$$

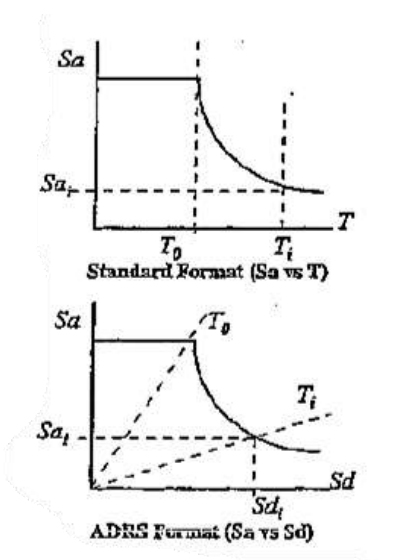


Figure I 10 Conversion to ADRS spectra (ATC 40)

According to (ATC 40) “The capacity spectrum method A, B, C (8.2.2.1) reduce the elastic spectrum to intersect the capacity curve in spectral coordinates to find a performance point a_p, d_p , the equal distance point a^*, d^* , is good starting point for the alternative process.

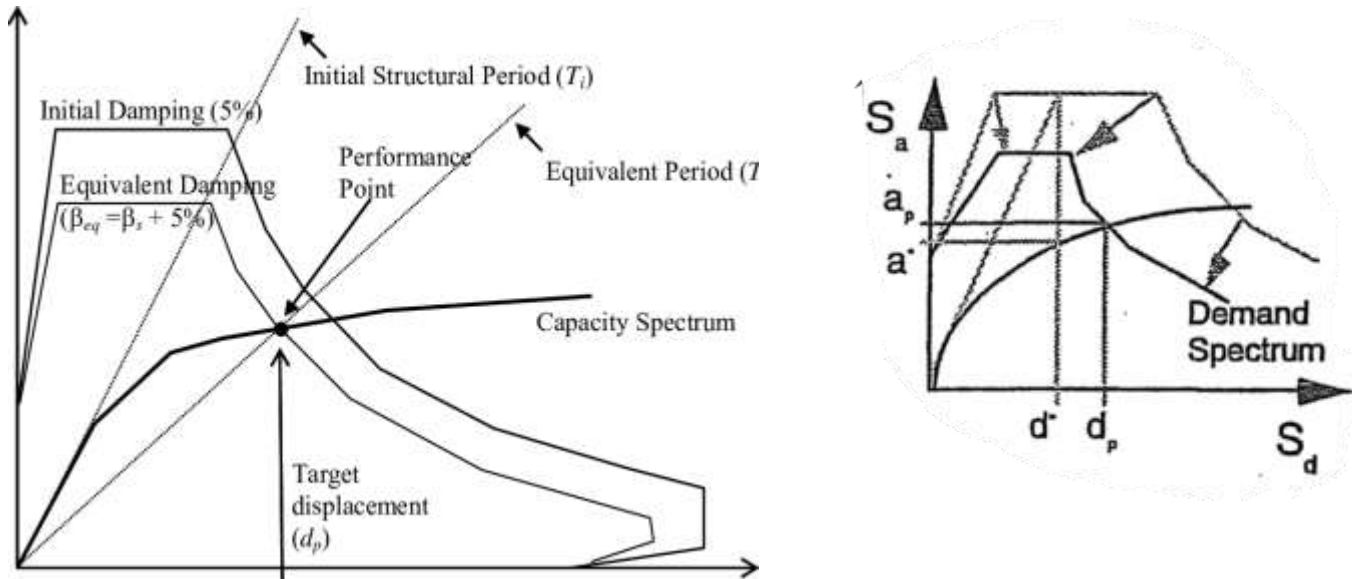


Figure I 11 Schematic representation of Capacity Spectrum Method (ATC 40)

Demand Spectrum should take Another form of response spectrum (ADRS Form) reduced based on effective damping (i.e., original inherent damping + additional hysteretic damping).

Reduction of Response Spectrum to get the Demand Spectrum

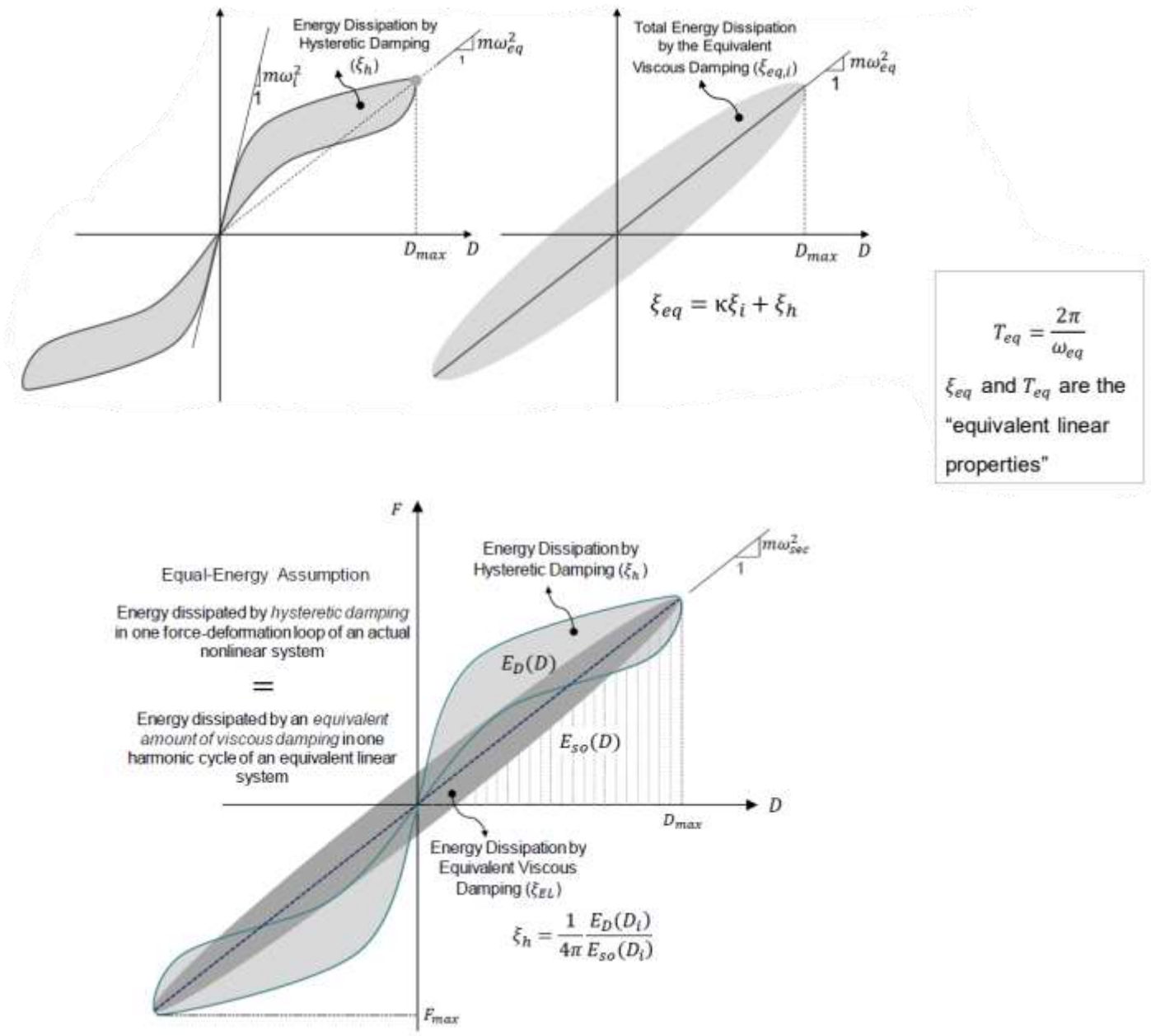


Figure I.12. Determination of Hysteretic

An Equivalent Linear System with Elongated Period and Additional Damping is the transformed form of. A nonlinear SDF system with initial circular natural frequency ω_i , and with initial inherent viscous damping ξ_i .

Reduction of Demand Spectrum

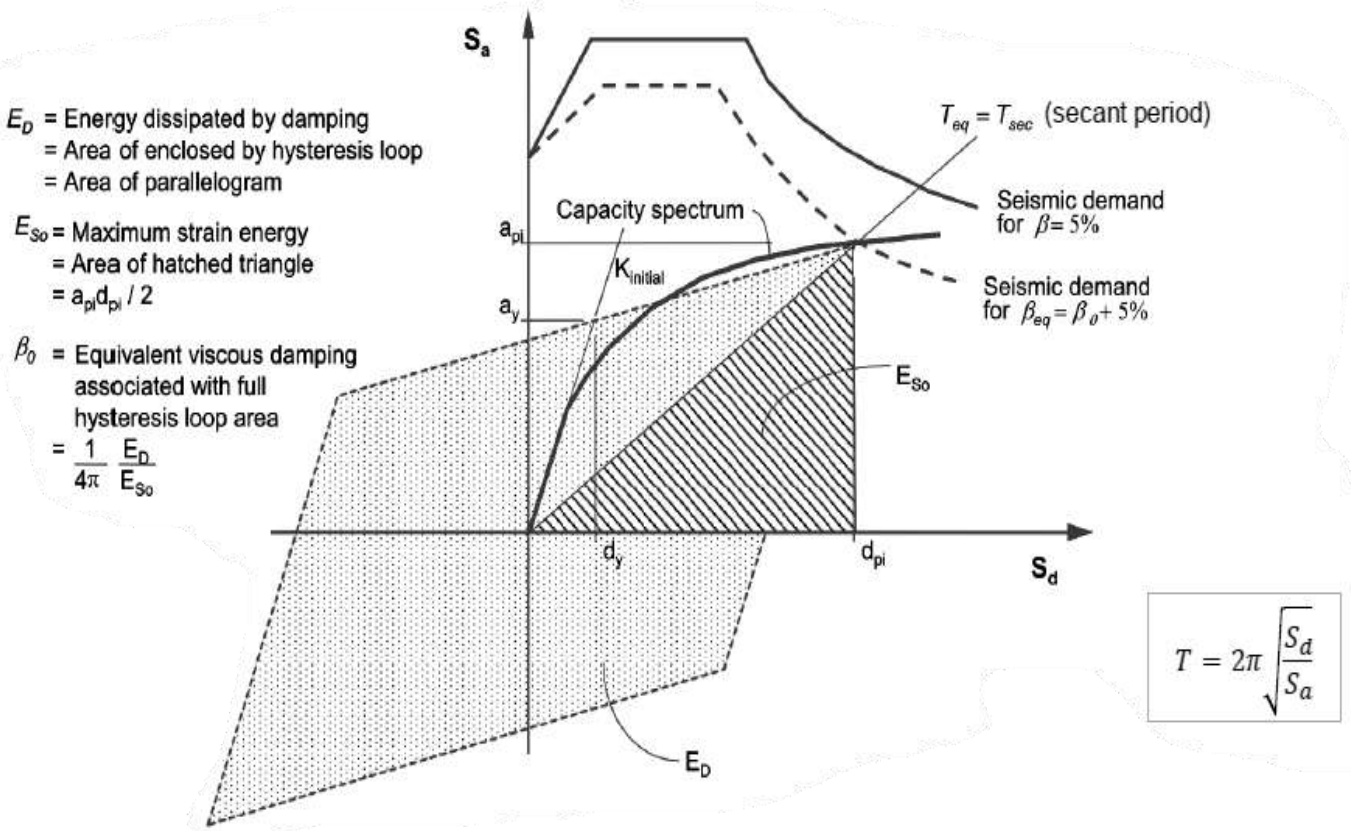


Figure I 13. Reduction of Demand Spectrum

Estimation of Damping and Reduction of 5 percent Damped Response Spectrum The damping that occurs when earthquake ground motion drives a structure into the inelastic range can be viewed as a combination of viscous damping that is inherent in the structure and hysteretic damping. Hysteretic damping is related to the area inside the loops that are formed when the earthquake force (base shear) is plotted against the structure displacement. (ATC 40)

To anticipate target displacement, the Demand Curve is utilized in conjunction with the Capacity Curve. To obtain the goal displacement, a trial-and-error approach is commonly utilized (ATC 40).

When the displacement at the intersection of the demand spectrum and the capacity spectrum, d_i , is within 5 percent ($0.95d_{pi} \leq d_i \leq 1.05d_{pi}$) of the displacement of the trial performance point, a_{pi} , d_{pi} , d_{pi} becomes the performance point. If the intersection of the demand spectrum and the capacity spectrum is not within the acceptable tolerance, then a new a_{pi} , d_{pi} point is selected and the process is repeated. The performance point represents the maximum structural displacement expected for the demand earthquake ground motion. When the capacity spectrum is a "sawtooth" curve, that is, the final composite capacity spectrum is constructed from several

different capacity spectra which account for strength degradation of elements, special care must be taken in determining the performance point. The bilinear representation of the capacity spectrum, that is used to determine the reduction factors for the 5 percent damped spectrum, is constructed for a single capacity spectrum curve, not the composite curve. For the analysis to be acceptable, the bilinear representation must be for the same single capacity spectrum curve that makes up the portion of the composite capacity spectrum where the intersection point occurs (ATC 40).

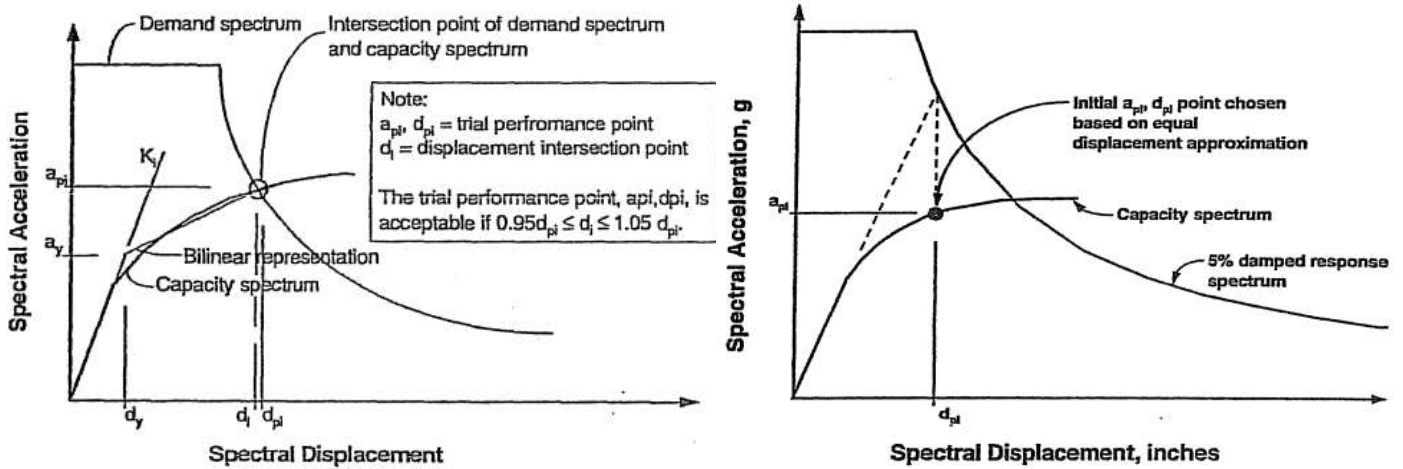


Figure I 14 Intersection point of Demand and capacity spectra Within Acceptable Tolerance (ATC 40)

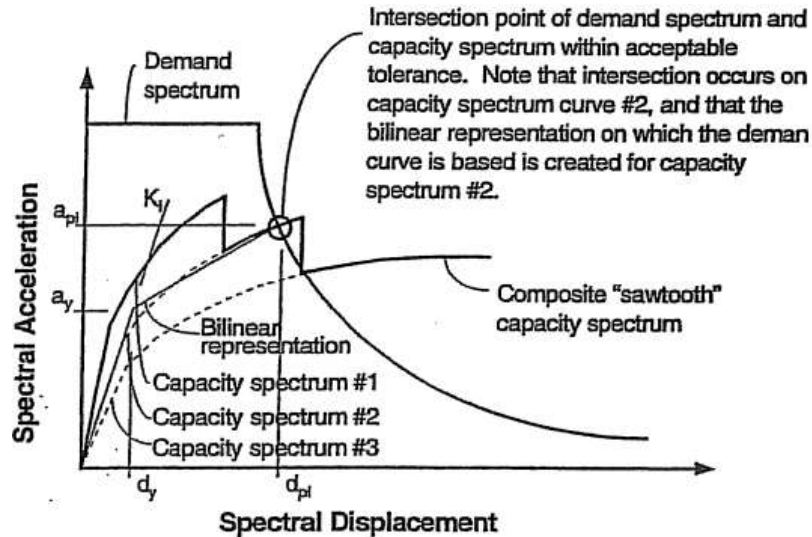


Figure I 15 The concept for a "sawtooth" capacity spectrum (ATC 40)

I.7 THE STRENGTHENING

Masonry buildings comprise a major share of existing structures worldwide. The experience of earthquakes has demonstrated that unreinforced masonry constructions may be significantly vulnerable to seismic activity. Several techniques for retrofitting masonry structures to increase seismic performance have been developed and applied during the last few decades. Surface treatment and external reinforcement are the two most common procedures for retrofitting masonry buildings.

I.7.1 Surface Treatment

The following methods can be used to reinforce masonry walls:

I.7.1.1.1 Adding reinforced concrete jackets to one or both sides of a wall

Reinforced concrete (RC) jackets are a technique for reinforcing masonry structures that involves applying jackets to one or both faces of masonry walls. This approach is utilized for both brick and stone masonry walls. To use reinforcing jackets, the plaster must first be removed from the walls. The mortar joints between the bricks have been cleaned. If there are any cracks in the masonry walls, they are first grouted. Anchor ties are placed in predrilled holes. The drill surface is cleaned and hydrated, then cement slurry is applied to the masonry surface and drills. The concrete is placed in two layers, separated by reinforcing mesh. Steel anchors hold the reinforcing mesh on both sides of the wall together. These anchors are soldered to the mesh or linked together using tying wire. The typical overall thickness of RC jackets is between 30mm and 100mm. The thickness of concrete layers is determined by the manner of application.

Reinforced Concrete Jacketing Guidelines for Masonry Wall Strengthening:

- The horizontal and vertical reinforcement should be no less than 0.25% of the jacket portion.
- The minimum reinforcement used to reinforce the ends of the wall should be 0.25% of the jacket section.
- The ties at the well ends shall have a minimum diameter of 8 mm and a maximum spacing of 150 mm.
- Dowels spaced no more than 600 mm apart in both directions must be used to secure the jacket to the previous concrete.

It is also significant that the jacket be capable of transferring forces to slab diaphragms. This may be accomplished by inserting epoxy grouted anchors and diagonal connecting bars through slab holes.

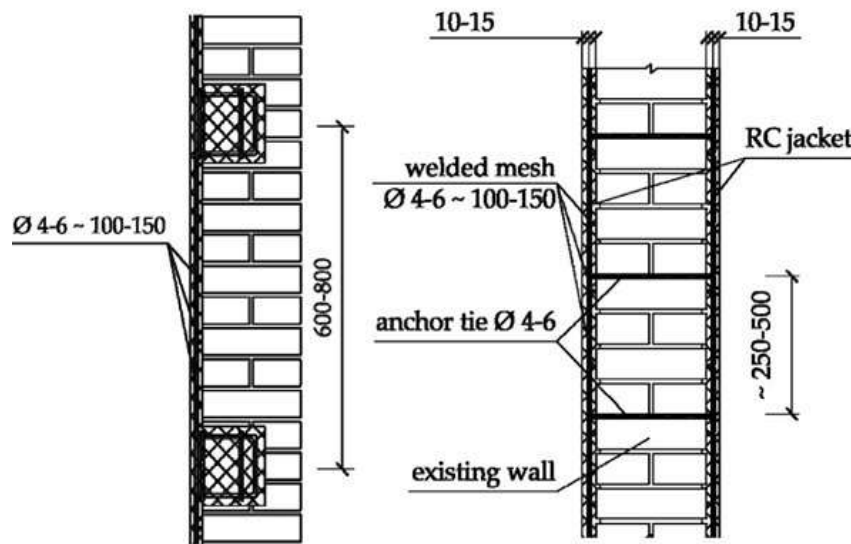


Figure I 16 Strengthening of Masonry Walls by Application of Single and Double sided reinforced concrete (RC) jackets

I.7.1.1.2 Frp structural repointing for masonry wall strengthening.

When compared to the usage of FRP laminates, structural repointing of masonry walls offers benefits. Because surface preparation (sandblasting and puttying) is not required, this method of masonry wall strengthening is straightforward. Also, the masonry's elegance is kept.

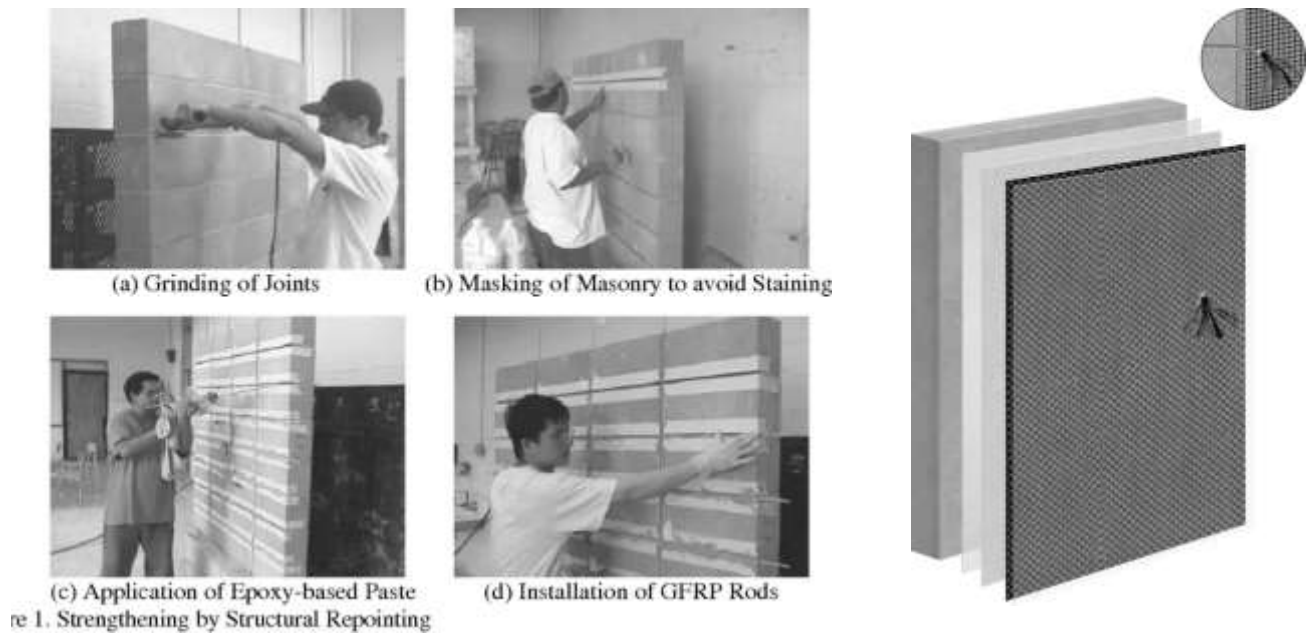


Figure I 17 Strengthening of Masonry Walls using FRP Structural Repointing

I.7.1.1.3 Fabric reinforced cementitious matrix (frmc)

Emerges as an alternative reinforcing technology for improving the mechanical characteristics of masonry buildings against seismic events. Fabric Reinforced Cementitious Matrix (FRCM) is a composite material composed of a mesh embedded in an inorganic mortar matrix that evolved as an alternative to the organic matrix of FRP (Fibre Reinforced Polymers). Because of its lower hazardous emissions, higher fire resistance, water vapor permeability, compatibility with inorganic substrates, and removability capability. On the other hand, FRCM composites have two technical drawbacks that must be overcome: first, the high stiffness of commonly used synthetic fiber meshes makes energy dissipation against cyclic loading difficult, resulting in stress concentration on the existing structure; and second, obtaining these used synthetic fibers has a high environmental and financial cost.



Figure I 18 Fabric Reinforced Cementitious Matrix (FRMC)

I.7.2 External Reinforcement

I.7.2.1.1 Post-tensioning strengthening

The post-tensioning strengthening technique is based on applying external pressures to masonry structural elements in order to counterbalance some or all of the effects of external stresses.

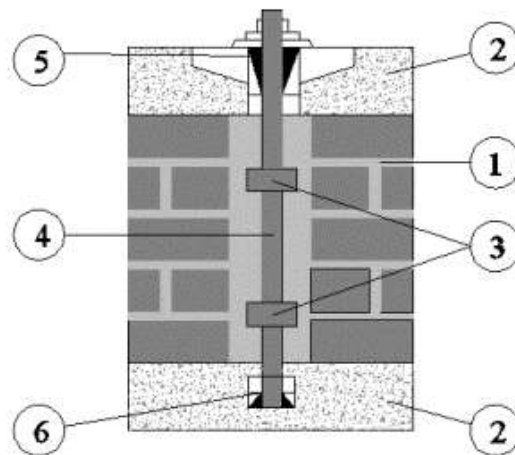
Strengthening using PT is very effective and cost-effective for big masonry walls and masonry dome structures, and it has been used successfully to enhance bending and shear resistance and reduce excessive deflections.

Post-tensioning in masonry provides a simple and possibly cost-effective structural method. Post-tensioning procedures may be used on a variety of masonry elements, including bonded and unbonded reinforcing walls that can be ungrouted, partially grouted, or completely grouted. When grout is used in the cells housing the post-tensioning (PT) bars in unbonded PT masonry walls, the PT bar is encased in a PVC tube and so is not

embedded in or bonded to the grout. An unbonded PT bar is intended to provide a restoring force to restore the wall to its original vertical alignment following a seismic event, hence eliminating residual drifts.

Externally or internally, the P-T strengthening method involves drilling vertical cores in the center of a masonry wall and inserting FRP tendons positioned inside a duct along the cores. FRP tendons are lightweight and strong, making them ideal for posttensioning applications. CFRP and aramid FRP are the most often used composite materials in P-T strengthening systems for masonry constructions.

The CFRP tendons feature fibers that are aligned in the longitudinal direction of the tendon, whereas aramid FRP tendons vary in strength according on the manufacturer.



1 - masonry; 2- reinforced concrete element; 3- threaded sleeve; 4 - FRP tendon; 5- stressing anchorage; 6- end of anchorage.

Figure I 19. Post-tensioning strengthening system

I.7.2.1.2 A steel ring-frame around the new opening

Certainly, steel frames are frequently selected over alternative brick wall strengthening solutions due to various advantages they provide. One of the primary benefits is their great reversibility, which means they may be quickly removed if necessary without causing harm to the existing brickwork. This is especially important in the case of historic buildings or structures that must be preserved.

Steel frames are also relatively easy to install, which can save time and labor costs compared to other techniques. Moreover, steel frames may give a high level of stiffness and strength without significantly increasing the self-weight of the structure, which is critical in buildings with weight limits or in seismic zones where excessive building weight can contribute to greater seismic loads.

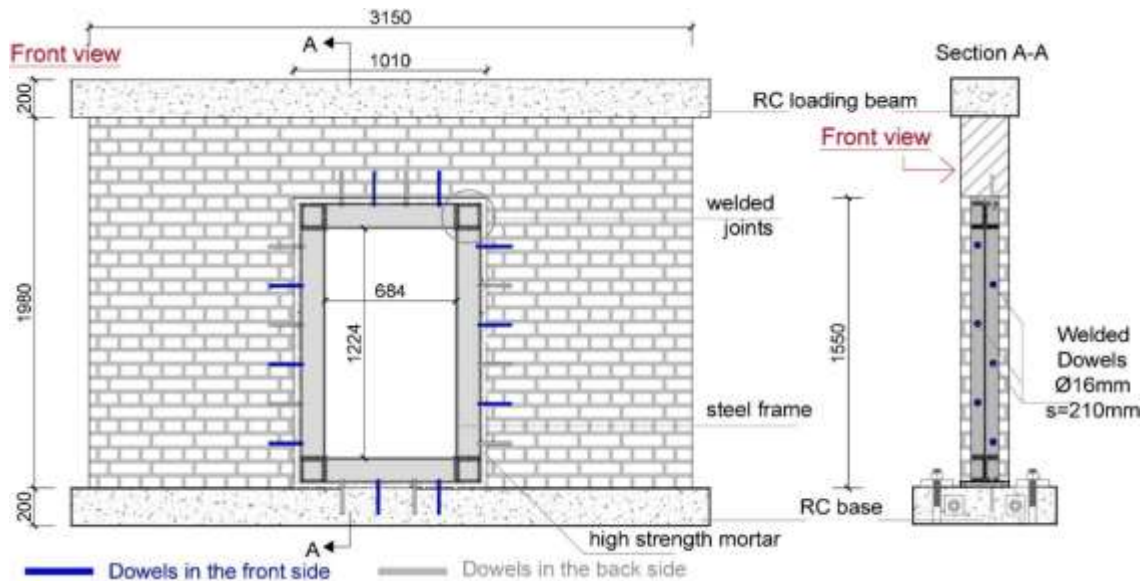


Figure I 20. steel ring-frame strengthening technique

I.7.2.1.3 The reinforced core technique

Is a strengthening method for masonry walls that involves adding vertical and/or horizontal reinforced concrete or steel columns within the core of the wall. This technique can be used to increase the load-carrying capacity of the wall and enhance its resistance to lateral loads, such as wind or seismic forces. To implement the reinforced core technique, vertical or horizontal holes are drilled into the masonry wall at regular intervals, and then reinforcing bars or steel columns are inserted into the holes and anchored into the surrounding masonry with grout or epoxy. The columns or bars are then connected at the top and bottom with steel plates or beams to create a rigid framework that reinforces the wall.

The reinforced core technique can be particularly effective in increasing the shear capacity of masonry walls, which is important in seismic design. This technique can also help mitigate the effects of cracking or spalling in the masonry by redistributing the load and reducing the stresses in the wall.

It's important to note that the reinforced core technique should only be implemented by a qualified contractor or structural engineer who has experience with this method. The proper design and installation of the reinforcement elements are critical to ensure the effectiveness and safety of the technique.

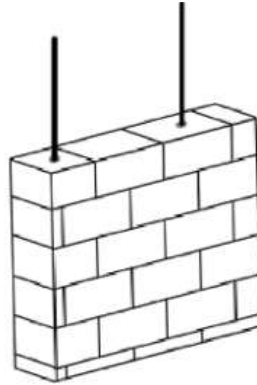


Figure I 21. The reinforced core technique

I.7.2.1.4 Tie rod strengthening

Is a type of structural element that is commonly used to provide lateral stability and support to masonry walls. It is essentially a steel rod or bar that is anchored into the masonry at both ends, and it is designed to resist tensile forces that can cause the wall to bow or bulge outward.

Tie rods are often used in pairs, with one rod running horizontally near the top of the wall and the other running diagonally from the top of the wall to a point near the base. The rods are usually connected to steel plates or anchors that are embedded into the masonry at each end, and they are tightened to a specified tension to provide the necessary support and stability to the wall.

The use of tie rods is particularly important in areas with high wind or seismic activity, as it can help to prevent masonry walls from collapsing or buckling under lateral loads. Tie rods can also be used to repair existing masonry walls that have become unstable or damaged over time.



Figure I 22. tie bars made of iron tension members

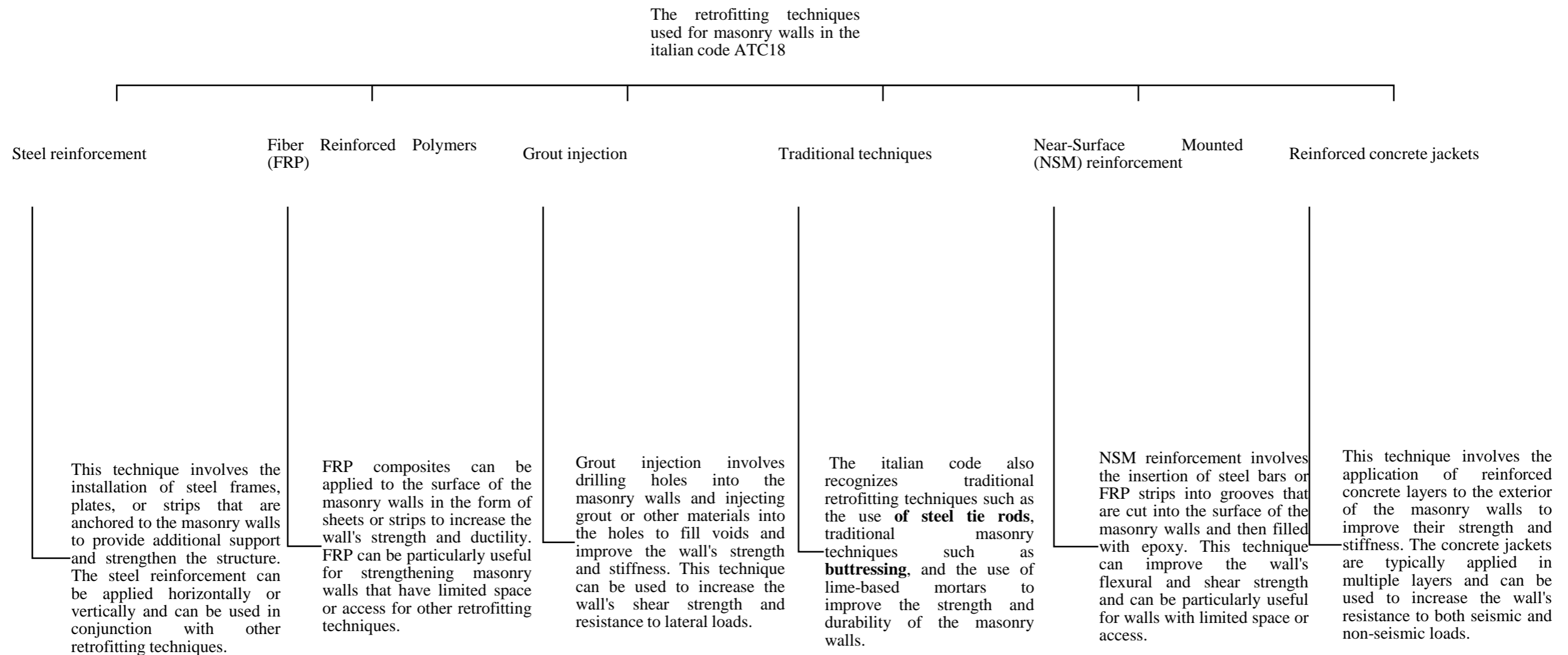


Figure I 23. the retrofitting techniques

I.8 CONCLUSION

In chapter 1 of the masonry bibliographic research, various aspects related to material properties and the assembly of masonry were discussed. The chapter covered topics such as the properties of masonry units and mortar, as well as the mechanical deterioration of masonry due to external and internal factors. Additionally, and we explored the estimation of mechanical properties of masonry, focusing on the italian code ntc18.

Moving forward, also we delved into masonry building behaviors, specifically emphasizing the domain of vulnerability modeling and seismic behavior mechanisms. The chapter touched upon the seismic analysis technique known as pushover analysis, providing an explanation for its utilization in the field. Furthermore, and introduced the concept of strengthening masonry structures, including techniques such as surface treatment and external reinforcement.

By investigating these diverse aspects, chapter 1 laid the foundation for a comprehensive understanding of masonry, enabling further exploration and analysis in subsequent chapters. The acquired knowledge will prove invaluable in comprehending the behavior and performance of masonry structures, ultimately contributing to the advancement of research and practices in this field.

CHAPTER II

TREMURI

MODELLING

II.1 INTRODUCTION:

3muri program is intended for nonlinear, pushover, and static analysis of masonry and mixed-material structures. 3muri employs a novel calculation approach (equivalent framework method "EFM") that can offer more information on the structure's real behaviour in terms of seismic stresses. The approach entails dividing the entire structure into macro-elements in order to determine the equivalent frame. 3muri provides a drawing area for structure insertion, an interface for selecting the calculation model and its answers, and a post processor for presenting the findings by showing the evolution of the building's state. During the push analysis, a calculation report is generated.

The reference seismic code is: seismic: Eurocode 8, and static: Eurocode 6

The program 3muri is a software created to execute the following analysis on masonry buildings:

- Non-linear static seismic analysis
- Analysis of vertical loads
- Kinematic analysis of masonry elements
- Local verification of structural and non-structural elements
- Management tool for retrofits on the structure

II.2 MACRO-ELEMENT MODELLING:

Micro-scale models and macro-scale models can be used to categorize the precise structural models utilized in simulation-based methodologies (calderini et al., 2009). The structure is discretized into finite elements in the micro-scale models, while the material level constitutive models are inelastic. Masonry piers and spandrels are modelled with force-deformation relationships at the structural member level in the macro-scale models, which discretize the structure into an equivalent frame model with main structural elements. The usage of micro-scale models is mostly restricted to the prediction of the behaviour of specific structural components (such as piers or spandrels) and the validation of the structural level accuracy of the macro-models due to their large computational complexity and expertise requirements.

3muri program is intended for nonlinear, pushover, and static analysis of masonry and mixed-material structures. 3muri employs a novel calculation approach (equivalent framework method "EFM") that can offer more information on the structure's real behaviour in terms of seismic stresses. The approach entails dividing the entire structure into macro elements in order to determine the equivalent frame. 3muri

provides a drawing area for structure insertion, an interface for selecting the calculation model and its answers, and a post processor for presenting the findings by showing the evolution of the building's state. During the push analysis, a calculation report is generated.

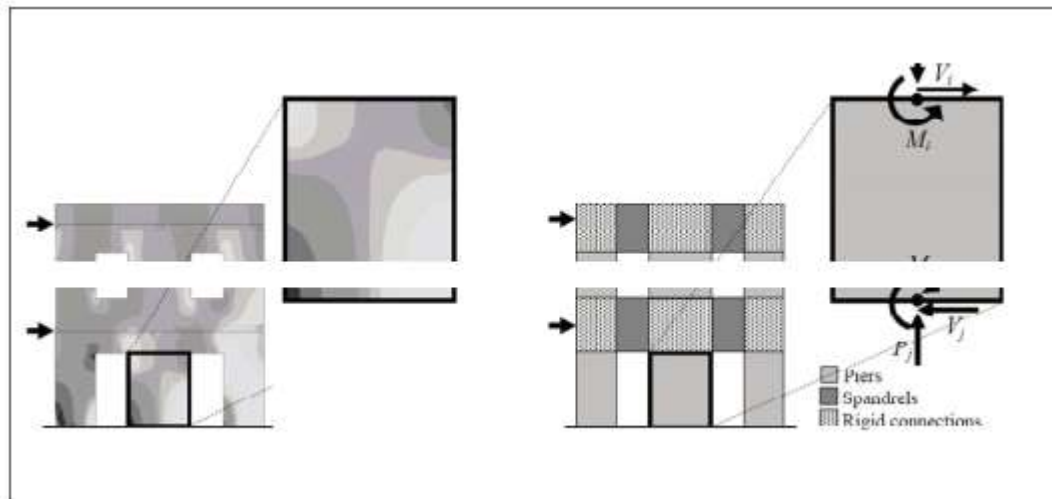


Figure II.1. Mef AND THE EFM

II.2.1 Macro-element approach:

Macro-element modelling is a numerical modelling approach in structural mechanics that uses enormous components to represent the behaviour of a complicated system. This method divides the structure into many macro-components, which are huge elements that comprise a major portion of the structure. Each macro-element is represented by a mixture of many sorts of simpler finite elements.

Macro-element modelling provides various benefits over other numerical modelling approaches, including a large reduction in the number of elements required to describe a particular structure, resulting in a significant reduction in computing time. Furthermore, for complicated structures such as reinforced concrete structures or complex metal structures, macro-element modelling can produce more precise and dependable results.

The design of a non-linear macroelement, representing a complete masonry panel, allows for the representation of a cinematic model describing deformation and damage mechanisms with a limited number of degrees of freedom. The macroelement proposed by gambarotta and lagomarsino is made up of three parts, which are depicted in the figure below. The two border sections 1 and 3, whose height is infinite, show a concentration of deformations caused by axial forces and flexion momentums. While at the middle 2 of height h , the concentrated effects are due to shear transversal forces.

To define the whole kinematic model of the macroelement, the three degrees of freedom of the nodes i and j corresponding to the interface of 1 and 3 must be considered. The following approximations can be used to simplify the kinematics of the following model:

$$U_1 = u_i \text{ et } u_2 = u_j \quad \text{because the ends parts are infinitely stiff in shear.}$$

$$W_1 = w_2 = \delta \text{ et } \varphi_1 = \varphi_2 = \Phi \quad \text{because the core section has infinite axial and bending rigidity.}$$

With w and u the axial and transverse displacements; φ rotation; δ and Φ represent the axial displacement and rotation of the central body respectively.

$$\text{A vector with eight degrees of freedom describes the kinematics; } A_T = \{u_i \ w_i \ \varphi_i \ u_j \ w_j \ \varphi_j \ \delta \ \Phi\}$$

Which is set for each macroelement. Because the brick wall has a relatively low tensile strength, it is also important to represent the element overturning. A mono-lateral elastic contact between surfaces 1 and 3 is used to describe the overturning mechanism (Lagomarsino et al., 2008b).

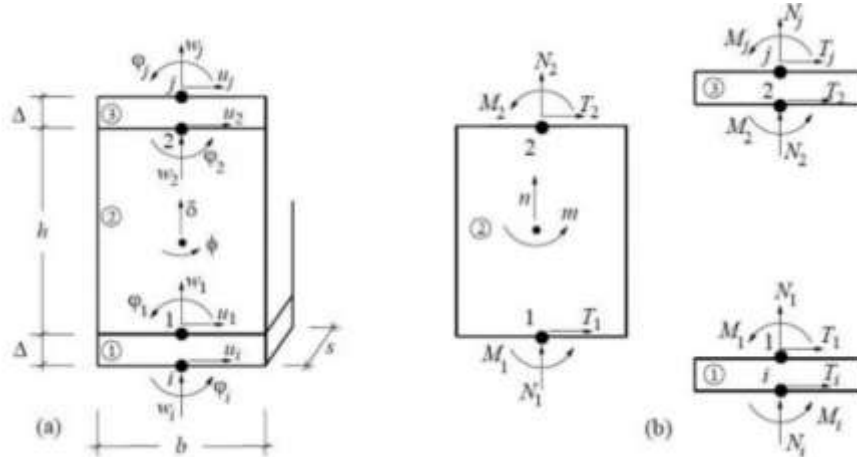


Figure II.2. Shema of macroelements taken from Lagomarsino et al (2008b)

II.2.2 Equivalent frame

The calculation code utilizes the EFM by macro elements approach to represent the masonry structure. This method enhances our understanding of seismic behaviour by dividing the structure into spandrels and piers. Each spandrel and pier are modelled as a unidirectional element, featuring rigid sections at the extremities and a deformable middle section to capture nonlinear characteristics. This approach

allows for a detailed analysis of the structural response and provides insights into the important nonlinear aspects of the masonry system.

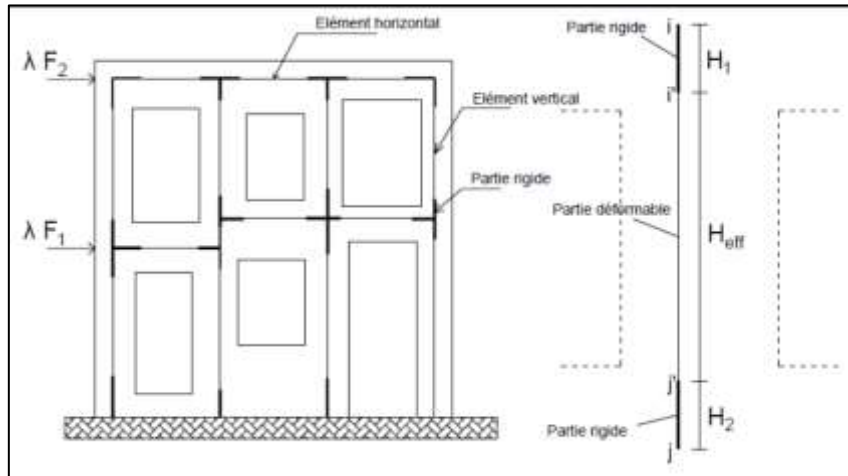


Figure II 3. Structure equivalent frame identification

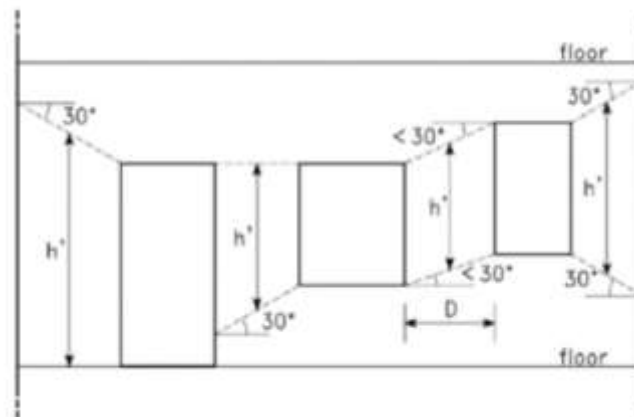


Figure II 4. Illustration of effective height identification method Taken from Dolce (1991)

$$H_{Eff} = H' + \left(\frac{1}{3}\right) \frac{D(\bar{H} - H')}{H'}$$

Definition of the effective height of the masonry walls (dolce, 1989).

Ultimate displacement of the reinforcement frame:

The yield and ultimate displacements of the frames are calculated using the expressions of the relative rotation capacity reported in circular no. 7 of 21 January 2019 (expressions (c8.7.2.7a) and (c8.7.2.1) respectively).

Strength of the reinforcement frame:

The resistance of the frame in the horizontal direction t is calculated using the relation:

$$T = 2M/h$$

In which:

M is the resistance to limb

H is the height of the frame

It is verified that this resistance does not exceed the maximum shear strength assessed according to the indications of the ministerial decree of 17.1.2018 (expression (4.1.29)).

Rigid elements at the ends, also known as rigid nodes, are intact components that convey vertical loads and inertial forces to the core section. The irregularity of the openings occasionally causes uncertainty in defining the effective height of the trumeau. Dolce (1991) provided a technique for determining the effective height that assumes a maximum inclination of 30° of the cracks from the corners of the openings, ensuring a steady rise in the height of the exterior pillars with regard to the dimensions of the opening. This approach was utilized in the creation of 3muri software; it handles the problem of irregular apertures as well as determining the effective height of an exterior pillar.

II.2.3 Structural element behaviour

After modelling the walls in an equivalent frame, it is essential to examine the behaviour of each element in order to derive the overall reaction of the structure. Masonry is the assembling of mortar and bricks, which results in a non-linear behaviour due to the intrinsic properties of the materials. The 3muri computation program employs a kind of basic and non-linear modelling of the elements to arrive at a result in terms of stiffness, resistance, and final displacement capacity.

To get reliable results of the structure's behaviour, as predicted by the capacity curve (force-displacement), it is necessary to consider the various ways of probable rupture of the macro-elements; there are two types of rupture for the trumeaux:

- 1) inflectional, which takes the shape of swinging rupture and.
- 2) shear, which manifests as sliding failure and diagonal tensile failure.

These forms of behaviour are fundamentally revealed in the center section by modelling the wall using macro-elements. Because of the multiple stress states that operate on them, a wall made of macro-elements might exhibit distinct failure behaviours for each partition. The axial force applied to a trumeau is important since it enables the collapse process to be identified. During the push analysis, an increase in horizontal load causes a redistribution phenomenon. As a result, depending on the progress of the nonlinear static analysis, the vertical load might assume different values for each trumeau. The maximum displacement must therefore be determined since beyond this value, the shear wall loses its resistance.

The identification of a macroelements failure process is thus dependent on the geometry of the panel, the intensity of the axial stress, and the mechanical properties of the material utilized. It should be emphasized that the forces only act at the node level. The shear and bending stiffness determine the elastic branch (the inclined section of the capacity curve). It is derived mostly from the shear's geometric and mechanical characteristics .

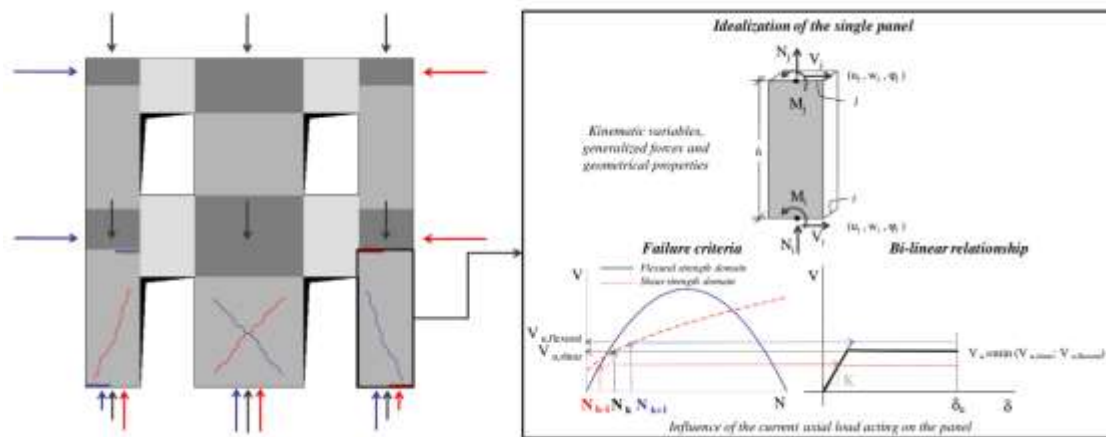


Figure II.5. Identification of failure modes for a microelement Taken from (Sergio Lagomarsino, 2013)

II.2.4 The structure's three-dimensional assembly

According to (Sergio Lagomarsino, 2013), some assumptions about the behaviour of the structure and the earthquake must be introduced into 3d modelling of masonry structures. Only when the structural parts are appropriately integrated in such a manner that the structure acts like a box can a complete reaction to earthquakes be achieved. In order to construct the many structural parts of a structure, a global coordinate system must be defined. The walls are defined by coordinates and the angle between the x axis and the plane of the wall. The equivalent framework approach was used to represent the walls. Lintels and macroelements are the two main types of elements.

A global cartesian coordinate system (x, y, z) is defined in order to create a 3d model. The coordinates of one point and the angle established with the global x axis are used to identify the wall vertical planes. In this manner, the walls may be represented as plane frames in the local coordinate system, while internal nodes can remain 2-dimensional nodes with 3 degrees of freedom. Three-dimensional nodes are utilized in corners and where two or more walls cross. They have 5 degrees of freedom (D.O.F.) In the global coordinate system $(u_x, u_y, u_z, \theta_x, \theta_y)$. Due to the membranous behaviour used for walls and floors, the rotating degree of freedom around the vertical z axis may be neglected.

These nodes may be created by assembling 2d stiff nodes acting in each wall plane and projecting the local D.O.F. Along global axes. The assemblage is then obtained by condensing the degrees of freedom

of two 2-dimensional nodes and assuming full coupling among the connected walls. This technique is highly effective for reducing the total number of D.O.F. And performing nonlinear analyses with a reasonable processing effort, even in the case of big and complicated building models.

Because the 2d nodes have no degrees of freedom along the orthogonal direction to the wall plane, the nodal mass component related to out-of-plane degrees of freedom is shared with the corresponding degrees of freedom of the two nearest 3d nodes of the same wall and floor.

This technique enabled the adoption of simplification hypotheses in the development of static studies with three acceleration components along the three primary directions and 3d dynamic analyses with three simultaneous input components.

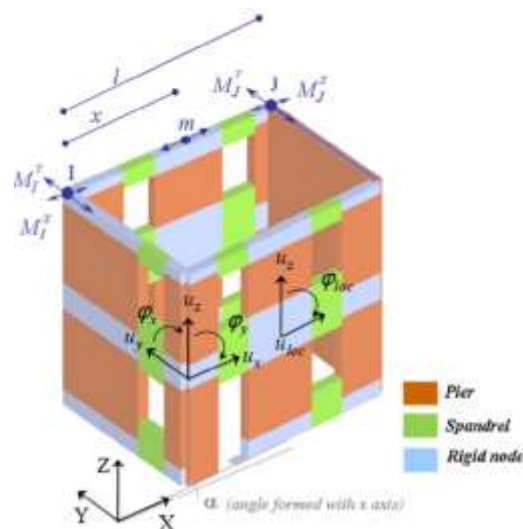


Figure II.6. 3D assembling of masonry walls: classification of 3D and 2D rigid nodes and out-of-plane mass sharing. (Sergio Lagomarsino, 2013)

II.3 MODELLING MASONRY PIERS AND SPANDRELS

A non-linear beam element model has been implemented in 3muri for modelling masonry piers and spandrels. Its main features are:

- Initial stiffness given by elastic (cracked) properties;

- Bilinear behaviour with maximum values of shear and bending moment as calculated in ultimate limit states;

- Redistribution of the internal forces according to the element equilibrium;

- Detection of damage limit states considering global and local damage parameters;

Stiffness degradation in plastic range;

Ductility control by defining maximum drift (δ_u). The maximum drift can be different for shear or axial bending. The regulations provide for different limit values depending on the failure type.

$$\delta_m^{DI} = \frac{\Delta_m}{h_m} = \delta_u$$

Element expiration at ultimate drift without interruption of global analysis.

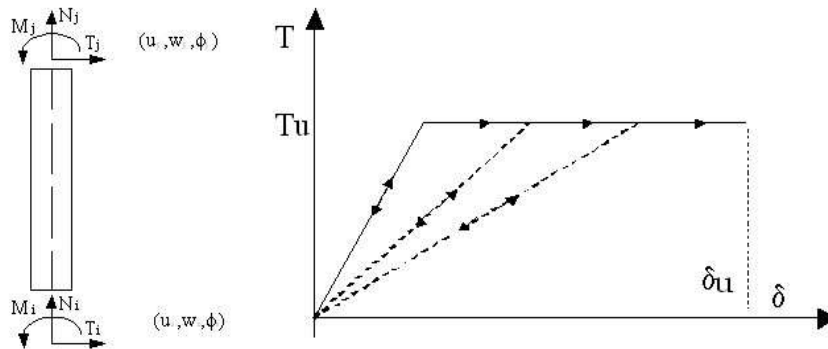


Figure II 7. Element BEHAVIOUR CURVE

Non-linear beam degrading behaviour

The elastic behaviour of this element is given by:

$$\begin{pmatrix} T_i \\ N_i \\ M_i \\ T_j \\ N_j \\ M_j \end{pmatrix} = \begin{bmatrix} \frac{12EJ}{H^3(1+\psi)} & 0 & -\frac{6EJ}{H^2(1+\psi)} & -\frac{12EJ}{H^3(1+\psi)} & 0 & -\frac{6EJ}{H^2(1+\psi)} \\ 0 & \frac{EA}{H} & 0 & 0 & -\frac{EA}{H} & 0 \\ -\frac{6EJ}{H^2(1+\psi)} & 0 & \frac{EJ(4+\psi)}{H(1+\psi)} & \frac{6EJ}{H^2(1+\psi)} & 0 & \frac{EJ(2+\psi)}{H(1+\psi)} \\ -\frac{12EJ}{H^3(1+\psi)} & 0 & \frac{6EJ}{H^2(1+\psi)} & \frac{12EJ}{H^3(1+\psi)} & 0 & \frac{6EJ}{H^2(1+\psi)} \\ 0 & -\frac{EA}{H} & 0 & 0 & \frac{EA}{H} & 0 \\ -\frac{6EJ}{H^2(1+\psi)} & 0 & \frac{EJ(4+\psi)}{H(1+\psi)} & \frac{6EJ}{H^2(1+\psi)} & 0 & \frac{EJ(2+\psi)}{H(1+\psi)} \end{bmatrix} = \begin{pmatrix} U_i \\ W_i \\ \Phi_i \\ U_j \\ W_j \\ \Phi_j \end{pmatrix}$$

Where

$$\psi = 24(1+\nu)X\left(\frac{H}{H}\right)^2 = 24\left(1 + \frac{E-2G}{2G}\right)1.2\frac{B^2}{12H^2} = 1.2\frac{B^2}{12H^2}$$

The nonlinear behaviour is activated when one of the nodal generalized forces reaches its maximum value estimated according to minimum of the following strength criteria: flexural-rocking, shear-sliding or diagonal shear cracking.

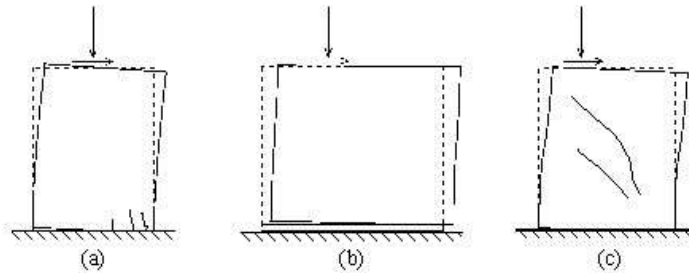


Figure 8. different types of failures (Raffaello, 2012)

Masonry in-plane failure modes: flexural-rocking (a), shear-sliding (b) e diagonal-cracking shear (c) (magenes et al., 2000)

II.4 STRENGTH AND FAILURE CRITERIA FOR URM PANELS IMPLEMENTED IN TREMURI PROGRAM

II.4.1 The failure modes

II.4.1.1 Bending ultimate moment

The resistance to compression bending can be evaluated by a parabolic curve which relates the normal stress and the ultimate moment, according to the hypothesis of material with no tensile strength. The ultimate bending moment is defined as:

$$M_U = \frac{L^2 T \Sigma_0}{2} \left(1 - \frac{\Sigma_0}{0.85 F_M} \right) = \frac{Nl}{2} \left(1 - \frac{N}{N_U} \right)$$

Where:

-L is the length of the panel,

-T is the thickness,

-\$\Sigma_0\$ is the average compression tension

-N is the axial compressive action (assumed positive in compression)

-Nu is the maximum axial compressive action of the panel and it is equal to 0.85 fm l t

- f_m is the average resistance in compression of the masonry.

This approach is based on a no-tension material where a non-linear reallocation of the stress is performed (rectangular stress-block with factor = 0.85)

In existing building, the average resistance f_m is to be divided by the “confidence factor” f_c according to the structural knowledge level.

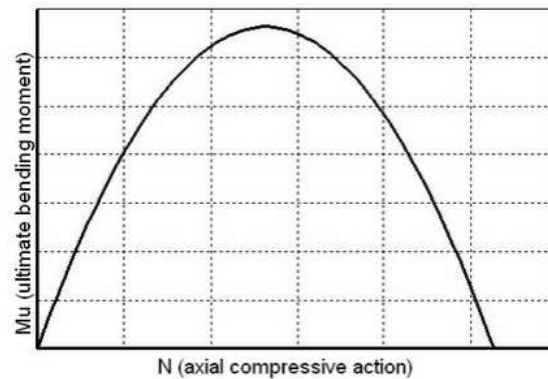


Figure II 9. Strength criterion in bending-rocking

II.4.1.2 Shear turnšek and cačovic criteria

According to Italian code, only for existing building, the shear failure can be computed according to turnšek and cačovic criterion; the ultimate shear is defined as:

$$V_u = l t \frac{1.5 T_0}{B} \sqrt{1 + \frac{\Sigma_0}{1.5 T_0}} = l t \frac{F_T}{B} \sqrt{1 + \frac{\Sigma_0}{F_T}} = l t \frac{1.5 T_0}{B} \sqrt{1 + \frac{N}{1.5 T_0 l t}}$$

Where f_t and τ_0 are the design value of tension resistance in diagonal cracking of masonry and its shear value, b is a coefficient defined according to the ratio of height and length of the wall:

$$B = \begin{cases} 1.5 & \frac{H}{L} > 1.5 \\ \frac{H}{L} & 1 \leq \frac{H}{L} \leq 1.5 \\ 1 & \frac{H}{L} < 1 \end{cases}$$

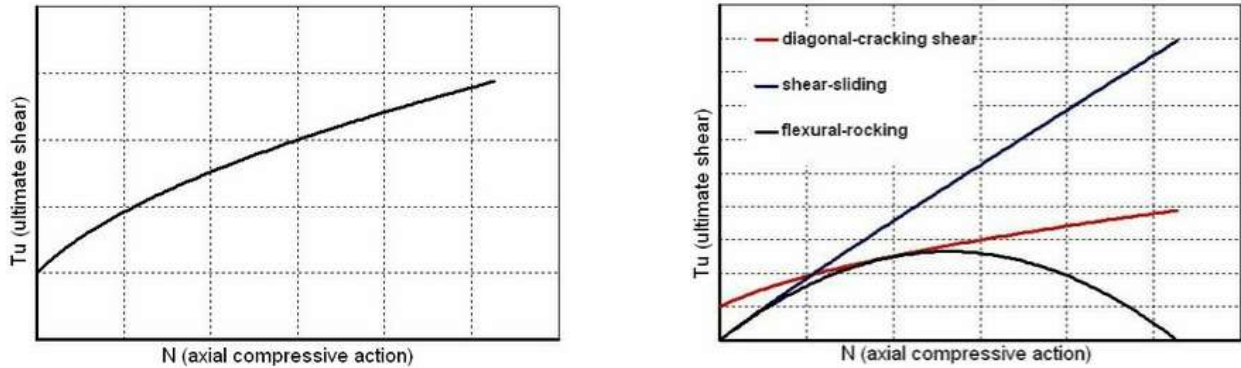


Figure ii 10. Turnšek and cačovic shear strength and strength criteria comparison

II.4.2 Strength criteria

Table ii 1. Strength criteria for urm panels implemented in tremuri program (Sergio Lagomarsino, 2013)

| Failure mode and element type | | Strength domain | Note |
|-------------------------------|-------------------|---|--|
| Rocking/crushing | Piers | $M_U = \frac{Nl}{2} \left(1 - \frac{N}{0.85F_U Lt} \right)$ | <p>F_u masonry compressive strength, l length of section, t thickness</p> <p>$H'p$ is assumed as the maximum value between the axial load n acting on spandrel and hp. Hp is the minimum value between the tensile strength of elements coupled to the spandrel (such as r.c. Beam or tie-rod) and $0.4f_{hu}dt$, where f_{hu} is the compression strength of masonry in horizontal direction, the limit domain is obtained by assuming an elasto-perfectly plastic constitutive law with limited ductility both in tension (ut) and compression (uc) and an equivalent tensile strength for spandrel f_{tu} (f_{bt} tensile strength of bricks; and c friction coefficient and cohesion of mortar joint, respectively; ϕ interlocking parameter; σ_s entity of compressive stresses acting at the end-sections of the spandrel)</p> <p>Coulomb criterion with: l' length of compressed part of cross section. A limit value ($v_{u, blocks}$) is imposed to take into account in approximate way the failure modes of blocks, h height</p> |
| | Spandrels | $M_U = \frac{Dh'p}{2} \left[1 - \frac{H'P}{0.85F_{Hu}Dt} \right]$ $M_u = f(N, \frac{F_{Tu}}{F_{Hu}} U_c, U_t)$ $F_{Tu} = \min \left(\frac{F_{Bt}}{2}; c + U\Sigma_S \Phi \right)$ | |
| Bed joint sliding | Piers | $V_{U,bjs} = L'Tc + UN \leq V_{U,blocks}$ | |
| | Spandrels | $V_U = htc$ | |
| Shear | Diagonal cracking | Piers / spandrels | $V_{U,dc,1} = lt \frac{1.5T_0}{B} \sqrt{1 + \left(\frac{1}{1.5T_0 Lt} \right)}$ $V_{U,dc,2} = \frac{1}{B} (Lt\hat{c} + \hat{u}n) \leq V_{U,block}$ |

| | | | | |
|--|--|--|--|--|
| | | | | <p>of spandrel transversal section (assumed only in case of a strut-and-tie mechanism may develop)</p> <p>τ_0 masonry shear strength, b stress distribution factor as function of slenderness</p> <p>Coulomb-type criterion with: \hat{u} and \hat{c} equivalent cohesion and friction parameters, related to the interlocking due to mortar head and bed joints, (with $b = 1$). The introduction of b, is implicitly justified by some comments on the shear stress distribution; a similar corrective factor is proposed</p> |
|--|--|--|--|--|

The calculation procedure is based on the comparison between the as installed and the as designed (introduction of a new opening).

The expression "as installed" means the schematization of the entire wall before the opening is made.

The expression "as designed" means the schematization of the entire wall after the opening has been made.

The comparison is made with respect to the variations of:

- resistance of the wall system

- Stiffness of the contained wall system (at the regulatory level there is no limit to this variation, alternative technical documentation suggests $\pm 15\%$)

- Deformation work, representative of the overall behaviour of the wall

The identification of the stiffness, strength and deformation work of the wall is carried out by calculating the contribution of the individual elements.

The mechanical characteristics of the individual elements can be calculated with the following formulations:

Table II 2. The MECHANICAL CHARACTERISTICS OF STEEL FRAMES IMPLEMENTED IN TREMURI PROGRAM

| | Strength domain | Note |
|----------------------------|---|--|
| Stiffness | $K_T = \frac{12e j}{H^3}$ | E: elastic modulus of the upright of the steel frame J, w: modulus of inertia and modulus of resistance H: height of the upright |
| Resistance | $V_T = \frac{2F_{Yk}W}{\Gamma_M H}$ | |
| Elastic limit displacement | $D_{Y, \text{ telaio}} = \frac{V_{\text{Telaio}}}{K_{\text{Telaio}}}$ | |

Table II 3. The MECHANICAL CHARACTERISTICS OF WALL PANEL IMPLEMENTED IN TREMURI PROGRAM

| | Strength domain | Note |
|--|--|---|
| Stiffness | $K_M = \frac{G l t}{1.2 h} \cdot \frac{1}{1 + \left(\left(\frac{1}{1.2} \right) \frac{G}{E} \left(\frac{H}{L} \right)^2 \right)}$ | E, g: elastic modulus H, l, t: height, length and thickness of the panel |
| Shear resistance | $V_M = l t \frac{Q \cdot 5T_0}{B} \cdot \sqrt{1 + \frac{\Sigma_0}{1.5T_0}}$ | |
| Axial bending resistance | $D_{Mpf} = \frac{P t \Sigma_0}{H} \left(1 - \frac{\Sigma_0}{0.85 \cdot F_M} \right)$ | |
| Elastic limit displacement assuming $v_t = \min(v_{mt}, v_{mpf})$ | $D_Y + V_T / K_M$ | |
| Ultimate displacement of a wall panel that is in crisis due to shear | $D_U = 0.005h$ | |
| Ultimate displacement of a wall panel that is in crisis due to axial bending | $D_U = 0.01 h$ | |

II.5 WALL MODELLING

Dividing the wall into vertical areas which correspond to the various levels, and noting the location of the openings, the portions of masonry, masonry piers, and spandrel beams, where deformability and damage are concentrated, can be determined. This can be verified by observing the damage caused by real earthquakes, and with experimental and numerical simulations. These areas are modelled with finite two-dimensional macro-elements, which represent masonry walls, with two nodes and three degrees of liberty per node (u_x , u_z , rot_y) and two additional internal degrees of liberty.

The resistant portions of the wall are considered as rigid two-dimensional nodes with finite dimensions, to which the macro-elements are connected. The macro-elements transfer the actions along the level's three degrees of liberty, at each incident node. In the description of each single wall, the nodes are identified by a pair of coordinates (x , z) in the level of the wall. The height, z , corresponds to that of the horizontal structures. The degrees of liberty are solely u_x , u_z , and rot_y (for two-dimensional nodes).

Thanks to the division of elements into nodes, the wall model becomes completely comparable to that of a frame plan.

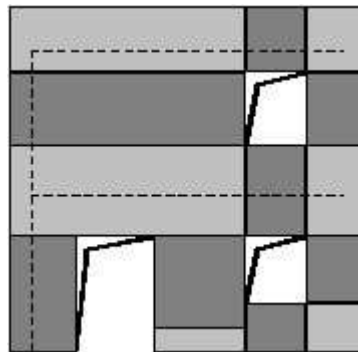


Figure II 11. The DIVISIONS OF WALL FRAME

During assembly of the wall, the possible eccentricities between the model nodes and the ends of the macro-elements are considered. Given the axes that are the center of mass for the elements, these cannot coincide with the node. Hence in the rigid blocks, it is possible that eccentricity may be found between the model node and that of the flexible element.

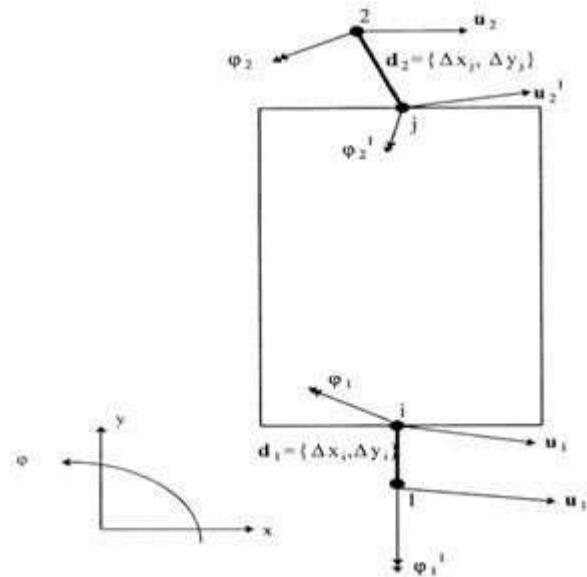


Figure II 12. Wall MODEL NODES AND THE ECCENTRICITIES

Structural modelling also requires the possibility of inserting beams, (elastic prisms with constant sections), identified in the level by the position of the two edge nodes. Once the length (prevalent dimension), the area, the inertial moment, and the elastic module are known, it is possible to reconstruct the rigidity matrix, applying elastic joint rules, and assuming that they remain indefinitely in the elastic field, the normal formulation of elastic joints are applied (petrini, et al., 2004; corradi dell'acqua, 1992).

In addition to the presence of actual beams (architraves or r.c. Tie beams), the model assumes the presence of tie rod structures. These metallic structures completely lack bending rigidity and lose all effectiveness if they are compressed. This detail adds an additional nonlinear element to the model. The total rigidity of the system must decrease if a stretched tie rod is compressed, and it must increase in the opposite case.

Another characteristic of these elements is the possibility to assign an initial deformation ϵ_0 , which determines a force $f_c = e a \epsilon_0$. From a static point of view, once the overall vector of the precompression forces f_c is determined, it is enough to apply it to the structure as if it were an external load.

The rigidity matrix for elements without bending rigidity is easily found by eliminating all the limits that contain j from the element matrix. To manage the non-linearity, all of the elastic contributions due to the tie rods must be kept distinct. At each step, it must be verified if the tie rod that previously was stretched is now compressed or vice versa. If the situation changes, the total rigidity matrix for the model must be corrected. (Raffaello, 2012)

II.6 SPATIAL MODELLING

In spatial modelling, the walls are resistant elements, with regards to vertical and horizontal loads. On the other hand, the horizontal structures (floors, vaults, ceilings) transfer their vertical loads to the walls and divide the horizontal actions onto the incident walls. In this way, the structure is modelled by assembly of the level structures: the walls and the horizontal structures, both lacking bending rigidity outside of the level.

The procedure for modelling macro-elements for masonry walls which receive forces from their own level was illustrated above. This instrument constitutes an important starting point for modelling of the overall behaviour, based on the behaviour of the walls on their level. In any case, extension of the procedure to three-dimensional modelling is not simple. The correct strategy is that of conserving the modelling of the walls on their level and assembling them with the horizontal structures, including those for which the membrane behaviour is modelled. In this way, the model of the structure takes on mass and rigidity on all of the three-dimensional degrees of liberty. At the same time, it locally takes into account the individual degrees of liberty of the levels (two-dimensional nodes).

In this way, an essential structural model is created, without adding the complication of computation of the response outside of the local level. This can of course be verified later. Once a single overall reference is established for the structural model, the local references are introduced for each wall. It is assumed that the walls rest on the vertical plane and they are found in the plan of the generic wall i through the coordinates of a point, the origin of the local reference $o_i (x_i, y_i, z_i)$, with respect to an overall cartesian reference system (x, y, z) .

The angle i is computed with respect to axis x .

In this way, the local reference system for the wall is unambiguously defined and the macroelement modelling can take place with the same modality used for the levels.

Macro-elements, such as beams and tie rods, maintain the behaviour of the level and do not require reformulation.

Connection nodes, belonging to a single wall, maintain their degrees of liberty at the local reference level. Nodes that belong to more than one wall (localized in the incidences of the walls) must have degrees of liberty in the overall reference (three-dimensional nodes). These nodes, due to the hypothesis that ignores the bending rigidity of the walls, do not need a rotational degree of liberty around the z axis, as they are not connected to any element able to provide local rotational rigidity limits. Three-dimensional rigid nodes, representing angle iron or hammer situations, are obtained as an assemblage of virtual two-dimensional rigid nodes identified in each of the incident walls. These have displacement components generalized using

five degrees of liberty: three displacement u_x , u_y and u_z . Two rotational φ_x and φ_y . The relationships between the five displacement and rotation components of the three-dimensional node and the three for the fictitious two-dimensional node, belonging to the single wall are given by:

$$\begin{cases} U = U_X \cos\theta + U_Y \sin\theta \\ \Omega = U_Z \\ \Phi = \Phi_X \sin\theta - \Phi_Y \cos\theta \end{cases}$$

In which u , w , and φ indicate the three displacement components according to the degrees of liberty found in the fictitious node that belongs to the generic wall facing the plan according to angle φ . Similarly, the forces applied to the three-dimensional nodes are displaced according to the directions identified by the middle level of the walls and then applied to the macro-elements in their level of resistance.

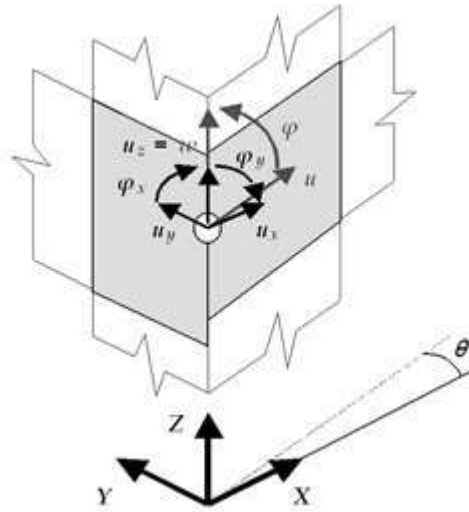


Figure II 13. Components DISPLACEMENTS ACCORDING TO DOF

The reactive forces transmitted by the macro-elements that belong to the individual walls to the fictitious two-dimensional nodes are carried over to the overall reference based on

$$\begin{cases} F_X = F_H^1 \cos\theta_1 + F_H^2 \cos\theta_2 \\ F_Y = F_H^1 \sin\theta_1 + F_H^2 \sin\theta_2 \\ F_Z = F_V^1 + F_V^2 \\ M_Y = -M^1 \cos\theta_1 - M^2 \cos\theta_2 \end{cases}$$

In which, as seen in the figure, the boundaries with apex 1 and 2 respectively make reference to the force limits corresponding with the virtual nodes identified in the walls 1 and 2 to which the three-dimensional node belongs.

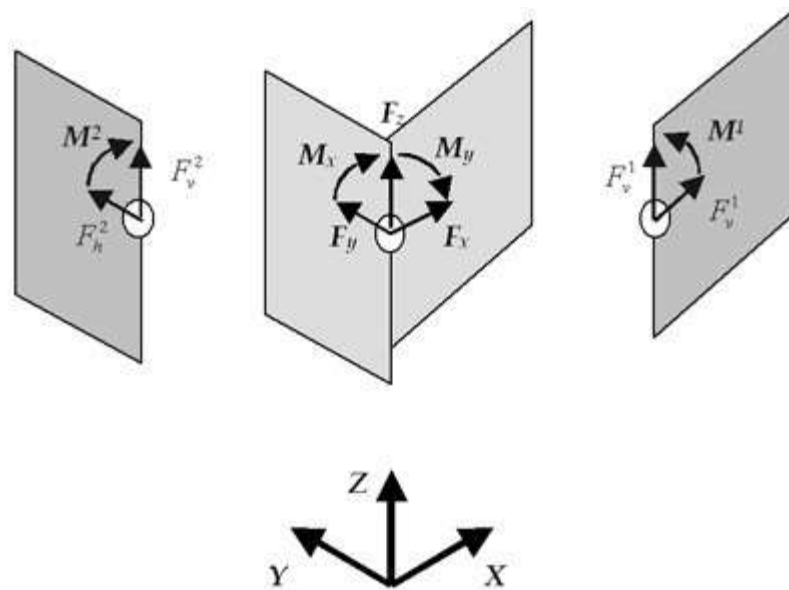


Figure II 14. The FORCES TRANSMITTED BY THE MACRO-ELEMENTS

In this way, modelling of the wall can take place on the level, recovering that described in the preceding chapter. The nodes that only belong to a single wall remain two-dimensional. They maintain only three degrees of liberty, rather than five.

The floors, modelled as finished orthotropic membrane three-node elements, with two degrees of liberty per node (displacements u_x and u_y), are identified with a warping direction, with respect to that characterized by an elastic module e_1 . E_2 is an elastic model with a direction perpendicular to the warping, while ν is the poisson coefficient and $g_{2,1}$ is the elasticity tangential model. E_1 and e_2 represent the degree of connection that the floor, thanks to the effects of the tie beams and tie rods, exercises on the element nodes on the level of the wall. $G_{2,1}$ represent the shear rigidity of the floor on its level and the division of the actions among the walls depends on this.

It is possible to position a floor element connecting it to the three-dimensional nodes. This is because the floor element functions principally to divide the horizontal actions between the various walls in proportion to their rigidity and its own. In this way it makes the model three-dimensional in a way that brings it close to the true structural performance.

The finished reference element to be considered is the level element, in a level state of tension, with three nodes.

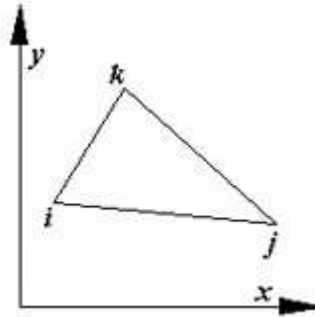


Figure II 15. The REFERENCE ELEMENT

The rigidity matrix involves the individual three-dimensional incidental nodes on the floor. The contribution of the vertical loads, self or borne, is attributed in terms of nodal mass added to all the nodes, including those with three degrees of freedom, that belong to the incident walls at the height of the level of the floor. This added mass is calculated based on the area of influence of each node, taking into account the warping direction of the floor. (Raffaello, 2012)

II.7 THE STRUCTURE AFTER MODELLING

The masonry structure was effectively modelled using the macro element method. Through successful meshing and division into equivalent frames, including spandrels and piers, the analysis captured the structure's behaviour accurately. This approach offers advantages in terms of efficiency and accuracy, providing valuable insights into the structural response and facilitating targeted evaluations for strengthening or rehabilitation purposes.

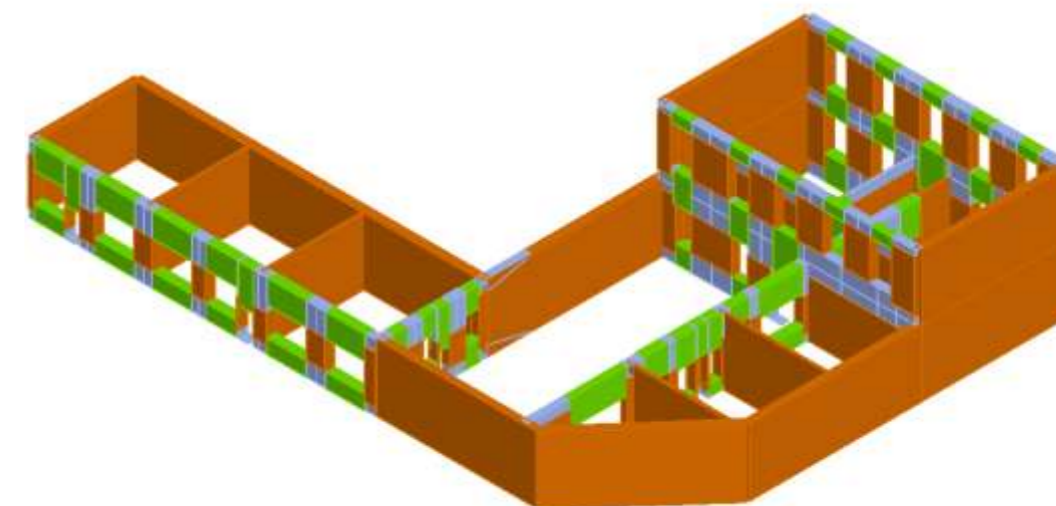
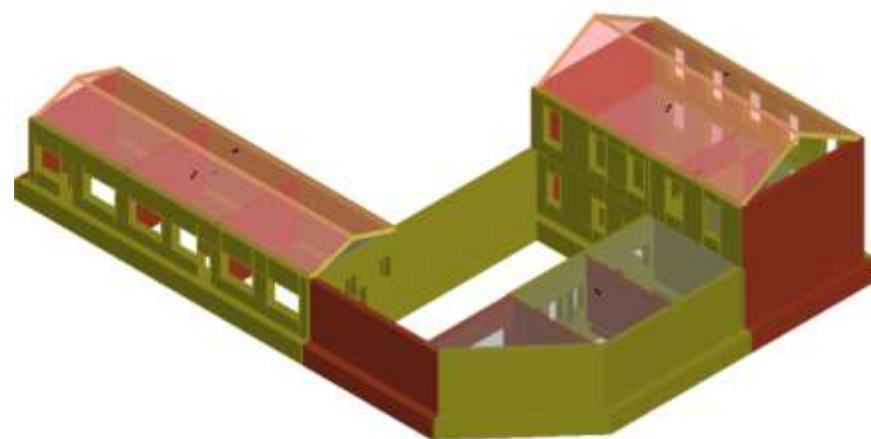
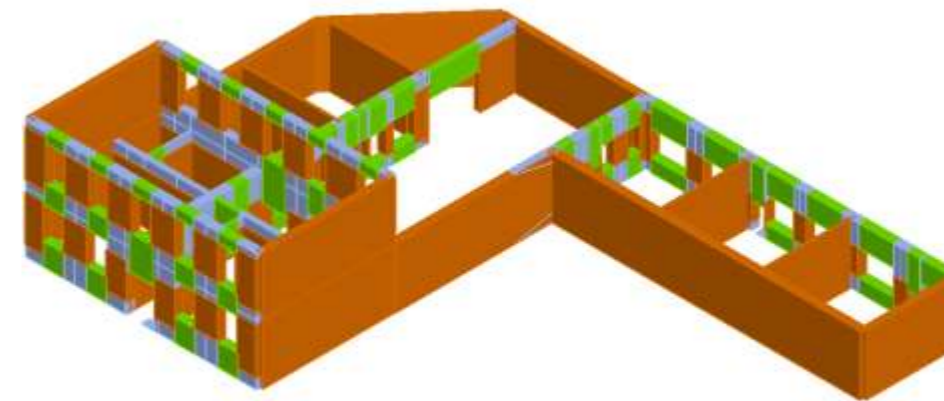
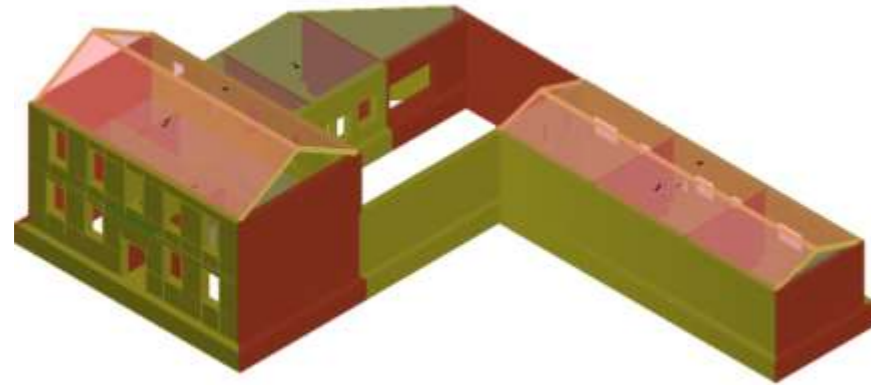


Figure II 16 3D VIEW OF THE BUILDING AFTER MODELLING AND THE MACROELEMENTS STRUCTURE MECH

II.8 CONCLUSION

Chapter II of the Masonry Bibliographic Research delves into tremuri modelling, focusing on different approaches and techniques. The chapter covers macro-element modelling, including the macro-element approach and the concept of an equivalent frame. It also explores the behaviour of structural elements and the three-dimensional assembly of masonry structures.

Further discusses the modelling of masonry piers, spandrels, and walls. It highlights the importance of considering spatial modelling to accurately represent the three-dimensional nature of masonry structures.

Additionally, addresses the strength and failure criteria for unreinforced masonry (URM) panels implemented in the Tremuri program. It examines various failure modes and strength criteria, providing insights into the structural behaviour of URM panels.

Overall, Chapter II provides valuable information and techniques for modelling tremuri, enabling researchers and practitioners to analyse and design masonry structures more effectively, particularly in seismic contexts. It offers advanced capabilities such as seismic analysis, pushover analysis, vulnerability assessment, and performance evaluation. With Tremuri, engineers can accurately model the behaviour of masonry buildings under seismic loads, assess their vulnerability to earthquakes, and evaluate their performance based on various criteria. The software provides visualizations and reporting features to effectively communicate analysis results. Overall, Tremuri is a valuable resource for engineers involved in the seismic assessment and design of masonry structures.

CHAPTER III CASE STUDY

III.1 INTRODUCTION

Annaba is a city in northeastern Algeria close to the Mediterranean Sea. The city has a long history, with human occupancy reaching back to ancient times. Annaba's beautiful masonry structures are one of its most noticeable attractions. Overall, Annaba's masonry structures reflect the city's rich history and cultural legacy. They serve as a reminder of the great workmanship and architectural brilliance of those who created them, and they continue to astonish and inspire visitors to the city.

Here are 10 outstanding examples of masonry architecture in Annaba:

- St. Augustine basilica - this great church, built in the late nineteenth century, combines Byzantine and Romanesque architectural elements. The façade of the basilica is ornamented with exquisite brickwork, while the inside features stunning vaulted ceilings and brilliant stained-glass windows.
- Palace of the Bey - built in the 18th century, this palace served as the residence of the local ruler. The building's exterior is clad in beautiful masonry and mixes French, Ottoman, and Islamic style features. The inside is lavishly adorned with ornate furniture and magnificent tilework.
- La Gare d'Annaba - built in the early twentieth century, this train station exhibits a unique combination of French and Islamic architectural elements. The façade of the station is distinguished by its red brickwork and ornate masonry.
- St. Jean Baptiste church - built in the early twentieth century, this church combines neo-Gothic and Romanesque architectural styles. The outside of the structure is clad in granite and has a big rose window and a high bell tower.
- Sidi Bou Merouane mosque - built in the 14th century, this mosque combines Andalusian, Moorish, and Ottoman architectural elements. The front is distinguished by beautiful brickwork, while the inside features magnificent tilework and decorative ornamentation.
- St. Augustine's college - built in the early twentieth century, this structure combines French and Islamic architectural elements. The outside of the building is distinguished by its red brickwork and exquisite masonry.
- St. Joseph's church - built in the early twentieth century, this church combines neo-Gothic and Romanesque architectural styles. The outside of the structure is clad in granite and has a high bell tower.
- The Khelifa Palace was built in the 18th century and served as the residence of the local governor. The exterior is clad in beautiful masonry and displays a blend of French, Ottoman, and Islamic style elements.

- Dar el hamra - this ancient edifice originates from the 18th century and was formerly the home of a wealthy merchant. The exterior of the building is adorned with elaborate masonry, while the inside is adorned with beautiful tilework.
- Governor's palace - built in the early twentieth century, this palace functioned as the local governor's house. The building's exterior is clad in elaborate masonry and shows a combination of french and islamic architectural elements.

These masonry buildings are only a small sample of the stunning architecture found throughout annaba. They serve as a tribute to the skill and inventiveness of the individuals who created them, as well as to the city's rich history and heritage of culture.

These structures exhibit a range of architectural styles, including byzantine, romanesque, gothic, and islamic, and are all examples of annaba's excellent masonry artistry.

III.2 STUDY CASE

III.2.1 Presentation of the assla hocine primary school

The elementary school "assela hocine" dates from the colonial era. It was erected in 1923 and is located in the city center, namely at the level of the anatole france- wheat market. It dates from the second phase of the colonial period, and it is the first secular, public school built on virgin ground within the second enclosure.



Figure III 1. main facade

III.2.2 Urban study

Although our intervention's field of action is confined to the building, it is critical to place it in its urban setting and define its interaction with its external environment in order to function within its boundaries.

III.2.2.1 Location and service of buildings

➤ **The situation in relation to the city:**

The project is located in the heart of downtown Annaba at the wheat market -place Anatole France.



Figure III 2. mass grounding plan

III.2.2.2 Immediate environment



Figure III 3. situation plan

III.2.3 Architectural study

The architectural analysis allows for the listing of existing spaces and their potential for use, the comparison of the surfaces offered with the program's demands, the understanding of the layout of the places and their operation, and the projection of the new image by comparing it to the previous appearance.

III.2.3.1 Limits and accessibility

- North side: the street zanine el arbi and the elementary school of the same name.
- South side: assela hocine and the elementary school for girls.
- East side: the street al kods and the place anatole france.
- West side: djemaa saci street and the civil protection.

III.2.3.2 Implantation

III.2.3.2.1 Siting types and structure dimensions

The elementary school is divided into three sections:

Table III 1 building block divisions

| Bloc | Descriptions | Heights |
|---------|---|---|
| Block 1 | (r+1) comprises the main entry hall access to the courtyard, the administration, the kitchen, the ground floor store, and a non-functional floor. | Ground floor height: 4.56 meters 1st story height: 9.1 meters Roof height: 11.96 meters |
| Block 2 | Represents two classrooms and the restrooms. The courtyard is represented by the unbuilt portion. | Ground floor height: 5.1 meters |
| Block 3 | Represents three separate classrooms. | Ground floor height: 4.26 meters Roof height: 6.27x37 meters |

III.2.3.2.2 Dimension in plan

- Total length along the axis (y -y): 36.70 m.
- Total width along the axis (x -x): 42.8 m.

III.2.3.2.3 Typology and plan

Dominant form: rectangular building (l form)

Table III 2 . Divisions dimensions and openings

| Space | Width (m) | Length (m) | Surface (m ²) | Height (m) | Openings |
|---------------------------|-----------|------------|---------------------------|------------|--|
| Class1 | 7.015 | 5.815 | 40.79 | 5.1 | (3.15*2) ;(1.45*3.41) |
| Class2 | 6.17 | 6.97 | 43 | 5.1 | (1.38*2.75) ;(0.82*2) ;(0.82*2) |
| Class3 | 8.38 | 7.57 | 63.43 | 4.26 | (1*1.85) ;(1*1.85) ;(0.65*2) ;(1*1.85) ;(2.8*2) ;(2.8*2) |
| Class4 | 7.85 | 7.335 | 57.579 | 4.26 | (2.8*2) ;(0.97*2) ;(2.14*2) |
| Class5 | 7.85 | 7.335 | 57.579 | 4.26 | (2.80*2) ;(0.97*2) ;(2.16*2) |
| 1st floor | 17.485 | 9.455 | 165.32 | 4.18 | 5 openings on each side (147*275) |
| Director's office | 5.89 | 7.355 | 43.32 | 4.56 | (1.5*2.5) |
| Director's office ancient | 7.345 | 6.117 | 44.92 | 4.56 | (1.5*2.5) |
| Store | 4.42 | 2.35 | 10.387 | 4.56 | (1*2.35) |
| Canteen | 2.49 | 2.35 | 5.85 | 4.56 | |
| Toilet | 1.18006d | 0.89 | 1.05 | 5.1 | (4*2.84) |
| Courtyard | 13.83 | 7.56 | 104.55 | | |
| Galleries | 19.38 | 10.345 | 200.486 | | |
| Entrance hall | 5.96 | 2.44 | 14.54 | 4.56 | |

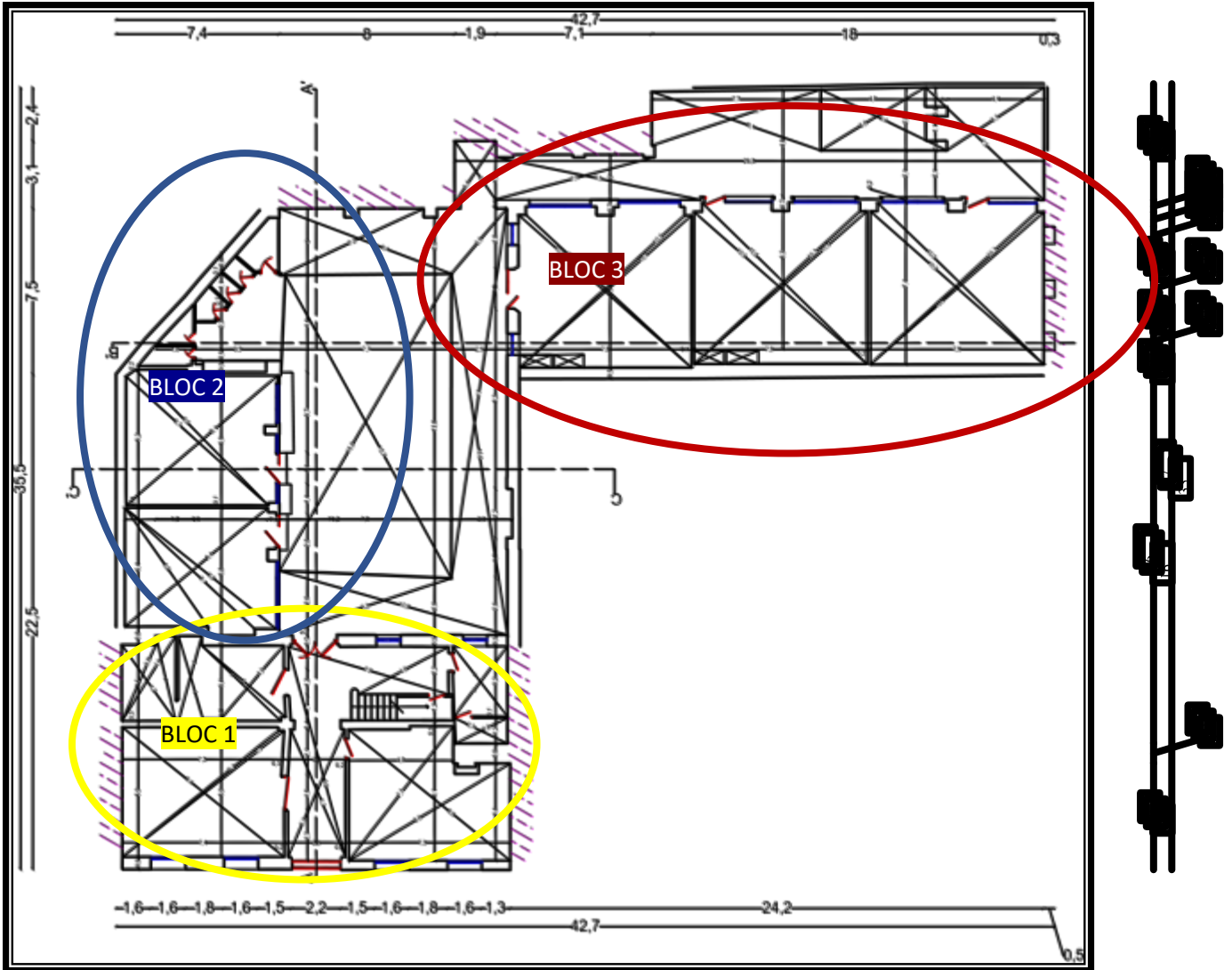


Figure III 4. ground floor plan and blocks divisions

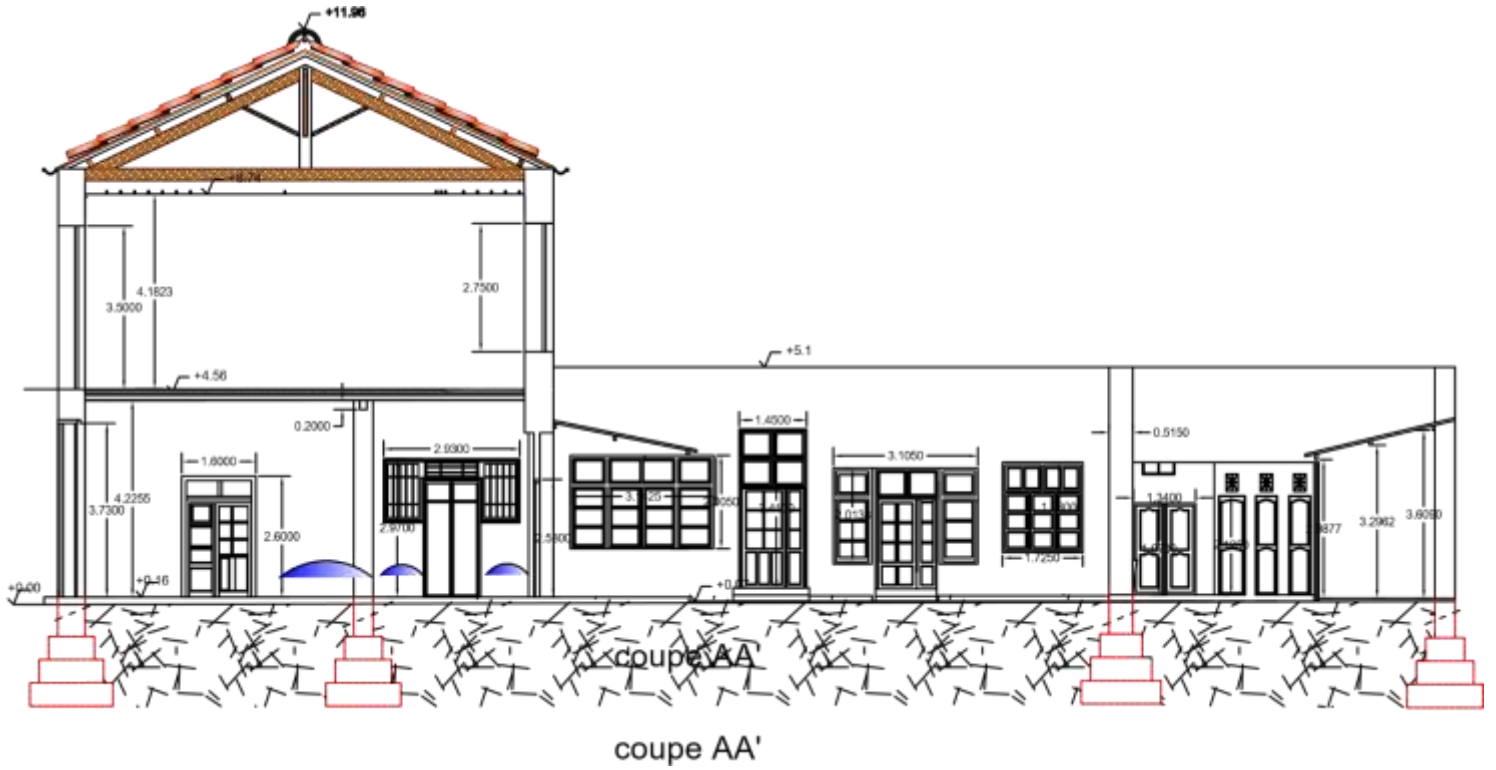


Figure III 5. architectural plan cut AA'

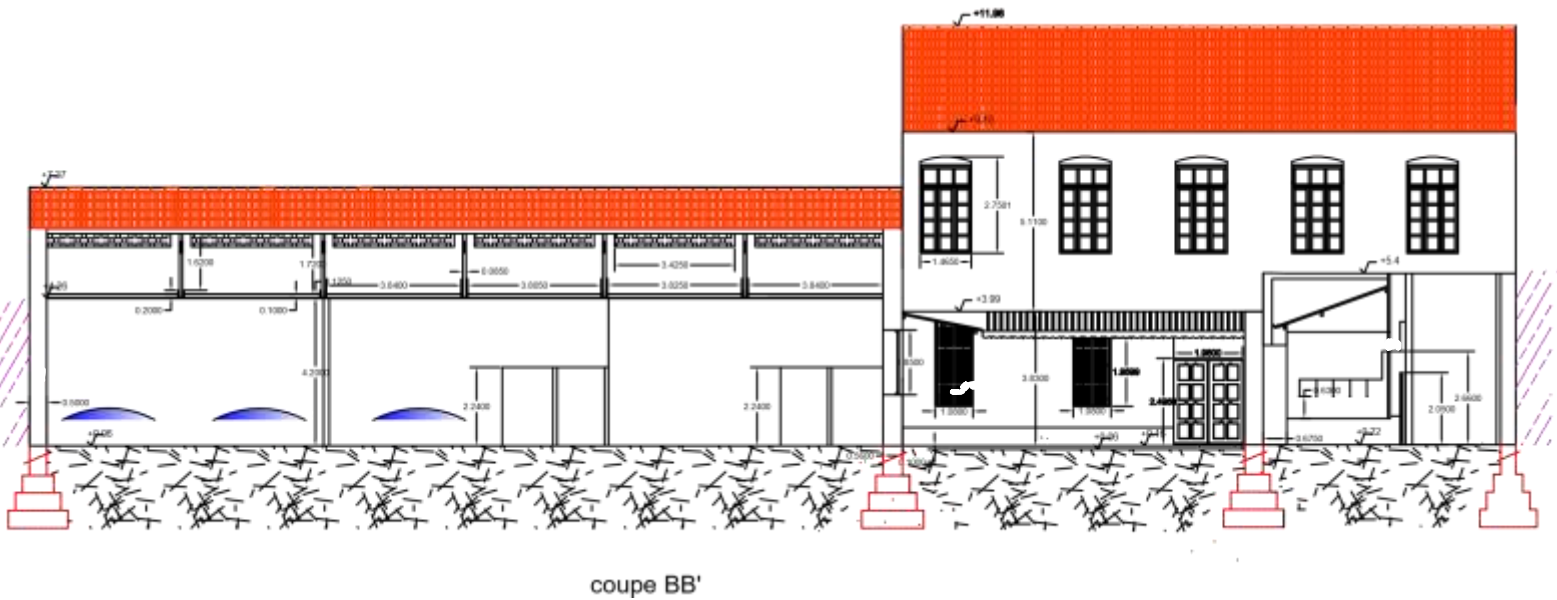
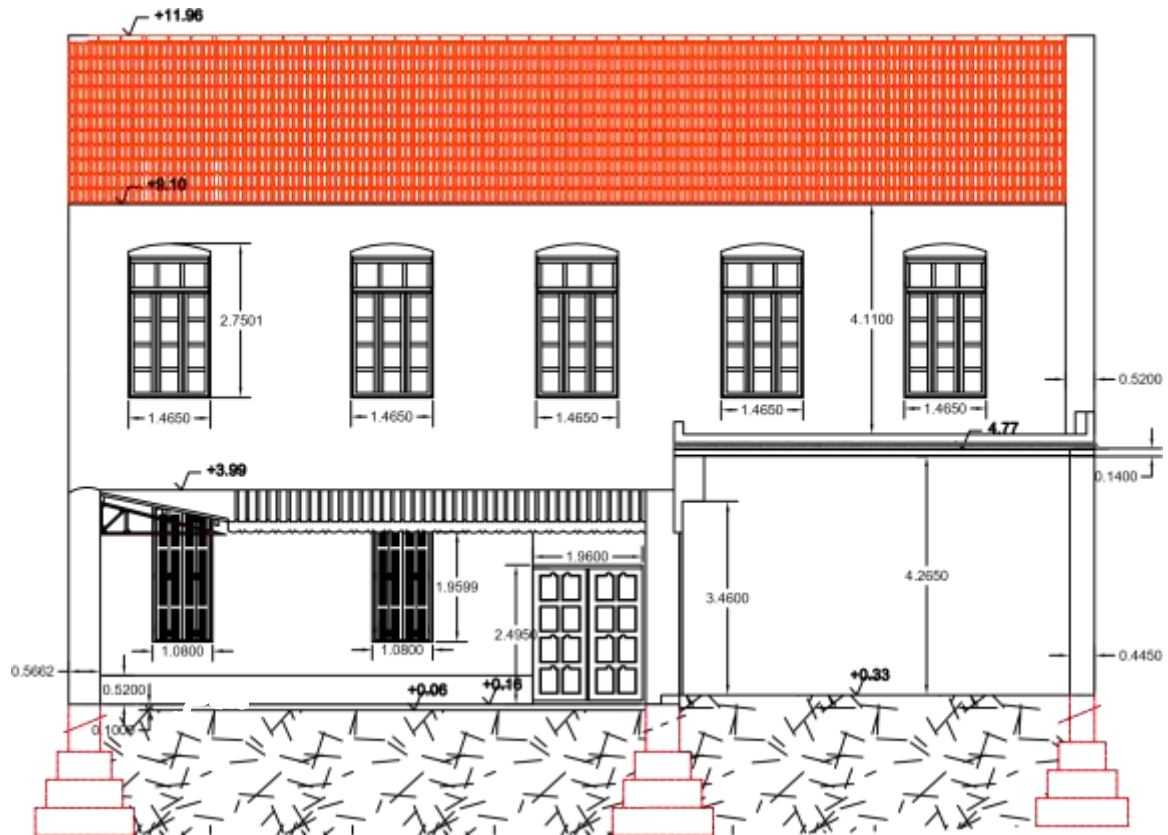


Figure III 6. architectural plan Cut BB'



coupe cc'

Figure III 7. architectural plan Cut CC'

III.3 STUDY CASE AND DIAGNOSIS

III.3.1 Constructive and structural analysis

A detailed comprehension of the structure of the building materials and building processes is required in order to evaluate its degree of conservation and offer an idea of its resistance to the various loads that this is of prior usage in the future.

The design of a civil engineering project is developed taking into account the functional aspects; structural and formal, which obliges the engineer to take into account the following data:

- the use of the building.
- resistance and stability.
- architectural, functional and aesthetic requirements.
- economic conditions.

III.3.1.1 Infrastructure

Access to infrastructure is an impossibility. We cannot recognise the sort of infrastructure; however, it is thought to have a continuous masonry foundation under walls.

III.3.1.2 Structure of the superstructure

The structure is made up of two major vertical and horizontal construction systems:

Table III 3. The structure elements

| Element | Materials | Dimensions |
|---------------------|---|---|
| Vertical elements | - load-bearing wall: - rubble masonry walls. - stones walls | - thicKness ranging between 40 to 60 cm. - thicKness of 40 cm. |
| Horizontal elements | Brick floor + ipe metal | - thicKness of 24.5 cm. (ipe 140) |
| Roof | The roof is slanted (wood frame + tile) at the floor level | - frame wood dimensions and joists of (7*17cm) ;(7*25cm) |
| Secondary system | Represent walls that do not contribute to load transmission but have the function of separating spaces, which made of bricks. | - thicKness ranging between 10 to 23 cm. |

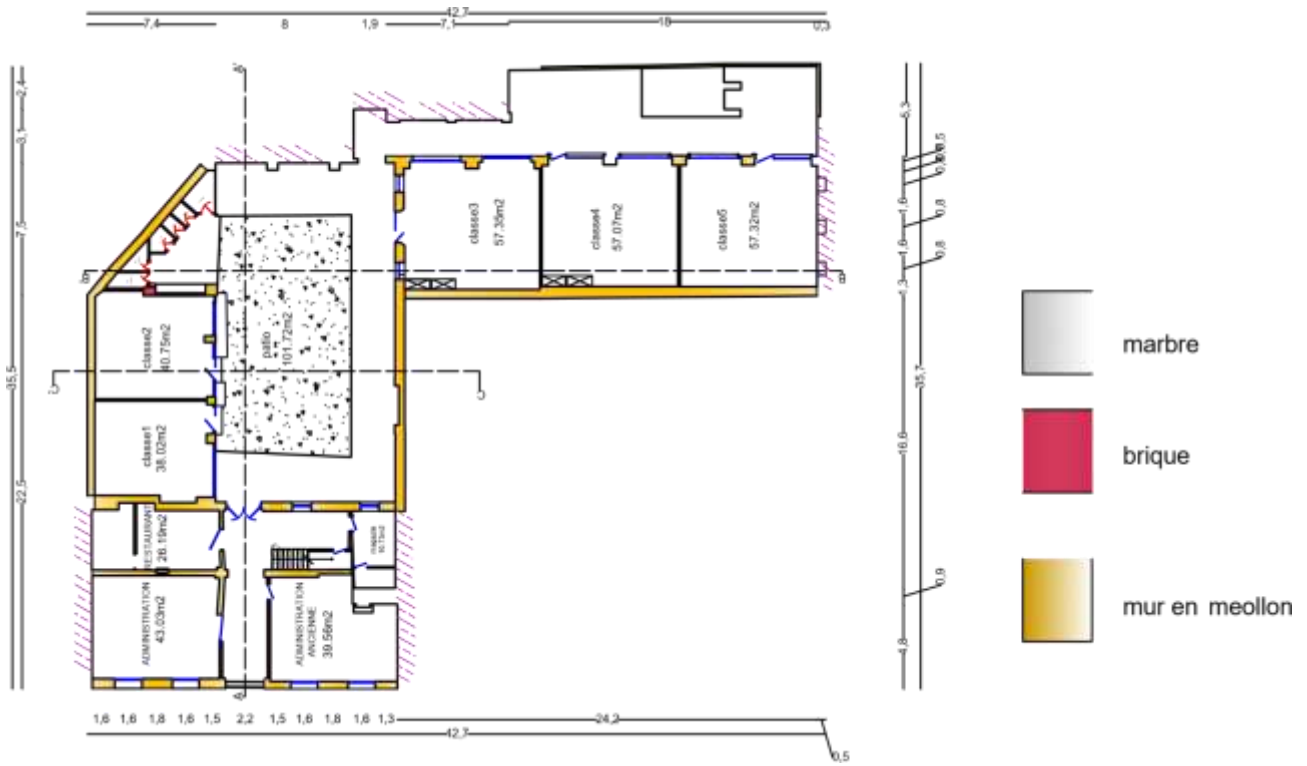


Figure III 8 . materials and architecture plan first floor

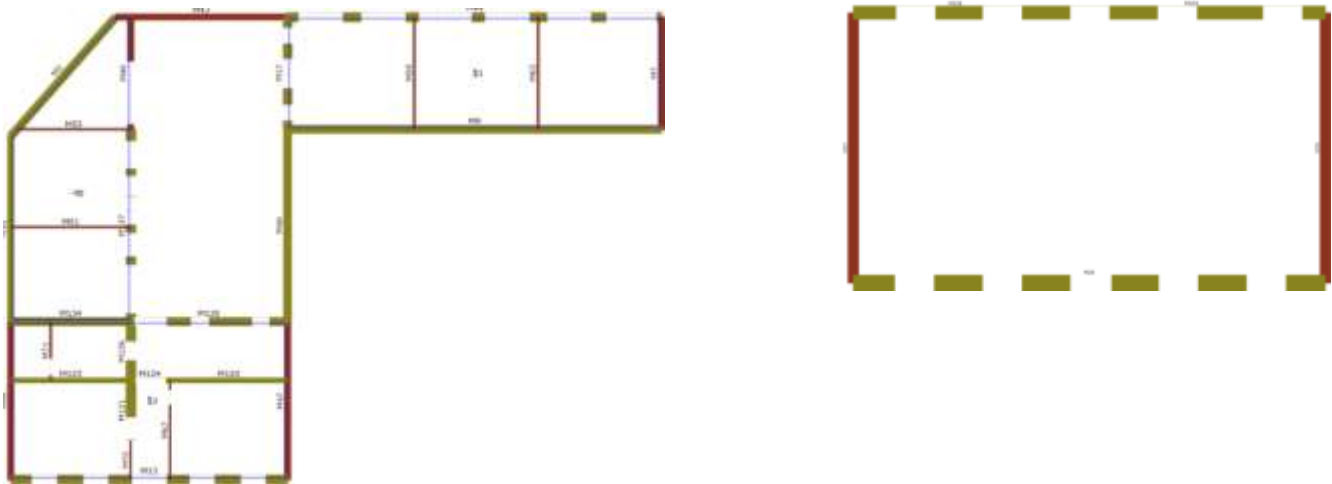






Figure III 9 material plan 1st floor and 2nd floor

Table III 4. The used material tables

| Name | Type | Colour | |
|--------------|---------|---|--------|
| C24 - en 338 | Timber |  | En 338 |
| Rubble | Masonry |  | |
| Stone | Masonry |  | |
| Bricks | Masonry |  | |

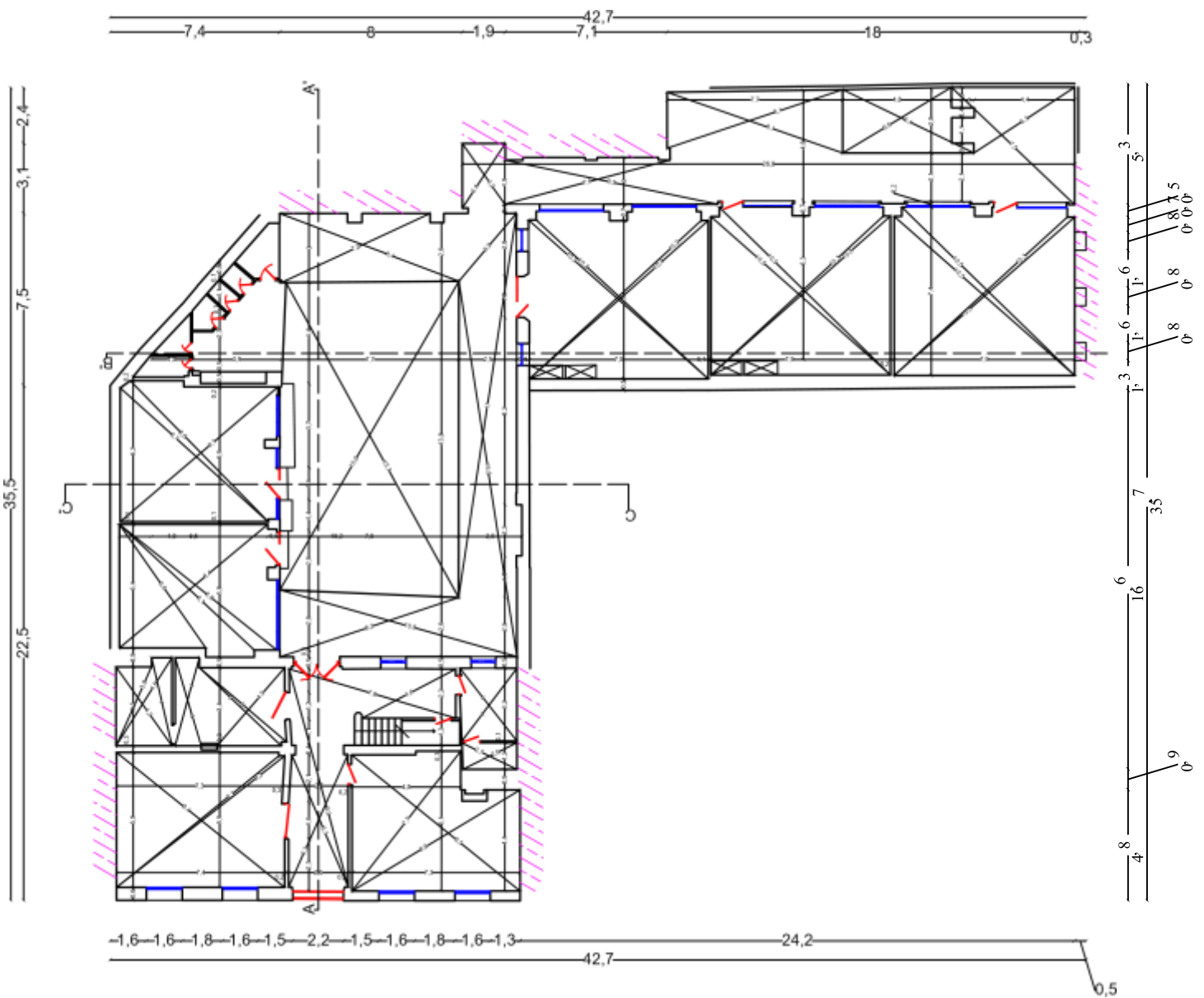


Figure III 10.RDC survey plan

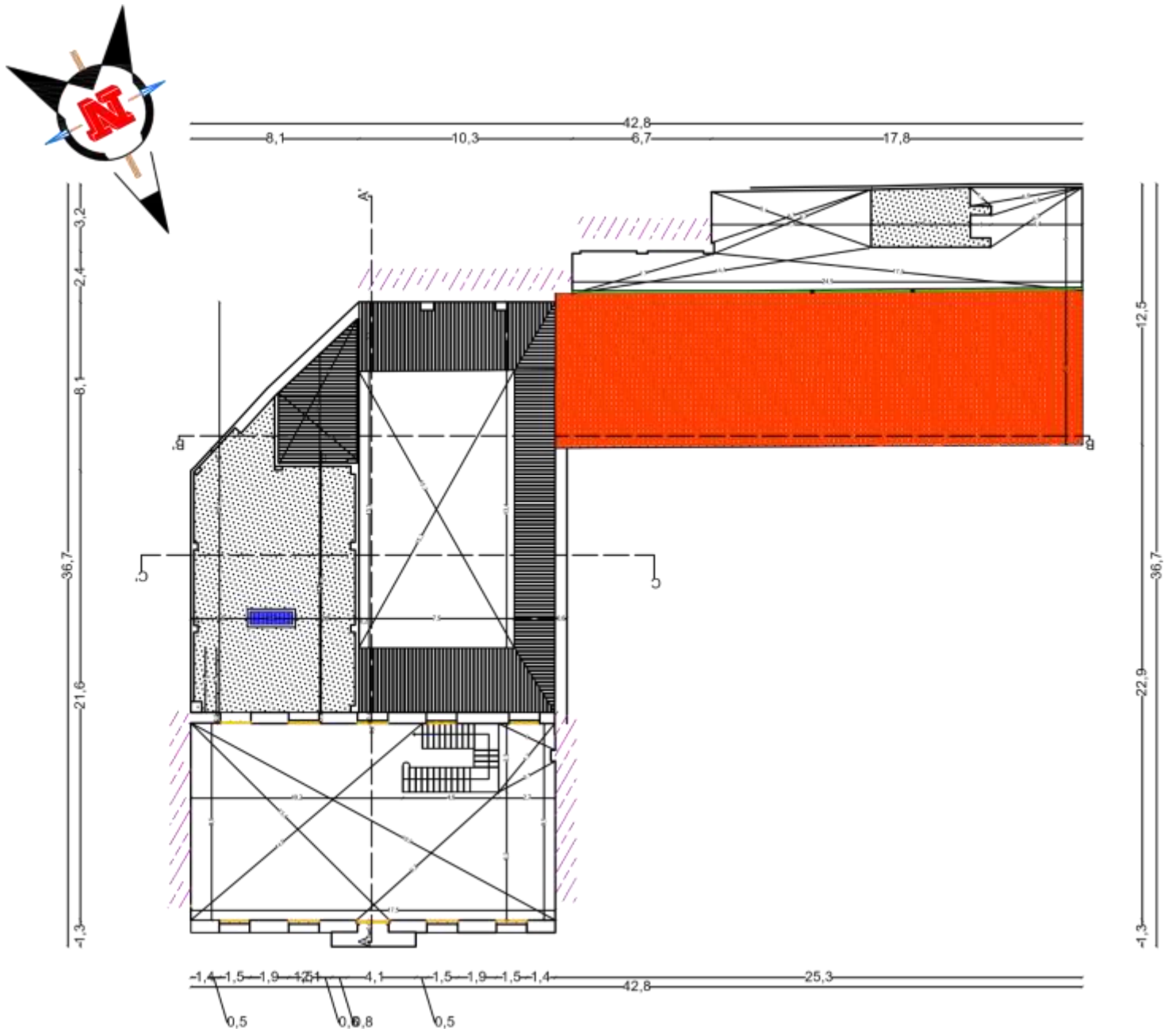


Figure III 11. 1st floor plan view

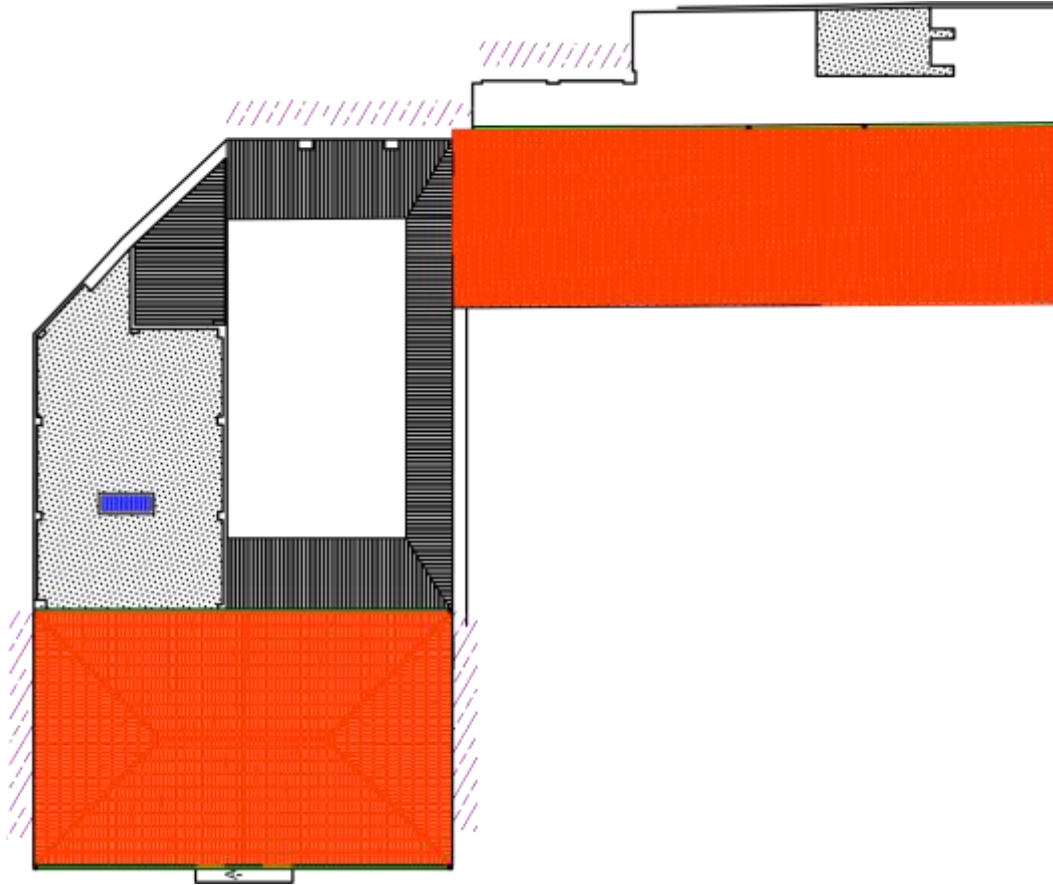


Figure III 12. Roof plan view

III.4 REFERENCE CODES

- Ntc 2018
- The algerian earthquake regulation "rpa" version 2003.
- Atc40
- Eurocode 8
- Eurocode 1
- Eurocode 6
- Fema 273, Fema 356

III.5 ACTIONS

III.5.1 Description of actions

The destination of the actions that will have to support the different floors of the building has been realistically designed in accordance with the writings of ntc 18 basis for structural calculation and eurocode 1: nf en 1991.1. Actions (2003-2008)

Loads classified by its nature can be distinguished between the direct actions include the self-weight of the structure, the rest of the dead loads, the operating overloads, etc.

The indirect actions consist of deformations or imposed accelerations capable of producing forces of indirect form. In this group there are the effects of settlement of foundations, rheological actions, seismic actions, etc.

According to the calculation rules, actions on structures can be classified into 3 different groups:

Permanent loads, operating loads and accidental loads (earthquake)

The characteristic value of an action is its main representative value. In general, for the proper weight of the structure, a unique value deduced from the nominal dimensions and the average specific weights will be adopted as characteristic action.

III.5.2 Permanent and variable loads

With regard to permanent and variable loads, the specific values of the Eurocode have been taken.

From the previous statements we go on to define the different actions that gravitate on the floors of each floor:

- The dead weight of the floors. The characteristic value of the self-weight of the elements constituting a building was determined on the basis of the average value obtained with the nominal dimensions and the average specific weights (an analytical method accepted by aeor-93).

Obtaining its value from these recommendations of various standards and instructions it should be mentioned that in some cases does not exist a single coating but more than one on top of the other) in these cases, the resulting wight have been taken into account.

- Operating overload: the value recommended by the Eurocode has been taken.

Overload of small brick partitions: to calculate their weight, different thicknesses measured on each dwelling have been taken into account. Also, and on the safety side, the empty by full criterion was followed.

III.5.3 General evaluation of the actions

In the first place, the presentations in the italian ntc 18 and eurocodes instruction was taken as reference values for the permanent charges and operating charges.

The weights of the constituent elements of a construction were calculated analytically by using the integrated codes, wich are from national regulations.

In particular, we used the values provided by italian regulations (and european regulations in general) through known eurocodes and not the algerians dtr's.

Then we present in the table below some constructive elements that have been taken into account.

Table III 5 . Some materials propre weights

| Materials | Proper weight |
|--------------------------------|-----------------------------|
| Steels | 7850 kg/m ³ |
| Cast iron | 7250 kg/m ³ |
| Aluminium | 2750 kg/m ³ |
| Bronze | 8600 kg/m ³ |
| Zinc | 7200 kg/m ³ |
| Concrete flows | 2200 kg/m ³ |
| Reinforced concrete | 2500 kg/m ³ |
| Cedar wood | 800kg/m ³ |
| Pine bowls | 600 kg/m ³ |
| Colonial wood | 1000 kg/m ³ |
| Wooden joists. | 25/45 kg/m ² |
| Hollow brick wall (perforated) | 1500 kg/m ³ |
| Solid brick wall | 1900 kg/m ³ |
| Rubble stone masonry | 2100/2600 kg/m ³ |
| Solid brick partitions | 120kg/m ² |
| Hollow brick partitions | 100kg/m ² |
| Coatings | 50/80 kg/m ² |

| | |
|---------------------------------|--------------------------|
| Large flat tile mold | 80/85 kg/m ² |
| Flat tile small mold | 60/70 kg/m ² |
| Flemish tile | 80/100 kg/m ² |
| Large mold flat tile | 80/85 kg/m ² |
| Corrugated asbestos cement tile | 15/20 kg/m ² |
| False ceiling | 5/10 kg/m ² |

III.6 THE LOADS

Table III 6. Floor loads

| No. Floor | Position | Gk1 [KN/m ²] | Gk2 [KN/m ²] | Qk [KN/m ²] | Leading variable action 1 | Ψ0 | Ψ2 |
|-----------|----------------------|-----------------------------|-----------------------------|----------------------------|---------------------------|------|------|
| 1 | Level 1 (+4.630 [m]) | 1.85 | 1.34 | 1.00 | No | 1.00 | 0.70 |
| 2 | Level 1 (+4.630 [m]) | 1.85 | 1.34 | 1.00 | No | 1.00 | 0.70 |
| 3 | Level 1 (+4.630 [m]) | 1.85 | 1.34 | 2.50 | No | 1.00 | 0.70 |

Table III 7 . Balcony loads

| No. Balconies | Position | Gk1 [KN/m ²] | Gk2 [KN/m ²] | Qk [KN/m ²] | Leading variable action 1 | Ψ0 | Ψ2 |
|---------------|--------------------|-----------------------------|-----------------------------|----------------------------|---------------------------|------|------|
| 1 | Level (+9.100 [m]) | 2.67 | 1.34 | 1.50 | No | 1.00 | 0.70 |

Table III 8. Roof slope loads

| Roof slope | Position | Gk1 [KN/m ²] | Gk2 [KN/m ²] | Qk [KN/m ²] | Leading variable action 1 | Ψ0 | Ψ2 |
|------------|----------------------|-----------------------------|-----------------------------|----------------------------|---------------------------|------|------|
| 1 | Level 1 (+4.630 [m]) | 0.70 | 0.00 | 1.00 | No | 1.00 | 0.70 |
| 2 | Level 1 (+4.630 [m]) | 0.70 | 0.00 | 1.00 | No | 1.00 | 0.70 |
| 3 | Level (+9.100 [m]) | 0.70 | 0.00 | 1.00 | No | 1.00 | 0.70 |
| 4 | Level (+9.100 [m]) | 0.70 | 0.00 | 1.00 | No | 1.00 | 0.70 |

III.7 THE MECHANICAL CHARACTERISTICS

III.7.1 Masonry

Table III 9. Masonry element mechanical characteristics

| Name | The material's condition | Constitutive law | E [KN/m ²] | Eh [KN/m ²] | G [KN/m ²] | Specific weight [kg/m ³] | Fm [KN/m ²] |
|--------|--------------------------|-------------------------------------|---------------------------|----------------------------|---------------------------|---|----------------------------|
| Bricks | Existing | Irregular masonry (turnsek/cacovic) | 1,500,000.00 | 1,500,000.00 | 500,000.00 | 1,835 | 2,600.00 |
| Rubble | Existing | Irregular masonry (turnsek/cacovic) | 1,230,000.00 | 1,230,000.00 | 410,000.00 | 2,039 | 2,000.00 |
| Stone | Existing | Irregular masonry (turnsek/cacovic) | 870,000.00 | 870,000.00 | 290,000.00 | 1,937 | 1,000.00 |

The material's condition: existing

Constitutive law: irregular masonry (turnsek/cacovic)

Table III 10. Materials coefficients

| Name | Fk [KN/m ²] | T [KN/m ²] | Cf | Γm |
|--------|----------------------------|---------------------------|------|------|
| Bricks | 1348.10 | 50.00 | 1.35 | 3.00 |
| Rubble | 1037.00 | 35.00 | 1.35 | 3.00 |
| Stone | 518.50 | 18.00 | 1.35 | 3.00 |

III.7.2 Timber

Table III 11. Timber mechanical characteristics

| Name | E [KN/m ²] | G [KN/m ²] | Specific weight [kg/m ³] | Fwm [KN/m ²] | Fwk [KN/m ²] | Γ w |
|--------------|---------------------------|---------------------------|---|-----------------------------|-----------------------------|------|
| C24 - en 338 | 11,000,000.00 | 690,000.00 | 428 | 34,000.00 | 24,000.00 | 1.30 |

III.7.3 Steel

Table III 12 structural steel mechanical characteristics

| Name | E [n/m ²] | G [n/m ²] | Specific weight [kg/m ³] | F _{ym} [n/m ²] | F _{yk} [n/m ²] | Γ _s |
|------------------|--------------------------|--------------------------|---|--|--|----------------|
| S 235 (t ≤ 40mm) | 2.10e+11 | 8.08e+10 | 8.00e+03 | 2.53e+08 | 2.35e+08 | 1.05 |

III.7.4 Floors

Steel-beam and vault

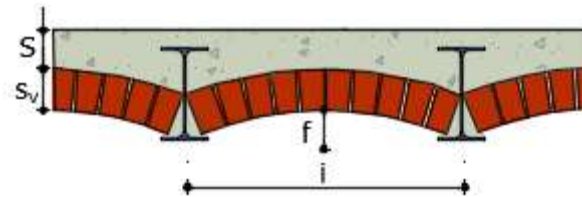


Figure III 13. Floor concept

Table III 13 . Floor dimensions

| Name | Materials | Description |
|-------|--|---|
| Vault | Steel: s 235 (t ≤ 40mm) Concrete: c8/10 Vaulted: brick | Steel-beam and vault Profile: ipe 140 I [mm] = 500; f [mm] = 100; sv [mm] = 70; a flat/m [mm ²] = 0.00; s [mm] = 100 |

Table III 14. Floor mechanical characteristics

| Archive | Elevation [m] | ThicKness [mm] | G [KN/m ²] | Ex [KN/m ²] | Ey [KN/m ²] | Mass loading | Type |
|---------|------------------|-------------------|---------------------------|----------------------------|----------------------------|----------------|----------------------|
| Vault | 4.630 | 40 | 13,593,229.49 | 17,251,501.95 | 0.00 | Unidirectional | Steel-beam and vault |

III.7.5 Roof elements

NOTE:

we considered the roof as a rigid element because it's so rotten and old and it will affect the analysis

1) Wooden beam

Table III 15. Roof materials

| Material | Area [mm ²] | J [mm ⁴] | W [mm ³] |
|--------------|-------------------------|----------------------|----------------------|
| C24 - en 338 | 17,500.00 | 91,145,800.8 | 729,170.0 |

2) Roof slope

Table III 16 the resistance direction of the floor

| Mass loading | Type |
|----------------|-------------|
| Unidirectional | Rigid floor |

III.8 CONCLUSION

In conclusion, Chapter III focuses on the study case of the Asla Hocine Primary School. Includes a presentation of the school, an urban study, and an architectural study. It also covers a constructive and structural analysis, reference codes, actions, loads, and the mechanical characteristics of the building's elements.

This comprehensive study provides valuable insights into the condition, performance, and design of the school building. It serves as a practical example for assessing and diagnosing masonry structures.

CHAPTER IV

STATIC

VERIFICATION

IV.1 INTRODUCTION

Static analysis of a building refers to the process of evaluating the structural stability and strength of a building using engineering principles and mathematical calculations. It involves assessing the building's ability to withstand various loads, such as dead loads (weight of the building itself), live loads (occupant loads, furniture, equipment), wind loads, seismic loads, and other external forces.

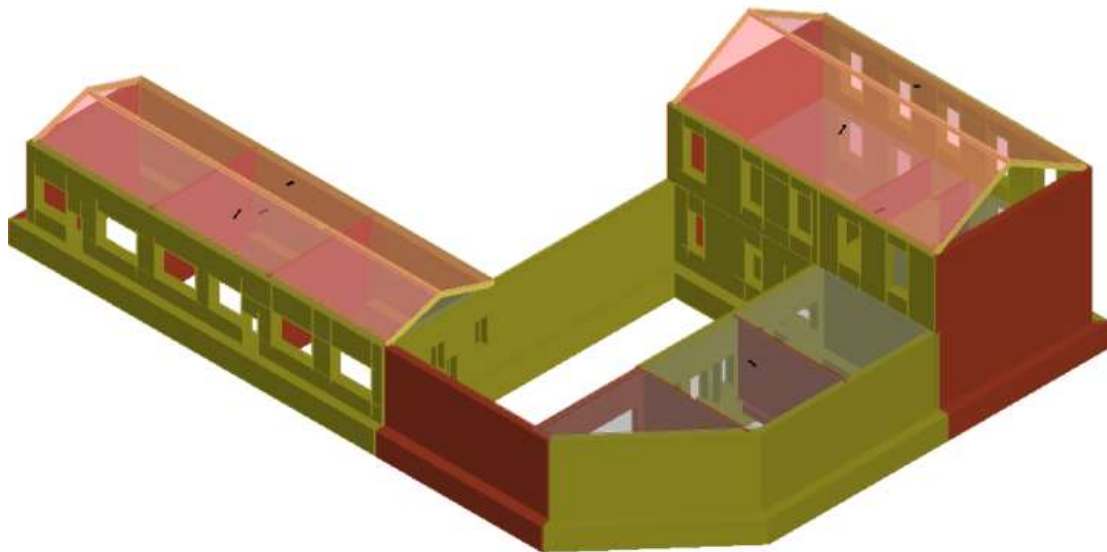


Figure IV 1. 3D view of the structure model

IV.2 REFERENCE CODE

For the analyzes described below, the principles and rules set out in the following regulations have been implemented:

Ministerial Decree of 17 January 2018 - "Technical standards for construction"(italy)

Application Circular No. 7 of 21 January 2019

IV.3 ANALYSIS METHOD

The modelling of the building is achieved by inserting walls that are discretized into macro-elements, representative of masonry piers and deformable floor strips; the rigid nodes are indicated in the portions of masonry which are typically less subject to seismic damage. Usually, the piers and spandrels are contiguous to the openings, the rigid nodes represent connecting elements between piers and spandrels. The mathematical conception that is hidden in the use of this element, allows to recognize the damage mechanism, by shear in its central part or by bending on the edges of the element in order to perceive the dynamics of the damage as it actually occurs in reality.

The nodes of the model are three-dimensional nodes with 5 degrees of freedom (the three components of displacement in the global reference system and the rotations around the X and Y axes) or two-dimensional nodes with 3 degrees of freedom (two translations and the rotation in the plane of the wall). The three-dimensional ones are used to allow the transfer of actions, from a first wall to a second one arranged transversally with respect to the first. The two-dimensional type nodes have degrees of freedom only in the plane of the wall allowing the transfer of stress states between the various points of the wall.

The horizontal elements, are modeled with three-node floor elements connected to the three-dimensional nodes, and can be loaded perpendicularly to their plane by accidental and permanent loads; seismic actions load the floor along the mid-story direction. For this reason, the floor finite element is defined with an axial stiffness, but no flexural stiffness, since the main mechanical behavior to be investigated is that under horizontal load due to the earthquake.

IV.3.1 Type of analysis performed

In order to carry out the necessary checks on the building in question, it was decided to proceed with the execution of a static analysis.

The required verifications take the form of a comparison between the value of the acting vertical load and the resistant vertical load. This evaluation is carried out by examining the slenderness and eccentricity values [2018 Technical Standards §4.5.6].

IV.4 MODEL DESCRIPTION

IV.4.1 materials

IV.4.1.1 Mechanical behaviour of the masonry

The mechanical properties of the masonry material are defined in order to best identify its behaviour in the non-linear field.

The main features are:

- Initial stiffness according to the elastic characteristics (cracked) of the material;
- Redistribution of the internal stresses of the element such as to guarantee equilibrium;
- Setting of the damage state according to the global and local parameters;
- Stiffness degradation in the plastic branch;
- Ductility control by defining the maximum drift (δu) differentiated according to the provisions of the regulations in force according to the damage mechanism acting on the panel;
- Elimination of the element, when the limit conditions are reached without interrupting the analysis.

The non-linear behaviour is activated when a force value reaches its maximum value defined as the minimum between the bending and shear resistance criteria.

The behaviour of the masonry piers associated with the shear and bending mechanisms can be described through different traits that represent the progressive levels of damage.

IV.4.1.2 Wall with shear mechanism

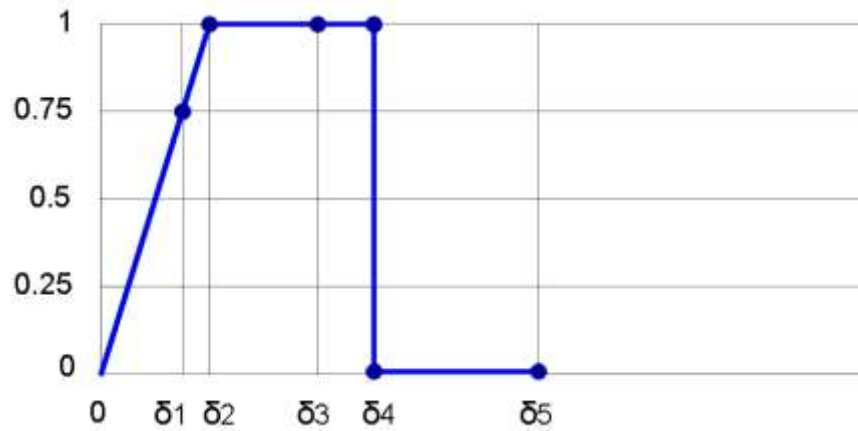


Figure IV 2 Wall behaviour curve with shear mechanism

The behavior of the masonry in shear can be described through the following sections, representative of the progressive levels of damage relative to the previous diagram:

Table IV 1 The behaviour of the masonry in shear and the related level of damage

| | |
|-------------------------|-------------------------|
| 0 – δ_1 | elasticity |
| δ_1 – δ_2 | incipient plasticity |
| δ_2 – δ_3 | plastic for cutting |
| δ_3 – δ_4 | incipient shear failure |
| δ_4 – δ_5 | shear breakage |
| δ_5 – ∞ | severe crisis |

IV.4.1.3 Wall with bending mechanism

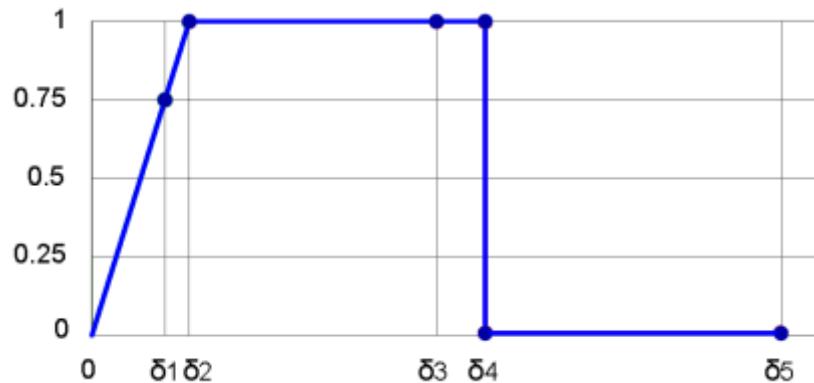


Figure IV 3 Wall behaviour curve with bending mechanism

On the other hand, the behavior of the bending wall masonry can be described by the following features:

Table IV 2 The behaviour of the masonry in bending mechanism and the related level of damage

| | |
|-------------------------|----------------------------------|
| 0 – δ_1 | elasticity |
| δ_1 – δ_2 | incipient plasticity |
| δ_2 – δ_3 | plastic for bending |
| δ_3 – δ_4 | incipient rupture due to bending |
| δ_4 – δ_5 | bending failure |
| δ_5 – ∞ | severe crisis |

Some of these failure levels are necessary to describe the progress of the crisis more accurately, allowing a more accurate prediction of the interventions and the level of deterioration of the masonry:

- Incipient plasticity: When an element is still in the elastic range but is close to plasticity
- Incipient failure: When an element is in the plastic range but is close to failure
- Serious crisis: When, following the failure of the element, the deformations become so significant as to be able to generate a local collapse.
- The software provides three bond categories:
- With Strength Degradation to a Residual Value (Multiline Link)

- With resistance equal to the residual value (Bilinear bond)
- No residual strength
- Among these, the bond categories used within the project in question are:
- In the absence of residual resistance

IV.4.1.4 In the absence of residual resistance

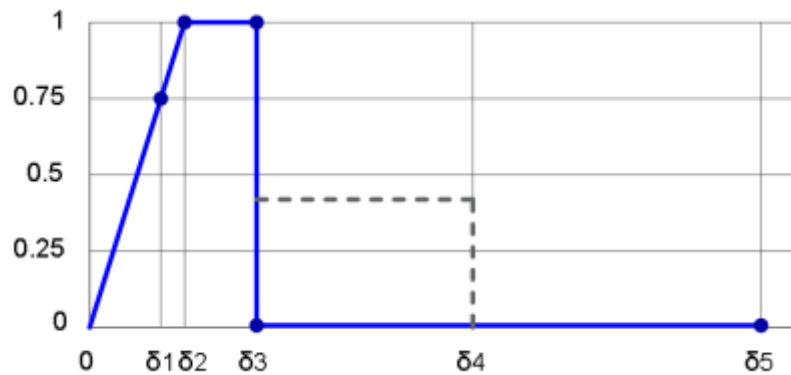


Figure IV 4 Wall behaviour curve in case of absence of residual resistance

This type of link represents a variant logic of the previous links starting from the multilinear link but is not currently contemplated in the current regulations. For the identifications and Explanations of details look in the **Appendix I**

IV.5 LOADS

IV.5.1 Seismic load:

Checks at the ultimate limit state (SLV) and at the serviceability limit state (SLD; SLO); must be carried out for the following combination [Technical Standards 2018 §2.5.3].

$$E + G_{K1} + G_{K2} + \sum_i \Psi_{2i} Q_{Ki}$$

The effects of the seismic action will be evaluated taking into account the masses associated with the following gravitational loads:

$$G_{K1} + G_{K2} + \sum_i \Psi_{2i} Q_{Ki}$$

IV.5.2 Static Load:

The ultimate limit state verification for static loads is conducted with the following combination of loads.

$$\gamma_{G1} G_{k1} + \gamma_{G2} G_{k2} + \gamma_Q \Psi_0 Q_k$$

Where:

| | |
|--|---|
| E | seismic action for the limit state in question; |
| G_{k1} | self-weight of all structural elements; |
| G_{k2} | self-weight of all non-structural elements; |
| Q_{ki} | characteristic value of the variable action; |
| γ_2 | combination coefficient; |
| γ_0 | combination factor for variable loads |
| γ_{G1} ; γ_{G2} ; γ_Q : | partial safety factors |

The values of the various coefficients are chosen on the basis of the intended use of the various floors as indicated in the standard. [2018 Technical Standards Table 2.5.1].

IV.6 GLOBAL STATIC VERIFICATION

The static checks performed on the structure in question are as follows:

IV.6.1 Slenderness of the masonry

The slenderness check is performed in accordance with what is reported in point 4.5.4. of the DM2018.

The slenderness of a masonry is defined as the ratio h_0/t in which:

h_0 : free buckling length of the wall equal to $\alpha r h$;

t : wall thickness.

h : the internal height of the floor;

r : the lateral constraint factor.

The slenderness check is satisfied if the following is true:

$$h_0/t < 20$$

IV.6.2 Load eccentricity

The slenderness check is performed in accordance with what is reported in point 4.5.6.2. of the DM2018.

This verification is satisfied if the following conditions are verified:

$$e_1/t \leq 0.33$$

$$e_2/t \leq 0.33$$

in which:

t: wall thickness

$$e_1 = |e_s| + |e_a| ; e_2 = \frac{e_1}{2} + |e_v|$$

es: total eccentricity of vertical loads

ea: h/200

ev: eccentricity due to wind $e_v = M_v / N$

IV.6.3 Verification at vertical loads

The slenderness check is performed in accordance with what is reported in point 4.5.6.2. of the DM2018.

This verification is satisfied if the following is verified:

$$N_d \leq N_r$$

in which:

N_d : acting vertical load

N_r : resistant vertical load; $N_r = f d A$

A: area of the horizontal section of the wall net of openings;

fd: design resistance of the masonry;

f: coefficient of reduction of the resistance of the wall

These checks were carried out in each masonry of the structure, in the three main sections (lower, central, upper).

The values of the normal resistant stress will be calculable only if the checks of slenderness and eccentricity of the loads are satisfied. We report below the verification details for the individual walls.

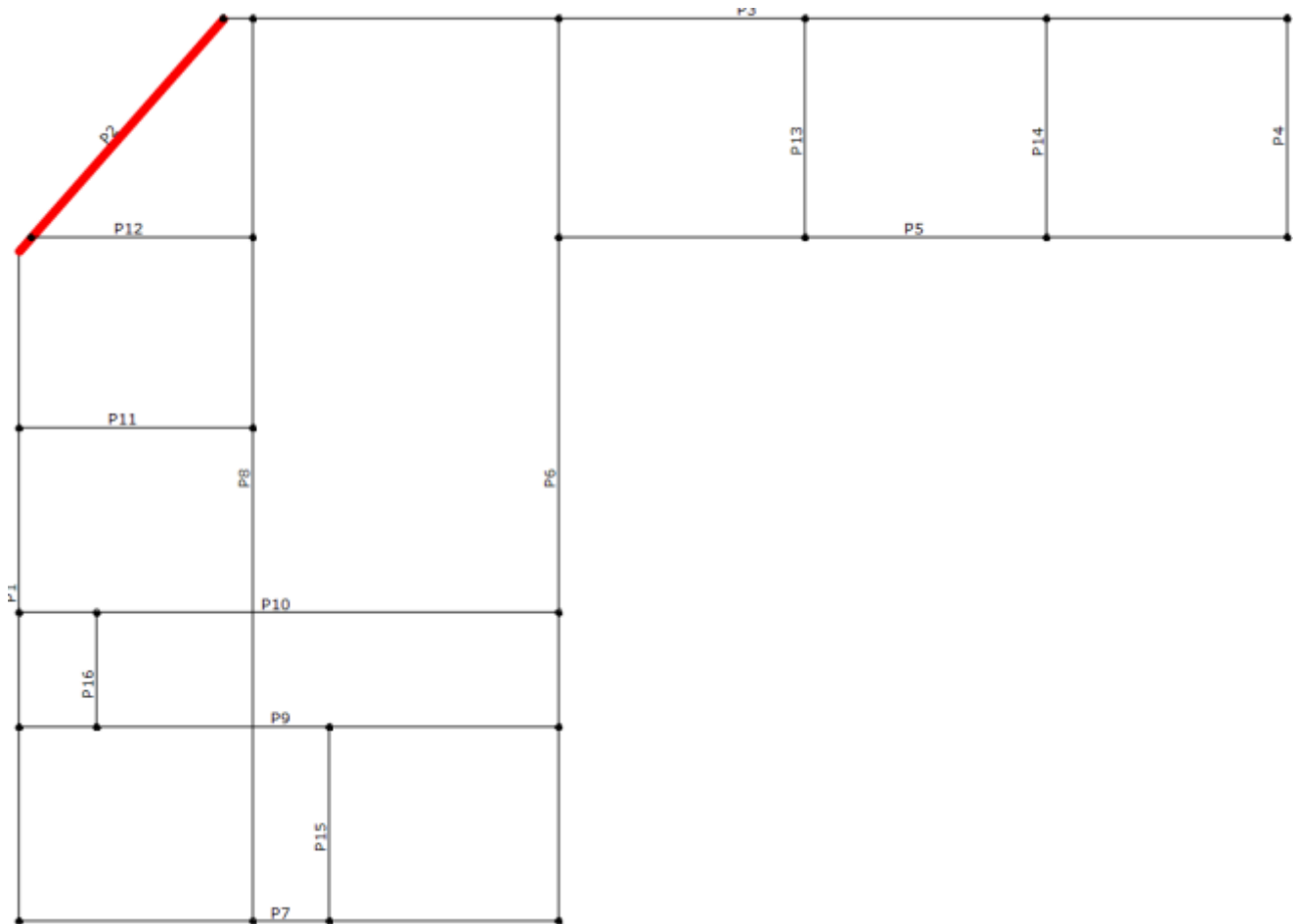


Figure IV 5. the structure walls numbers

IV.6.4 the results

a static verification process is conducted to assess the structural integrity of the building's elements. The non-verified (red) elements are scrutinized for potential vulnerabilities, while the verified (green) elements have been thoroughly examined and deemed structurally sound. This differentiation helps identify areas that require further analysis or reinforcement to ensure the overall safety and stability of the building.

Table IV 3 the legend table for verification of element status

| Legend | |
|----------------------|--|
| Verified element | |
| Not verified element | |

IV.6.4.1 Wall: 1



Figure IV 6 wall 1 element verification

Table IV 4 slenderness and eccentricity verification for wall 1

| Pier | ho [m] | t [m] | ho/t | e1/t Bottom | e2/t Middle | e1/t Top | Satisfied |
|------|--------|-------|--------|-------------|-------------|----------|-----------|
| 1 | 4.510 | 0.400 | 11.275 | 0.056 | 0.056 | 0.056 | Yes |
| 2 | 4.510 | 0.400 | 11.275 | 0.122 | 0.077 | 0.245 | Yes |
| 3 | 4.350 | 0.400 | 10.875 | 0.054 | 0.054 | 0.054 | Yes |

Table IV 5 vertical load bearing resistance verification for wall 1

| Pier | Top | | | | Middle | | | | Bottom | | | | Satisfied |
|------|-----|-------|-----|-------|--------|-------|-------|-------|--------|-------|-------|-------|-----------|
| | Nd | F | Nr | Nd/Nr | Nd | F | Nr | Nd/Nr | Nd | F | Nr | Nd/Nr | |
| 1 | 426 | 0.654 | 659 | 0.646 | 659 | 0.654 | 659 | 1.000 | 893 | 0.654 | 659 | 1.354 | No |
| 2 | 308 | 0.255 | 604 | 0.511 | 597 | 0.595 | 1,408 | 0.424 | 885 | 0.503 | 1,188 | 0.745 | Yes |
| 3 | 155 | 0.672 | 677 | 0.229 | 356 | 0.672 | 677 | 0.527 | 582 | 0.672 | 677 | 0.859 | Yes |

IV.6.4.2 Wall: 3

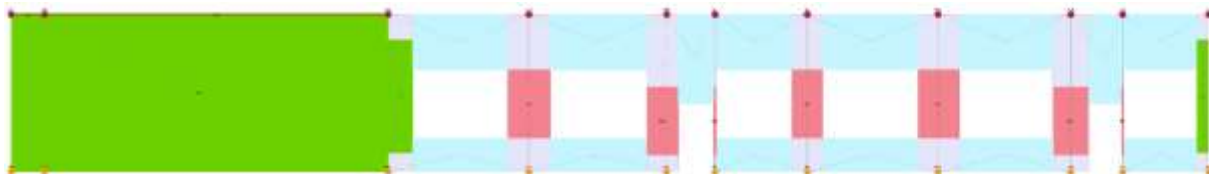


Figure IV 7 wall 3 element verification

Table IV 6 slenderness and eccentricity verification for wall 3

| Pier | ho [m] | t [m] | ho/t | e1/t Bottom | e2/t Middle | e1/t Top | Satisfied |
|------|--------|-------|--------|-------------|-------------|----------|-----------|
| 19 | 4.630 | 0.400 | 11.575 | 0.058 | 0.058 | 0.058 | Yes |
| 20 | 4.510 | 0.600 | 7.517 | 0.087 | 0.049 | 0.116 | Yes |
| 21 | 4.510 | 0.600 | 7.517 | 0.179 | 0.096 | 0.207 | Yes |
| 22 | 4.510 | 0.600 | 7.517 | 0.174 | 0.092 | 0.196 | Yes |
| 23 | 4.510 | 0.600 | 7.517 | 0.174 | 0.091 | 0.191 | Yes |
| 24 | 4.510 | 0.600 | 7.517 | 0.178 | 0.094 | 0.201 | Yes |
| 25 | 4.510 | 0.600 | 7.517 | 0.183 | 0.098 | 0.214 | Yes |
| 26 | 4.510 | 0.600 | 7.517 | 0.171 | 0.090 | 0.191 | Yes |
| 27 | 4.510 | 0.600 | 7.517 | 0.182 | 0.094 | 0.196 | Yes |
| 28 | 4.510 | 0.600 | 7.517 | 0.074 | 0.040 | 0.089 | Yes |

Table IV 7 vertical load bearing resistance verification for wall 3

| Pier | Top | | | | Middle | | | | Bottom | | | | Satisfied |
|------|-----|-------|-----|-------|--------|-------|-----|-------|--------|-------|-----|-------|-----------|
| | Nd | F | Nr | Nd/Nr | Nd | F | Nr | Nd/Nr | Nd | F | Nr | Nd/Nr | |
| 19 | 58 | 0.642 | 703 | 0.083 | 302 | 0.642 | 703 | 0.429 | 555 | 0.642 | 703 | 0.790 | Yes |
| 20 | 65 | 0.597 | 128 | 0.506 | 84 | 0.764 | 164 | 0.509 | 102 | 0.652 | 140 | 0.730 | Yes |
| 21 | 197 | 0.418 | 156 | 1.263 | 217 | 0.636 | 237 | 0.913 | 237 | 0.475 | 178 | 1.332 | No |
| 22 | 177 | 0.440 | 120 | 1.475 | 192 | 0.643 | 176 | 1.091 | 206 | 0.485 | 133 | 1.555 | No |
| 23 | 22 | 0.450 | 12 | 1.911 | 24 | 0.645 | 17 | 1.416 | 25 | 0.484 | 13 | 1.994 | No |
| 24 | 175 | 0.431 | 117 | 1.491 | 189 | 0.639 | 174 | 1.087 | 204 | 0.477 | 130 | 1.566 | No |
| 25 | 182 | 0.404 | 146 | 1.249 | 201 | 0.631 | 228 | 0.884 | 220 | 0.466 | 168 | 1.309 | No |
| 26 | 212 | 0.450 | 139 | 1.529 | 228 | 0.647 | 199 | 1.145 | 245 | 0.491 | 152 | 1.613 | No |
| 27 | 15 | 0.439 | 6 | 2.351 | 16 | 0.639 | 9 | 1.700 | 17 | 0.469 | 7 | 2.425 | No |
| 28 | 45 | 0.650 | 67 | 0.669 | 54 | 0.792 | 82 | 0.658 | 63 | 0.688 | 71 | 0.885 | Yes |

IV.6.4.3 Wall: 6

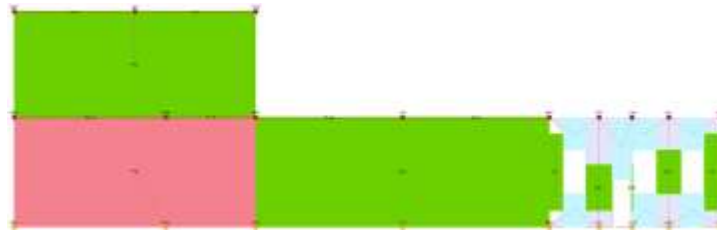


Figure IV 8 wall 6 element verification

Table IV 8 slenderness and eccentricity verification for wall 6

| Pier | ho [m] | t [m] | ho/t | e1/t Bottom | e2/t Middle | e1/t Top | Satisfied |
|------|--------|-------|--------|-------------|-------------|----------|-----------|
| 38 | 4.510 | 0.400 | 11.275 | 0.056 | 0.056 | 0.056 | Yes |
| 39 | 4.630 | 0.500 | 9.260 | 0.046 | 0.046 | 0.046 | Yes |
| 40 | 4.350 | 0.400 | 10.875 | 0.054 | 0.054 | 0.054 | Yes |
| 41 | 4.510 | 0.550 | 8.200 | 0.041 | 0.041 | 0.041 | Yes |
| 42 | 4.510 | 0.550 | 8.200 | 0.041 | 0.041 | 0.041 | Yes |
| 43 | 4.510 | 0.550 | 8.200 | 0.041 | 0.041 | 0.041 | Yes |
| 44 | 4.510 | 0.550 | 8.200 | 0.041 | 0.041 | 0.041 | Yes |
| 45 | 4.510 | 0.550 | 8.200 | 0.041 | 0.041 | 0.041 | Yes |

Table IV 9 vertical load bearing resistance verification for wall 6

| Pier | Top | | | | Middle | | | | Bottom | | | | Satisfied |
|------|-----|-------|-------|-------|--------|-------|-------|-------|--------|-------|-------|-------|-----------|
| | Nd | F | Nr | Nd/Nr | Nd | F | Nr | Nd/Nr | Nd | F | Nr | Nd/Nr | |
| 38 | 390 | 0.654 | 659 | 0.592 | 624 | 0.654 | 659 | 0.946 | 857 | 0.654 | 659 | 1.300 | No |
| 39 | 296 | 0.737 | 2,257 | 0.131 | 669 | 0.737 | 2,257 | 0.297 | 1,043 | 0.737 | 2,257 | 0.462 | Yes |
| 40 | 163 | 0.672 | 677 | 0.240 | 369 | 0.672 | 677 | 0.545 | 594 | 0.672 | 677 | 0.877 | Yes |
| 41 | 29 | 0.775 | 124 | 0.236 | 43 | 0.775 | 124 | 0.346 | 56 | 0.775 | 124 | 0.456 | Yes |
| 42 | 85 | 0.775 | 235 | 0.362 | 100 | 0.775 | 235 | 0.428 | 116 | 0.775 | 235 | 0.493 | Yes |

| | | | | | | | | | | | | | |
|----|----|-------|-----|-------|----|-------|-----|-------|-----|-------|-----|-------|-----|
| 43 | 5 | 0.775 | 15 | 0.357 | 6 | 0.775 | 15 | 0.422 | 7 | 0.775 | 15 | 0.488 | Yes |
| 44 | 73 | 0.775 | 219 | 0.333 | 87 | 0.775 | 219 | 0.396 | 101 | 0.775 | 219 | 0.459 | Yes |
| 45 | 51 | 0.775 | 146 | 0.349 | 67 | 0.775 | 146 | 0.459 | 83 | 0.775 | 146 | 0.569 | Yes |

IV.6.4.4 Wall: 7

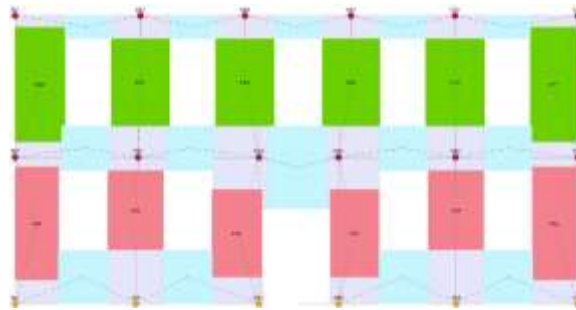


Figure IV 9 wall 7 element verification

Table IV 10 slenderness and eccentricity verification for wall 7

| Pier | ho [m] | t [m] | ho/t | e1/t Bottom | e2/t Middle | e1/t Top | Satisfied |
|------|--------|-------|-------|-------------|-------------|----------|-----------|
| 60 | 4.510 | 0.600 | 7.517 | 0.087 | 0.047 | 0.102 | Yes |
| 61 | 4.510 | 0.600 | 7.517 | 0.123 | 0.066 | 0.141 | Yes |
| 62 | 4.510 | 0.600 | 7.517 | 0.125 | 0.067 | 0.146 | Yes |
| 63 | 4.510 | 0.600 | 7.517 | 0.122 | 0.066 | 0.144 | Yes |
| 64 | 4.510 | 0.600 | 7.517 | 0.122 | 0.065 | 0.141 | Yes |
| 65 | 4.510 | 0.600 | 7.517 | 0.082 | 0.044 | 0.097 | Yes |
| 66 | 4.350 | 0.600 | 7.250 | 0.036 | 0.036 | 0.036 | Yes |
| 67 | 4.350 | 0.600 | 7.250 | 0.036 | 0.036 | 0.036 | Yes |
| 68 | 4.350 | 0.600 | 7.250 | 0.036 | 0.036 | 0.036 | Yes |
| 69 | 4.350 | 0.600 | 7.250 | 0.036 | 0.036 | 0.036 | Yes |
| 70 | 4.350 | 0.600 | 7.250 | 0.036 | 0.036 | 0.036 | Yes |
| 71 | 4.350 | 0.600 | 7.250 | 0.036 | 0.036 | 0.036 | Yes |

Table IV 11 vertical load bearing resistance verification for wall 7

| Pier | Top | | | | Middle | | | | Bottom | | | | Satisfied |
|------|-----|-------|-----|-------|--------|-------|-----|-------|--------|-------|-----|-------|-----------|
| | Nd | F | Nr | Nd/Nr | Nd | F | Nr | Nd/Nr | Nd | F | Nr | Nd/Nr | |
| 60 | 247 | 0.624 | 255 | 0.970 | 285 | 0.772 | 315 | 0.906 | 324 | 0.653 | 267 | 1.214 | No |
| 61 | 323 | 0.549 | 285 | 1.133 | 357 | 0.714 | 371 | 0.963 | 392 | 0.583 | 303 | 1.291 | No |
| 62 | 272 | 0.539 | 252 | 1.077 | 306 | 0.709 | 332 | 0.920 | 339 | 0.580 | 272 | 1.250 | No |
| 63 | 265 | 0.544 | 249 | 1.061 | 298 | 0.713 | 327 | 0.911 | 331 | 0.585 | 268 | 1.235 | No |
| 64 | 319 | 0.550 | 286 | 1.116 | 354 | 0.715 | 372 | 0.950 | 388 | 0.585 | 304 | 1.274 | No |
| 65 | 248 | 0.634 | 269 | 0.920 | 288 | 0.779 | 331 | 0.868 | 327 | 0.662 | 282 | 1.163 | No |
| 66 | 60 | 0.809 | 379 | 0.159 | 105 | 0.809 | 379 | 0.277 | 149 | 0.809 | 379 | 0.394 | Yes |
| 67 | 39 | 0.809 | 445 | 0.087 | 78 | 0.809 | 445 | 0.176 | 118 | 0.809 | 445 | 0.265 | Yes |
| 68 | 40 | 0.809 | 445 | 0.091 | 80 | 0.809 | 445 | 0.180 | 120 | 0.809 | 445 | 0.270 | Yes |
| 69 | 39 | 0.809 | 434 | 0.089 | 78 | 0.809 | 434 | 0.179 | 116 | 0.809 | 434 | 0.268 | Yes |
| 70 | 39 | 0.809 | 445 | 0.087 | 78 | 0.809 | 445 | 0.176 | 118 | 0.809 | 445 | 0.266 | Yes |
| 71 | 58 | 0.809 | 361 | 0.160 | 100 | 0.809 | 361 | 0.278 | 143 | 0.809 | 361 | 0.395 | Yes |

IV.6.4.5 Wall: 8

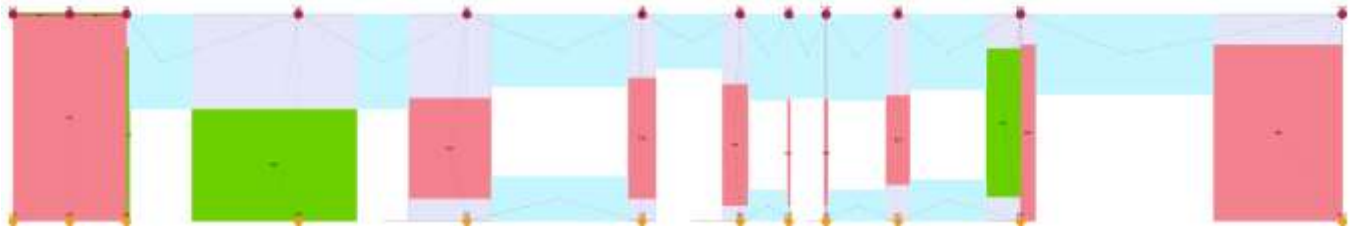


Figure IV 10 wall 8 element verification

Table IV 12 slenderness and eccentricity verification for wall 8

| Pier | ho [m] | t [m] | ho/t | e1/t Bottom | e2/t Middle | e1/t Top | Satisfied |
|------|--------|-------|--------|-------------|-------------|----------|-----------|
| 85 | 4.510 | 0.100 | 45.100 | 0.226 | 0.226 | 0.226 | Yes |
| 86 | 4.510 | 0.600 | 7.517 | 0.038 | 0.038 | 0.038 | Yes |
| 87 | 4.510 | 0.600 | 7.517 | 0.038 | 0.038 | 0.038 | Yes |

| | | | | | | | |
|----|-------|-------|--------|-------|-------|-------|-----|
| 88 | 4.510 | 0.600 | 7.517 | 0.113 | 0.060 | 0.130 | Yes |
| 89 | 4.510 | 0.600 | 7.517 | 0.172 | 0.093 | 0.203 | Yes |
| 90 | 4.510 | 0.600 | 7.517 | 0.167 | 0.091 | 0.202 | Yes |
| 91 | 4.510 | 0.600 | 7.517 | 0.174 | 0.092 | 0.195 | Yes |
| 92 | 4.510 | 0.600 | 7.517 | 0.175 | 0.092 | 0.196 | Yes |
| 93 | 4.510 | 0.600 | 7.517 | 0.174 | 0.091 | 0.192 | Yes |
| 94 | 4.510 | 0.600 | 7.517 | 0.123 | 0.069 | 0.160 | Yes |
| 95 | 4.510 | 0.400 | 11.275 | 0.171 | 0.105 | 0.286 | Yes |
| 96 | 4.510 | 0.400 | 11.275 | 0.112 | 0.068 | 0.189 | Yes |

Table IV 13vertical load bearing resistance verification for wall 8

| Pier | Top | | | | Middle | | | | Bottom | | | | Satisfied |
|------|-----|-------|-------|-------|--------|-------|-------|-------|--------|-------|-------|-------|-----------|
| | Nd | F | Nr | Nd/Nr | Nd | F | Nr | Nd/Nr | Nd | F | Nr | Nd/Nr | |
| 85 | 39 | 0.000 | n / d | n / d | 53 | 0.000 | n / d | n / d | 67 | 0.000 | n / d | n / d | No |
| 86 | 5 | 0.800 | 17 | 0.312 | 7 | 0.800 | 17 | 0.440 | 10 | 0.800 | 17 | 0.568 | Yes |
| 87 | 368 | 0.800 | 879 | 0.419 | 441 | 0.800 | 879 | 0.501 | 513 | 0.800 | 879 | 0.584 | Yes |
| 88 | 286 | 0.570 | 312 | 0.915 | 318 | 0.730 | 400 | 0.795 | 350 | 0.603 | 330 | 1.061 | No |
| 89 | 113 | 0.425 | 79 | 1.424 | 126 | 0.641 | 120 | 1.055 | 140 | 0.489 | 91 | 1.528 | No |
| 90 | 90 | 0.428 | 73 | 1.233 | 103 | 0.645 | 110 | 0.930 | 115 | 0.500 | 85 | 1.343 | No |
| 91 | 12 | 0.441 | 7 | 1.779 | 13 | 0.643 | 10 | 1.316 | 14 | 0.485 | 8 | 1.874 | No |
| 92 | 20 | 0.440 | 10 | 1.880 | 21 | 0.642 | 15 | 1.385 | 23 | 0.482 | 11 | 1.973 | No |
| 93 | 128 | 0.447 | 71 | 1.807 | 136 | 0.644 | 102 | 1.337 | 144 | 0.484 | 76 | 1.889 | No |
| 94 | 91 | 0.512 | 117 | 0.778 | 111 | 0.703 | 160 | 0.691 | 131 | 0.584 | 133 | 0.982 | Yes |
| 95 | 13 | 0.000 | n/d | n / d | 20 | 0.536 | 18 | 1.108 | 27 | 0.408 | 14 | 1.941 | No |
| 96 | 82 | 0.370 | 106 | 0.779 | 139 | 0.622 | 178 | 0.781 | 196 | 0.521 | 149 | 1.311 | No |

IV.6.4.6 Wall: 9

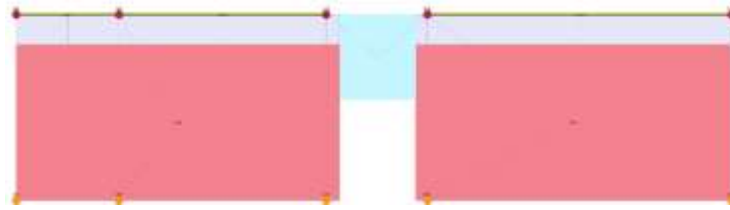


Figure IV 11 wall 9 element verification

Table IV 14 slenderness and eccentricity verification for wall 9

| Pier | ho [m] | t [m] | ho/t | e1/t Bottom | e2/t Middle | e1/t Top | Satisfied |
|------|--------|-------|--------|-------------|-------------|----------|-----------|
| 98 | 4.510 | 0.300 | 15.033 | 0.092 | 0.075 | 0.105 | Yes |
| 99 | 4.510 | 0.300 | 15.033 | 0.104 | 0.075 | 0.123 | Yes |

Table IV 15 vertical load bearing resistance verification for wall 9

| Pier | Top | | | | Middle | | | | Bottom | | | | Satisfied |
|------|-----|-------|-----|-------|--------|-------|-----|-------|--------|-------|-----|-------|-----------|
| | Nd | F | Nr | Nd/Nr | Nd | F | Nr | Nd/Nr | Nd | F | Nr | Nd/Nr | |
| 98 | 332 | 0.437 | 523 | 0.635 | 454 | 0.500 | 597 | 0.760 | 576 | 0.462 | 552 | 1.044 | No |
| 99 | 383 | 0.404 | 472 | 0.812 | 502 | 0.500 | 584 | 0.861 | 622 | 0.439 | 513 | 1.213 | No |

IV.6.4.7 Wall: 10

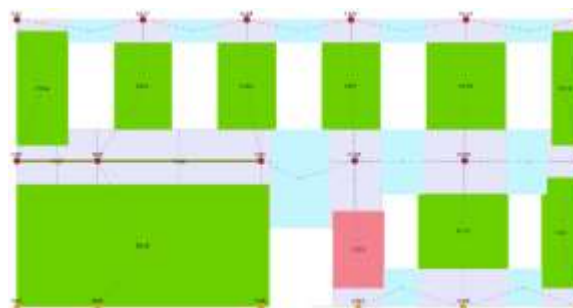


Figure IV 12 wall 10 element verification

Table IV 16 slenderness and eccentricity verification for wall 10

| Pier | ho [m] | t [m] | ho/t | e1/t Bottom | e2/t Middle | e1/t Top | Satisfied |
|------|--------|-------|-------|-------------|-------------|----------|-----------|
| 110 | 4.510 | 0.500 | 9.020 | 0.104 | 0.060 | 0.147 | Yes |
| 111 | 4.510 | 0.500 | 9.020 | 0.105 | 0.056 | 0.119 | Yes |
| 112 | 4.510 | 0.500 | 9.020 | 0.099 | 0.053 | 0.113 | Yes |
| 113 | 4.510 | 0.500 | 9.020 | 0.083 | 0.045 | 0.103 | Yes |
| 114 | 4.350 | 0.500 | 8.700 | 0.043 | 0.043 | 0.043 | Yes |
| 115 | 4.350 | 0.500 | 8.700 | 0.043 | 0.043 | 0.043 | Yes |
| 116 | 4.350 | 0.500 | 8.700 | 0.043 | 0.043 | 0.043 | Yes |
| 117 | 4.350 | 0.500 | 8.700 | 0.043 | 0.043 | 0.043 | Yes |
| 118 | 4.350 | 0.500 | 8.700 | 0.043 | 0.043 | 0.043 | Yes |
| 119 | 4.350 | 0.500 | 8.700 | 0.043 | 0.043 | 0.043 | Yes |

Table IV 17 vertical load bearing resistance verification for wall 10

| Pier | Top | | | | Middle | | | | Bottom | | | | Satisfied |
|------|-----|-------|-------|-------|--------|-------|-------|-------|--------|-------|-------|-------|-----------|
| | Nd | F | Nr | Nd/Nr | Nd | F | Nr | Nd/Nr | Nd | F | Nr | Nd/Nr | |
| 110 | 553 | 0.507 | 1,001 | 0.552 | 755 | 0.700 | 1,383 | 0.546 | 956 | 0.590 | 1,165 | 0.821 | Yes |
| 111 | 215 | 0.561 | 222 | 0.968 | 241 | 0.714 | 283 | 0.851 | 266 | 0.588 | 233 | 1.141 | No |
| 112 | 333 | 0.572 | 402 | 0.829 | 377 | 0.722 | 507 | 0.742 | 420 | 0.599 | 421 | 0.998 | Yes |
| 113 | 101 | 0.591 | 176 | 0.575 | 128 | 0.744 | 221 | 0.580 | 156 | 0.631 | 188 | 0.830 | Yes |
| 114 | 59 | 0.757 | 304 | 0.193 | 97 | 0.757 | 304 | 0.319 | 135 | 0.757 | 304 | 0.444 | Yes |
| 115 | 31 | 0.757 | 337 | 0.093 | 63 | 0.757 | 337 | 0.188 | 96 | 0.757 | 337 | 0.284 | Yes |
| 116 | 33 | 0.757 | 344 | 0.095 | 65 | 0.757 | 344 | 0.190 | 98 | 0.757 | 344 | 0.286 | Yes |
| 117 | 30 | 0.757 | 344 | 0.087 | 63 | 0.757 | 344 | 0.183 | 96 | 0.757 | 344 | 0.278 | Yes |
| 118 | 40 | 0.757 | 469 | 0.085 | 85 | 0.757 | 469 | 0.181 | 130 | 0.757 | 469 | 0.277 | Yes |
| 119 | 42 | 0.757 | 165 | 0.253 | 62 | 0.757 | 165 | 0.379 | 83 | 0.757 | 165 | 0.505 | Yes |

IV.7 FINDS

The results of the static verification process have revealed that a significant number of masonry elements are represented in red, indicating potential concerns. Specifically, these elements have been verified for slenderness and eccentricity but have not been verified for their ability to bear vertical loads effectively.

The identification of these red-colored masonry elements raises concerns about their structural integrity and their capacity to handle the vertical loads imposed upon them. It suggests that further investigation and analysis are required to ensure their ability to safely support vertical loads.

Addressing the issues related to the vertical load-bearing capacity of these masonry elements is crucial to maintain the overall stability and safety of the building. Measures such as additional reinforcement, modifications, or design alterations might be necessary to enhance their load-bearing capacity and minimize the risk of structural failure.

. The slenderness ratio of a masonry structure provides insights into its stability and vulnerability to excessive deflection or failure under vertical loads.

Excessive eccentricity can result in uneven stress distribution, compromising the overall stability and load-carrying capacity of the structure.

Without the required verifications, comparing the acting vertical load to the resistant vertical load, considering slenderness and eccentricity values, offers a preliminary understanding of the potential structural adequacy or vulnerability of the masonry building, which may mean that the failure is about the wall resistance.

By giving proper attention to these red-colored masonry elements, the building's structural performance can be improved, providing a secure environment for occupants and ensuring the long-term integrity of the structure.

Therefore, it is essential to prioritize the verification of the vertical load-bearing capacity of these masonry elements to address any potential weaknesses and ensure their ability to effectively carry the required loads within the building.

IV.8 CONCLUSION

The study delves into the static verification of the masonry structure. The analysis method used and the type of analysis performed are described, providing a framework for the evaluation process. A comprehensive model description, including the materials behaviour hypothesis utilized, is provided to establish the context for the verification. The loads considered, such as seismic and static loads, are discussed in relation to their influence on the structural behavior.

The global static verification process focuses on three key aspects: the slenderness of the masonry, load eccentricity, and the verification of vertical loads. These factors are crucial in assessing the structural stability and load-bearing capacity of the masonry elements. The chapter presents the results of the verification, highlighting the findings of the analysis. These findings offer valuable insights into the behavior and performance of the masonry structure, enabling a comprehensive assessment of its structural integrity and its ability to withstand various loads and external forces.

CHAPTE V
SEISMIC
PERFORMANCE
ANALYSIS

V.1 INTRODUCTION

A building prototype's seismic vulnerability is determined by the probability that it will encounter some sort of financial loss at a specific level of seismic activity. It is generated by combining the fragility model, the probability of experiencing each state of damage for a specific degree of seismic intensity, and the resulting economic losses for each condition of damage.

Analysing the seismic reaction of a building prototype is necessary for the fragility model. The capacity model or pushover curve is a representation of a building's physical response to seismic pressures. The performance point of the prototype can be obtained by combining the capacity curve with the seismic demand, which is represented by the seismic response spectrum. There are various ways to determine the performance point. The degree of damage established according to quantitative parameters (such as displacement) or qualitative ones (such as state of cracking) is compared to the performance point to identify the state of damage obtained by the prototype (light, moderate, extensive, and complete).

It is possible to identify the distinctive characteristics of the fragility curves and derive the probability for each state of damage (light, moderate, extensive, and complete) thanks to the variability of the capacity model, seismic demand, and specification of the degrees of damage. Finally, the creation of vulnerability curves allows for the economic losses caused by physical damage indicated by the risk ratio to be translated.

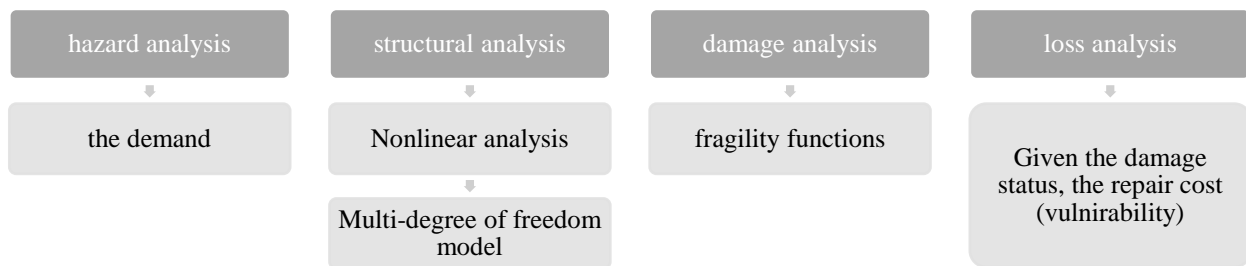


Figure V 1. risk assessment formwork

V.2 SEISMIC SPECTRUM ASSESSMENT

According to the (ATC40), the maximum reaction of any simple linear oscillator exposed to a given stress is summarized by the elastic response spectrum. The response spectrum is created by classifying the maximal elastic response values for each oscillator by vibration period. For a fixed value

of the damping coefficient, the response values are calculated. The graphs used to show the spectral acceleration (S_a) as a function of the period (T) are called spectra.

The elastic Response spectrum: Curves used to assess the maximum response of a building to a past or future earthquake, and according to the **Algerian seismic regulation (RPA 99 2003)** we can determine the demand spectrum as follows:

V.2.1 SITE SELECTION

Site selection should take into account adverse conditions such as active faults, unstable ground, compacts, waterlogged, poorly drained or flood-prone land, underground cavities, uncompacted backfill, uneven surface topography, alluvium, different geological formations, and seismic microzoning studies. The final choice of the site will be decided on the basis of the results of investigations, the importance of which will be related to that of the planned work.

V.2.2 Reconnaissance and soil studies

Soil reconnaissance and studies are essential for structures of medium or greater importance located in areas of medium to high seismicity. These studies must be able to classify the site and detect liquefiable and/or unstable zones, as well as consider the dynamic properties of the soils in calculations.

V.2.3 Modelling and calculation methods

The choice of calculation methods and modelling of the structure must aim to reproduce the real behaviour of the structure as well as possible. It is accepted that structures subjected to seismic action may undergo deformations in the post-elastic range, so linear calculation methods are used. A unique behaviour coefficient is used to determine the design forces of the structure and estimate the inelastic deformations. More elaborate calculation methods may be used, subject to scientific justification.

V.2.4 Seismic zone classification

The national territory is divided into four zones of increasing seismicity, defined on the map of seismicity zones and the associated table.

- Zone O is negligible
- Zone I is low
- Zone IIa is average

- Zone IIb and III is high.

The seismic classification by wilaya and municipality is different when the wilaya is shared between two different seismic zones.

V.2.5 Classification Of Works According to Their Importance

The minimum level of seismic protection granted to a structure depends on its destination and importance to the community. This classification recommends minimum protection thresholds that a client can modify only by upgrading the structure for increased protection, taking into account the nature and destination of the structure with regard to the objectives targeted. Structures must be classified in one of the four (04) groups defined below:

- **Group 1A** includes works of vital importance that must remain operational after a major earthquake. These include strategic decision-making centres, emergency and/or national defense personnel and equipment, public health establishments, public communication establishments, public works of a cultural or historical nature, energy production or distribution centers, and administrative or other buildings that must remain functional in the event of an earthquake.
- **Group 1B** includes works of great importance such as mosques, office buildings, industrial and commercial buildings, schools, universities, sports and cultural buildings, penitentiaries, large hotels, collective housing or office use, public works of national interest or socio-cultural and economic importance, libraries or archive buildings of regional importance, health establishments other than those of group 1A, energy production or distribution centers, and large to medium size water towers and reservoirs.
- **Group 2** is composed of structures that can accommodate up to 300 people simultaneously, such as collective housing, office buildings, industrial buildings, and public car parks.
- **Group 3:** Structures of minor importance, Industrial, agricultural, and temporary buildings are suitable for low-value goods, with limited risk for people.

V.2.6 Site classification

The sites are classified into four categories based on the mechanical properties of the soils.

Table V 1. the sites classifications

| Category | Description | qc(MPA) (c) | N (d) | pl(MPA) (e) | Ep(MPA) (e) | qu (MPA) (f) | Vs (m/s) (g) |
|----------|--|----------------|---------|-------------|----------------|-----------------|--------------|
| S1 | Rocky (a) | - | - | >5 | >100- | >10 | ≥800 |
| S2 | Firm | >15 | >50 | >2 | >20 | >0.4 | ≥400 - <800 |
| S3 | loose soil | 1.5 ~ 15 | 10 ~ 50 | 1 ~ 2 | 5 ~ 20 | 0.1 ~ 0.4 | ≥200 - <400 |
| S4 | Very Loose or Presence of at least 3m of soft clay (b) | <1.5 | <10 | <1 | <5 | <0.1 | ≥100 <200 |

V.2.7 Calculation response Spectrum

The seismic action is represented by the following calculation spectrum.

$$\frac{S_a}{g} = \begin{cases} 1.25A \left(1 + \frac{T}{T_1} \left(2.5\eta \frac{Q}{R} - 1 \right) \right) & 0 \leq T \leq T_1 \\ 2.5\eta(1.25A) \left(\frac{Q}{R} \right) & T_1 \leq T \leq T_2 \\ 2.5\eta(1.25A) \left(\frac{Q}{R} \right) \left(\frac{T_2}{T} \right)^{2/3} & T_2 \leq T \leq 3.0s \\ 2.5\eta(1.25A) \left(\frac{T_2}{3} \right)^{2/3} \left(\frac{3}{T} \right)^{5/3} \left(\frac{Q}{R} \right) & T > 3.0s \end{cases}$$

A : zone acceleration coefficient

Table V 2. The zones acceleration

| Group | Zone | | |
|-------|------|------|------|
| | I | II | III |
| 1A | 0,12 | 0,25 | 0,35 |
| 1B | 0,10 | 0,20 | 0,30 |

| | | | |
|---|------|------|------|
| 2 | 0,08 | 0,15 | 0,25 |
| 3 | 0,05 | 0,10 | 0,15 |

η : damping correction factor for the elastic spectrum $\xi=5\%$ $\eta = \sqrt{7/(2+\xi)} \geq 0.7$

T1, T2 : characteristic periods associated with the category of site

Table V 3. sites periods

| Site | S ₁ | S ₂ | S ₃ | S ₄ |
|---------------------|----------------|----------------|----------------|----------------|
| T _{1(sec)} | 0,15 | 0,15 | 0,15 | 0,15 |
| T _{2(sec)} | 0,30 | 0,40 | 0,50 | 0,70 |

Q : quality factor $Q = 1 + \sum_1^5 P_q$

Table V 4. quality factors index

| Criteria q » | P _q | |
|---------------------------------------|----------------|------------|
| | Observed | N/observed |
| 1. Minimum conditions on bracing rows | 0 | 0,05 |
| 2. In-plane redundancy | 0 | 0,05 |
| 3. Regularity in plan | 0 | 0,05 |
| 4. Regularity in elevation | 0 | 0,05 |
| 5. Material quality control | 0 | 0,05 |
| 6. Execution quality control | 0 | 0,10 |

W : total weight of the structure,
W is equal to the sum of the weights

W_i, calculated at each level (i):

$$W = \sum_{i=1}^n W_i \quad \text{with} \quad W_i = W_{Gi} + \beta W_{Qi}$$

W_{Gi} : weight due to permanent loads and those of fixed equipment possible, integral to the structure

W_{Qi} : charges exploitation

β : weighting coefficient, depending on the nature and duration of the operating load

Table V 5. weighting coefficient

| Case | Type of work | β |
|------|--|------------------|
| 1 | Residential buildings, offices or similar | 0,20 |
| 2 | Buildings open to the public temporarily: - Exhibition halls, sports halls, places of worship, meeting rooms with standing room. - classrooms, restaurants, dormitories, meeting rooms with Seating places | 0,30 0,40 |
| 3 | Warehouses, sheds | 0,50 |
| 4 | Archives, libraries, repositories and similar works | 1,00 |
| 5 | Other premises not referred to above | 0,60 |

R: global behaviour coefficient of the structure

For the elastic spectrum the value of the coefficient $R = 1$ and $\xi = 5$

V.2.8 Observance of Algerian seismic regulations

Because rules change and develop with time, the regulatory review is a critical stage in bringing the building up to code in order to:

- To avoid the technical and legal risks involved with rehabilitation operations.
- Ensure the implementation and follow-up of rehabilitation projects in accordance with continually changing requirements.

The school will be made comply with the current building rules, which concern:

- The Algerian earthquake regulation "RPA" version 2003.
- Fire and panic restrictions.

The classification is required for the definition of the seismic setting investigated which will aid in the selection of the technique of calculation and the identification of the seismic force calculation parameters in order to simulate the building to the earthquake once it has been modelled.

- **Seismic Zone:**

This entails categorizing the structure based on the following criteria:

The school is located in the town of **Annaba**, the latter is in the seismic zone

"Zone II a" which is characterized by an average seismicity.

- **Importance of the building:** classified in the group "medium-sized work in "the category 1A".

site soil classification: Category S2 (firm site): Deposits of very dense sand and gravel and/or over consolidated clay 10 to 20 m thick with $V_S \geq 400$ m/s from a depth of 10 m.

Values of ξ (%): where ξ (%) is percentage of critical damping function of the constituent material, type of structure and the importance of the fillings **adopted: for elastic spectrum " $\xi = 5\%$ "**

- " **$\eta = 1$** ": damping factor
- **R: global behaviour coefficient of the structure:** Value of " **$R = 1$** ".
- **Q: quality factor:** " **$Q = 1$** "
- " **$CT = 0.5$** ": coefficient, depending on the bracing system, the type of filling
- Value of " **$T_1=0.15$ et $T_2=0.40$** "

The response spectrum for the city of Annaba for a category S2 site is shown in the accompanying figure 2.

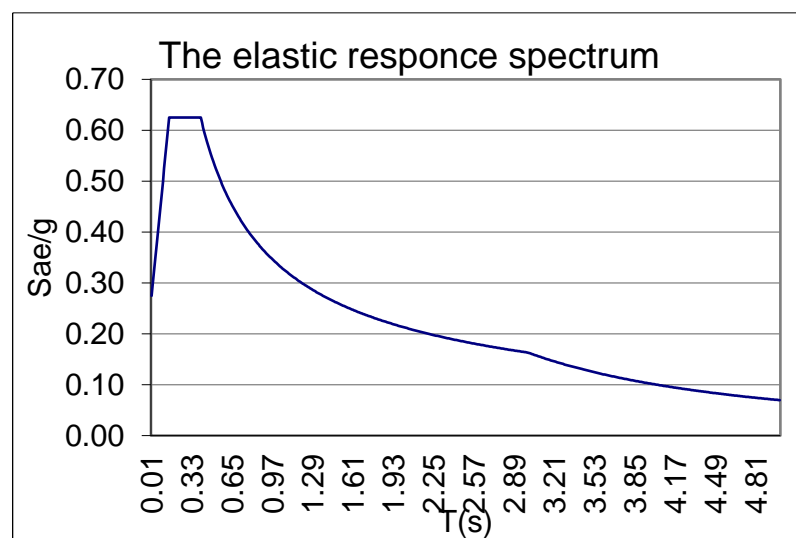


Figure V 2. The elastic response spectrum for A=0.2

V.3 PUSHOVER ANALYSIS DESCRIPTION

In order to carry out the necessary checks on the building in question, it was decided to proceed with the execution of a non-linear static analysis.

The required verifications take the form of a comparison between the capacity curve for the various conditions envisaged and the travel demand envisaged by the legislation.

The capacity curve is identified by means of a maximum displacement-shear diagram at the base.

According to the provisions of the legislation, the load conditions to be examined must consider at least two distributions of inertia forces, one falling into the main distributions (Group 1) and the other into the secondary distributions (Group 2) illustrated below.

- distribution proportional to static forces (Group 1)
- uniform distribution of forces, to be understood as derived from a uniform distribution of accelerations along the height of the building (Group 2);

The analysis, performed in displacement control, proceeds with the calculation of the distribution of forces which generates the value of the required displacement. The analysis is continued until the shear decays to 80% of its peak value. Thus, the value of the maximum displacement at the base of the building generated by that distribution of forces is calculated. This displacement value forms the ultimate value of the building.

The displacement taken into consideration for drawing the capacity curve is that of a point of the building called the control node.

The legislation requires the drawing of a bi-linear capacity curve of an equivalent system (SDOF). The tracing of this curve must take place with a straight line which, passing through the origin, intersects the curve of the real system in correspondence with 70% of the peak value; the second straight line will be parallel to the displacement axis such as to generate the equivalence of the areas between the diagrams of the real system and the equivalent one.

The determination of the curve relating to the equivalent system makes it possible to determine the period with which to obtain the maximum displacement required by the earthquake, according to the spectra reported in the regulations.

The legislation defines an accidental eccentricity of the center of the masses equal to 5% of the maximum dimension of the building in a direction perpendicular to the earthquake.

Based on the type of building and the design choices that are deemed most suitable, the seismic load condition to be taken into consideration can be decided.

- Seismic load: Identify which of the two types of distributions (proportional to the masses or the first way) to take into consideration.
- Direction: Identifies the direction along which the structure is loaded (X or Y of the global system) by the seismic load.

In order to identify the most severe seismic load condition, it was decided to carry out separate analyses by type of load, direction of the earthquake and any accidental eccentricities.

Table V 6 direction of the earthquake

| No. | Seism dir. | Uniform pattern of lateral loads | Eccentricity [mm] | Level | node |
|-----|------------|----------------------------------|-------------------|-------|------|
| 1 | +X | Uniform | 0 | 2 | 3 |
| 2 | +X | Static forces | 0 | 2 | 3 |
| 3 | -X | Uniform | 0 | 2 | 3 |
| 4 | -X | Static forces | 0 | 2 | 3 |
| 5 | +Y | Uniform | 0 | 2 | 3 |
| 6 | +Y | Static forces | 0 | 2 | 3 |
| 7 | -Y | Uniform | 0 | 2 | 3 |
| 8 | -Y | Static forces | 0 | 2 | 3 |

V.4 DATA VALIDATION

V.4.1 Domain resistance calculation

V.4.1.1 Ordinary masonry

As indicated in paragraph C8.7.1.3.1.1 of the Circular n. 7 on 21st January 2019, three main methods of failure can be distinguished:

- by compression bending
- by sliding shear
- by diagonal cracking, dominated by diagonal traction in irregular masonry and in the form of "ladder" through the mortar joints.

The resistant shear is equal to the minimum of the values obtained by using, as appropriate, the verification criteria described below. Look ‘data validation’ in **APPENDIX II**.

V.4.1.1.1 Compression bending

The resistant moment of the section is equal to:

$$M_u = \frac{\sigma_o l^2 t}{2} \left(1 - \frac{\sigma_o}{k f_d} \right) \quad (1)$$

where: $\sigma_o = \frac{N}{lt}$ is the average compression normal stress,

N is the normal force acting on the section,

l is the length of the panel,

t is the thickness of the panel,

f_d is the compressive resistance of the masonry,

κ defines the amplitude of the stress-block (usually $\kappa = 0.85 \div 1$),

The value of k used in the present work is 0.85

Once the value of the resisting moment in the plane is known, the resistive shear of the panel can be calculated as:

$$V_f = \frac{M_u}{\alpha H} \quad (2)$$

where H is the height of the panel and α is a parameter that depends on the static diagram of the panel and is defined as:

$$\alpha = \left| \frac{M_{max}}{M_{max} + M_{min}} \right|$$

M_{max} and M_{min} are respectively the bending moments acting at the upper and lower extremities of the pier. Consequently, in the case in which the panel is comparable to a cantilever $\alpha = 1$ while in the case it is comparable to a beam fixed at both ends $\alpha = 0.5$.

V.4.1.1.2 Sliding shear (new masonry)

The ultimate sliding shear resistance for new masonry can be obtained as described in paragraph 7.8.2.2.2 of Circular no. 7 of 21 January 2019:

$$V_s = f_v l' t \quad (3)$$

where:

- f_v is the shear resistance of the masonry,
- l' is the length of the compressed area of the section,
- t is the thickness of the panel.

The shear resistance f_v is calculated using the Mohr-Coulomb resistance criterion by adding the contribution due to cohesion and the one due to friction:

$$f_v = f_{v0} + \mu \sigma_0 \leq f_{v,lim} \quad (4)$$

where: $\sigma_0 = \frac{N}{l' t}$ is the normal stress acting on the compressed part of the section (partialized section),

- μ is the coefficient of friction (usually assumed to be 0.4),
- f_{v0} is the initial shear resistance in the absence of compression,
- $f_{v,lim}$ is the upper limit value of the shear resistance (cracking of the elements).

Considering the section partialization condition, the length of the compressed portion can be determined (GUIDO MAGENES, 2002).

V.4.1.1.3 Sliding shear (existing regular masonry)

The ultimate sliding shear resistance for regular existing masonry can be obtained using the equation C8.7.1.17 of the Circular which takes into account the equivalent shear resistance of the masonry \tilde{f}_{v0} and an equivalent coefficient of friction \tilde{m} as a function of the local friction parameters of the joint:

$$V_s = \frac{l t}{b} (\tilde{f}_{v0} + \tilde{m} \sigma_0) = \frac{l t}{b} \left(\frac{f_{v0a}}{1 + \mu \phi} + \frac{\mu}{1 + \mu \phi} \sigma_0 \right) \quad (5)$$

where:

- b varies with the h / l aspect ratio of the masonry panel (usually $1 \leq b \leq 1.5$),
- m in the absence of more accurate assessments it can be assumed equal to 0.577,
- F masonry meshing coefficient (in the absence of more accurate assessments it can be assumed equal to 0.5),

$\sigma_o = \frac{N}{lt}$ is the average normal stress acting on the section

f_{v0} is the initial shear strength in the absence of compression

Furthermore, it is necessary that the shear strength thus calculated does not exceed the value evaluated using the same formulas valid for the new masonry and illustrated in the previous paragraph.

V.4.1.1.4 Shear by diagonal cracking (existing irregular masonry)

The ultimate shear-traction resistance can be obtained using the Turnšek - Cacovic resistance criterion (equation C8.7.1.16 of the Circular):

$$V_t = lt \frac{f_{tu}}{b} \sqrt{1 + \frac{\sigma_o}{F_{tu}}} = lt \frac{1.5\tau_{0d}}{b} \sqrt{1 + \frac{\sigma_o}{1.5\tau_{0d}}} \quad (6)$$

where: $\sigma_o = \frac{N}{lt}$ is normal stress of average compression,

b varies with the aspect ratio h/l (usually $1 \leq b \leq 1.5$),

$f_{tu} = 1.5\tau_o$ is the conventional tensile strength of masonry,

t_o reference shear resistance of the masonry.

V.4.1.1.5 Shear by diagonal cracking (existing regular masonry)

In the case of existing regular masonry, the shear resistance for diagonal cracking is equal to the upper limit of the equation C8.7.1.17 of the Circular, i.e. the value $V_{t,lim}$ which can be estimated, approximately, as a function of the tensile failure of the f_{bt} blocks, and taking into account the geometry of the panel. This value can be deduced using the Mann-Muller Resistance Criterion defined in equation C8.7.1.18 of the Circular:

$$V_{t,lim} = \frac{lt}{b} \frac{f_{btd}}{2.3} \sqrt{1 + \frac{\sigma_o}{f_{btd}}} \quad (7)$$

where f_{btd} can be obtained from literature data or through direct characterization tests in the laboratory of samples taken on site, eventually estimating it from the compressive strength of the f_b block, as $f_{btd} = 0.1f_b$.

V.4.1.1.6 Summarizing table of the verification criteria

In summary, the verification of an ordinary masonry wall panel can be summarized using the following table:

Table V 7 summary of verification equations for masonry wall

| | Type of masonry | | |
|------------------|--|--|--|
| | New | Existing regular | Existing irregular |
| Shear resistance | Minimum between: Equation (2) Equation (3) | Minimum between: Equation (2) Equation (3) Equation (5) Equation (7) | Minimum between: Equation (2) Equation (6) |
| Input parameters | l, t, H, a, fd, N, fv0, fv,lim | l, t, H, a, fd, N, fv0, fv,lim, m, F, fbtd | l, t, H, a, fd, N, t0 |

V.5 RESULTS

According to the indications of the law, the following checks must be carried out:

Limit State Collapse (SLC):

D_u^{SLC} : Maximum displacement offered by the structure corresponding to the lesser of:

- the value of the residual basic cut equal to 80% of the maximum one
- the value corresponding to the achievement of the limit threshold of the angular deformation at SLC in all vertical piers of any level in any wall considered significant for safety purposes.

Limit State Life (SLV):

$$D_{max}^{SLV} \leq D_u^{SLV}$$

D_{max}^{SLV} : Maximum displacement required by the standard identified by the elastic spectrum.

D_u^{SLV} : Maximum displacement offered by the structure identified at $0.75 \cdot D_u^{SLC}$.

$$q^* < 3.0$$

q^* : ratio between the elastic response force and the yield strength of the equivalent system

V.5.1 Result details

Table V 8 verification of the critical direction of the earthquake

| No. | Seism dir. | Seismic load | Ecc. [mm] | Dmax ULS [mm] | Du ULS [mm] | q* ULS | ULS Ver. |
|-----|------------|---------------|--------------|------------------|----------------|--------|----------|
| 1 | +X | Uniform | 0 | 22.32 | 40.21 | 2.02 | Yes |
| 2 | +X | Static forces | 0 | 08.33 | 35.07 | 2.63 | Yes |
| 3 | -X | Uniform | 0 | 23.75 | 51.30 | 2.18 | Yes |
| 4 | -X | Static forces | 0 | 29.47 | 38.80 | 3.61 | No |
| 5 | +Y | Uniform | 0 | 09.15 | 10.50 | 2.55 | No |
| 6 | +Y | Static forces | 0 | 18.62 | 17.39 | 3.17 | No |
| 7 | -Y | Uniform | 0 | 15.21 | 12.88 | 2.58 | No |
| 8 | -Y | Static forces | 0 | 18.70 | 18.21 | 3.20 | No |

Table V 9 pushover critical direction of the earthquake

| No. | Seism dir. | Seismic load | Ecc. [mm] | α ULS |
|-----|------------|---------------|--------------|--------------|
| 1 | +X | Uniform | 0 | 1,485 |
| 2 | +X | Static forces | 0 | 1.056 |
| 3 | -X | Uniform | 0 | 1,378 |
| 4 | -X | Static forces | 0 | 0.830 |
| 5 | +Y | Uniform | 0 | 0.760 |
| 6 | +Y | Static forces | 0 | 0.944 |
| 7 | -Y | Uniform | 0 | 0.878 |
| 8 | -Y | Static forces | 0 | 0.938 |

V.5.2 Results legend

Table V 10 colours legend

| RC | |
|----|---------------------|
| | undamaged |
| | Shear failure |
| | Bending damage |
| | Bending failure |
| | Compression failure |
| | Tension failure |
| | Shear failure |

| timber | |
|--------|---------------------|
| | undamaged |
| | Bending failure |
| | Compression failure |
| | Tension failure |

| Steel | |
|-------|---------------------------|
| | undamaged |
| | Bending damage |
| | Compressive damage |
| | tensile damage |
| | Ineffective element |
| | Back to elastic condition |

| masonry | |
|---------|------------------------------|
| | undamaged |
| | Incipient plasticity |
| | Shear damage |
| | Incipient shear failure |
| | Shear failure |
| | Bending damage |
| | Incipient bending failure |
| | Bending failure |
| | Serious crisis |
| | Compression failure |
| | Tension failure |
| | Failure during elastic phase |
| | Ineffective element |

V.5.3 Seismic analysis no. 4 Direction X

We will only show the walls that are most vulnerable.

V.5.3.1 Seismic analysis no. 4 Wall 10

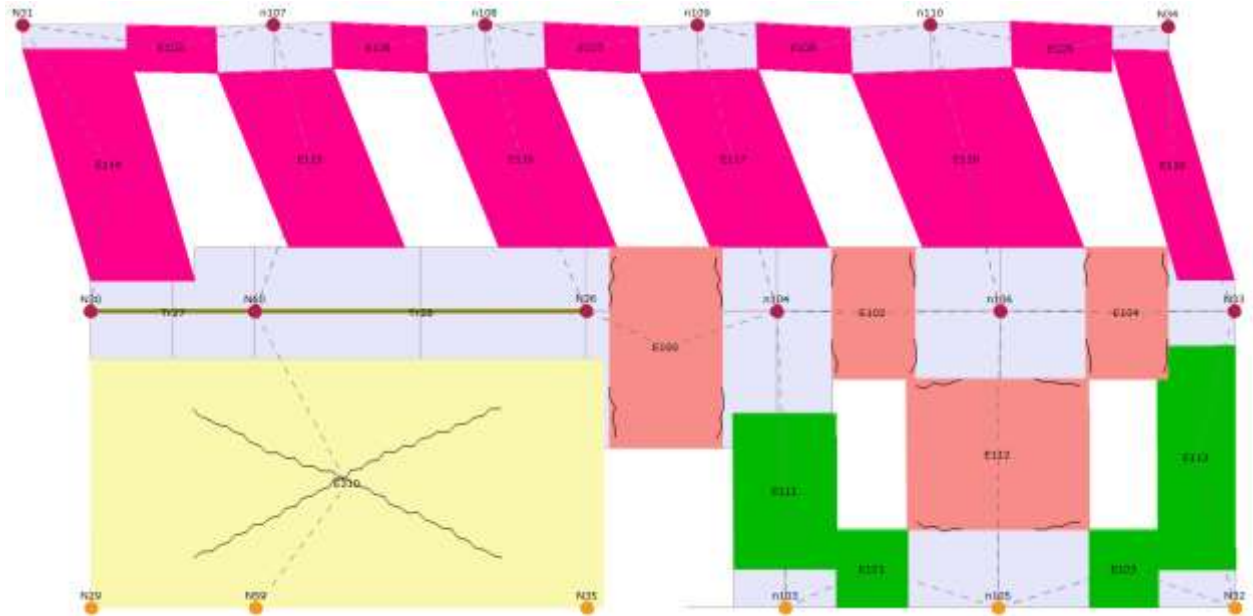


Figure V 3 wall 10 deformations result for X direction

V.5.3.1.1 General data

Table V 11 wall 10 analysis damage results X direction

| Code | Technical standards 2018 |
|------------------|--------------------------|
| Wall | 10 |
| Piers | 110 |
| Analysis | 4 |
| Substep | 47/50 |
| Limit Drift | 0.005 |
| Drift in Step | 0.001 |
| Damage condition | Shear damage |

V.5.3.1.2 Input data from Model

Table V 12 wall 10 input conditions

| | |
|--------------------------|-------------------------------------|
| Typology | Common masonry |
| The material's condition | Existing |
| Constitutive law | Irregular masonry (Turnsek/Cacovic) |

V.5.3.1.2.1 Geometry

Table V 13 wall 10 geometry

| Name | Value | Description |
|-------|-------|-----------------------------|
| h [m] | 3.883 | Height (deformable portion) |
| l [m] | 7.999 | Length |
| t [m] | 0.500 | Thickness |

V.5.3.1.2.2 Masonry: rubble

Table V 14 wall 10 mechanical characteristics

| Name | Value | Description |
|-----------------------------|----------|--|
| f_m [kN/m ²] | 2,000.00 | Average compressive strength of masonry |
| τ [kN/m ²] | 35.00 | Average shear strength in the absence of normal stresses |
| CF | 1.35 | Confidence factor |

V.5.3.1.3 Applied forces (from pushover analysis)

Table V 15 wall 10 applied forces for X direction

| Name | Value | Description |
|----------------|-------|------------------------------|
| N [kN] | 527 | Axial force |
| Vd [kN] | 263 | Shear |
| M top [kNm] | -225 | Upper section bending moment |
| M bottom [kNm] | -794 | Lower section bending moment |

V.5.3.1.4 Resistance forces and verification

Table V 16 wall 10 resistance forces verifications for X direction

| Name | Value | Description |
|---------|-------|---|
| N [kN] | 527 | Axial force (coincident with applied) |
| Vf [kN] | 624 | Shear (principle bending) calculated by interpolation on the resistance domain |
| Vs [kN] | 326 | Shear (principal shear) calculated by interpolation on the resistance domain |
| Vr [kN] | 326 | Shear (minimum between Vf and Vs) |
| Vd/Vr | 0.806 | Safety factor |

V.5.3.1.5 Resistance domain diagram

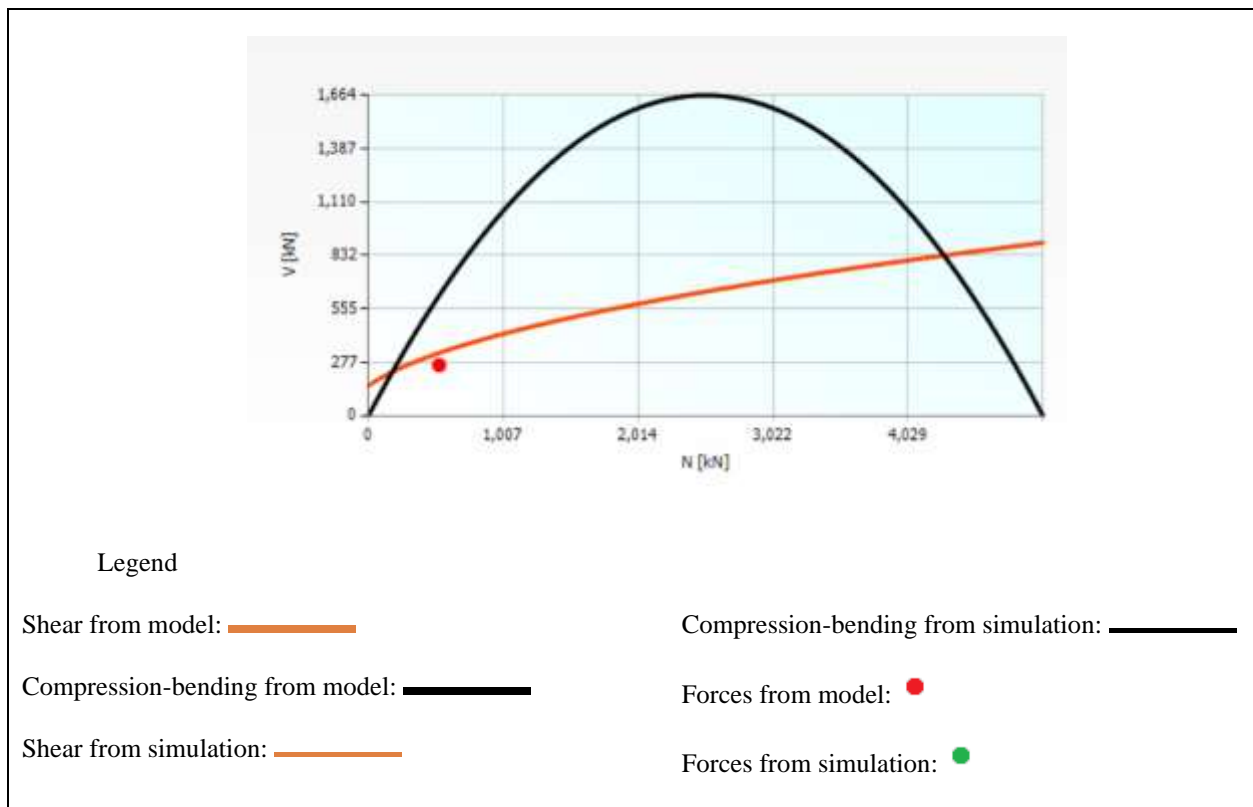
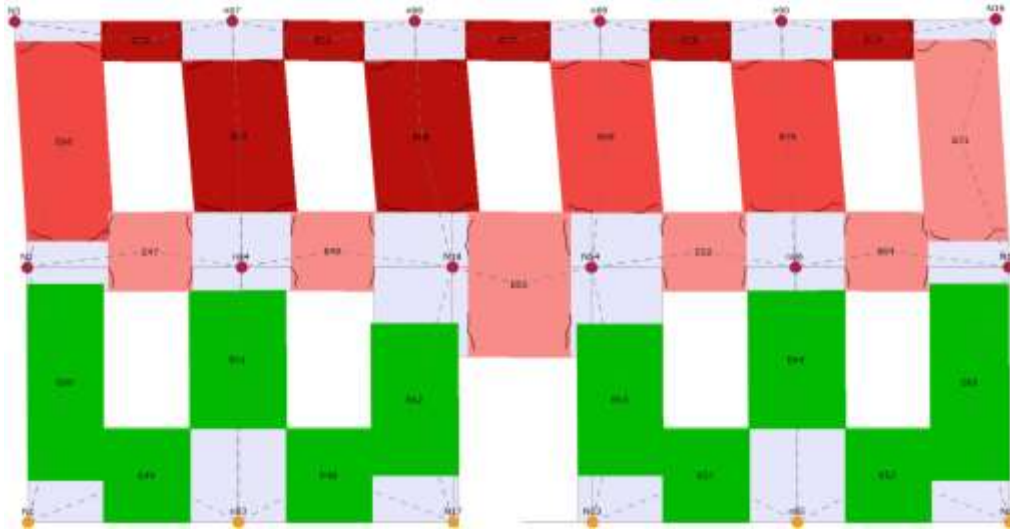


Figure V 4 wall 10 Resistance domain diagram

For the calculation domain look table 1 and 2 on the **APPENDIX II**



V.5.3.2 Seismic analysis no. 4 Wall 7

V.5.3.2.1 General data

Table V 17 wall 7 analysis damage results X direction

| | |
|------------------|---------------------------|
| Code | Technical standards 2018 |
| Wall | 7 |
| Piers | 66 |
| Analysis | 4 |
| Substep | 45/50 |
| Limit Drift | 0.010 |
| Drift in Step | 0.008 |
| Damage condition | Incipient bending failure |

V.5.3.2.2 Input data from Model

Table V 18 wall 7 input conditions

| | |
|--------------------------|-------------------------------------|
| Typology | Common masonry |
| The material's condition | Existing |
| Constitutive law | Irregular masonry (Turnsek/Cacovic) |

V.5.3.2.2.1 Geometry

Table V 19 wall 7 geometry

| Name | Value | Description |
|-------|-------|-----------------------------|
| h [m] | 3.610 | Height (deformable portion) |
| l [m] | 1.580 | Length |
| t [m] | 0.600 | Thickness |

V.5.3.2.2.2 Masonry "rubble"

Table V 20 wall 7 mechanical characteristics

| Name | Value | Description |
|-----------------------------|----------|--|
| f_m [kN/m ²] | 2,000.00 | Average compressive strength of masonry |
| τ [kN/m ²] | 35.00 | Average shear strength in the absence of normal stresses |
| CF | 1.35 | Confidence factor |

V.5.3.2.3 Applied forces (from pushover analysis)

Table V 21 wall 7 applied forces for X direction

| Name | Value | Description |
|----------------|-------|------------------------------|
| N [kN] | 17 | Axial force |
| Vd [kN] | 7 | Shear |
| M top [kNm] | -13 | Upper section bending moment |
| M bottom [kNm] | -13 | Lower section bending moment |

V.5.3.2.4 Resistance forces and verification

Table V 22 wall 7 resistance forces verifications for X direction

| Name | Value | Description |
|---------|-------|---|
| N [kN] | 17 | Axial force (coincident with applied) |
| Vf [kN] | 7 | Shear (principle bending) calculated by interpolation on the resistance domain |

| | | |
|---------|-------|---|
| Vs [kN] | 30 | Shear (principal shear) calculated by interpolation on the resistance domain |
| Vr [kN] | 7 | Shear (minimum between Vf and Vs) |
| Vd/Vr | 1.002 | Safety factor |

V.5.3.2.5 Resistance domain diagram

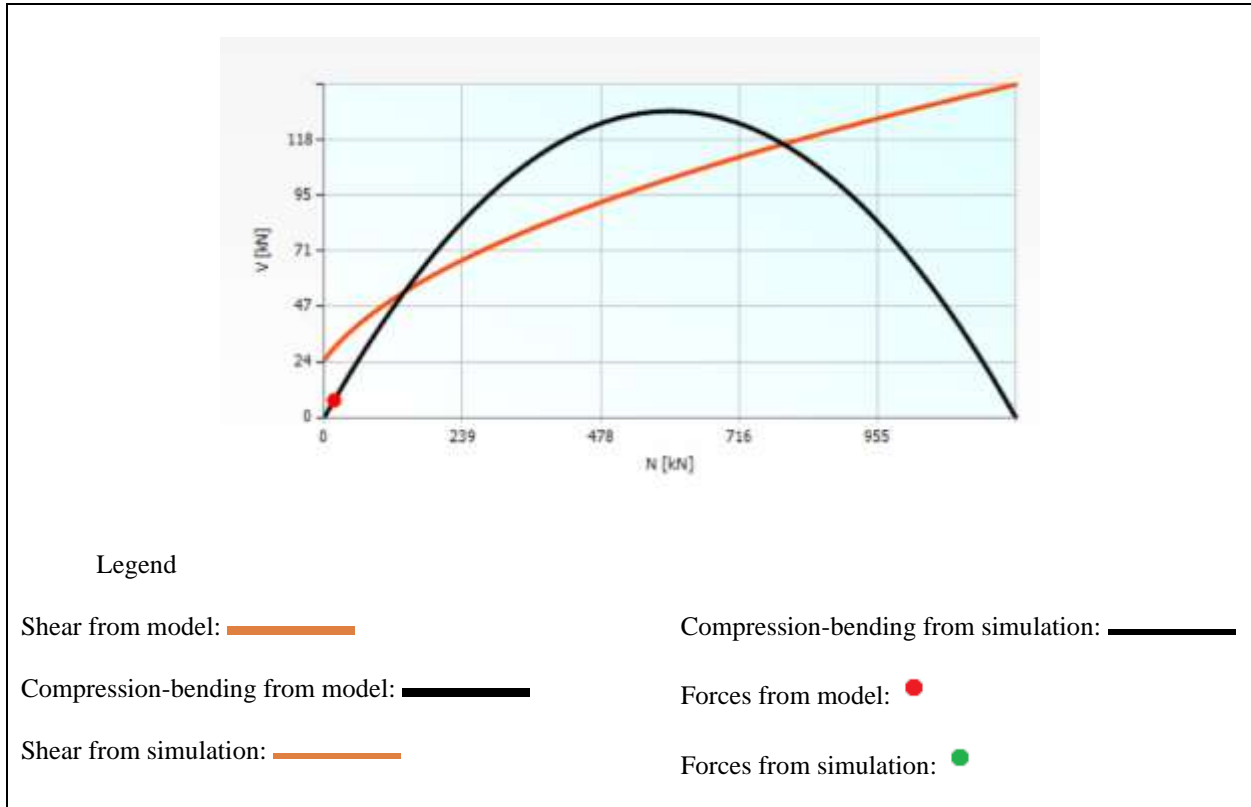


Figure V 6 wall 7 Resistance domain diagram

For the calculation domain look table 3 and 4 on the **APPENDIX II**

V.5.3.3 Plan deformed shape

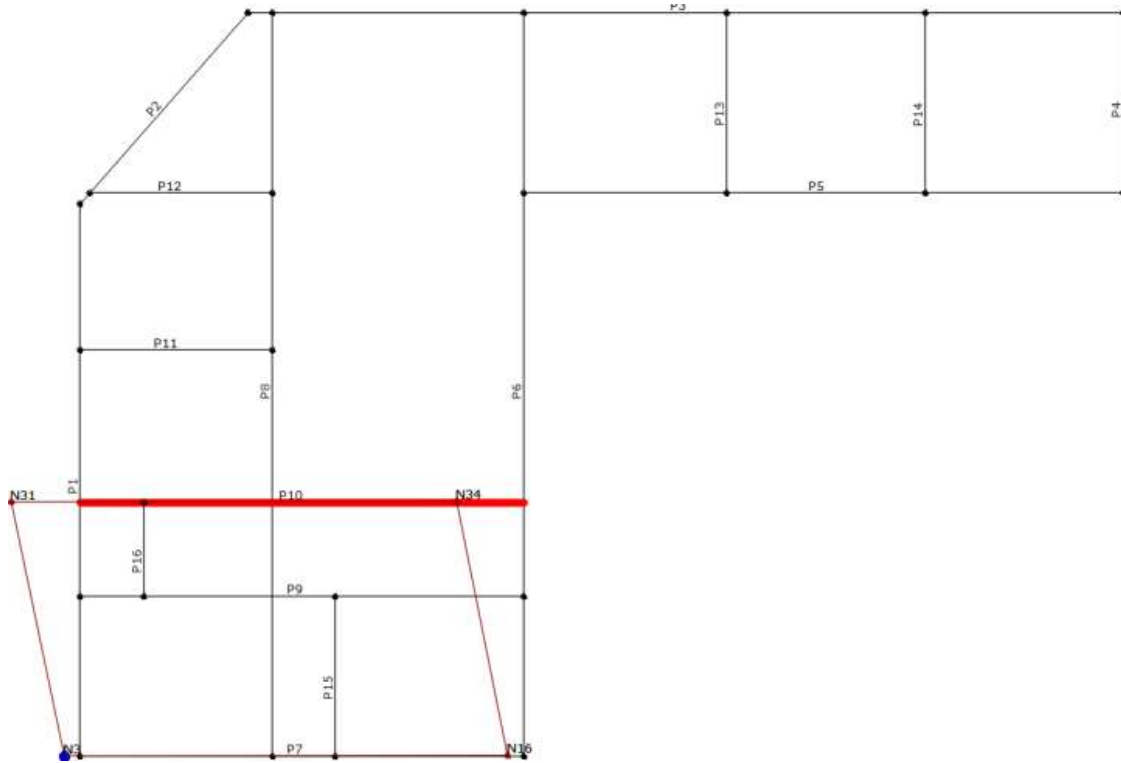


Figure V 7 Plan deformed shape for X direction

V.5.3.4 Pushover curves (analysis n. 4)

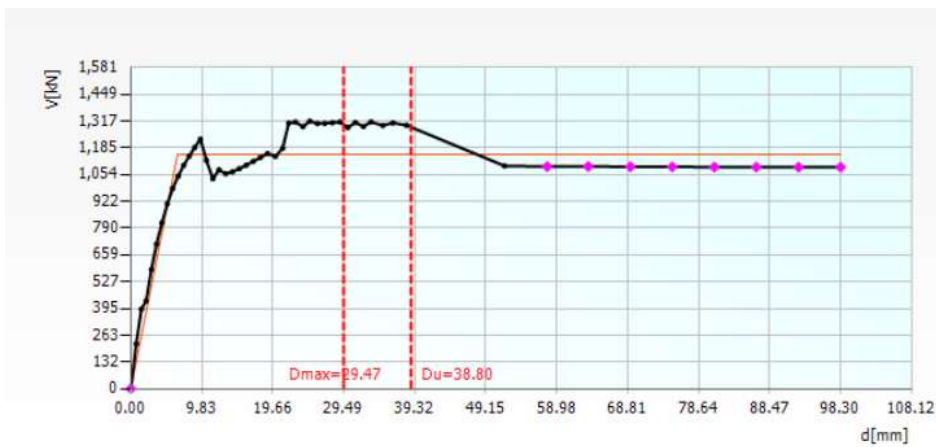


Figure V 8 Pushover curves for X direction

V.5.4 Seismic analysis no. 5 Direction Y

Wi will only show the walls that are most vulnerable.

V.5.4.1 Seismic analysis no. 5 Wall 8

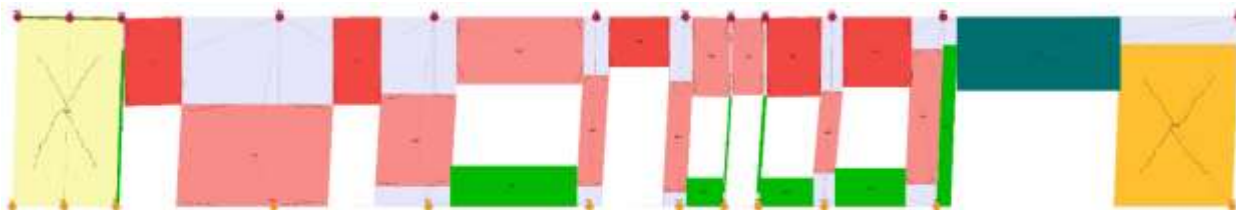


Figure V 9 wall 8 Resistance domain diagram

V.5.4.1.1 General data

Table V 23 wall 8 deformations result for Y direction

| Code | Technical standards 2018 |
|------------------|--------------------------|
| Wall | 8 |
| Piers | 88 |
| Analysis | 5 |
| Substep | 14/15 |
| Limit Drift | 0.005 |
| Drift in Step | 0.003 |
| Damage condition | Shear damage |

V.5.4.1.2 Input data from Model

Table V 24 wall 8 input conditions

| | |
|--------------------------|-------------------------------------|
| Typology | Common masonry |
| The material's condition | Existing |
| Constitutive law | Irregular masonry (Turnsek/Cacovic) |

V.5.4.1.2.1 Geometry

Table V 25 wall 8 geometry

| Name | Value | Description |
|-------|-------|-----------------------------|
| h [m] | 2.250 | Height (deformable portion) |
| l [m] | 1.848 | Length |
| t [m] | 0.600 | Thickness |

V.5.4.1.2.2 Masonry: rubble

Table V 26 wall 8 mechanical characteristics

| Name | Value | Description |
|-----------------------------|----------|--|
| f_m [kN/m ²] | 2,000.00 | Average compressive strength of masonry |
| τ [kN/m ²] | 35.00 | Average shear strength in the absence of normal stresses |
| CF | 1.35 | Confidence factor |

V.5.4.1.3 Applied forces (from pushover analysis)

Table V 27 wall 8 applied forces for Y direction

| Name | Value | Description |
|----------------|-------|------------------------------|
| N [kN] | 94 | Axial force |
| Vd [kN] | 63 | Shear |
| M top [kNm] | 71 | Upper section bending moment |
| M bottom [kNm] | 71 | Lower section bending moment |

V.5.4.1.4 Resistance forces and verification

Table V 28 wall 8 resistance forces verifications for Y direction

| Name | Value | Description |
|---------|-------|---|
| N [kN] | 94 | Axial force (coincident with applied) |
| Vf [kN] | 72 | Shear (principle bending) calculated by interpolation on the resistance domain |
| Vs [kN] | 63 | Shear (principal shear) |

| | | |
|------------|-------|--|
| | | calculated by interpolation on the resistance domain |
| V_r [kN] | 63 | Shear (minimum between V_f and V_s) |
| V_d/V_r | 1.000 | Safety factor |

V.5.4.1.5 Resistance domain diagram

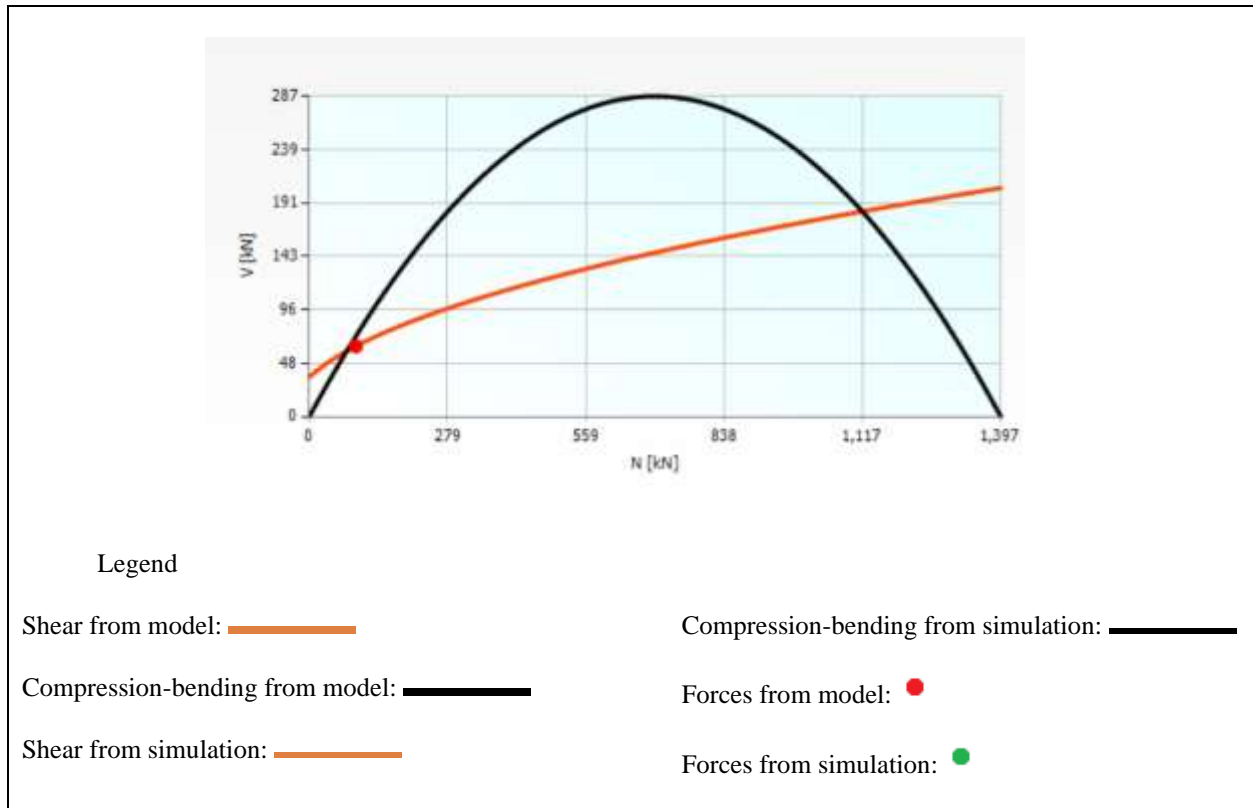


Figure V 10 wall 8 Resistance domain diagram

For the calculation domain look table 5 and 6 on the **APPENDIX II**

V.5.4.2 Plan deformed shape

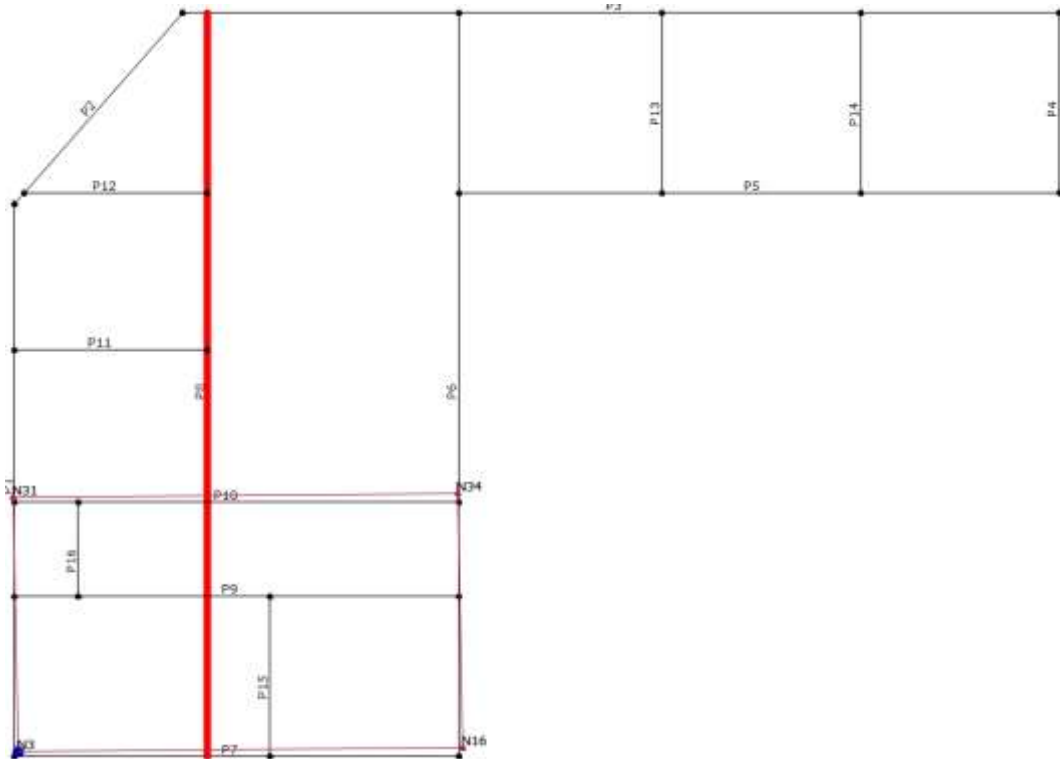


Figure V 11 Plan deformed shape Y direction

V.5.4.3 Pushover curves (analysis n. 4)

The mechanics-based approaches construct the strength, stiffness, and deformation parameters of single masonry walls using simplified structural mechanics concepts, and then combine those parameters to create the building's capacity curve.

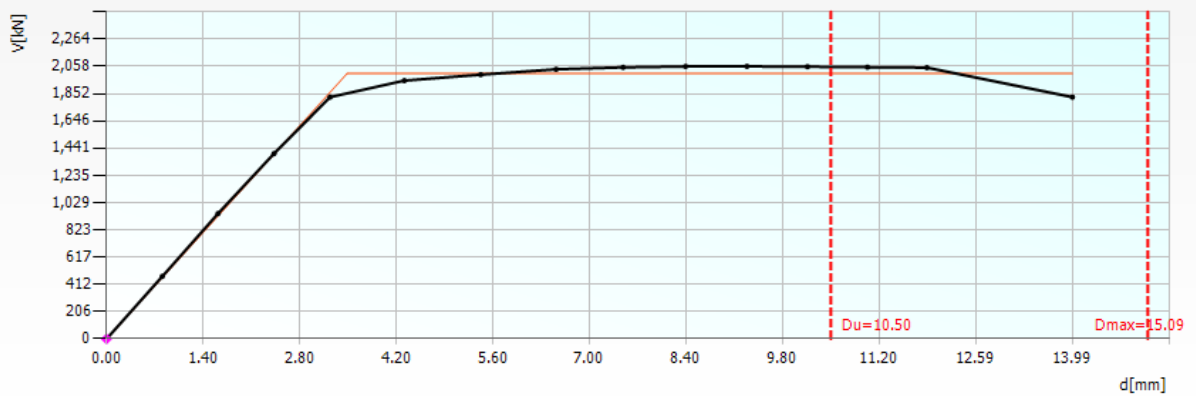


Figure V 12 Pushover curves Y direction

V.6 ASSESSMENT OF THE PERFORMANCE POINT (X DIRECTION)

The intersection of the demand spectrum and capacity curve is a critical point that determines the seismic performance of a structure. If the capacity curve lies above the demand spectrum, it indicates that the structure has sufficient strength to withstand the expected seismic forces. Conversely, if the capacity curve intersects or falls below the demand spectrum, it suggests that the structure may experience significant damage or failure during an earthquake.

To assess the performance point, we have seen choosing two different methods (graphical, and empirical).

All calculation details are in the table 7, 8, 9,10 **Appendix II**

V.6.1 Graphical ‘using excel table’:

The method used is the (N2) approach as described in the seismic analysis part:

V.6.1.1 SDOF to MDOF

The capacity curve can be transformed into an equivalent capacity curve relating the (shear, displacement) of a structure to a single degree of freedom. For all calculation look table 8 **Appendix II**

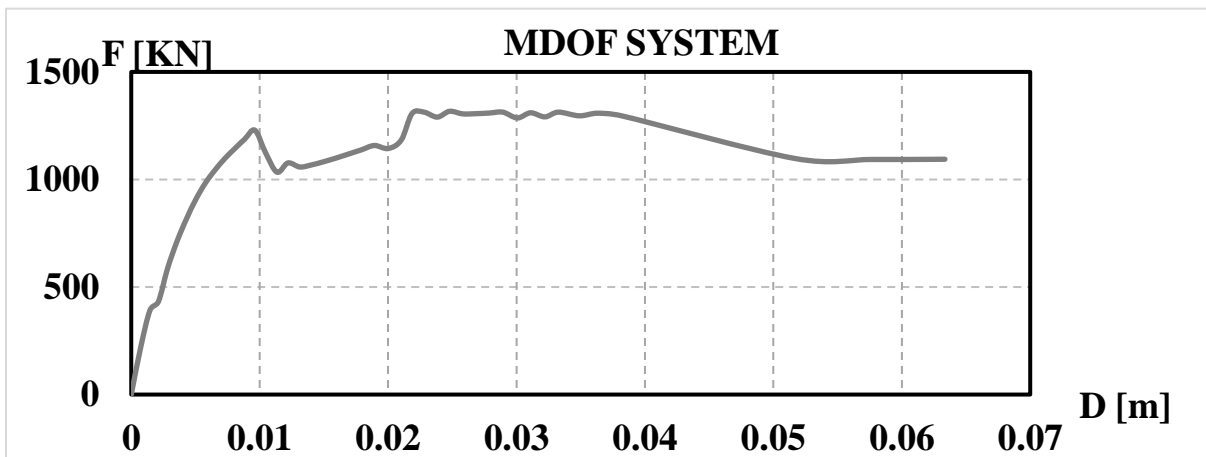


Figure V 13 MDOF capacity curve for X direction

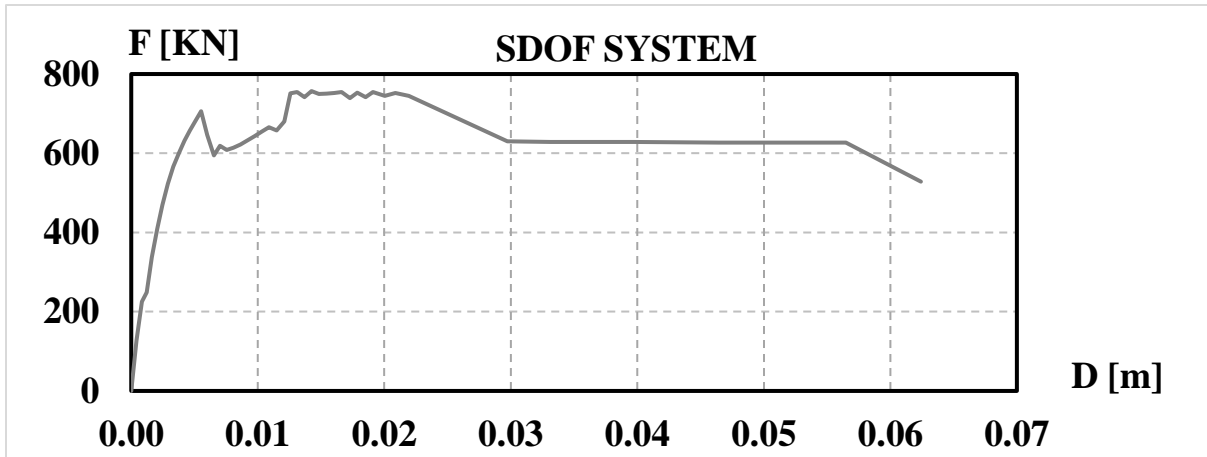


Figure V 14 SDOF capacity curve for X direction

V.6.1.2 The bi-linear equivalent capacity curve

The bi-linear equivalent capacity curve represents dual stiffness behaviour in a structure: elastic until yielding and post-yield with reduced stiffness. It indicates ultimate strength, ductility, and seismic performance. And characterized by the lateral resistance represented by a horizontal plateau bounded by the elastic displacement and the ultimate displacement at the top of the building. see table 7 **Appendix II**.

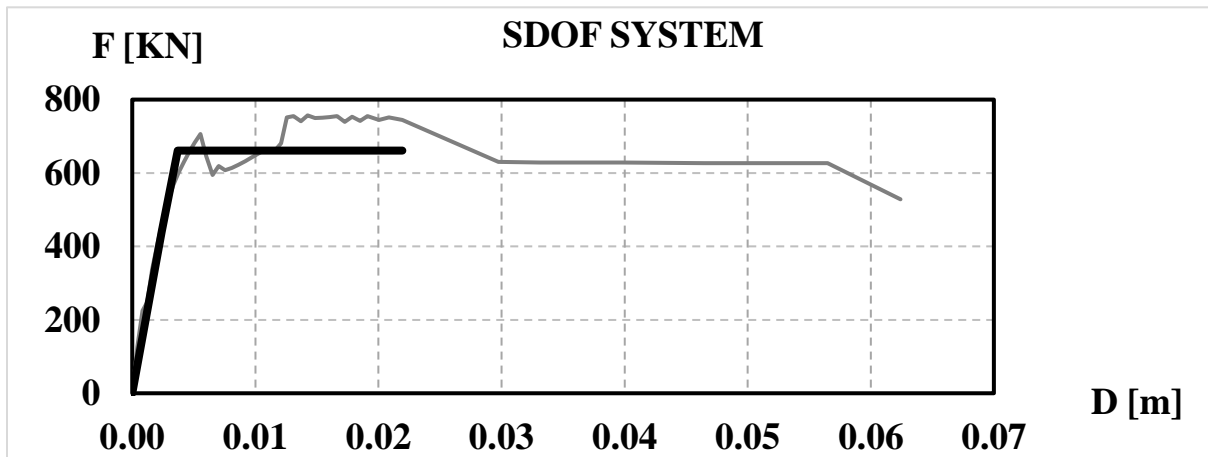


Figure V 15 bi-linear equivalent capacity curve X direction

V.6.1.3 The intersection

The intersection of the bi-linear equivalent capacity curve and the Acceleration-Displacement Response Spectrum (ADRS) demand is determined through a systematic analysis process. First, the bi-linear capacity curve is constructed, considering the structural properties such as stiffness, strength, and energy dissipation. Simultaneously, the ADRS demand curve is developed, representing the expected ground motion intensities. Plotting both curves on the same graph allows for the identification of the intersection point. By analysing the location of this point relative to the different segments of the bi-linear curve, the structure's ability to withstand the seismic demand can be assessed. If the intersection lies below the post-yield segment, it signifies that the structure can resist the seismic forces without exceeding its capacity, indicating a favorable (Transport, 2019) safety margin and reliable seismic performance.

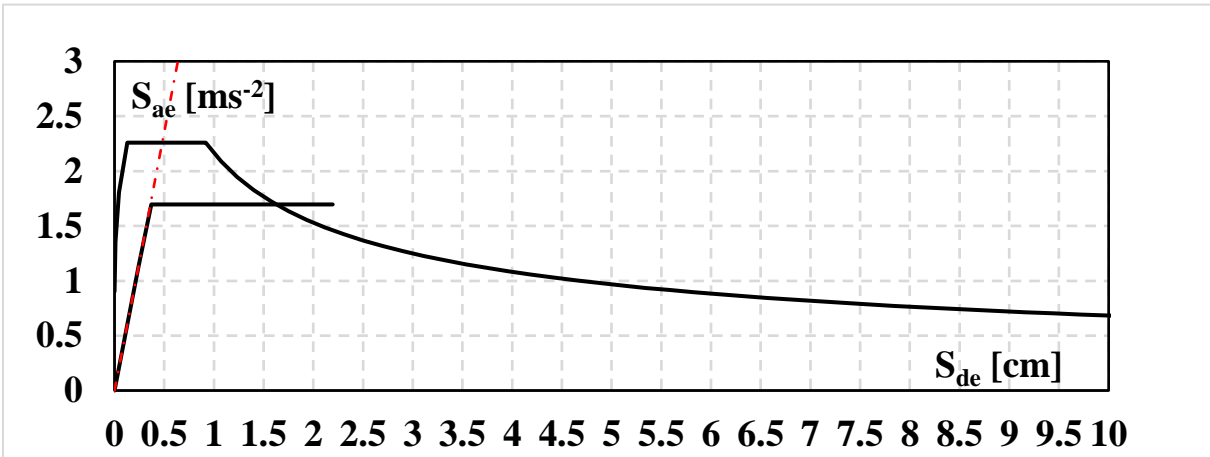


Figure V 16 intersection of the capacity curve and the demand X direction

V.6.2 Numerical:

According to (Sergio Lagomarsino, 2006)the performance point, Sd, in terms of displacement, is determined by a closed analytical function as a function of the demand and capacity curves:

$$S_d * = \begin{cases} \left[1 + \left(\frac{S_{ae}(T)}{a_y} - 1 \right) \left(\frac{T_c}{T} \right) \right] dy & , \quad T < T_c \text{ and } \frac{S_{ae}(T)}{a_y} > 1 , \\ \left(\frac{S_{ae}(T)}{a_y} \right) dy & , \quad T_c \leq T < T_D \text{ or } \frac{S_{ae}(T)}{a_y} < 1 \\ \left(\frac{S_{ae}(T_D) T_D^2}{4\pi^2} \right) & , \quad T \geq T_D \end{cases}$$

Or even by:

$$S_d^* = \begin{cases} \left[1 + (q - 1) \left(\frac{T_c}{T} \right) \right] dy & , \quad T < T_c \text{ and } q > 1, \\ q dy & , \quad T_c \leq T < T_D \text{ or } q < 1 \\ \left(\frac{S_{ae}(T_D) T_D^2}{4\pi^2} \right) & , \quad T \geq T_D \end{cases}$$

With: $q = \frac{du}{dy}$

Table V 29 performance point X direction numerical method data

| T [sec] | TC [sec] | Sae [m/s ²] | ay [m/s ²] | Dy [m] | Sd*[m] |
|-------------|----------|-------------------------|------------------------|--------|---------|
| 0.29 | 0.4 | 6.1 | 1.7 | 0.0037 | 0.01684 |

V.6.3 Finds

Using different methods to assess the performance point gave an approximate value which around ‘1.7cm’

V.7 ASSESSMENT OF THE PERFORMANCE POINT (Y DIRECTION)

V.7.1 Graphical ‘using excel table’

The method used is the (N2) approach as described in the seismic analysis part:

all calculation details are in the table 11, 12, 13,14 **Appendix II**

V.7.1.1 SDOF to MDOF

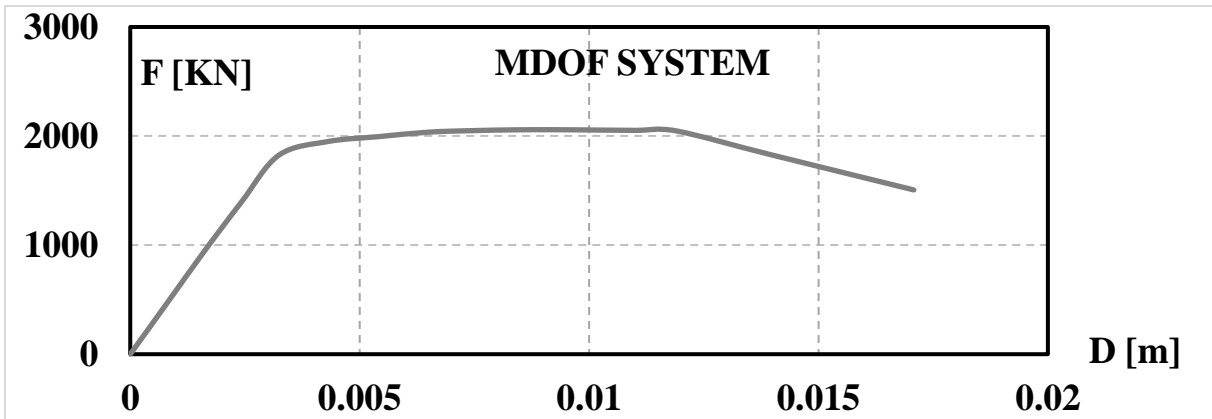


Figure V 17 MDOF capacity curve Y direction

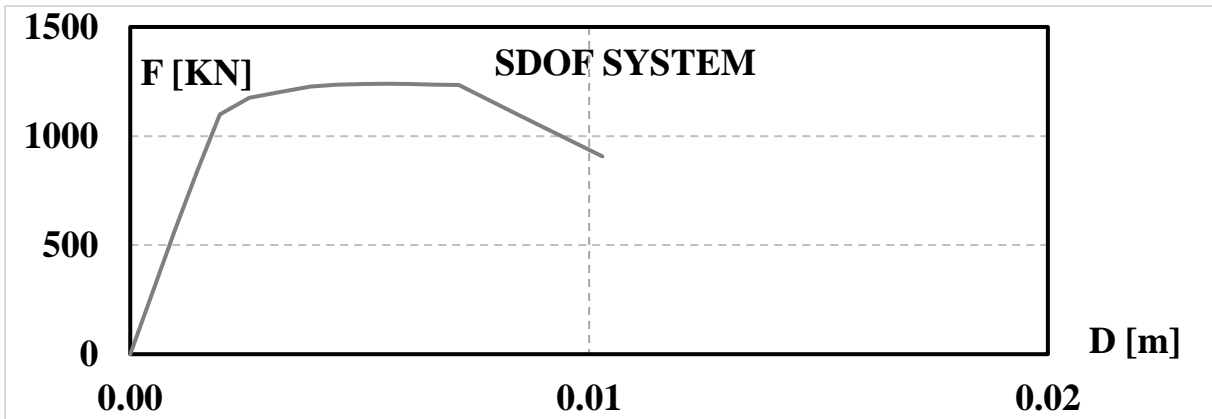


Figure V 18 SDOF capacity curve Y direction

V.7.1.2 The bi-linear equivalent capacity curve

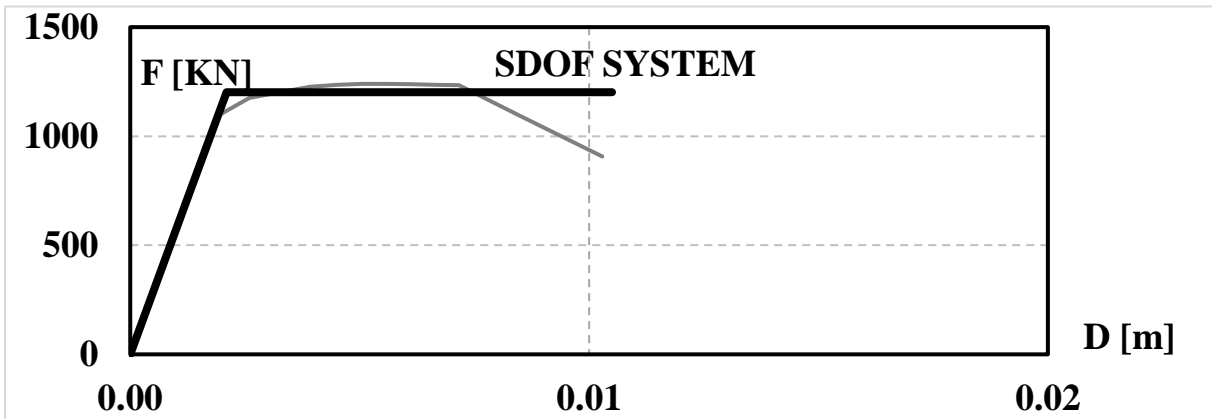


Figure V 19 bi-linear equivalent capacity curve Y direction

V.7.1.3 The intersection

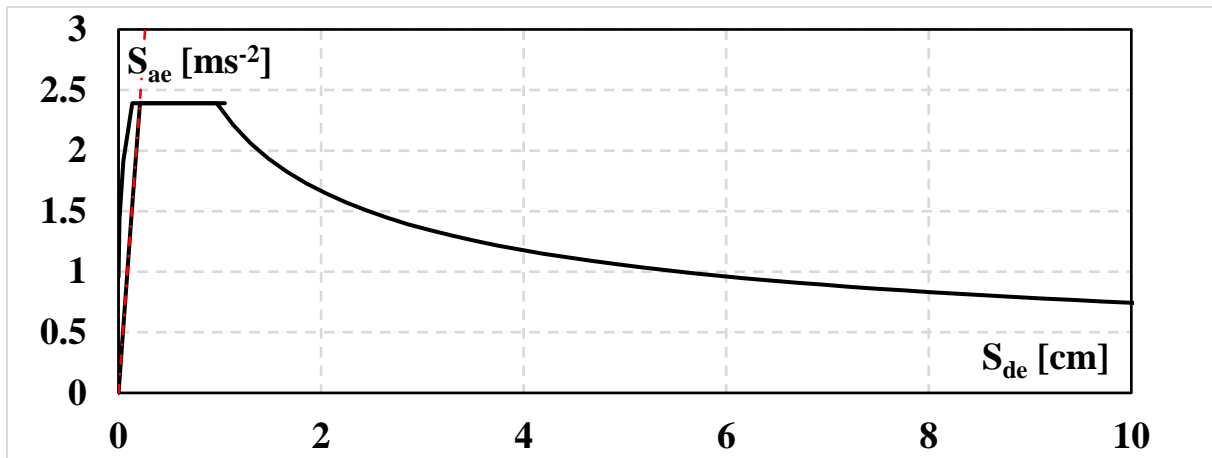


Figure V 20 intersection of the capacity curve and the demand Y direction

V.7.2 Numerical

According to (Sergio Lagomarsino, et al,2006), performance point, S_d , in terms of displacement, is determined by a closed analytical function as a function of the demand and capacity curves:

$$S_d * = \begin{cases} \left[1 + \left(\frac{S_{ae}(T)}{ay} - 1 \right) \left(\frac{T_c}{T} \right) \right] dy & , \quad T < T_c \text{ and } \frac{S_{ae}(T)}{ay} > 1, \\ \left(\frac{S_{ae}(T)}{ay} \right) dy & , \quad T_c \leq T < TD \text{ or } \frac{S_{ae}(T)}{ay} < 1 \\ \left(\frac{S_{ae}(TD)TD^2}{4\pi^2} \right) & , \quad T \geq TD \end{cases}$$

Or even by :

$$S_d * = \begin{cases} \left[1 + (q - 1) \left(\frac{T_c}{T} \right) \right] dy & , \quad T < T_c \text{ and } q > 1, \\ q dy & , \quad T_c \leq T < TD \text{ or } q < 1 \\ \left(\frac{S_{ae}(TD)TD^2}{4\pi^2} \right) & , \quad T \geq TD \end{cases}$$

With: $q = \frac{du}{dy}$

Table V 30 performance point Y direction numerical method data

| T [sec] | TC [sec] | Sae [m/s ²] | ay [m/s ²] | Dy [m] | Sd*[m] |
|--------------|----------|-------------------------|------------------------|--------|--------|
| 0.186 | 0.4 | 6.1 | 2.39 | 0.0021 | 0.0093 |

V.7.3 Finds:

Using different methods to assess the performance point gave an approximate value which around ‘1cm’

V.8 VULNERABILITY ANALYSIS:

Since vulnerability modelling is typically confined by a lack of knowledge and information, there may be an important amount of uncertainty throughout the assessment process. The exposure and vulnerability models are mostly affected by epistemic uncertainties, whereas the definition of the seismic hazard is affected by both epistemic and aleatory uncertainty. A risk assessment study's overall findings and conclusions may be significantly impacted by the use of various input models, such as ground motion models, structural capacity models, or repair cost data. Therefore, regardless of the methodology used, identifying, quantifying, and incorporating the uncertainties associated with each input parameter is one of the most crucial parts in the creation of a seismic vulnerability model.

V.8.1 Fragility and vulnerability functions

The terms fragility functions and vulnerability functions, which are both related to seismic damageability, must be distinguished in this context. An intensity measure, is used to define a seismic fragility function, which quantifies the probability that some unwanted event or physical damage will occur as a function of the intensity measure. As a function of a structure independent intensity measure, a seismic vulnerability function determines the economic loss, the damage factor defined as the repair to replacement cost ratio. For instance, a fragility function can indicate the probability that a structure will collapse given a certain amount of trembling. The damage factor (in terms of repair to replacement cost ratio) for the building given the intensity of the shaking would be provided by analogous vulnerability functions.

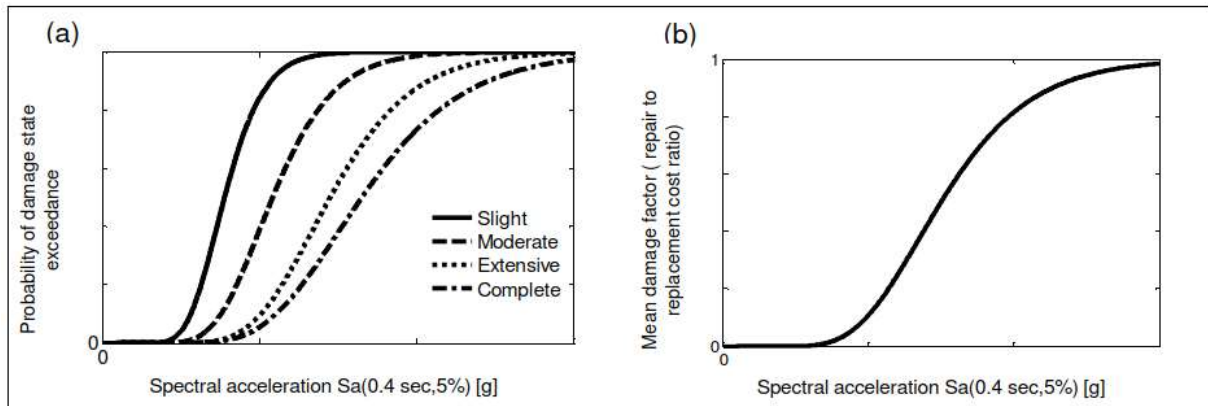


Figure V 21 fragility curves stages

The fragility functions may also depend on a structural response parameter, such as the inter-storey drift ratio or the roof displacement transformed to spectral displacement (Kircher et al. 1997a). They are described as a displacement fragility function in this instance. These fragility functions are a crucial part of the seismic vulnerability modelling, which uses displacements to gauge the severity of damage caused by earthquakes.

According to Rossetto and Elnashai (2005), fragility and vulnerability functions can be derived from empirical data, expert judgment, analytical models, or any combination of these approaches. There are uncertainties in the evaluation processes and data used regardless of the method employed to anticipate the seismic damageability. They consist of measurements with observational uncertainty:

- the analysis and database's quality are inconsistent.
- the ground's motion is variable.
- uncertainty over the experts' opinions.
- the strength and stiffness of structural materials and components are subject to ambiguity because of model simplification.
- Uncertainties in the definition of the damage states, variances in the geometry and material qualities of the structures, and their seismic demand and capability.

V.8.1.1 Analytical functions for fragility curve

according to (Giovinazzi, 2005), The probability of a particular damage state occurring or exceeding a given damage state for a structural response parameter (such as spectral inelastic displacement demand) is typically given in the form of a lognormal distribution in analytical displacement

fragility functions. The following equation describes the conditional possibility of achieving a specific damage state, DS, given the spectral displacement, Sd:

$$p [DS|Sd] = \Phi \left[\frac{1}{\beta_{ds}} \ln \left(\frac{Sd}{\bar{S}_d \cdot DS} \right) \right]$$

$$B_{ds} = \sqrt{\text{CONV}(\beta_c, \beta_d)^2 + \beta_t^2}$$

Or even: $B_{ds} = B_k$ and $B_k = 0.4 \ln(q)$

Damage limit states **SD,k(k = 1/4)** are identified directly on the capacity curve as a consequence of the yielding **dy** and the ultimate displacements **du** to determine the damage suffered by the structures.

$$\left\{ \begin{array}{l} DS1 = 0.7 dy \\ DS2 = 1.5 dy \\ DS3 = 0.5(du + dy) \\ DS4 = du \end{array} \right.$$

q: is the behaviour factor behaviour factor and du; dy are the displacements

Recent vulnerability modelling has a heavy emphasis on analytical techniques. Analytical methods take into account all uncertainties. However, analytical techniques must require substantial computational effort.

Sd,DS is the median spectral displacement value at which the building enters the damage state DS.

β_{ds} stand for the natural logarithm of spectral displacement standard deviation for damage state DS.

Φ stands for the standard normal cumulative distribution function. Any given damage state's total variability comes from three main sources, including the variation in the **capacity** model β_c .

the variability in the **demand** model β_d . and the variability in the **damage** state threshold from the damage model β_t .

By performing seismic demand studies on capacity curves and calculating the probability that certain damage states would be reached or exceeded, the convolution (CONV) is assessed.

Ps1 is the fragility curve for the probability of damage state 1 and so on ..etc

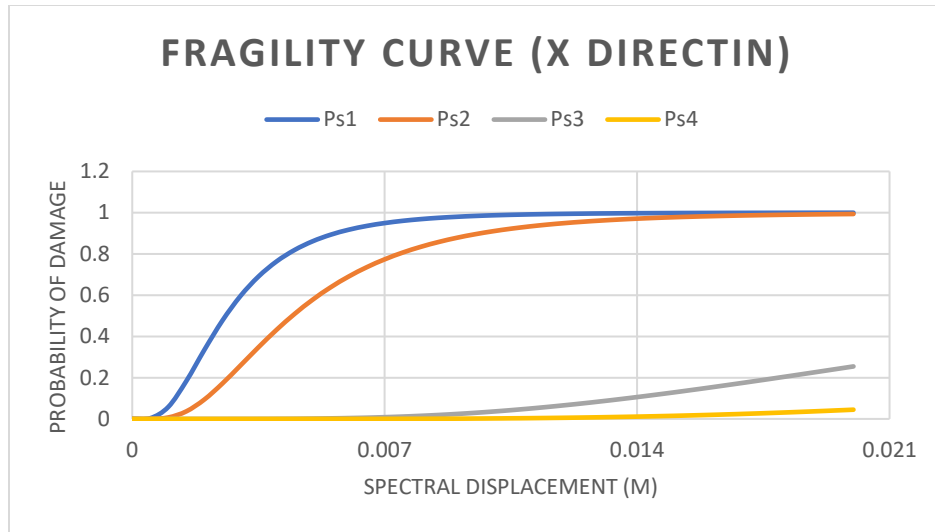


Figure V 22 fragility curve (X direction)

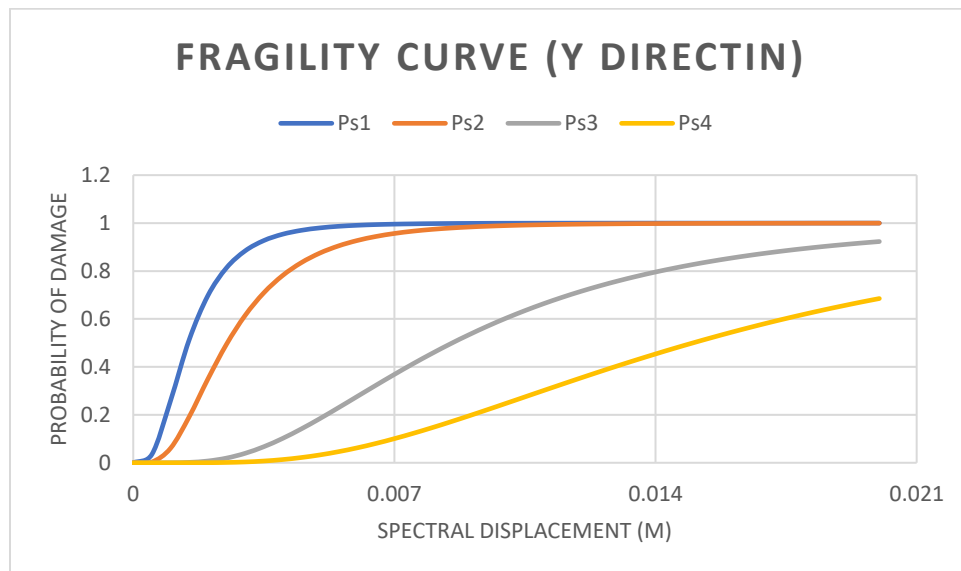


Figure V 23 fragility curve (Y direction)

V.8.1.2 Damage distribution of the studied structure

A vulnerability histogram for a structure and its damages due to seismic demand provides insights into the distribution of vulnerability levels and the resulting damages caused by earthquakes. This assessment involves evaluating various parameters such as construction materials, structural design, age, maintenance, and location to determine the vulnerability of the structure. By assigning vulnerability levels, such as low, medium, and high, or numerical values, a vulnerability profile can be created. Additionally, considering the seismic demand or the forces imposed on the structure during an earthquake, can be conducted to determine the expected damages.

Making reference to the EMS-98 scale with is the macroseismic method and the mechanical method to best understanding of the damage level is summarised in the table 31 form (Sergio Lagomarsino, et al,2006).

Table V 31. Correspondence between damage level D_{sk} and damage grades D_k related to structural and non-structural damage, (Sergio Lagomarsino, et al,2006).

| D_{sk} | D_k | Structural (SD) and non-structural (N-SD) damage |
|---|---|---|
| Slight (D_{s1}) Moderate (D_{s2}) Extensive (D_{s3}) Complete (D_{s4}) | Slight (D_1) Moderate (D_{s2}) Heavy (D_3) Very heavy (D_4) Destruction (D_5) | No SD slight N-SD Slight SD moderate N-SD Moderate SD heavy N-SD Heavy SD very heavy N-SD Very heavy SD |

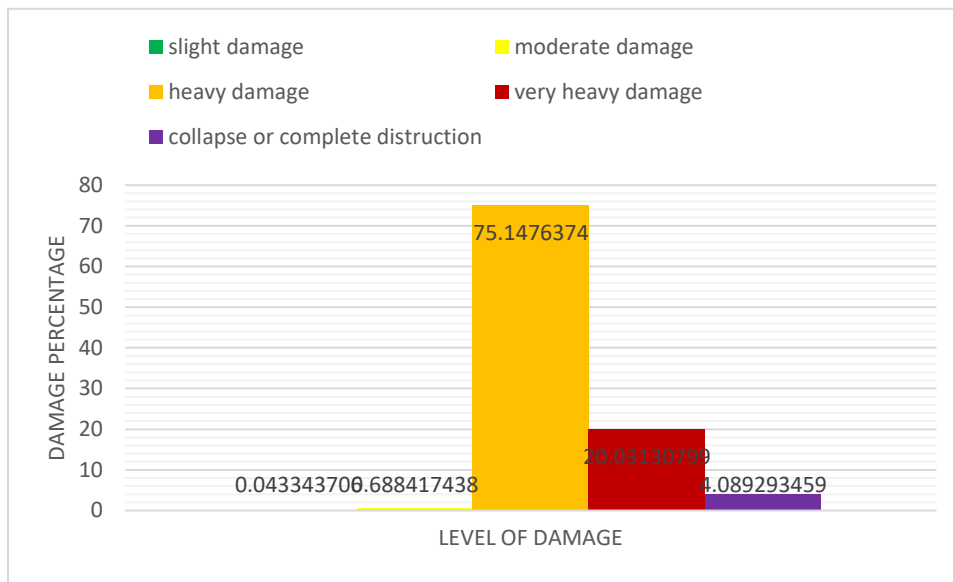


Figure V 24 damage histogram (X direction)

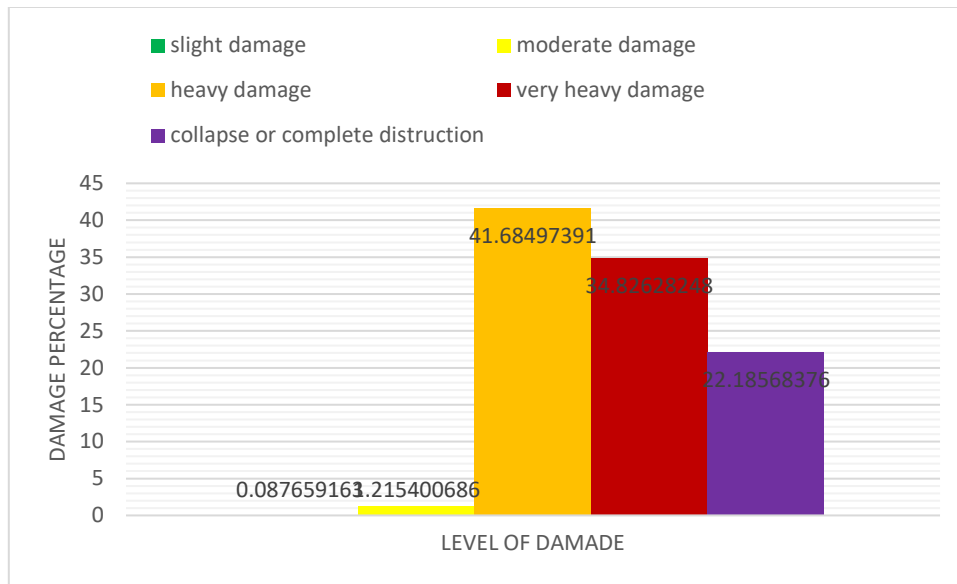


Figure V 25 Vulnerability histogram (Y direction)

V.8.1 Finds

Upon conducting an extensive seismic and vulnerability analysis of the masonry structure, it has become evident that the seismic behaviour and vulnerability of the structure exhibit notable variations across its different sides. The analysis has provided valuable insights, revealing that while the structure as a whole has not suffered from complete or irreparable damage, specific elements within it have experienced severe degradation. In light of these findings, it is imperative to implement targeted repair and rehabilitation measures to address the areas that have been adversely affected.

V.9 CONCLUSION

We have undertaken an extensive evaluation of the masonry structure's behaviour when subjected to seismic forces, while also investigating its susceptibility to damage. The chapter encompasses a comprehensive range of crucial aspects related to seismic spectrum assessment. It commences with a meticulous calculation of the response spectrum, ensuring strict adherence to the Algerian seismic regulations that govern the structural safety within the region.

Moreover, we delve into the methodology of pushover analysis, providing a meticulous and detailed description of the structure's response under the influence of seismic loads. Stringent data validation techniques, including domain resistance calculation, are employed to establish the utmost accuracy and reliability of the analysis outcomes.

The subsequent presentation of results showcases an in-depth examination of the seismic analysis, featuring comprehensive result details, an illustrative results legend, and detailed findings from the seismic analyses conducted for both the X and Y directions. These findings offer invaluable insights into the structure's behaviour, pinpointing areas of concern and potential vulnerability, thus empowering decision-makers with critical information.

In addition to the seismic analysis, the chapter encompasses a meticulous vulnerability analysis that entails the development of fragility and vulnerability functions. These functions are meticulously designed to assess the likelihood and severity of damage, allowing for a comprehensive understanding of the structure's vulnerability. The findings derived from this analysis not only enhance our comprehension of the structure's behaviour but also serve as a foundation for proposing effective mitigation measures.

Considering the outcomes and recommendations derived from the seismic and vulnerability analyses, it is crucial to propose targeted solutions to address the identified vulnerabilities. These solutions may encompass the implementation of retrofitting techniques, reinforcing critical structural elements, or considering architectural modifications to enhance the structure's resilience in the face of potential seismic events. By embracing and implementing these recommended measures, stakeholders can ensure the long-term safety, stability, and robustness of the masonry structure, thus safeguarding lives and preserving invaluable assets.

CHAPTER VI
REINFORCEMENT
ANALYSIS

VI.1 INTRODUCTION

Masonry structure reinforcement is the process of strengthening and enhancing the load-bearing capacity of existing masonry buildings or structures. It involves the application of various techniques such as steel reinforcement, fiber reinforcement, composite materials, and grouting or injection. These methods aim to improve the structural integrity, durability, and resistance of the masonry to external forces. The choice of reinforcement technique depends on factors such as the condition of the masonry, the desired level of reinforcement, and the specific load requirements of the structure.

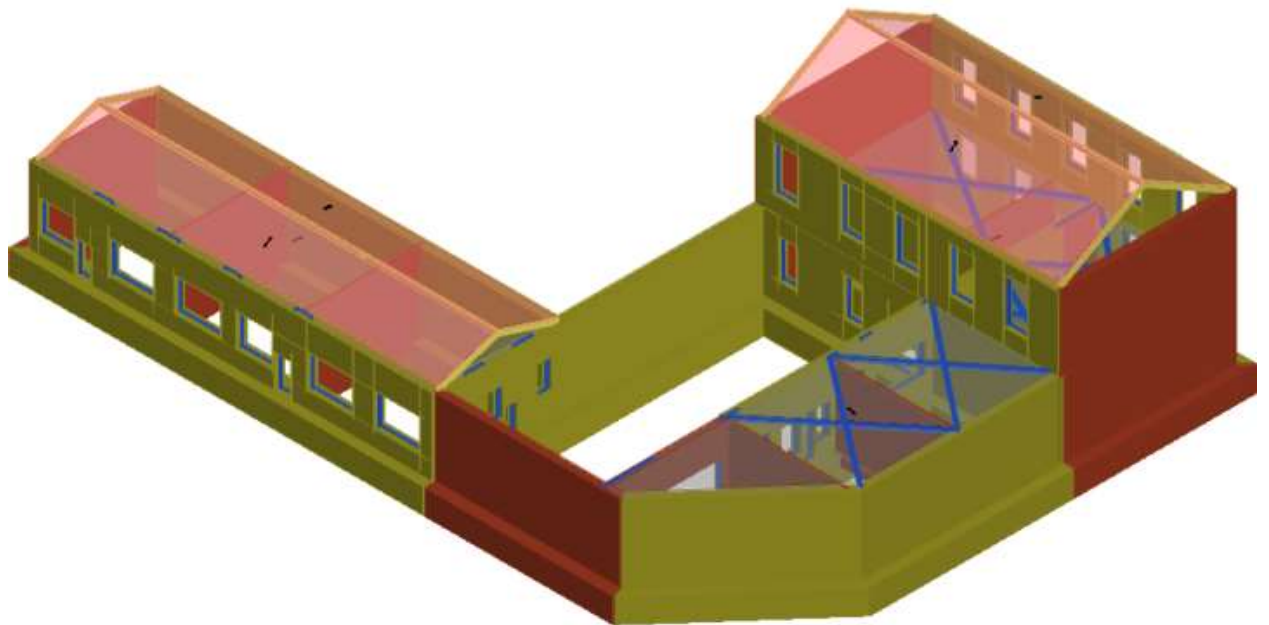


Figure VI 1 3d view after reinforcement

VI.2 TYPES OF REINFORCEMENT USED

Our masonry structures is often need to require reinforcement. Two common methods of masonry structure reinforcement are the use of wall frames and Fiber-Reinforced Cementitious Matrix (FRCM) systems.

VI.2.1 Wall frames

Wall frames are typically used as an external reinforcement system for masonry structures. They consist of steel or timber frames that are attached to the existing masonry walls. The frames are designed to bear a significant portion of the applied loads, such as wind or seismic forces, and transfer them to the foundation.

The installation of wall frames involves attaching horizontal and vertical members to the masonry wall, creating a framework that distributes the loads more evenly. These frames provide additional strength, stability, and ductility to the masonry structure, reducing the risk of failure under extreme conditions.

VI.2.2 Frcm systems

Fiber-Reinforced Cementitious Matrix (FRCM) systems are a relatively new technology used for the reinforcement of masonry structures. FRCM comprises high-strength fibers embedded in a cementitious matrix. The fibers can be made of materials like carbon, glass, or basalt, while the matrix is typically a cement-based mortar.

FRCM systems are applied directly to the masonry surface, providing both flexural and shear reinforcement. The fibers enhance the tensile strength and ductility of the masonry, while the cementitious matrix acts as a bonding agent between the fibers and the masonry substrate. This combination improves the overall structural performance and resists cracking, deformation, and delamination.

The installation of FRCM systems involves cleaning and preparing the masonry surface, applying a primer, and then applying multiple layers of the FRCM composite. Once cured, the FRCM becomes an integral part of the masonry structure, providing enhanced strength and durability.

VI.3 REINFORCEMENT TYPE CHARACTERISTICS

VI.3.1 Reinforcements frcm (walls)

Table VI 1 Block mechanical characteristics

| Name | Masonry | Masonry type | Exposure class | F _{bm} [n/m ²] | F _{btm} [n/m ²] | Dist. Application [m] |
|------------------------------|---------|------------------------------------|----------------|-------------------------------------|--------------------------------------|-----------------------|
| Frcm (Rubble Masonry Wall) | Rubble | Limestone or leccese stone masonry | External | 4.40e+06 | 4.00e+05 | 0.00e+00 |
| Frcm (Stone Wall) | Stone | Brick masonry | Internal | 2.20e+06 | 2.00e+05 | 0.00e+00 |

VI.3.1.1 Piers

Table VI 2 piers element type of reinforcement

| Name | Effect typology | Application | Bending anchor |
|----------------------------|-----------------|-------------|----------------|
| FRCM (Rubble Masonry Wall) | Shear | Double side | Efficacious |
| FRCM (Stone Wall) | Shear | Double side | Efficacious |

Table VI 3 Piers FRCM geometrics

| Name | tf [mm] | η_a | E _f [N/m ²] |
|------------------------------|---------|----------|------------------------------------|
| FRCM (Rubble Masonry Wall) | 0.062 | 0.80 | 6.00E+10 |
| FRCM (Stone Wall) | 0.062 | 0.90 | 6.00E+10 |

Table VI 4 FRCM on piers mechanical characteristics

| Name | $\varepsilon (\alpha)$ lim,conv [%] | $\sigma (\alpha)$ lim,conv [N/mm ²] | ε_{fd} [%] | f _{fd} /f _{added} [N/m ²] |
|------------------------------|-------------------------------------|---|------------------------|--|
| FRCM (Rubble Masonry Wall) | 2.80000 | 1,680.00000 | 1.49333 | 1.26E+20 |
| FRCM (Stone Wall) | 2.80000 | 1,680.00000 | 1.68000 | 1.01E+15 |

VI.3.1.2 Spandrel beam

Table VI 5 spandrel element type of reinforcement

| Name | Effect typology | Application | Bending anchor |
|-----------------------------|-----------------|-------------|----------------|
| FRCM (Rubble Masonry Wall) | Shear | Double side | Efficacious |
| FRCM (Stone Wall) | Shear | Single side | Efficacious |

Table VI 6 spandrel FRCM geometrics

| Name | tf [mm] | $\eta\alpha$ | Ef [N/m ²] |
|------------------------------|---------|--------------|------------------------|
| FRCM (Rubble Masonry Wall) | 0.062 | 0.80 | 6.00E+10 |
| FRCM (Stone Wall) | 0.062 | 0.90 | 6.00E+10 |

Table VI 7 FRCM on spandrel mechanical characteristics

| Name | $\varepsilon(\alpha)$ lim,conv [%] | $\sigma(\alpha)$ lim,conv [N/mm ²] | ε_{fd} [%] | f fd /f fdd [N/m ²] |
|------------------------------|------------------------------------|--|------------------------|---------------------------------|
| FRCM (Rubble Masonry Wall) | 2.80000 | 1,680.00000 | 1.49333 | 1.26E+20 |
| FRCM (Stone Wall) | 2.80000 | 1,680.00000 | 1.68000 | 1.01E+15 |

VI.3.2 Reinforcements wall (Steel frames)

Table VI 8 wall frame reinforcement characteristics for walls

| Material | Profile | Area [m ²] | J [m ⁴] | W [m ³] |
|-------------------|---------|------------------------|---------------------|---------------------|
| S 235 (t <= 40mm) | IPE 180 | 2.40E-03 | 1.32E-05 | 1.46E-04 |
| S 235 (t <= 40mm) | IPE 140 | 1.64E-03 | 5.41E-06 | 7.73E-05 |

VI.3.3 Reinforcements horizontal elements (Steel frame “tie rod “)

Table VI 9 tie rod reinforcement characteristics for horizontal elements

| Category | Profile | Material | Area [m ²] | J [m ⁴] | W [m ³] |
|----------|---------|-------------------|------------------------|---------------------|---------------------|
| Floor | HEA 180 | S 235 (t <= 40mm) | 3.88E-03 | 1.67E-05 | 2.20E-04 |
| Floor | HEA 160 | S 235 (t <= 40mm) | 4.53E-03 | 2.51E-05 | 2.94E-04 |

VI.4 MASONRY WITH FRCM REINFORCEMENT

VI.4.1 Compression bending

For the calculation of the moment of bending resisting moment it is possible to carry out a simplified calculation (see APPENDIX 1 of the CNR-DT 215/2018), on which the resisting moment of calculation can be evaluated by assuming a stress diagram of constant compression stress equal to $\alpha_m f_{md}$, extended to a portion of deep section βy_n , being y_n the distance of the neutral axis from the compressed end. α_m and β are two reduction coefficients, determined on empirical tests, described in the CNR -DT 215/2018.

In the case of crisis due to the achievement of the ε_{mu} deformation at the compressed end ($\varepsilon_m = \varepsilon_{mu}$) and of the neutral axis that cuts the section, the resistant moment of calculation is:

$$M_{Rd}(N_{sd}) = \frac{\alpha_m \beta f_{md} t y_n}{2} (H - \beta y_n) + \frac{\varepsilon_{mu}}{y_n} \frac{(d_f - y_n)^2}{12} E_f t_{2f} (2y_n + 4d_f - 3H)$$

being y_n the distance of the neutral axis from the compressed end, given by:

$$y_n = \frac{N_{sd} - E_f t_{2f} d_f \varepsilon_{mu} + \sqrt{N_{sd}^2 + 2E_f t_{2f} d_f \varepsilon_{mu} (\alpha_m \beta f_{md} d_f - N_{sd})}}{2\alpha_m \beta f_{md} t - E_f t_{2f} \varepsilon_{mu}}$$

Note the deformed configuration, it is necessary to verify that the maximum deformation of the reinforcement is less than the ultimate deformation.

In the case that the deformation of the reinforcement exceeds the maximum, it means that the hypothesis previously made (achievement of the ultimate deformation of the masonry) is not true, and therefore we proceed by assuming that the crisis occurs due to the achievement of the deformation ε_{fd} in the reinforcement ($\varepsilon_f = \varepsilon_{fd}$) and of neutral axis that cuts the section. In this case, the resistant moment of calculation is:

$$M_{Rd}(N_{sd}) = \frac{\alpha_m \beta f_{md} t y_n}{2} (H - \beta y_n) + \varepsilon_{fd} E_f t_{2f} \frac{d_f - y_n}{12} (2y_n + 4d_f - 3H)$$

being y_n the distance of the neutral axis from the compressed end, given by:

$$y_n = \frac{\varepsilon_{fd} E_f t_{2f} d_f + 2N_{sd}}{2\alpha_m \beta f_{md} t + \varepsilon_{fd} E_f t_{2f}}$$

where:

H is the length of the wall (section height);

t is the wall thickness (section width);

t_{2f} is the total equivalent thickness of the fibers applied on the two sides;

d_f is the distance between the compressed end and the fiber of the reinforcement furthest away from it;

N_{sd} is the normal compressive stress applied (possibly zero in the case of the floor strips).

VI.4.2 Shear

With reference to paragraph 4.1.1 of CNR-DT 215/2018, the shear strength of the reinforced wall (V_s) is calculated as the sum of the contribution of the non-reinforced masonry (V_t), evaluated in accordance with the Current legislation for non-reinforced walls that are in crisis due to traction shear, and that of the reinforcement (v_{tf}).

The latter is evaluated with the following equation:

$$V_{t,f} = \frac{1}{\gamma_{Rd}} \eta_f t_{vf} l_f \alpha_t \varepsilon_{fd} E_f$$

where:

γ_{Rd} it is a partial model factor to which value 2 is attributed, to the state of current knowledge;

n_f is the total number of reinforcement layers arranged on the sides of the wall;

t_{vf} is the equivalent thickness of a layer of mesh with fibers arranged in a direction parallel to the shear force;

l_f is the calculation dimension of the reinforcement measured orthogonally to the shear force, and in any case it cannot be assumed to be greater than the dimension H of the wall.

ε_{fd} is the calculation deformation of the reinforcement;

E_f is the elastic modulus of the reinforcement.

The α_t coefficient takes into account the reduced extensional resistance of the fibers when in shear. In the absence of proven experimental results, it can be assigned the value 0.80.

In the presence of fibers orthogonal to the direction of the shear and effectively anchored, it must also be

verified that the effective shear does not exceed the following diagonal crushing value of the masonry:

$$V_{s,lim} = 0.25 f_{md} t d_f$$

where:

t is the thickness of the wall;

f_{md} is the design compressive resistance of the masonry;

d_f is the distance between the compressed end of the masonry and the extreme of the FRCM reinforcement subject to traction

VI.5 STATIC REINFORCEMENT VERIFICATIONS

Retrofitting the most affected element of a masonry structure is a critical step in reinforcing the overall stability and performance of the building. The identification of the most vulnerable element, such as a weakened wall, is crucial to ensure targeted reinforcement. Proper retrofitting not only addresses existing weaknesses but also improves the structure's ability to withstand external forces and extends its service life.

For this we have used steel frames for the weakened elements (Pierses) and for the openings, and so far, we have applied the FRCM for the rest of walls in wish we did not apply steel frames.

VI.5.1 Wall: 1

Table VI 10 wall 1 static state after reinforcement


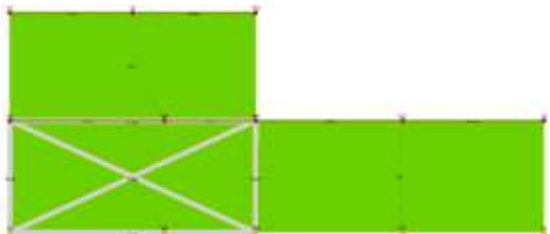
| before | AFTER |
|---|--|
|  |  |

Table VI 11 wall 1slanderness and eccentrecity verification after reinforcement

| Pier | ho [m] | t [m] | ho/t | e1/t Bottom | e2/t Middle | e1/t Top | Satisfied |
|------|-----------|----------|--------|-------------|-------------|----------|-----------|
| 1 | 4.52E+00 | 4.00E-01 | 11.300 | 0.056 | 0.056 | 0.056 | Yes |
| 2 | 4.52E+00 | 4.00E-01 | 11.300 | 0.118 | 0.075 | 0.248 | Yes |
| 89 | 4.36E+00 | 4.00E-01 | 10.900 | 0.055 | 0.055 | 0.055 | Yes |

Table VI 12 wall 1 vertical load bearing verification after reinforcement

| Pier | Top | | | | Middle | | | | Bottom | | | | Satisfied |
|------|----------|-------|----------|-------|----------|-------|----------|-------|----------|-------|----------|-------|-----------|
| | Nd | F | Nr | Nd/Nr | Nd | F | Nr | Nd/Nr | Nd | F | Nr | Nd/Nr | |
| 1 | 5.41E+04 | 0.653 | 6.58E+05 | 0.082 | 1.78E+05 | 0.653 | 6.58E+05 | 0.270 | 4.11E+05 | 0.653 | 6.58E+05 | 0.624 | Yes |
| 2 | 2.75E+05 | 0.247 | 5.85E+05 | 0.470 | 5.63E+05 | 0.600 | 1.42E+06 | 0.397 | 8.51E+05 | 0.509 | 1.20E+06 | 0.708 | Yes |
| 89 | 1.55E+05 | 0.671 | 6.76E+05 | 0.229 | 3.49E+05 | 0.671 | 6.76E+05 | 0.516 | 5.74E+05 | 0.671 | 6.76E+05 | 0.850 | Yes |

VI.5.2 Wall: 6

Table VI 13 wall 6 static state after reinforcement

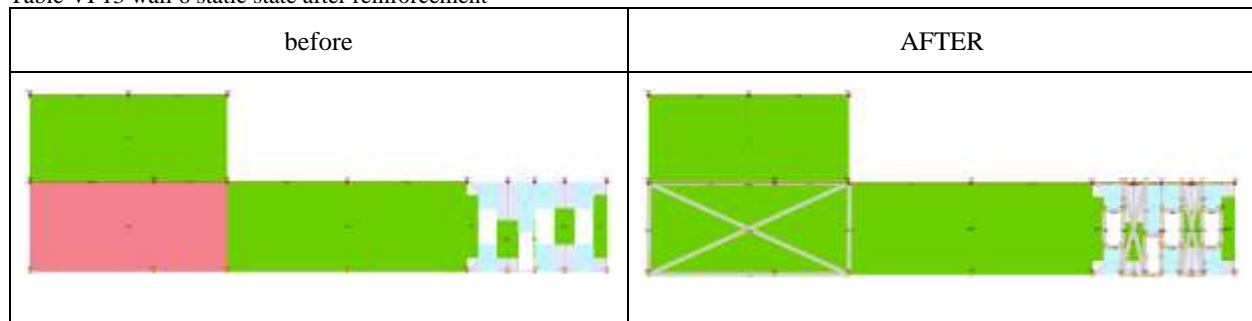


Table VI 14 wall 6 slanderness and eccentrecity verification after reinforcement

| Pier | ho [m] | t [m] | ho/t | e1/t Bottom | e2/t Middle | e1/t Top | Satisfied |
|------|-----------|----------|--------|-------------|-------------|----------|-----------|
| 33 | 4.52E+00 | 4.00E-01 | 11.300 | 0.056 | 0.056 | 0.056 | Yes |

| | | | | | | | |
|----|----------|----------|--------|-------|-------|-------|-----|
| 34 | 4.52E+00 | 5.50E-01 | 8.218 | 0.041 | 0.041 | 0.041 | Yes |
| 35 | 4.52E+00 | 5.50E-01 | 8.218 | 0.041 | 0.041 | 0.041 | Yes |
| 36 | 4.52E+00 | 5.50E-01 | 8.218 | 0.041 | 0.041 | 0.041 | Yes |
| 37 | 4.52E+00 | 5.50E-01 | 8.218 | 0.041 | 0.041 | 0.041 | Yes |
| 38 | 4.52E+00 | 5.50E-01 | 8.218 | 0.041 | 0.041 | 0.041 | Yes |
| 94 | 4.63E+00 | 5.00E-01 | 9.260 | 0.046 | 0.046 | 0.046 | Yes |
| 95 | 4.36E+00 | 4.00E-01 | 10.900 | 0.055 | 0.055 | 0.055 | Yes |

Table VI 15 wall 6 vertical load bearing verification after reinforcement

| Pie r | Top | | | | Middle | | | | Bottom | | | | Satisf ied |
|----------|--------------|-----------|--------------|-----------|--------------|-----------|--------------|-----------|--------------|-----------|--------------|-----------|---------------|
| | Nd | F | Nr | Nd/ Nr | Nd | F | Nr | Nd/ Nr | Nd | F | Nr | Nd/ Nr | |
| 33 | 1.40E +05 | 0.6 53 | 6.58E +05 | 0.21 3 | 3.74E +05 | 0.6 53 | 6.58E +05 | 0.56 8 | 6.07E +05 | 0.6 53 | 6.58E +05 | 0.92 2 | Yes |
| 34 | 1.44E +02 | 0.7 74 | 1.24E +05 | 0.00 1 | 6.89E +02 | 0.7 74 | 1.24E +05 | 0.00 6 | 1.43E +04 | 0.7 74 | 1.24E +05 | 0.11 6 | Yes |
| 35 | 0.00E +00 | 0.7 74 | 2.34E +05 | 0 | 6.98E- 01 | 0.7 74 | 2.34E +05 | 0.00 0 | 1.53E +04 | 0.7 74 | 2.34E +05 | 0.06 5 | Yes |
| 36 | 0.00E +00 | 0.7 74 | 1.47E +04 | 0 | 7.76E- 02 | 0.7 74 | 1.47E +04 | 0.00 0 | 9.64E +02 | 0.7 74 | 1.47E +04 | 0.06 6 | Yes |
| 37 | 0.00E +00 | 0.7 74 | 2.19E +05 | 0 | 4.13E- 01 | 0.7 74 | 2.19E +05 | 0.00 0 | 1.38E +04 | 0.7 74 | 2.19E +05 | 0.06 3 | Yes |
| 38 | 6.31E +01 | 0.7 74 | 1.46E +05 | 0.00 0 | 1.53E +02 | 0.7 74 | 1.46E +05 | 0.00 1 | 1.63E +04 | 0.7 74 | 1.46E +05 | 0.11 1 | Yes |
| 94 | 4.79E +04 | 0.7 37 | 2.26E +06 | 0.02 1 | 2.29E +05 | 0.7 37 | 2.26E +06 | 0.10 2 | 6.03E +05 | 0.7 37 | 2.26E +06 | 0.26 7 | Yes |
| 95 | 1.65E +05 | 0.6 71 | 6.76E +05 | 0.24 4 | 3.74E +05 | 0.6 71 | 6.76E +05 | 0.55 3 | 5.99E +05 | 0.6 71 | 6.76E +05 | 0.88 6 | Yes |

VI.5.3 Wall: 7

Table VI 16 wall 7 static state after reinforcement

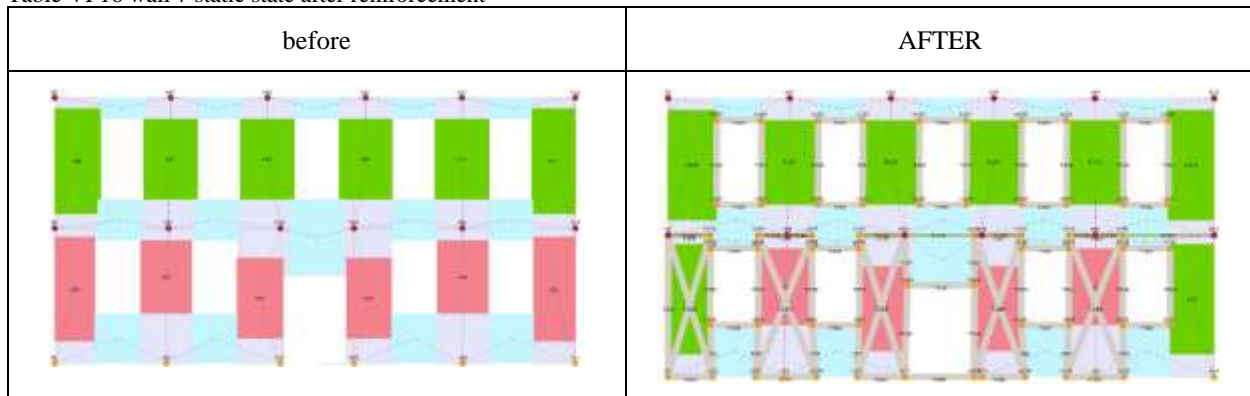


Table VI 17 wall 7 slenderness and eccentricity verification after reinforcement

| Pier | ho [m] | t [m] | ho/t | e1/t Bottom | e2/t Middle | e1/t Top | Satisfied |
|------|-----------|----------|-------|-------------|-------------|----------|-----------|
| 48 | 4.52E+00 | 6.00E-01 | 7.533 | 0.038 | 0.038 | 0.079 | Yes |
| 49 | 4.52E+00 | 6.00E-01 | 7.533 | 0.038 | 0.038 | 0.402 | No |
| 50 | 4.52E+00 | 6.00E-01 | 7.533 | 0.038 | 0.044 | 0.396 | No |
| 51 | 4.52E+00 | 6.00E-01 | 7.533 | 0.038 | 0.038 | 0.336 | No |
| 52 | 4.52E+00 | 6.00E-01 | 7.533 | 0.038 | 0.046 | 0.346 | No |
| 53 | 4.52E+00 | 6.00E-01 | 7.533 | 0.099 | 0.056 | 0.132 | Yes |
| 106 | 4.36E+00 | 6.00E-01 | 7.267 | 0.036 | 0.036 | 0.036 | Yes |
| 107 | 4.36E+00 | 6.00E-01 | 7.267 | 0.036 | 0.036 | 0.036 | Yes |
| 108 | 4.36E+00 | 6.00E-01 | 7.267 | 0.036 | 0.036 | 0.036 | Yes |
| 109 | 4.36E+00 | 6.00E-01 | 7.267 | 0.036 | 0.036 | 0.036 | Yes |
| 110 | 4.36E+00 | 6.00E-01 | 7.267 | 0.036 | 0.036 | 0.036 | Yes |
| 111 | 4.36E+00 | 6.00E-01 | 7.267 | 0.036 | 0.036 | 0.036 | Yes |

Table VI 18 wall 7 vertical load bearing verification after reinforcement

| Pie r | Top | | | | Middle | | | | Bottom | | | | Satisf ied |
|----------|--------------|-----------|--------------|-----------|--------------|-----------|--------------|-----------|--------------|-----------|--------------|-----------|---------------|
| | Nd | F | Nr | Nd/ Nr | Nd | F | Nr | Nd/ Nr | Nd | F | Nr | Nd/ Nr | |
| 48 | 2.33E +01 | 0.6 72 | 2.74E +05 | 0.00 0 | 1.11E +02 | 0.7 99 | 3.26E +05 | 0.00 0 | 3.84E +04 | 0.7 99 | 3.26E +05 | 0.11 8 | Yes |
| 49 | 8.23E- 01 | 0.0 00 | 0 | 0 | 1.19E +01 | 0.7 99 | 4.15E +05 | 0.00 0 | 3.42E +04 | 0.7 99 | 4.15E +05 | 0.08 2 | Yes |
| 50 | 1.38E +01 | 0.0 00 | 0 | 0 | 9.81E +01 | 0.7 80 | 3.65E +05 | 0.00 0 | 3.40E +04 | 0.7 99 | 3.74E +05 | 0.09 1 | Yes |
| 51 | 1.16E +00 | 0.0 00 | 0 | 0 | 1.69E +01 | 0.7 99 | 3.66E +05 | 0.00 0 | 3.32E +04 | 0.7 99 | 3.66E +05 | 0.09 1 | Yes |
| 52 | 2.95E +00 | 0.0 00 | 0 | 0 | 1.70E +01 | 0.7 75 | 4.03E +05 | 0.00 0 | 3.43E +04 | 0.7 99 | 4.16E +05 | 0.08 2 | Yes |
| 53 | 1.46E +05 | 0.5 65 | 2.40E +05 | 0.60 7 | 1.86E +05 | 0.7 43 | 3.16E +05 | 0.58 8 | 2.26E +05 | 0.6 29 | 2.68E +05 | 0.84 3 | Yes |
| 10 6 | 7.14E +04 | 0.8 09 | 3.79E +05 | 0.18 9 | 1.16E +05 | 0.8 09 | 3.79E +05 | 0.30 6 | 1.60E +05 | 0.8 09 | 3.79E +05 | 0.42 4 | Yes |
| 10 7 | 3.80E +04 | 0.8 09 | 4.45E +05 | 0.08 6 | 7.78E +04 | 0.8 09 | 4.45E +05 | 0.17 5 | 1.18E +05 | 0.8 09 | 4.45E +05 | 0.26 5 | Yes |
| 10 8 | 3.73E +04 | 0.8 09 | 4.45E +05 | 0.08 4 | 7.71E +04 | 0.8 09 | 4.45E +05 | 0.17 3 | 1.17E +05 | 0.8 09 | 4.45E +05 | 0.26 3 | Yes |
| 10 9 | 3.57E +04 | 0.8 09 | 4.34E +05 | 0.08 2 | 7.45E +04 | 0.8 09 | 4.34E +05 | 0.17 2 | 1.13E +05 | 0.8 09 | 4.34E +05 | 0.26 1 | Yes |
| 11 0 | 4.57E +04 | 0.8 09 | 4.45E +05 | 0.10 3 | 8.55E +04 | 0.8 09 | 4.45E +05 | 0.19 2 | 1.25E +05 | 0.8 09 | 4.45E +05 | 0.28 2 | Yes |
| 11 1 | 5.26E +04 | 0.8 09 | 3.61E +05 | 0.14 6 | 9.51E +04 | 0.8 09 | 3.61E +05 | 0.26 3 | 1.38E +05 | 0.8 09 | 3.61E +05 | 0.38 1 | Yes |

VI.5.4 Wall: 10

Table VI 19 wall 10 static state after reinforcement

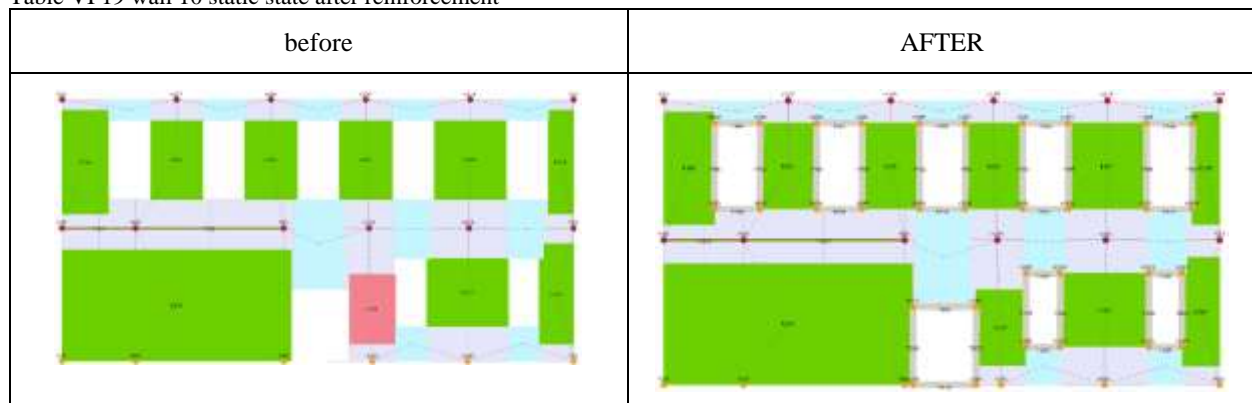


Table VI 20 wall 10 slenderness and eccentricity verification after reinforcement

| Pier | ho [m] | t [m] | ho/t | e1/t Bottom | e2/t Middle | e1/t Top | Satisfied |
|------|----------|----------|-------|-------------|-------------|----------|-----------|
| 126 | 4.52E+00 | 5.00E-01 | 9.040 | 0.091 | 0.058 | 0.194 | Yes |
| 127 | 4.52E+00 | 5.00E-01 | 9.040 | 0.097 | 0.052 | 0.112 | Yes |
| 128 | 4.52E+00 | 5.00E-01 | 9.040 | 0.099 | 0.053 | 0.114 | Yes |
| 129 | 4.52E+00 | 5.00E-01 | 9.040 | 0.083 | 0.048 | 0.121 | Yes |
| 130 | 4.36E+00 | 5.00E-01 | 8.720 | 0.044 | 0.044 | 0.044 | Yes |
| 131 | 4.36E+00 | 5.00E-01 | 8.720 | 0.044 | 0.044 | 0.044 | Yes |
| 132 | 4.36E+00 | 5.00E-01 | 8.720 | 0.044 | 0.044 | 0.044 | Yes |
| 133 | 4.36E+00 | 5.00E-01 | 8.720 | 0.044 | 0.044 | 0.044 | Yes |
| 134 | 4.36E+00 | 5.00E-01 | 8.720 | 0.044 | 0.044 | 0.044 | Yes |
| 135 | 4.36E+00 | 5.00E-01 | 8.720 | 0.044 | 0.044 | 0.044 | Yes |

Table VI 21 wall 10 vertical load bearing verification after reinforcement

| Pier | Top | | | | Middle | | | | Bottom | | | | Satisfied |
|------|----------|-------|----------|-------|----------|-------|----------|-------|----------|-------|----------|-------|-----------|
| | Nd | F | Nr | Nd/Nr | Nd | F | Nr | Nd/Nr | Nd | F | Nr | Nd/Nr | |
| 126 | 1.83E+05 | 0.412 | 8.14E+05 | 0.225 | 3.85E+05 | 0.706 | 1.39E+06 | 0.276 | 5.87E+05 | 0.614 | 1.21E+06 | 0.484 | Yes |
| 127 | 1.76E+05 | 0.574 | 2.27E+05 | 0.772 | 2.01E+05 | 0.725 | 2.87E+05 | 0.700 | 2.26E+05 | 0.603 | 2.39E+05 | 0.947 | Yes |

| | | | | | | | | | | | | | |
|-----|----------|-------|----------|-------|----------|-------|----------|-------|----------|-------|----------|-------|-----|
| 128 | 3.07E+05 | 0.571 | 4.01E+05 | 0.765 | 3.50E+05 | 0.722 | 5.07E+05 | 0.690 | 3.94E+05 | 0.600 | 4.21E+05 | 0.934 | Yes |
| 129 | 5.40E+04 | 0.557 | 1.66E+05 | 0.326 | 8.13E+04 | 0.737 | 2.19E+05 | 0.371 | 1.09E+05 | 0.631 | 1.88E+05 | 0.579 | Yes |
| 130 | 6.14E+04 | 0.756 | 3.03E+05 | 0.202 | 9.95E+04 | 0.756 | 3.03E+05 | 0.328 | 1.38E+05 | 0.756 | 3.03E+05 | 0.454 | Yes |
| 131 | 3.09E+04 | 0.756 | 3.37E+05 | 0.092 | 6.31E+04 | 0.756 | 3.37E+05 | 0.187 | 9.54E+04 | 0.756 | 3.37E+05 | 0.283 | Yes |
| 132 | 3.30E+04 | 0.756 | 3.43E+05 | 0.096 | 6.58E+04 | 0.756 | 3.43E+05 | 0.192 | 9.87E+04 | 0.756 | 3.43E+05 | 0.287 | Yes |
| 133 | 2.87E+04 | 0.756 | 3.43E+05 | 0.084 | 6.16E+04 | 0.756 | 3.43E+05 | 0.179 | 9.45E+04 | 0.756 | 3.43E+05 | 0.275 | Yes |
| 134 | 3.86E+04 | 0.756 | 4.69E+05 | 0.082 | 8.35E+04 | 0.756 | 4.69E+05 | 0.178 | 1.28E+05 | 0.756 | 4.69E+05 | 0.274 | Yes |
| 135 | 4.14E+04 | 0.756 | 1.64E+05 | 0.252 | 6.21E+04 | 0.756 | 1.64E+05 | 0.378 | 8.28E+04 | 0.756 | 1.64E+05 | 0.503 | Yes |

VI.6 SEISMIC VULNERABILITY ANALYSIS

After undergoing demand spectrum analysis and implementing the necessary reinforcement measures, the masonry structure should exhibit improved performance and enhanced resilience against seismic forces.

The reinforcement works, such as steel bracing, fiber wrapping, concrete jacketing, aim to increase the structure's strength, stiffness, and ductility. These measures help to redistribute and dissipate the forces generated during a seismic event, reducing the risk of structural failure and minimizing damage in the structure elements. The reinforced structure should demonstrate improved resistance to deformation, cracking, and displacement, providing a higher level of safety for occupants and preserving the integrity of the building.

VI.6.1 Results

Table VI 22 verification of the critical direction of the earthquake after reinforcement

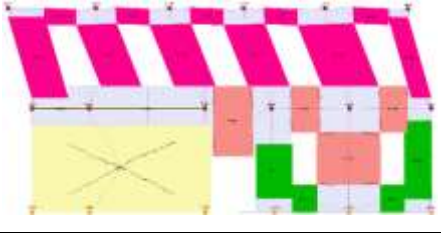
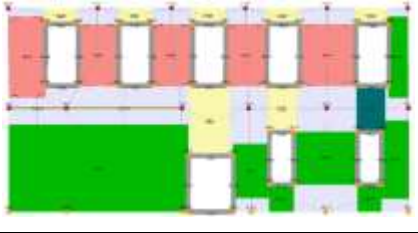
| No. | Seism dir. | Seismic load | Ecc. [m] | Dmax ULS [m] | Du ULS [m] | q* ULS | ULS Ver. |
|-----|------------|---------------|-------------|-----------------|---------------|--------|----------|
| 1 | +X | Uniform | 0.00E+00 | 1.08E-03 | 2.77E-02 | 0.46 | Yes |
| 2 | +X | Static forces | 0.00E+00 | 2.16E-03 | 2.77E-02 | 0.85 | Yes |
| 3 | -X | Uniform | 0.00E+00 | 1.85E-03 | 3.55E-02 | 0.70 | Yes |
| 4 | -X | Static forces | 0.00E+00 | 5.83E-03 | 4.03E-02 | 1.39 | Yes |
| 5 | +Y | Uniform | 0.00E+00 | 1.43E-03 | 2.83E-02 | 0.32 | Yes |
| 6 | +Y | Static forces | 0.00E+00 | 2.73E-03 | 2.88E-02 | 0.64 | Yes |
| 7 | -Y | Uniform | 0.00E+00 | 1.44E-03 | 1.53E-02 | 0.36 | Yes |
| 8 | -Y | Static forces | 0.00E+00 | 2.73E-03 | 1.36E-01 | 0.66 | Yes |

Table VI 23 pushover critical direction of the earthquake after reinforcement

| No. | Seism dir. | Seismic load | Ecc. [m] | α ULS |
|-----|------------|---------------|-------------|--------------|
| 1 | +X | Uniform | 0.00E+00 | 6.472 |
| 2 | +X | Static forces | 0.00E+00 | 3.512 |
| 3 | -X | Uniform | 0.00E+00 | 4.259 |
| 4 | -X | Static forces | 0.00E+00 | 2.153 |
| 5 | +Y | Uniform | 0.00E+00 | 6.876 |
| 6 | +Y | Static forces | 0.00E+00 | 4.178 |
| 7 | -Y | Uniform | 0.00E+00 | 4.570 |
| 8 | -Y | Static forces | 0.00E+00 | 4.557 |

VI.6.1.1 Seismic analysis Wall 10 for the X direction

Table VI 24 wall 10 dynamic state after reinforcement

| | before | After |
|------------------|---|---|
| |  |  |
| Limit Drift | 0.005 | 0.010 |
| Drift in Step | 0.001 | 0.000 |
| Damage condition | Shear damage | Undamaged |

VI.6.1.1.1 General data

Table VI 25 wall 10 analysis damage results X direction after reinforcement

| Code | Technical standards 2018 |
|------------------|--------------------------|
| Wall | 10 |
| Piers | 116 |
| Analysis | 4 |
| Substep | 2/32 |
| Limit Drift | 0.010 |
| Drift in Step | 0.000 |
| Damage condition | Undamaged |

VI.6.1.1.2 Input data from Model

Table VI 26 wall 10 input conditions

| | |
|--------------------------|-------------------------------------|
| Typology | FRCM reinforced masonry |
| The material's condition | Existing |
| Constitutive law | Irregular masonry (Turnsek/Cacovic) |

VI.6.1.1.2.1 Geometry

Table VI 27 wall 10 geometry

| Name | Value | Description |
|-------|----------|-----------------------------|
| h [m] | 3.88E+00 | Height (deformable portion) |
| l [m] | 8.00E+00 | Length |
| t [m] | 5.00E-01 | Thickness |

VI.6.1.1.2.2 Masonry: rubble

Table VI 28 wall 10 mechanical characteristics

| Name | Value | Description |
|----------------------------|----------|--|
| f_m [N/m ²] | 2.00E+06 | Average compressive strength of masonry |
| τ [N/m ²] | 3.50E+04 | Average shear strength in the absence of normal stresses |
| CF | 1.35 | Confidence factor |

VI.6.1.1.2.3 Reinforcement FRCM

Table VI 29 wall 10 reinforcement typology applied

| Name | Value | Description |
|---------------------------|----------|---|
| Effect typology | Shear | |
| Layers | 2 | Number of layers applied |
| E_f [N/m ²] | 6.00E+10 | Young's modulus |
| tf [mm] | 0.062 | Equivalent thickness of the single layer of the FRCM system |

VI.6.1.1.3 Applied forces (from pushover analysis)

Table VI 30 wall 10 applied forces for X direction after reinforcement

| Name | Value | Description |
|---------------|-----------|------------------------------|
| N [N] | 2.98E+05 | Axial force |
| Vd [N] | 6.88E+03 | Shear |
| M top [Nm] | 6.12E+04 | Upper section bending moment |
| M bottom [Nm] | -8.79E+04 | Lower section bending moment |

VI.6.1.1.4 Resistance forces and verification

Table VI 31 wall 10 resistance forces verifications for X direction after reinforcement

| Name | Value | Description |
|--------|----------|---|
| N [N] | 2.98E+05 | Axial force (coincident with applied) |
| Vf [N] | 8.77E+04 | Shear (principle bending) calculated by interpolation on the resistance domain |
| Vs [N] | 4.38E+05 | Shear (principle shear) calculated by interpolation on the resistance domain |
| Vr [N] | 8.77E+04 | Shear (minimum between Vf and Vs) |
| Vd/Vr | 0.078 | Safety factor |

VI.6.1.1.5 Resistance domain diagram

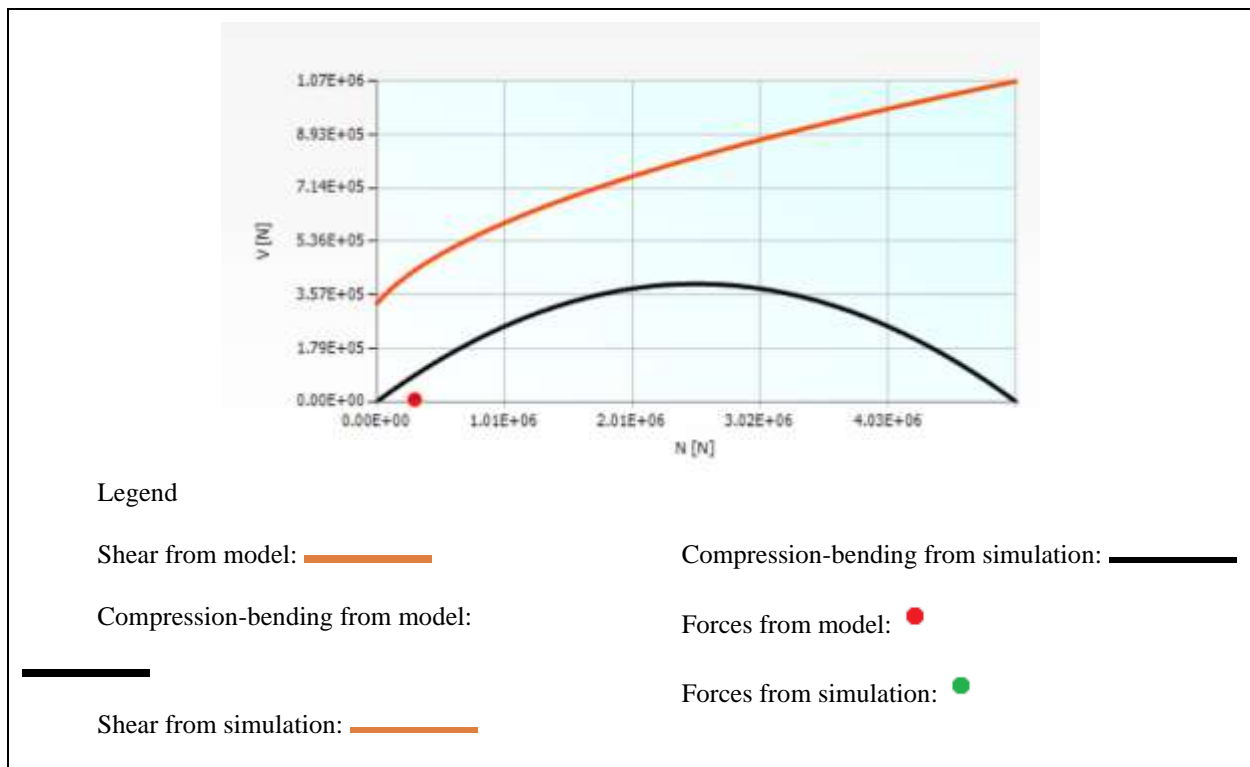
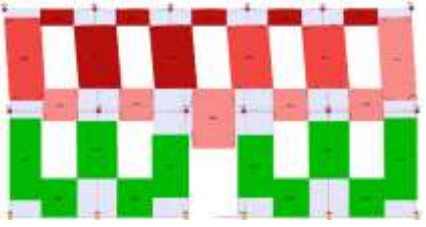
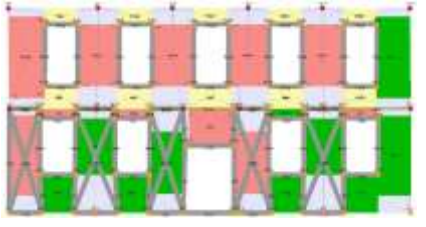


Figure VI 2 wall 10 Resistance domain diagram after reinforcement

For the calculation domain look the **APPENDIX III**

VI.6.1.2 Seismic analysis Wall 7 for the X direction

Table VI 32 wall 7 dynamic state after reinforcement

| | before | After |
|------------------|---|---|
| |  |  |
| Limit Drift | 0.010 | 0.010 |
| Drift in Step | 0.008 | 0.001 |
| Damage condition | Incipient bending failure | Bending damage |

VI.6.1.2.1 General data

Table VI 33 wall 7 analysis damage results X direction after reinforcement

| Code | Technical standards 2018 |
|------------------|--------------------------|
| Wall | 7 |
| Piers | 72 |
| Analysis | 4 |
| Substep | 3/32 |
| Limit Drift | 0.010 |
| Drift in Step | 0.001 |
| Damage condition | Bending damage |

VI.6.1.2.2 Input data from Model

Table VI 34 wall 7 input conditions

| | |
|--------------------------|-------------------------------------|
| Typology | FRCM reinforced masonry |
| The material's condition | Existing |
| Constitutive law | Irregular masonry (Turnsek/Cacovic) |

VI.6.1.2.2.1 Geometry

Table VI 35 wall 7 geometry

| Name | Value | Description |
|-------|----------|-----------------------------|
| h [m] | 2.75E+00 | Height (deformable portion) |
| l [m] | 1.86E+00 | Length |
| t [m] | 6.00E-01 | Thickness |

VI.6.1.2.2.2 Masonry: rubble

Table VI 36 wall 7 mechanical characteristics

| Name | Value | Description |
|----------------------------|----------|--|
| f_m [N/m ²] | 2.00E+06 | Average compressive strength of masonry |
| τ [N/m ²] | 3.50E+04 | Average shear strength in the absence of normal stresses |
| CF | 1.35 | Confidence factor |

VI.6.1.2.2.3 Reinforcement FRCM

Table VI 37 wall 7 reinforcement typology applied

| Name | Value | Description |
|---------------------------|----------|---|
| Effect typology | Shear | |
| Layers | 2 | Number of layers applied |
| E_f [N/m ²] | 6.00E+10 | Young's modulus |
| t_f [mm] | 0.062 | Equivalent thickness of the single layer of the FRCM system |

VI.6.1.2.3 Applied forces (from pushover analysis)

Table VI 38 wall 7 applied forces for X direction after reinforcement

| Name | Value | Description |
|---------------|-----------|------------------------------|
| N [N] | 6.09E+04 | Axial force |
| Vd [N] | 2.13E+04 | Shear |
| M top [Nm] | -4.60E+03 | Upper section bending moment |
| M bottom [Nm] | -5.41E+04 | Lower section bending moment |

VI.6.1.2.4 Resistance forces and verification

Table VI 39 wall 7 resistance forces verifications for X direction after reinforcement

| Name | Value | Description |
|--------|----------|---|
| N [N] | 6.09E+04 | Axial force (coincident with applied) |
| Vf [N] | 2.13E+04 | Shear (principle bending) calculated by interpolation on the resistance domain |
| Vs [N] | 1.28E+05 | Shear (principle shear) calculated by interpolation on the resistance domain |
| Vr [N] | 2.13E+04 | Shear (minimum between Vf and Vs) |
| Vd/Vr | 1.000 | Safety factor |

VI.6.1.2.5 Resistance domain diagram

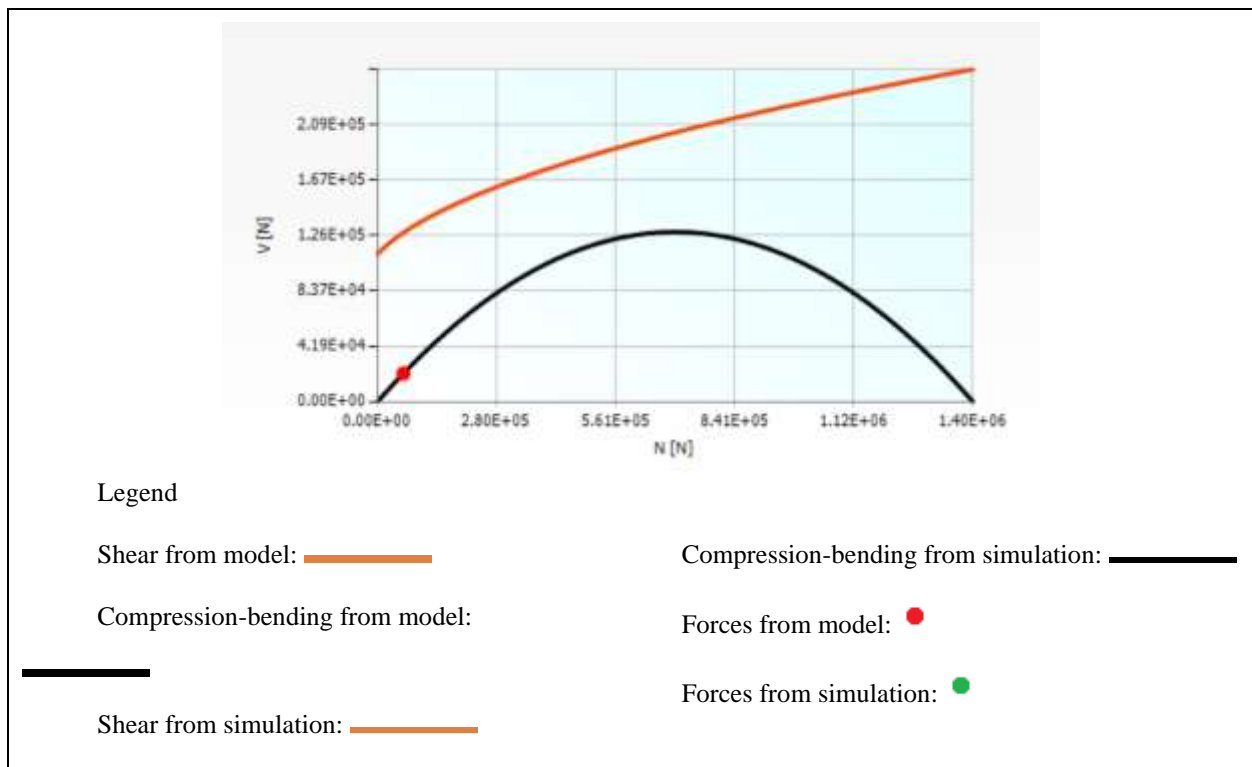


Figure VI 3 wall 7 Resistance domain diagram after reinforcement

For the calculation domain look the **APPENDIX III**

VI.6.1.2.6 Plan deformed shape

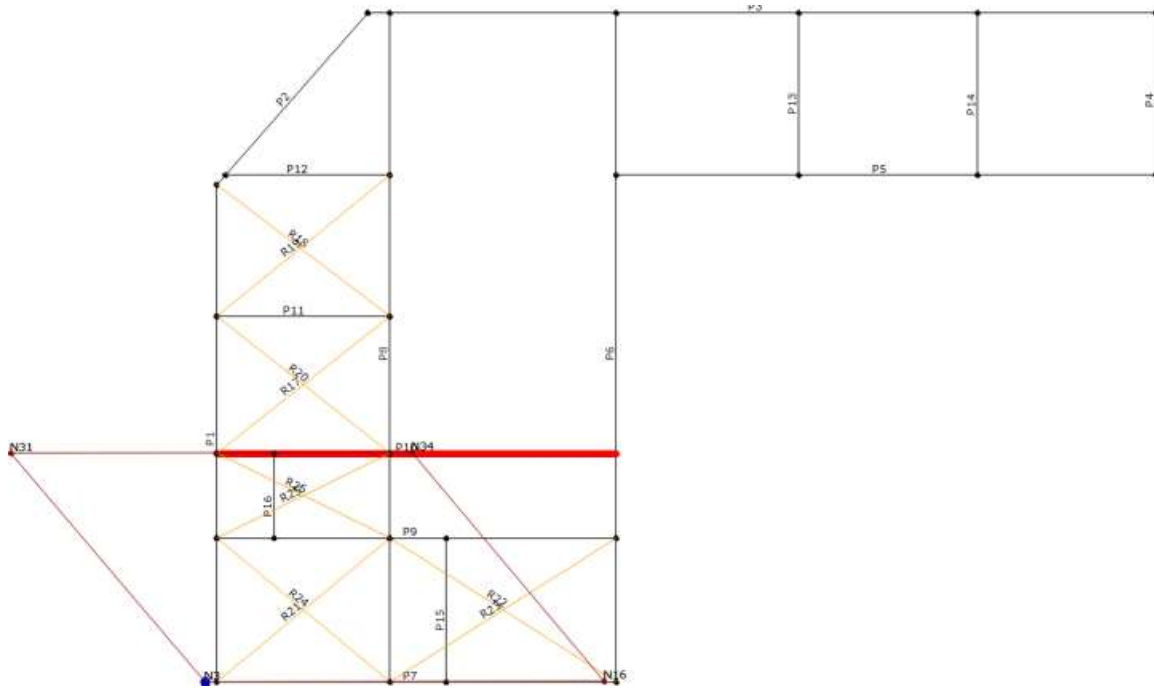


Figure VI 4 Plan deformed shape for X direction after reinforcement

VI.6.1.2.7 Pushover curve (analysis n. 4)

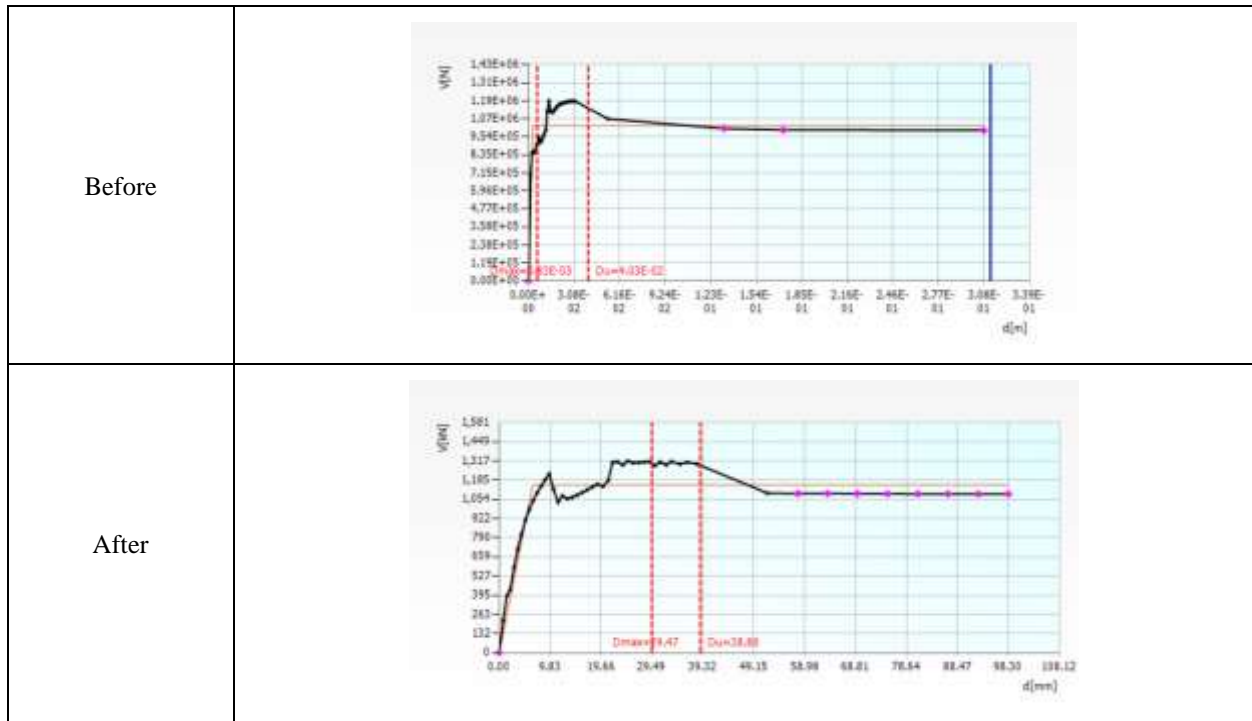
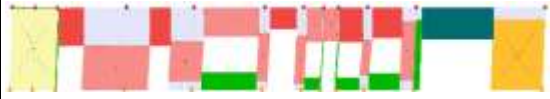



Figure VI 5 Pushover curves for X direction before and after reinforcement

VI.6.1.3 Seismic analysis Wall 8 for the Y direction

Table VI 40 wall 8 dynamic state after reinforcement

| | before | After |
|------------------|---|--|
| |  |  |
| Limit Drift | 0.005 | 0.010 |
| Drift in Step | 0.003 | 0.000 |
| Damage condition | Shear damage | Bending damage |

VI.6.1.3.1 General data

Table VI 41 wall 8 analysis damage results Y direction after reinforcement

| Code | Technical standards 2018 |
|------------------|--------------------------|
| Wall | 8 |
| Piers | 77 |
| Analysis | 6 |
| Substep | 2/46 |
| Limit Drift | 0.010 |
| Drift in Step | 0.000 |
| Damage condition | Bending damage |

VI.6.1.3.2 Input data from Model

Table VI 42 wall 8 input conditions

| | |
|--------------------------|-------------------------------------|
| Typology | Common masonry |
| The material's condition | Existing |
| Constitutive law | Irregular masonry (Turnsek/Cacovic) |

VI.6.1.3.2.1 Geometry

Table VI 43 wall 8 geometry

| Name | Value | Description |
|-------|----------|-----------------------------|
| h [m] | 4.63E+00 | Height (deformable portion) |
| l [m] | 2.55E+00 | Length |
| t [m] | 1.00E-01 | Thickness |

VI.6.1.3.2.2 Masonry: rubble

Table VI 44 wall 8 mechanical characteristics

| Name | Value | Description |
|----------------------------|----------|--|
| f_m [N/m ²] | 2.60E+06 | Average compressive strength of masonry |
| τ [N/m ²] | 5.00E+04 | Average shear strength in the absence of normal stresses |
| CF | 1.35 | Confidence factor |

VI.6.1.3.3 Applied forces (from pushover analysis)

Table VI 45 wall 8 applied forces for Y direction after reinforcement

| Name | Value | Description |
|---------------|----------|------------------------------|
| N [N] | 2.24E+03 | Axial force |
| Vd [N] | 9.51E+02 | Shear |
| M top [Nm] | 1.57E+03 | Upper section bending moment |
| M bottom [Nm] | 2.83E+03 | Lower section bending moment |

VI.6.1.3.4 Resistance forces and verification

Table VI 46 wall 8 resistance forces verifications for Y direction after reinforcement

| Name | Value | Description |
|--------|----------|---|
| N [N] | 2.24E+03 | Axial force (coincident with applied) |
| Vf [N] | 9.46E+02 | Shear (principle bending) calculated by interpolation on the resistance domain |

| | | |
|--------|----------|---|
| Vs [N] | 1.01E+04 | Shear (principle shear) calculated by interpolation on the resistance domain |
| Vr [N] | 9.46E+02 | Shear (minimum between Vf and Vs) |
| Vd/Vr | 1.005 | Safety factor |

VI.6.1.3.5 Resistance domain diagram

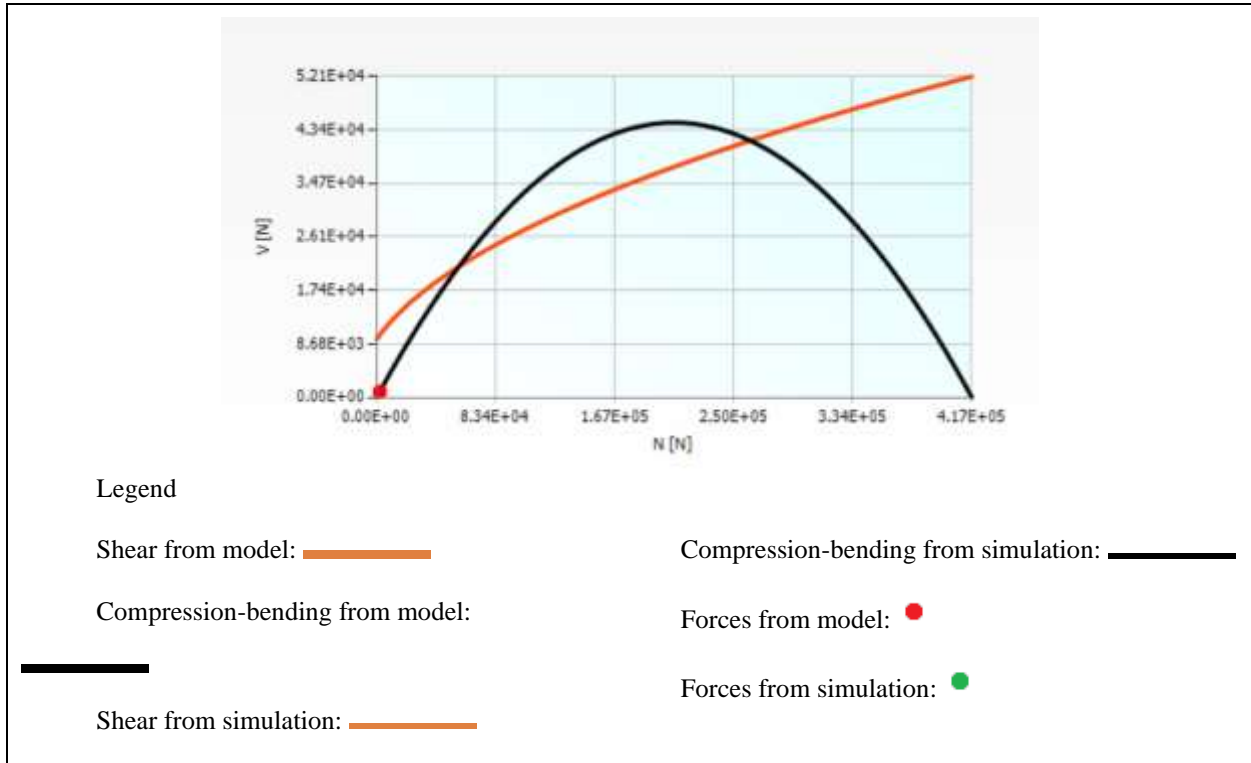


Figure VI 6 wall 8 Resistance domain diagram

For the calculation domain look the **APPENDIX III**

VI.6.1.3.6 Plan deformed shape

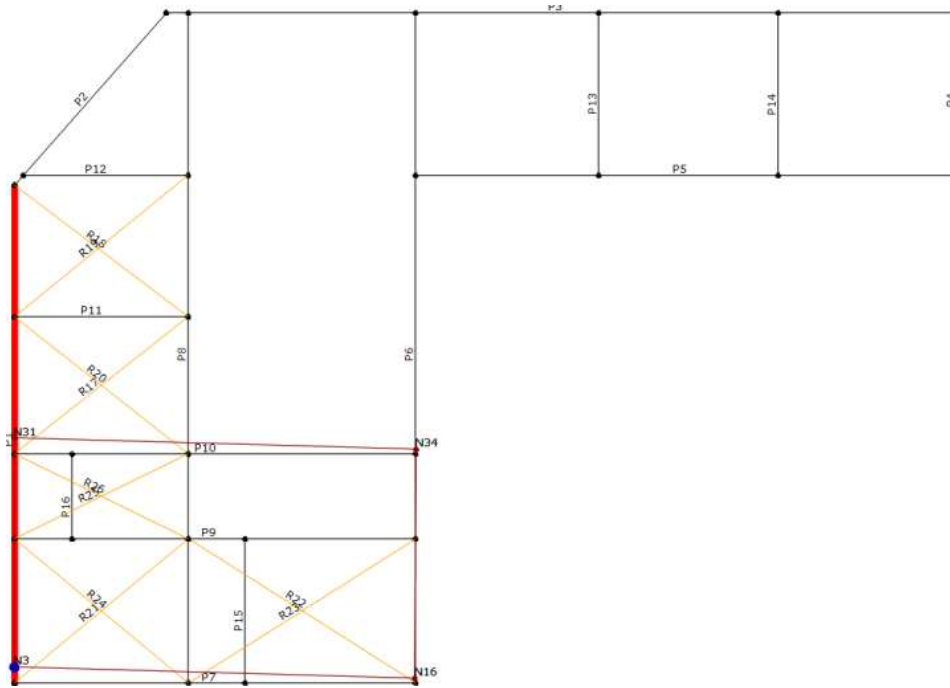


Figure VI 7 Plan deformed shape for Y direction after reinforcement

VI.6.1.3.7 Pushover curve (analysis n. 6)

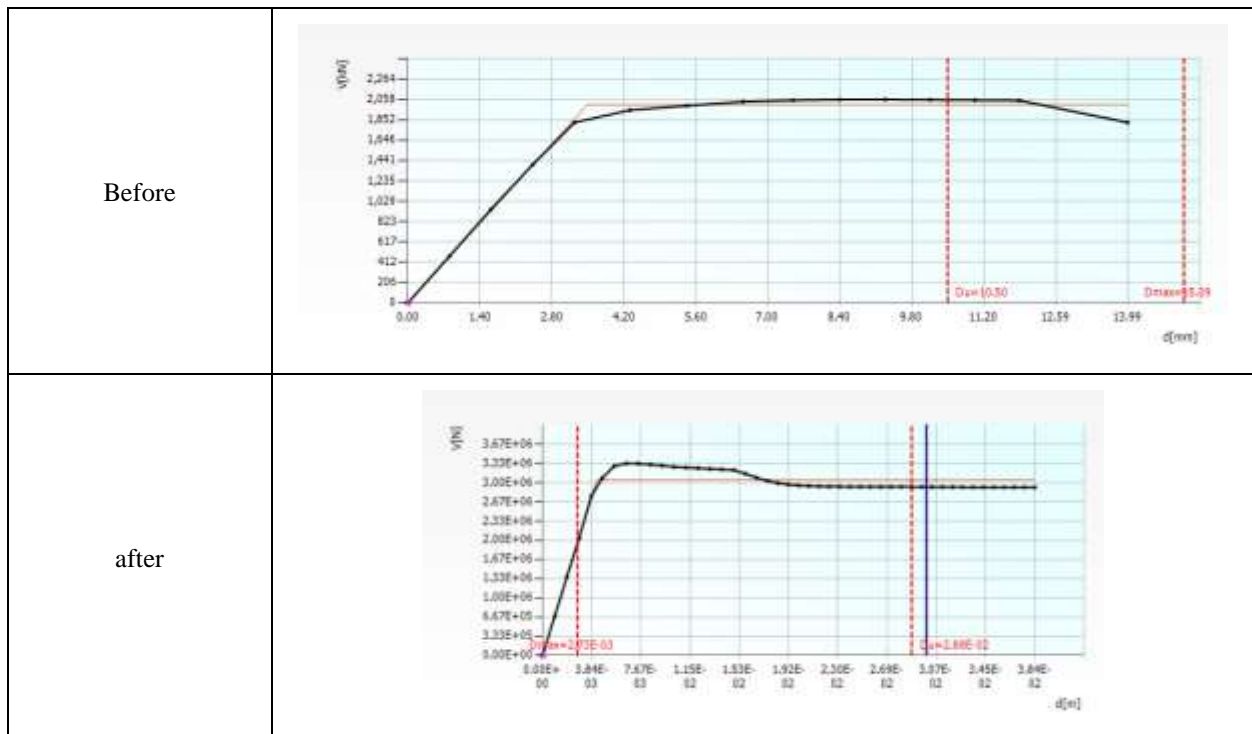


Figure VI 8 Pushover curves for Y direction before and after reinforcement

VI.7 ASSESSMENT OF THE PERFORMANCE POINT (X DIRECTION)

To assess the performance point, we have seen choosing two different methods (graphical, and empirical).

VI.7.1 Graphical ‘‘using excel table’’

The method used is the (N2) approach as described in the seismic analysis part:

For all calculation look **APPENDIX III**

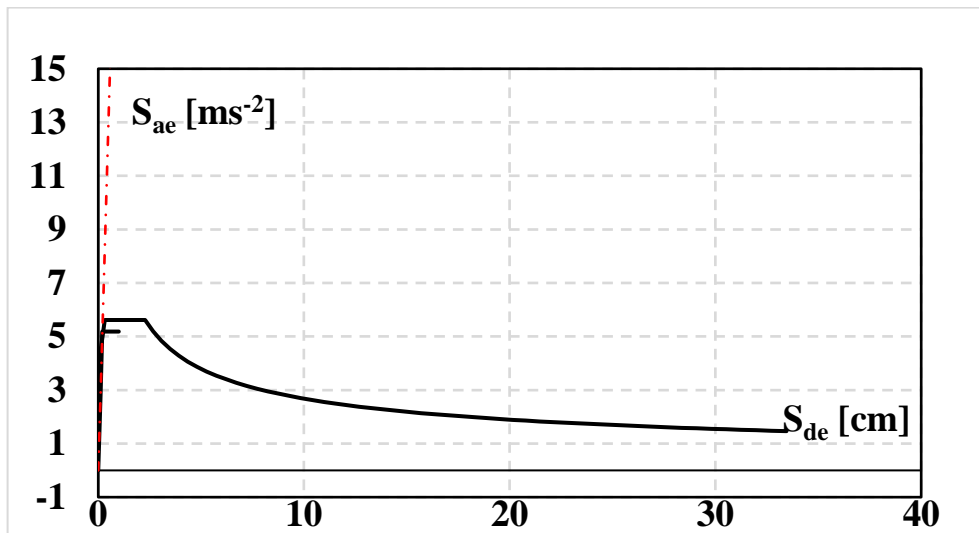


Figure VI.9 intersection of the capacity curve and the demand X direction after reinforcement

VI.7.2 Numerical

According to (Sergio Lagomarsino and al), the performance point, S_d , in terms of displacement, is determined by a closed analytical function.

Table VI.47 performance point X direction numerical method data after reinforcement

| T [sec] | TC [sec] | Sae[m/s ²] | ay[m/s ²] | Dy [m] | Sd*[m] |
|---------|----------|------------------------|-----------------------|--------|--------|
| 0.122 | 0.4 | 7.5 | 0.25 | 0.002 | 0.004 |

Using different methods to assess the performance point gave an approximate value which around ‘‘0.4 cm’’

all calculation details are in the **Appendix III**

VI.8 ASSESSMENT OF THE PERFORMANCE POINT (Y DIRECTION)

To assess the performance point, we have seen choosing two different methods (graphical, and empirical).

VI.8.1 Graphical ‘using excel table’

The method used is the (N2) approach as described in the seismic analysis part:

For all calculation look table **APPENDIX III**

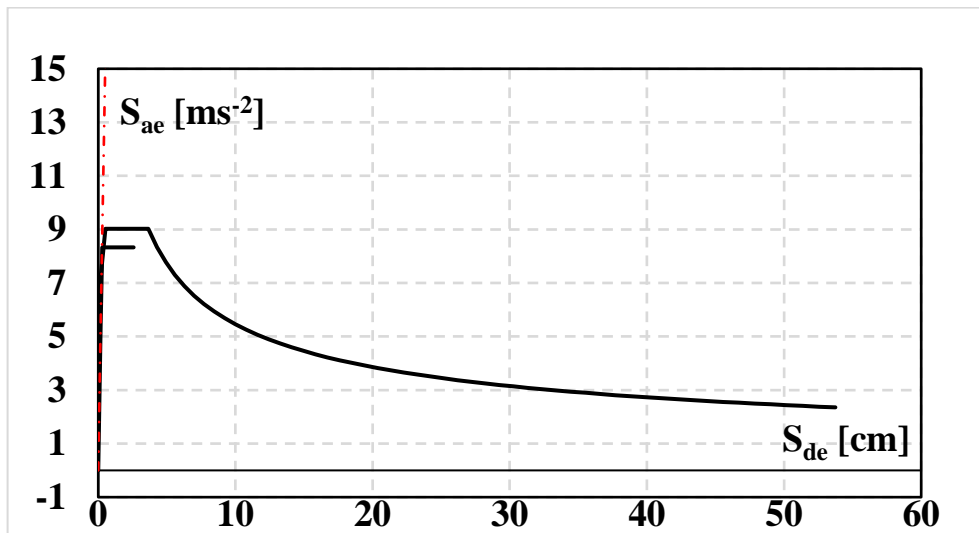


Figure VI 10 intersection of the capacity curve and the demand Y direction after reinforcement

VI.8.2 Numerical

According to (Sergio Lagomarsino and al), the performance point, S_d , in terms of displacement, is determined by a closed analytical function.

Table VI 48 performance point Y direction numerical method data after reinforcement

| T [sec] | TC [sec] | Sae[m/s ²] | ay[m/s ²] | Dy [m] | Sd*[m] |
|---------|----------|------------------------|-----------------------|--------|--------|
| 0.116 | 0.4 | 7.5 | 0.3 | 0.002 | 0.002 |

Using different methods to assess the performance point gave an approximate value which around ‘0.02 cm’

all calculation details are in the **Appendix III**

VI.9 VULNERABILITY ANALYSIS

VI.9.1 Analytical functions for fragility curve

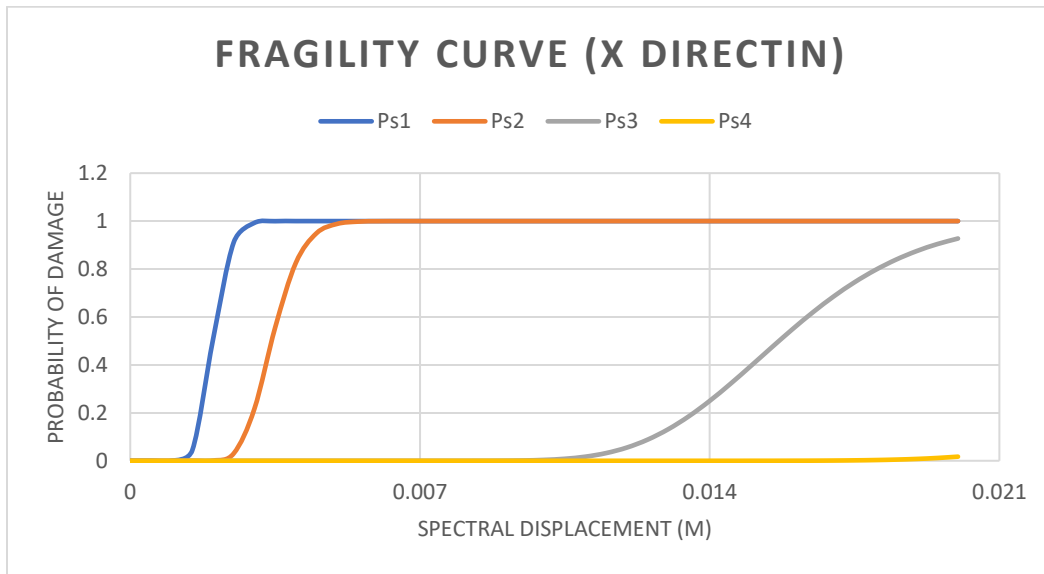


Figure VI 11 fragility curve for X directin after reinforcement

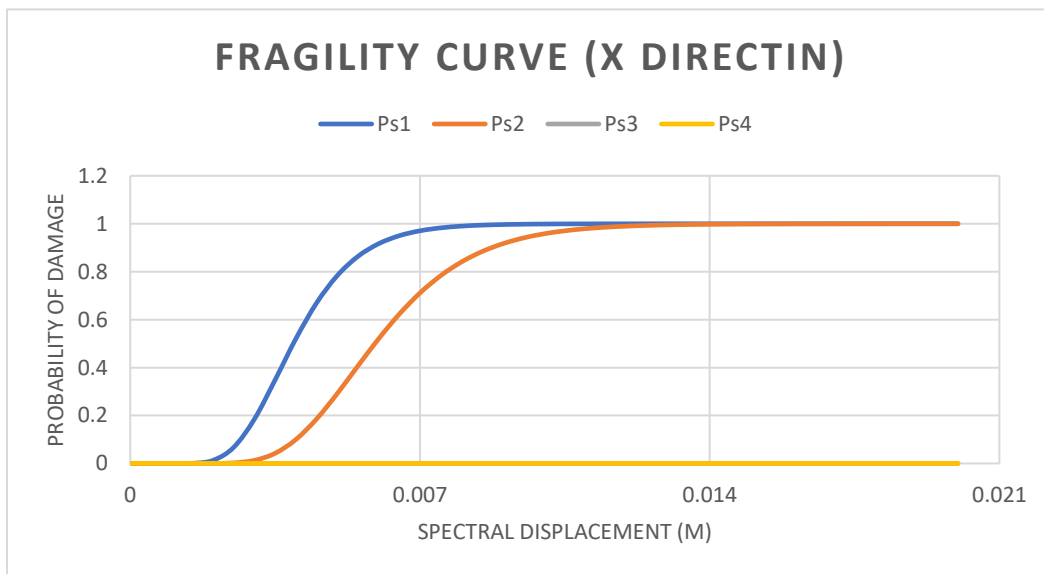


Figure VI 12 fragility curve for Y directin after reinforcement

V.1.1 Damage distribution of the studied structure

Table VI 49. Correspondence between damage level D_{Sk} and damage grades D_k related to structural and non structural damage.

| D_{Sk} | D_k | Structural (SD) and non-structural (N-SD) damage |
|--|-----------------------|--|
| Slight (D_{S1}) | Slight (D_1) | No SD slight N-SD |
| Moderate (D_{S2}) | Moderate (D_{S2}) | Slight SD moderate N-SD |
| Extensive (D_{S3}) | Heavy (D_3) | Moderate SD heavy N-SD |
| Complete (D_{S3}) | Very heavy (D_4) | Heavy SD very heavy N-SD |
| | Destruction (D_5) | Very heavy SD |

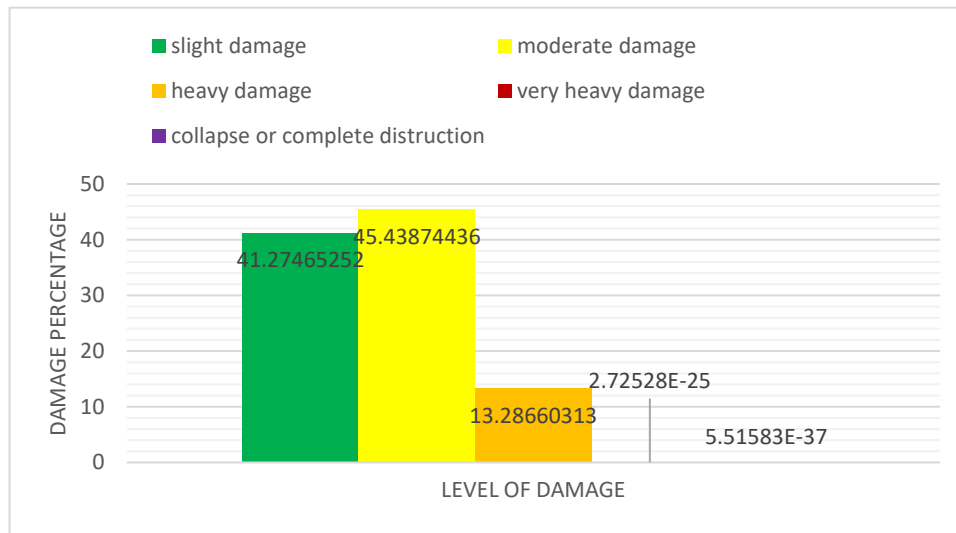


Figure VI 13 damage histogram after reinforcement (X direction)

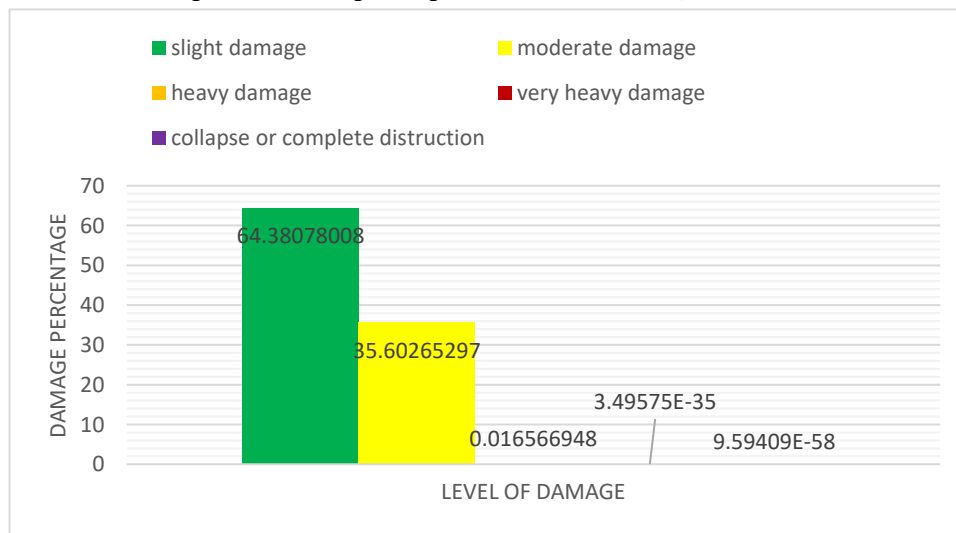


Figure VI 14 damage histogram after reinforcement (Y direction)

VI.9.2 Finds

In conclusion, the reinforcement of the masonry wall has proven to be an effective measure in reducing the vulnerability of elements to seismic demand.

Table VI 50 comparison of the damage histograms before and after reinforcement for both seismic directions

| | Before | After | | | | | | | | | | | | | | | | | | |
|-----------------|--|-----------------|-------------------|---------|---|---------|----|---------|----|---------|----|--|-----------------|-------------------|---------|----|---------|----|---------|----|
| X direction | <table border="1"> <caption>Damage Histogram - X direction Before</caption> <thead> <tr> <th>Level of Damage</th> <th>Damage Percentage</th> </tr> </thead> <tbody> <tr> <td>Level 1</td> <td>1</td> </tr> <tr> <td>Level 2</td> <td>75</td> </tr> <tr> <td>Level 3</td> <td>20</td> </tr> <tr> <td>Level 4</td> <td>5</td> </tr> </tbody> </table> | Level of Damage | Damage Percentage | Level 1 | 1 | Level 2 | 75 | Level 3 | 20 | Level 4 | 5 | <table border="1"> <caption>Damage Histogram - X direction After</caption> <thead> <tr> <th>Level of Damage</th> <th>Damage Percentage</th> </tr> </thead> <tbody> <tr> <td>Level 1</td> <td>42</td> </tr> <tr> <td>Level 2</td> <td>45</td> </tr> <tr> <td>Level 3</td> <td>13</td> </tr> </tbody> </table> | Level of Damage | Damage Percentage | Level 1 | 42 | Level 2 | 45 | Level 3 | 13 |
| Level of Damage | Damage Percentage | | | | | | | | | | | | | | | | | | | |
| Level 1 | 1 | | | | | | | | | | | | | | | | | | | |
| Level 2 | 75 | | | | | | | | | | | | | | | | | | | |
| Level 3 | 20 | | | | | | | | | | | | | | | | | | | |
| Level 4 | 5 | | | | | | | | | | | | | | | | | | | |
| Level of Damage | Damage Percentage | | | | | | | | | | | | | | | | | | | |
| Level 1 | 42 | | | | | | | | | | | | | | | | | | | |
| Level 2 | 45 | | | | | | | | | | | | | | | | | | | |
| Level 3 | 13 | | | | | | | | | | | | | | | | | | | |
| Y direction | <table border="1"> <caption>Damage Histogram - Y direction Before</caption> <thead> <tr> <th>Level of Damage</th> <th>Damage Percentage</th> </tr> </thead> <tbody> <tr> <td>Level 1</td> <td>1</td> </tr> <tr> <td>Level 2</td> <td>42</td> </tr> <tr> <td>Level 3</td> <td>35</td> </tr> <tr> <td>Level 4</td> <td>22</td> </tr> </tbody> </table> | Level of Damage | Damage Percentage | Level 1 | 1 | Level 2 | 42 | Level 3 | 35 | Level 4 | 22 | <table border="1"> <caption>Damage Histogram - Y direction After</caption> <thead> <tr> <th>Level of Damage</th> <th>Damage Percentage</th> </tr> </thead> <tbody> <tr> <td>Level 1</td> <td>65</td> </tr> <tr> <td>Level 2</td> <td>35</td> </tr> </tbody> </table> | Level of Damage | Damage Percentage | Level 1 | 65 | Level 2 | 35 | | |
| Level of Damage | Damage Percentage | | | | | | | | | | | | | | | | | | | |
| Level 1 | 1 | | | | | | | | | | | | | | | | | | | |
| Level 2 | 42 | | | | | | | | | | | | | | | | | | | |
| Level 3 | 35 | | | | | | | | | | | | | | | | | | | |
| Level 4 | 22 | | | | | | | | | | | | | | | | | | | |
| Level of Damage | Damage Percentage | | | | | | | | | | | | | | | | | | | |
| Level 1 | 65 | | | | | | | | | | | | | | | | | | | |
| Level 2 | 35 | | | | | | | | | | | | | | | | | | | |

Through the implementation of appropriate reinforcement techniques, the structural integrity of the wall has been enhanced, leading to improved resistance against seismic forces. This reinforcement effort serves as a vital step in ensuring the overall safety and resilience of the structure, providing greater protection for occupants and minimizing potential damage during seismic events.

VI.10 CONCLUSION

In conclusion, the reinforcement of the School of Asla Hocine's masonry structure in Annaba has significantly improved its stability and resilience. Various types of reinforcement, including wall frames, FRCM systems, and steel elements, were employed to address structural weaknesses. Static verifications confirmed the adequacy of the reinforcements, while seismic and vulnerability analyses demonstrated improved performance and reduced susceptibility to damage. The resulting histogram of the damage degree highlights the structure's enhanced resistance and durability. Overall, the successful reinforcement

efforts ensure the long-term preservation of this heritage building and provide valuable insights for similar projects in the future.

GENERAL CONCLUSION

The study focuses on the analysis and assessment of masonry structures, particularly historical buildings. It delves into various aspects such as material properties, including units and mortar, and examines the mechanisms of deterioration, encompassing both external and internal factors such as mechanical, chemical, and biodeterioration. The research further aims to estimate the mechanical properties of masonry, considering relevant codes and guidelines. Seismic behaviour and vulnerability modelling are explored, utilizing techniques such as pushover analysis to evaluate the response of structures to seismic forces. The study also investigates different strengthening methods, including surface treatment and external reinforcement, to enhance the performance and longevity of masonry structures. By conducting case studies and diagnoses, the research provides valuable insights into the behaviour of masonry under various loads and conditions. Ultimately, the findings contribute to a deeper understanding of masonry behaviour and provide valuable guidance for the effective strengthening and preservation of historical buildings.

Following the modelling and analysis of the structure, it became evident that the building was highly vulnerable to seismic actions, with severe damage observed on several elements. Consequently, the decision was made to reinforce the structure, and the outcome was remarkably positive. The behaviour of all elements, both statically and dynamically, improved significantly, addressing the vulnerabilities identified during the analysis. Notably, the damage histogram demonstrated highly satisfactory results, indicating the effectiveness of the reinforcement measures implemented. Overall, the reinforcement efforts proved successful in enhancing the structural integrity and resilience of the building, mitigating the potential damage caused by seismic events.

The findings obtained from the analysis clearly indicate the urgent need for a thorough reassessment of all structures throughout Algeria. These results serve as a wake-up call, underscoring the imperative to prioritize the preservation and careful management of our cherished heritage and historical buildings. Despite their profound significance in embodying the essence of Algerian culture, it is disheartening to observe the state of neglect that many of these structures have fallen into over the years.

Compounding the issue is the scarcity of research in this specific field, which is remarkably limited and, in some cases, virtually non-existent. The dearth of scholarly exploration into the conservation and restoration of historical buildings not only perpetuates the cycle of neglect but also inhibits our ability to develop effective strategies and approaches tailored to the unique challenges faced by these structures. This scarcity of research is further exacerbated by the absence of a dedicated

Algerian guideline or code, specifically designed to address the intricacies of preserving and maintaining heritage structures within the country.

Moreover, the prevailing laws and regulations governing heritage conservation in Algeria present a formidable obstacle to progress in this field. The stringent nature of these legal frameworks restricts innovation and hampered the development of a comprehensive approach to heritage preservation. There is an urgent need to review and revise these regulations, fostering an environment that encourages research, innovation, and collaboration in the field of heritage conservation.

By acknowledging the critical state of our historical buildings and acknowledging the lack of attention they have received, we can pave the way for transformative change. It is imperative to advocate for the establishment of a robust research framework that actively supports investigations into heritage conservation and restoration. Simultaneously, efforts must be made to formulate a comprehensive Algerian guideline or code that provides clear and practical directives for the management, maintenance, and seismic reinforcement of heritage structures.

In embracing these measures, we can foster a renewed commitment to our shared cultural legacy and ensure its preservation for generations to come. By safeguarding our historical buildings and investing in their protection, we honor our heritage, strengthen our national identity, and contribute to the sustainable development and prosperity of Algeria.

REFERENCES

- MASONRY - ROOF - FLOOR CONSTRUCTION. (2020). Retrieved from www.sathyabama.ac.in
- SEBOUI Hatem, A.A. (2022). Literature review on the mechanical properties estimation.
- Valek, j. J. (2003). Literature review mortars in historic buildings. Historic Scotland.
- Raffaello, C. (2012). 3 muri project. Retrieved from STADATA: www.3muri.com
- Sergio Lagomarsino, A.P. (2013). TREMURI program: An equivalent frame model for the nonlinear seismic analysis of masonry buildings. elsevier.
- Giovinazzi, S. (2005). THE VULNERABILITY ASSESSMENT AND THE DAMAGE SCENARIO IN SEISMIC RISK ANALYSIS. the Department of Civil Engineering of the Technical University Carolo-Wilhelmina at Braunschweig.
- GUIDO MAGENES, S.P. (2002). non_liar modeling and seismic analysis of masonry structure . Journal of Earthquake Engineering.
- Sergio Lagomarsino, S.G. (2006). Macroseismic and mechanical models for vulnerability and damage assessment. Springer Science.
- Transport, M.o. (2019). circular no 7.
- (RPA99/version 2003): Règlement Parasismique Algériennes.
- NTC 2018: Norme Techniche per le Costruzioni (2018). Italian Ministry of Infrastructure and Transport.
- ATC-40: Seismic Evaluation and Retrofit of Concrete Buildings (1996). Applied Technology Council.
- Eurocode 8: Design of Structures for Earthquake Resistance - Part 1: General Rules, Seismic Actions, and Rules for Buildings (2004). European Committee for Standardization.
- Eurocode 1: Actions on Structures - Part 1-1: General Actions - Densities, Self-Weight, Imposed Loads for Buildings (2002). European Committee for Standardization.
- Eurocode 6: Design of Masonry Structures - Part 1-1: General Rules for Reinforced and Unreinforced Masonry Structures (2005). European Committee for Standardization.
- FEMA 273: Guidelines for the Seismic Rehabilitation of Buildings (1997). Federal Emergency Management Agency.
- FEMA 356: Prestandard and Commentary for the Seismic Rehabilitation of Buildings (2000). Federal Emergency Management Agency.

APPENDIX I

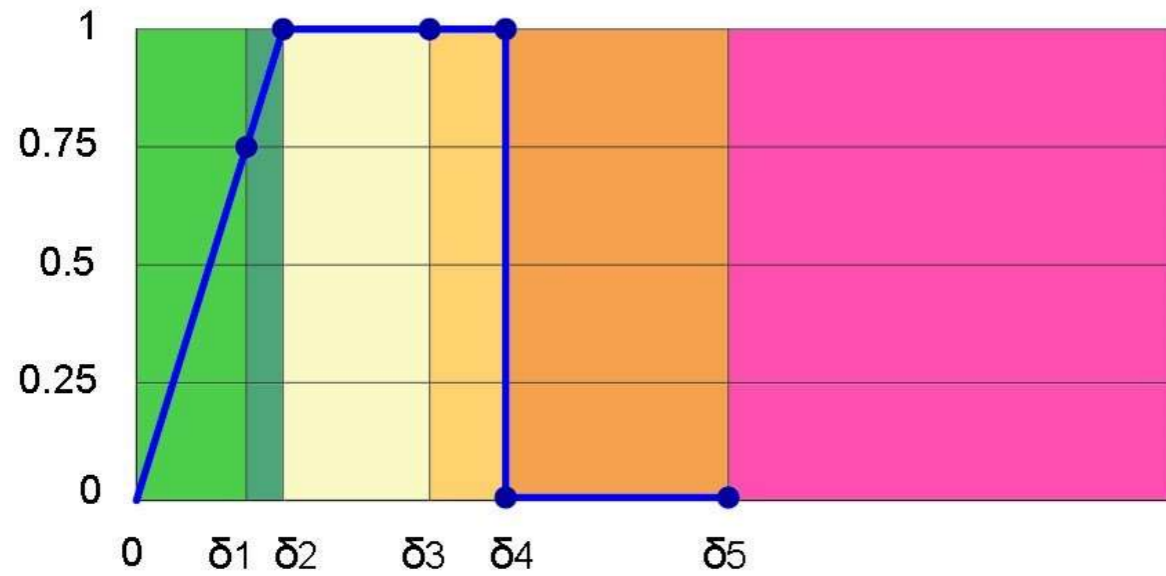
I.1 CONSTITUENT BONDS

Subsequently, the constituent bonds associated with the shear and bending mechanisms acting on the load-bearing masonry are analyzed.

The colored areas used on diagrams, refer to the color legend dedicated to "Masonry", present on 3Muri.

| Masonry | |
|--------------|------------------------------|
| Green | Undamaged |
| Light Green | Plasticity incipient |
| Yellow | Shear damage |
| Light Orange | Incipient shear failure |
| Orange | Shear failure |
| Light Red | Bending damage |
| Red | Incipient bending failure |
| Dark Red | Bending failure |
| Pink | Serious crisis |
| Dark Purple | Compression failure |
| Light Blue | Tension failure |
| Blue | Failure during elastic phase |

· Pier with shear mechanism

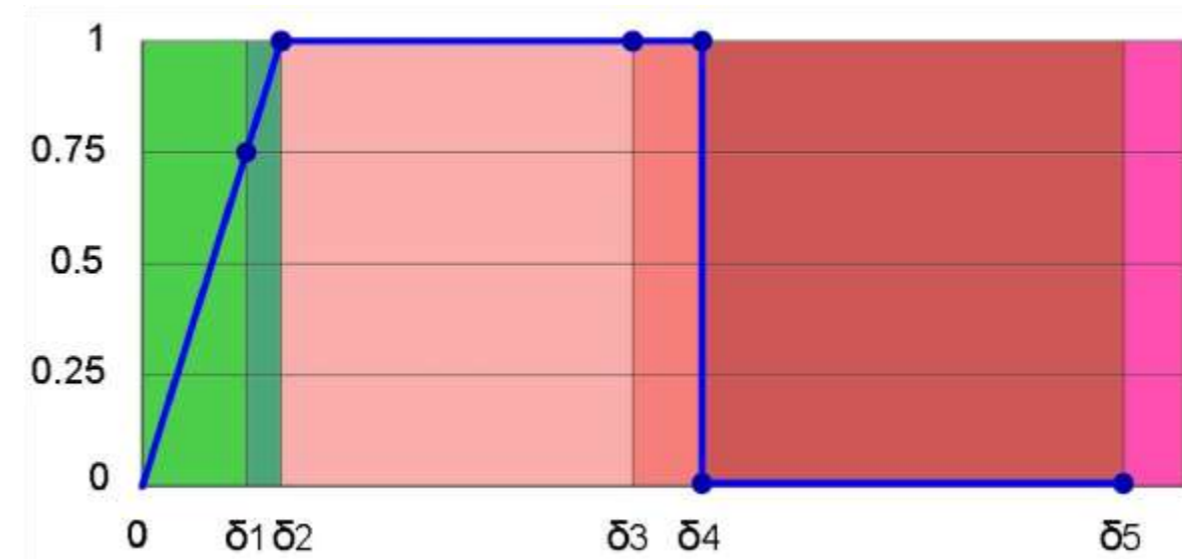


The behavior of the pier wall shear can be described through the following traits, representative of the progressive levels of damage relating to the previous diagram:

| | |
|-------------------------|-------------------------|
| 0 - δ_1 | elasticity |
| δ_1 - δ_2 | incipient of plasticity |

| | |
|-------------------------|-------------------------|
| δ_2 - δ_3 | plastic for shear |
| δ_3 - δ_4 | shear rupture incipient |
| δ_4 - δ_5 | shear rupture |
| δ_5 - ∞ | serious crisis |

· Pier with bending mechanism



The behavior of the pier wall to bending, however, can be described through the following traits:

| | |
|-------------------------|---------------------------|
| 0 - δ_1 | elasticity |
| δ_1 - δ_2 | incipient of plasticity |
| δ_2 - δ_3 | plastic for bending |
| δ_3 - δ_4 | bending rupture incipient |
| δ_4 - δ_5 | bending rupture |
| δ_5 - ∞ | serious crisis |

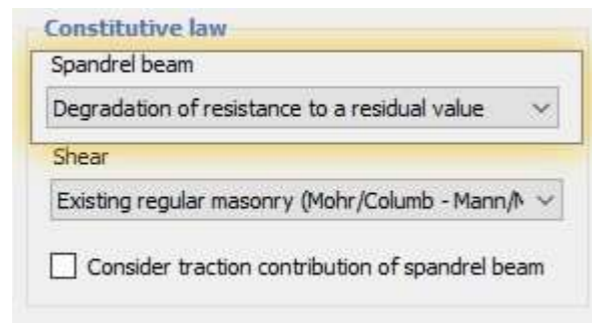
Some levels of damage are used to describe more carefully the progress of the crisis:

- incipient of plasticity: When an element is in the elastic field but it is next to the plasticity
- incipient of rupture : When an element is in the plastic field but is close to rupture

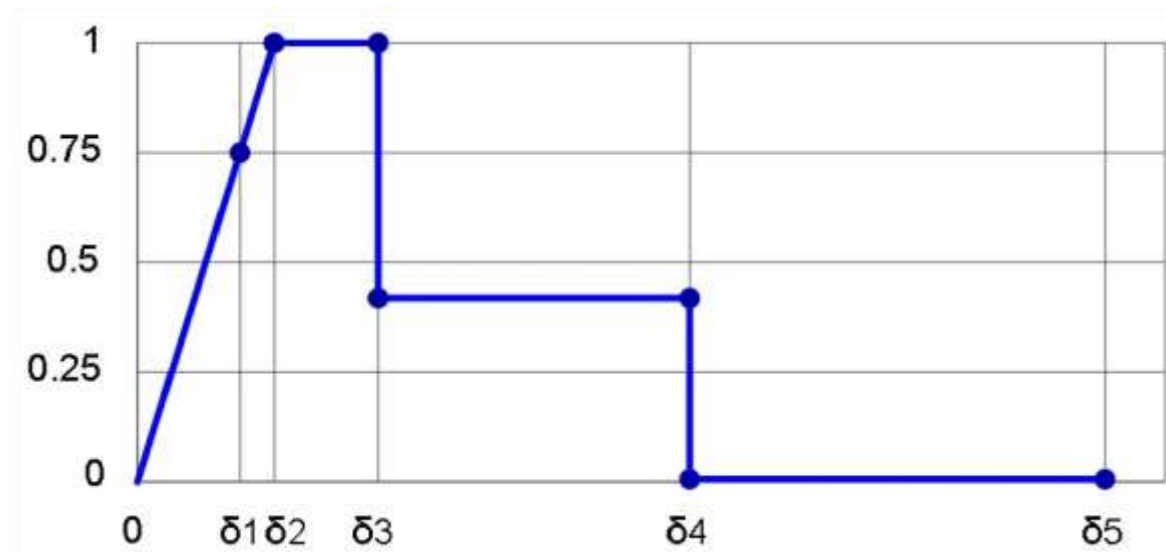
· Serious crisis: When afterwards the rupture element, the deformations become so significant that they can generate a local collapse.

These new levels of damage enable a more accurate prediction of the interventions and the degradation level of the masonry.

Through the drop-down menu, exclusively dedicated to the "Spandrel beams", present in the main screen of masonry materials, the software provides three types of analysis:



· With degradation of resistance to residual value (Multiline bond)



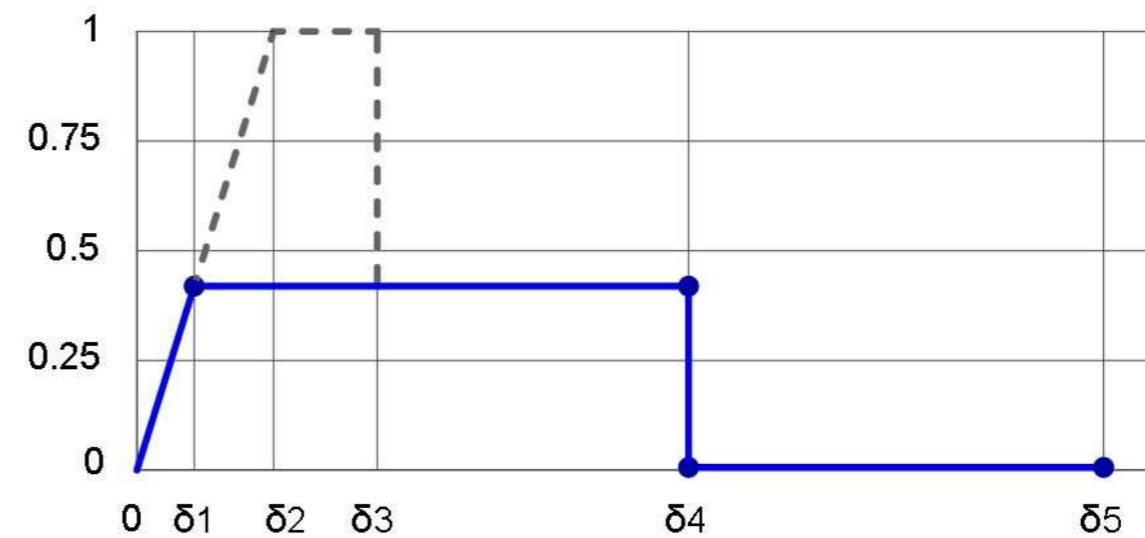
This type of bond is defined in the Circular at §C8.7.1.3.1 assuming:

δ_1 : $0.75 \cdot \delta_2$ (0.75 is the default value of the "incipient factor bond plasticity" defined in the parameter window.

| [1] Materials | |
|---|-------|
| Pier drift shear | 0,005 |
| Pier drift bending | 0,01 |
| Spandrel beams drift shear | 0,015 |
| Spandrel beam drift bending | 0,015 |
| Paired spandrel beam drift | 0,02 |
| Existing: FC-LC1 | 1,35 |
| Existing: FC-LC2 | 1,2 |
| Existing: FC-LC3 | 1 |
| Reduction factor for cracked stiffness | 2 |
| Concrete/steel lintel residual resistance | 0,6 |
| Timber lintel residual resistance | 0,4 |
| Masonry arch residual resistance | 0,1 |
| Incipient factor bond plasticity | 0,75 |
| [2] Static calculation | |
| γ_{G1} | 1,3 |
| γ_{G2} | 1,5 |
| γ_Q | 1,5 |

δ_2 : deformation in correspondence with the elastic limit defined by the stiffness and limit resistance δ_3 : 0.005
 δ_4 : 0.015 δ_5 : $2 \cdot \delta_4$: This deformation represents the state of "serious crisis" not directly required in the standard but useful as a "warning" for the designer.

· With resistance equal to residual value (bilinear bond)

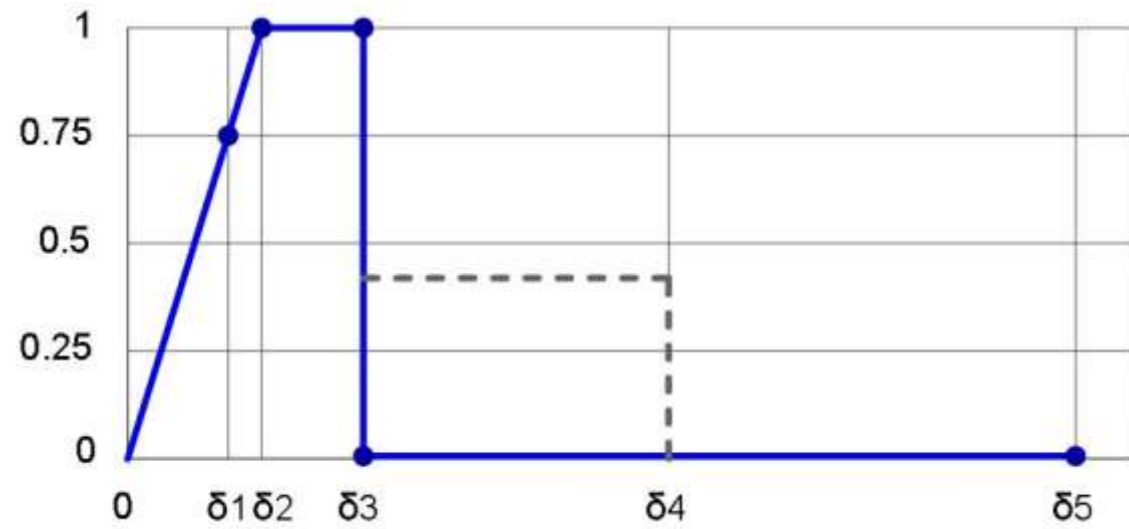


This type of bond is defined in the Circular at §C8.7.1.3.1 assuming:

δ_4 : 0.015 δ_5 : $2 \cdot \delta_4$: This deformation represents the state of "serious crisis" not directly required in the standard but useful as a "warning" for the designer.

This type of bond is produced by limiting the multiline bond to the residual resistance.

· Without residual resistance



This type of bond represents a logical variation of the earlier bond starting from the multiline bond but is currently not covered by current regulations.

I.1.1 Definition of residual resistance

The definition of residual resistance is explained on section C8.7.1.3.1 of the Circolare

(...) In the absence of more accurate formulations, it is possible to choose values of residual strength, such as the maximum one provided by (8.7.1.16), equal to:

- lintel in reinforced concrete or steel, as long as it is supported by an extension force in the masonry: 60%;
- wooden lintel, with good characteristics and well clamped: 40%; -masonry arch: 10%. (...)

I.1.2 Tension failure

One of the colors in the legend represents tension failure.

Reinforced masonry: The traction caused the rupture of the reinforcement, this is an irreversible state.

I.1.3 Ineffective element

One of the colors of the legend represents the ineffective element.

Ordinary masonry: The masonry is not effective; this is not a real rupture but a reversible temporary state that could evolve into any other type of rupture.

I.2 EUROCODE 6

Let's present below the checks that are carried out:

| | |
|---|---|
| Slenderness check: EN 1996-1-1 § 5.5.1.4 | $h_{ef}/t_{ef} \leq \lambda_{lim}$: di default=27 |
| Verification subjected to vertical loading EN 1996-1-1 § 6.1.2 | $N_{Ed} \leq N_{Rd} = \Phi f_d A$ |
| | N_{Ed} : design value of the vertical load applied to a masonry wall; A: is the loaded horizontal gross cross-sectional area of the wall; f_d : design compressive strength of the masonry; Φ : is the capacity reduction factor |

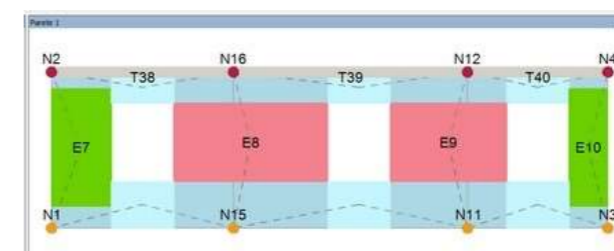
The static checks are performed in an area that is accessed using the associated button.



The following screen will appear:



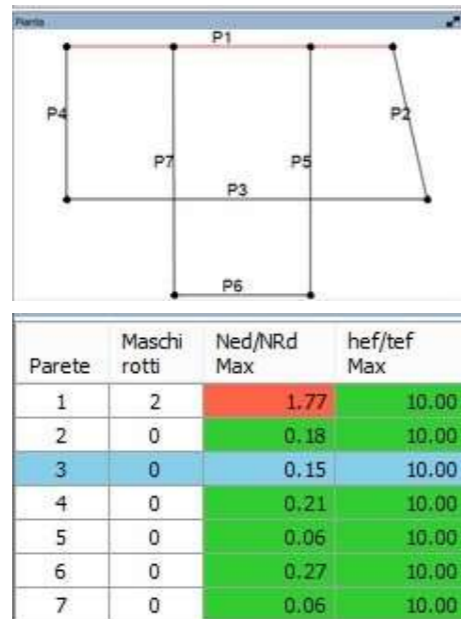
This video is very similar to that which presents the results of non-linear analysis. Let's describe it in detail.



In the upper right side appears the wall mesh.

In this case, does not exist the legend with colors indicating different phases of damage.

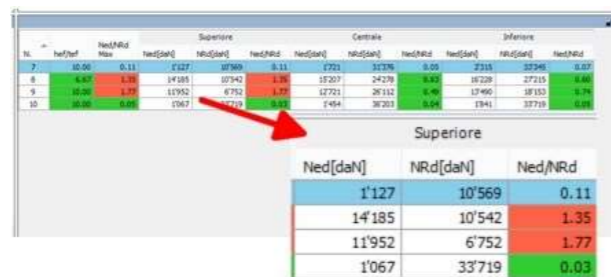
Elements that passed the check appear in green and in different color those that do not exceed the check.



At the lower left side, is shown the plan view. The wall shown in the precedent view is highlighted with a thick line.

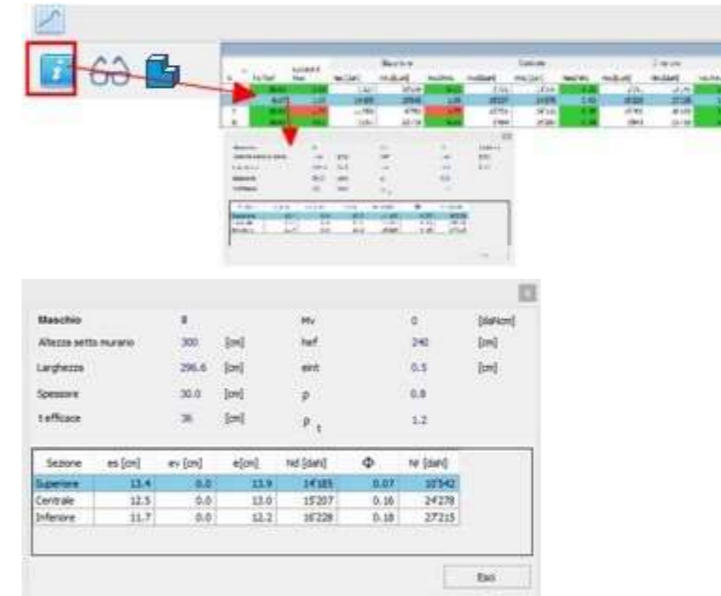
On the upper left side there is a list of the walls in the model, with the number of elements that did not pass the check and the values associated with the individual checks. The values found in the table are for the wall elements examined in which the limit values are the most restrictive of all the piers.

Clicking on the line of a wall (highlighting it in blue) brings that wall to the view on the right side.



At the lower right side, the elements detail window is shown for the selected wall.

For each masonry element, the checks are performed for three different sections (higher, central, lower). For each section the value for normal forces strain is shown (N_{Rd} : computed based on the masses and the combinations of the loads) and the normal resistant strain ($N_{Rd} = \Phi f_d A$). The check is satisfied if the ratio $N_{Ed}/N_{Rd} \leq 1$. In this case, the corresponding cell appears in green, otherwise in red color. In some cases, as shown in the example, N_{Rd} cannot be calculated (n/d: not defined). This happens when the slenderness or eccentricity checks are not satisfactory.



When a masonry pier is chosen from the list and the information button is pressed, a window will appear which contains the calculation details.

The window shows all the details of the parameters used in the computation of the various check coefficients. The text in red near the bottom gives relative informations to conditions where the check was not satisfied. This window can remain open and be moved to any point of the drawing area while working (floating window). This gives to the user the possibility to select various elements in different wall and still have the details for each individual check visible.

| ID | h0 / t | Higher e1 / t | Central e2 / t | Lower e1 / t |
|----|--------|------------------|-------------------|-----------------|
| 35 | 7,50 | 0,300 | 0,144 | 0,263 |
| 36 | 7,50 | 0,306 | 0,145 | 0,276 |
| 37 | 7,50 | 0,360 | 0,172 | 0,331 |
| 38 | 7,50 | 0,332 | 0,150 | 0,274 |
| 39 | 7,50 | 0,451 | 0,187 | 0,268 |
| 40 | 7,50 | 0,401 | 0,175 | 0,311 |
| 41 | 7,50 | 0,448 | 0,202 | 0,369 |
| 42 | 7,50 | 0,470 | 0,186 | 0,309 |

Here we see the check details for slenderness and eccentricity. The green values indicate that the check was passed.

In order to help the user in the results interpretations, some of the tables offer the possibility of reordering the rows according to a characteristic shown in a column by simply clicking on the title of the column.

APPENDIX II

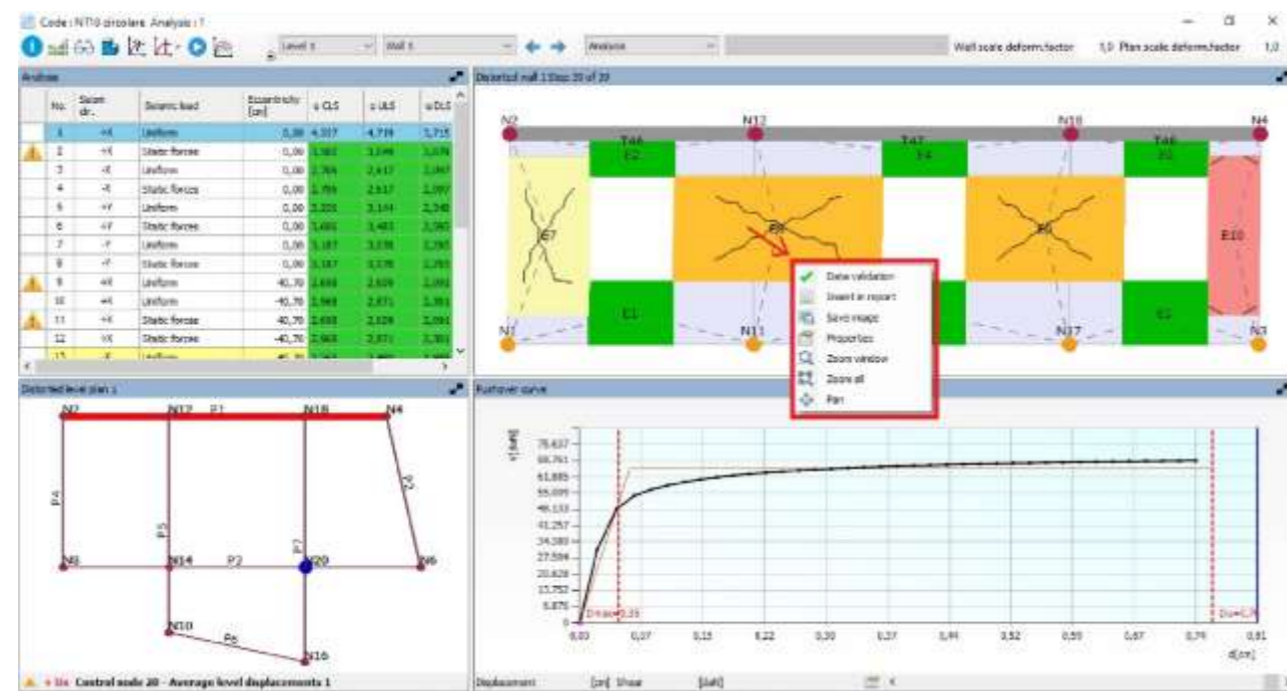
I Data validation

This validation tool allows the user to evaluate the stress state of the masonry walls in a quick, simple and intuitive way, graphically displaying, for each step of the non-linear seismic analysis, the drift value, the resistance domain and the mechanism of collapse.

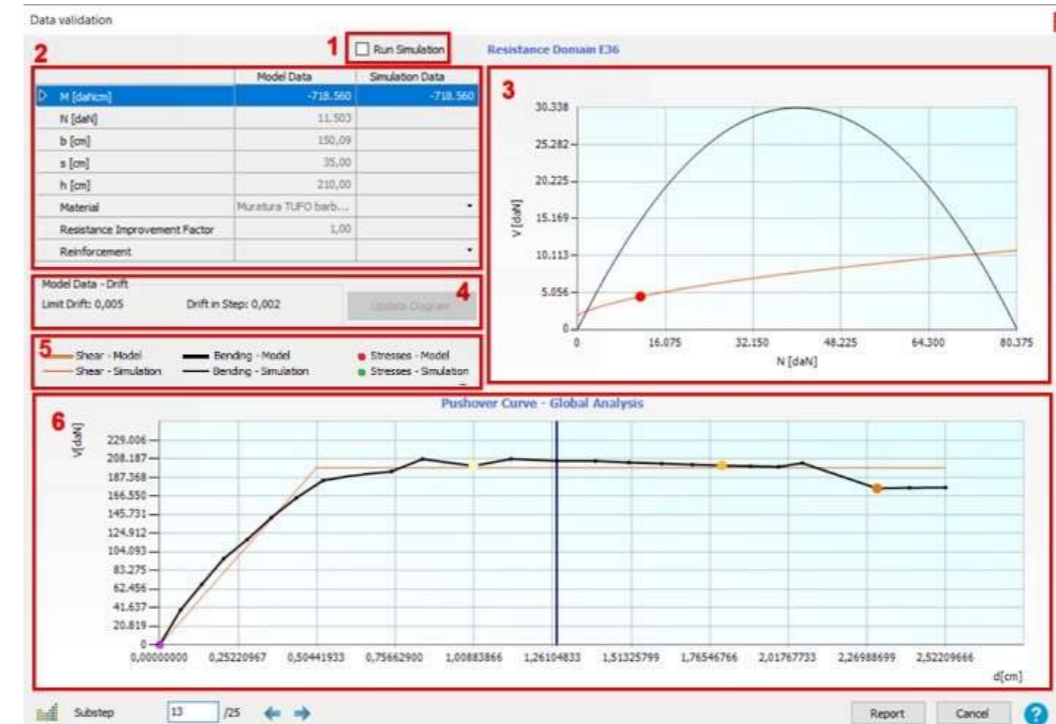
This function is designed both to help the user understand the behavior of the structure, but above all to help and guide him in the phase of validating the results provided by the software.

For this purpose, within the results window, at each point of the global pushover curve, for each masonry wall it is possible to view the state (first yielding, incipient failure, breaking) in which the element is located. This allows the designer to have a transversal view of the behavior, and therefore of the influence, of the individual wall panels within the structure. In the event that improvements need to be made to an existing building (reinforcements with FRP and FRCM), using this validation tool, the designer can easily understand on which wall panels it is appropriate to intervene, or if the interventions are effective or if they can be optimized.

From the window containing the results of the pushover analysis, by right clicking on the wall of interest, the following dropdown menu opens:



Once you have clicked on the "data validation" option, the following window appears:



It allows to start a simulation by entering the simulation data in the third column of the table at the top left, and click on "Update diagram".

The table contains in the second column the geometric and mechanical data of the masonry wall in question, while in the third column, which can be activated by checking the "Run simulation" box, the respective parameters used to determine the simulated resistance domains can be entered.

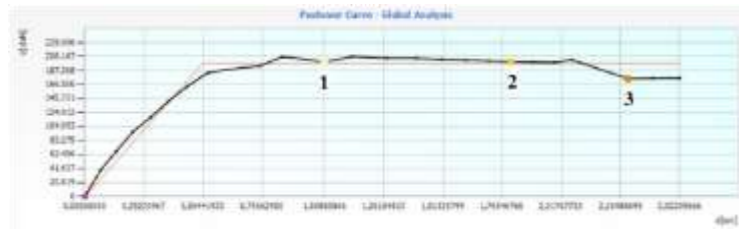
Resistance domains diagram.

Values of the element's limit drift (depends on the breaking mechanism) and the drift to the pace. As is known, the element reaches the break when the drift at the step reaches the drift limit.

Legend related to the diagrams of the resistance domains.

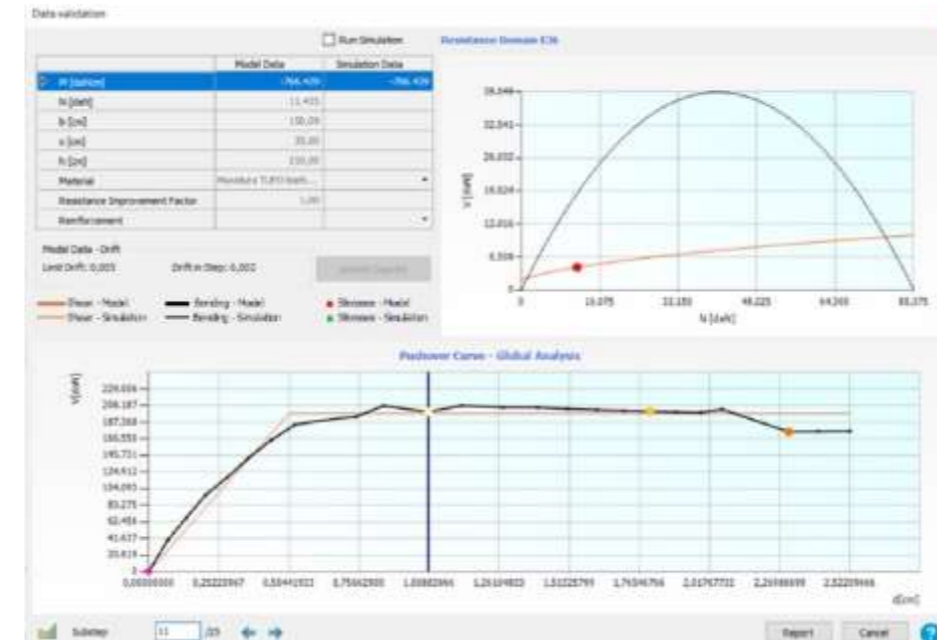
The orange line indicates the shear resistance domain, while the black line indicates the bending resistance domain. The solid lines represent the resistance domain evaluated for the geometric and mechanical characteristics of the modeled masonry wall, while the dashed lines indicate the simulated resistance domains. The two circular indicators, red and green, respectively indicate the stress state of the element resulting from the pushover analysis and the simulated stress state.

Global pushover curve on which there are colored indicators that indicate the calculation step in which the state change of the wall occurs (beginning of plastification, incipient breaking, breaking).



The colored indicators, which designate the state in which the wall under examination is located, allow us to quickly understand that the wall under examination exhibits an elastic behavior until point 1 is reached, step in which the first plastification by shear takes place. Moving further along the curve, the wall changes state in correspondence with the step identified by point 2, that is when he reaches 75% of the drift limit. In this step, in fact, the color legend indicates that the element is in a state of incipient breakage due to shear, which occurs at the step identified in point 3, when the drift limit is reached. As can be easily understood from this result, it can be deduced that the wall in question is well sized and effectively contributes to the strength of the building as its breakage is close to the collapse of the entire building, coinciding with the last point of the curve.

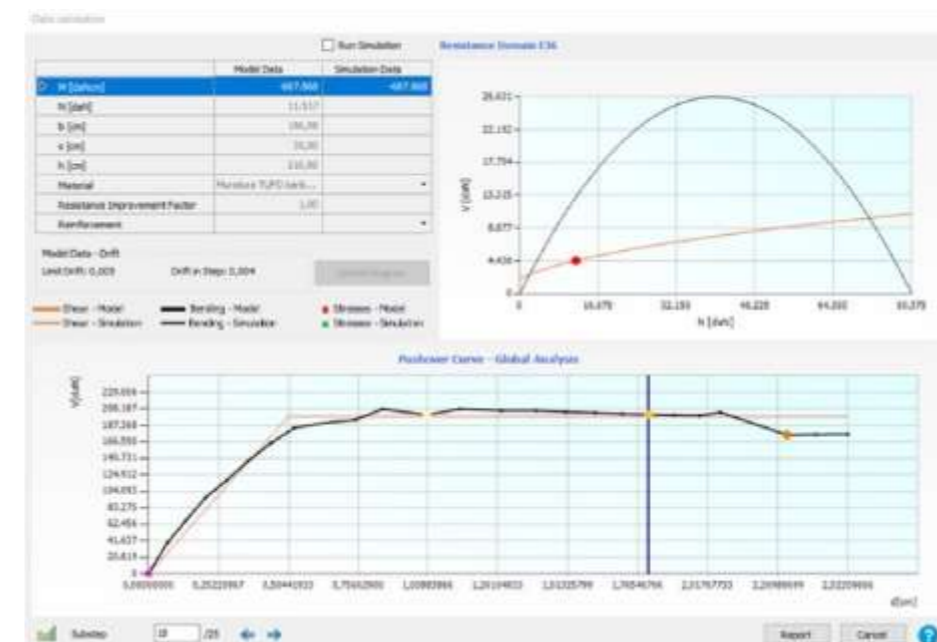
For each point of the pushover curve, it is also possible to visualize the resistance domains of the masonry wall. As already said, in the stretch of curve between step 0 and point 1, the masonry wall is in the elastic phase, in fact, from the resistance domain we can observe that the point indicating the state of stress at the step (red indicator), is placed within the domain.



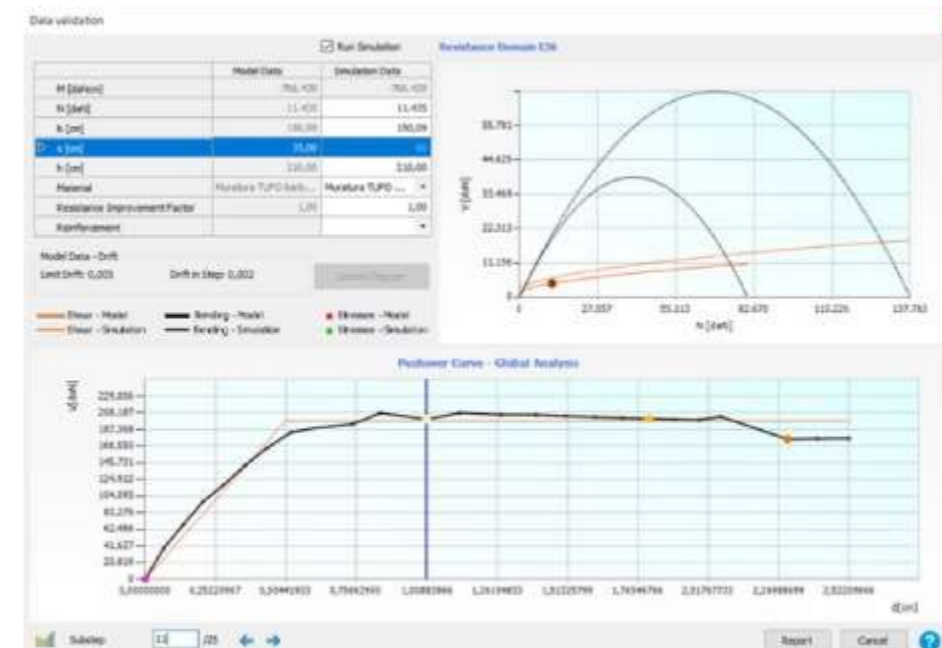
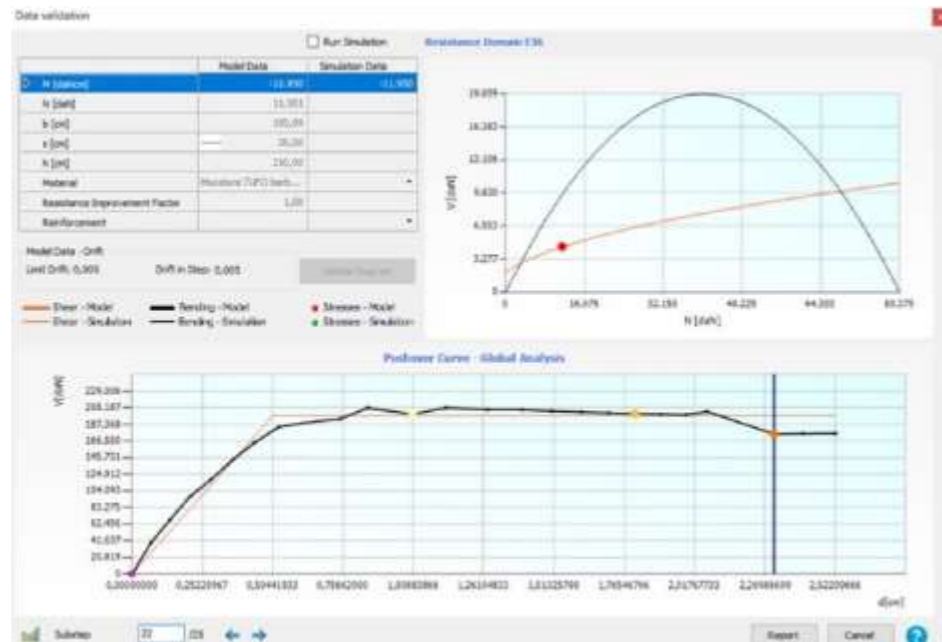
By creating the diagrams of the resistance domains for the step of the pushover curve corresponding to point 2 (incipient collapse due to shear), it is observed that the red indicator always coincides with the orange curve, while the drift at the step is equal to 0.004 or coincides with 75% of the drift limit rounded to three decimal places.



Positioning instead in correspondence with the step of the pushover curve where the first yielding occurs (point 1), from the graph it can be observed that the stressing point (red indicator) is exactly on the curve corresponding to the shear resistance criteria of the masonry wall (curve orange), but if we observe the drift value, it is lower than the breaking value (drift in step = 0.001; drift limit = 0.005).



Finally, positioning in correspondence with the step of the curve in which the breaking of the wall occurs, we observe that the red indicator always coincides with the orange curve, while the drift at the step is equal to 0.005 or coincides with the drift limit.



At the bottom left, using the following buttons, you can access the damage status legend and move between the various points of the pushover curve.



A similar result could be obtained by simulating the case in which the normal stress is greater, for example by increasing the weight of the floor that rests on this wall as a consequence of a reinforcement intervention on a floor which on the one hand improves the performance of the slab itself, and on the other hand it increases the load on the walls. In this case the curves of the domains remain unchanged as they are a function only of the geometric and mechanical parameters of the masonry and of the possible presence of the reinforcement, while the green indicator, which indicates the state of simulated stress, has moved to the right, re-entering the domain.

I.1 RUN SIMULATION Run Simulation

This function offers the possibility of simulating the resistance domain of a masonry wall in real time, simply by varying a few parameters that define its geometric and mechanical characteristics, or those of any reinforcement applied, without having to modify anything in the global model and without having to re-calculate.

If you want to start a simulation, you need to select the step of interest of the pushover curve, check the "Run simulation" box, enter the simulation data in the third column of the table at the top left, and click on "Calculate domain".

I.1.1 Example

In the following example, the simulation is started by positioning at point 1 of the pushover curve and increasing the thickness of the masonry.

As it can be seen from the following figure, the increase in thickness of the masonry wall has the effect of increasing its resistance, and therefore, under the same stress (the red indicator coincides with the green one due to the fact that in the simulation the normal stress has not been changed), in the simulation the element is in the elastic phase, while from the data entered in the model it would be in the plastic phase.

Ultimately, if the masonry wall had the geometric characteristics introduced with the simulation, it would be able to withstand a greater shear force.



What is described above should make us reflect on all those cases in which we try to make an improvement on the structure by lightening the floors.

This could bring the solicitor closer to the origin of the domain and consequently expose them outside the domain itself, creating a deterioration rather than the desired improvement.

These observations make us understand that the most efficient improvement choices should be made after having examined the resistance domain to clarify on which area it is good to act.

I.1.2 Quantifying the extent of improvement of a reinforcement

The application of a reinforcement (reinforced masonry, FRP or FRCM) acts on two different ways:

- Resistance
- Ductility (displacements)

The concept of "improvement" is therefore produced by the union of the two characteristics listed above, which can occur simultaneously or one of the two can have a greater weight than the other.

Strength affects plasticity, ductility affects rupture; ductility itself can be indirectly influenced by resistance by postponing the plasticity of the element due to greater resistance.

Modifying resistance and / or ductility alters the stiffness of the building as a whole and consequently the load that can potentially act on the element in question.

According to the theory of resistance domains, the performance of the element depends on the vertical load acting on it. It therefore follows a significant alteration of the shape of the resistance domains and of the element's ultimate ductility.

It is therefore impossible to numerically quantify the extent of the improvement resulting from the intervention as load, strength and ductility are linked to each other and cannot be schematized in a simplified way through a simple improvement factor of the compressive strength.

To define the benefits produced by an intervention of this nature, it is therefore necessary to simultaneously examine both the changes in the resistance domain (and not just the compressive capacity) and the increase in ductility provided by the reinforcement itself.

In some cases it may happen that the result obtained by recalculating the global analysis does not reflect what was previously simulated through the change of some characteristics.

In fact, when the simulation is carried out on an element, it is considered as an isolated element exempt from the interactions with the rest of the structure that will come into play only following the global calculation.

The modification of geometric or mechanical characteristics or the addition of any reinforcements have an influence not only on the element itself but on the behavior of the entire structure, modifying its configuration in

terms of ductility, stiffness and load. It is therefore important to consider the simulation result as approximate (compared to what would be obtained by redoing the global analysis of the structure) and to use the tool as an aid to the designer who otherwise, faced with an element that is not verified, would have to make changes to the structure based on more or less vague criteria, sometimes modifying the structure in an ineffective way, and spending time redoing the mesh each time and recomputing the seismic analysis.

II DOMAIN COORDINATES FROM MODEL WALL , SEISMIC ANALYSIS NO. 4 WALL 10 X DIRECTION

II.1 BENDING DOMAIN

Table 1 wall 10 bending domain

| N [kN] | V [kN] |
|--------|--------|
| 0 | 0 |
| 51 | 67 |
| 102 | 132 |
| 153 | 196 |
| 203 | 258 |
| 254 | 319 |
| 305 | 379 |
| 356 | 438 |
| 407 | 495 |
| 458 | 550 |
| 509 | 605 |
| 560 | 658 |
| 610 | 709 |
| 661 | 760 |
| 712 | 808 |
| 763 | 856 |
| 814 | 902 |
| 865 | 947 |
| 916 | 991 |
| 967 | 1,033 |
| 1,017 | 1,073 |
| 1,068 | 1,113 |
| 1,119 | 1,151 |
| 1,170 | 1,188 |
| 1,221 | 1,223 |
| 1,272 | 1,257 |

| | |
|-------|-------|
| 1,323 | 1,289 |
| 1,374 | 1,321 |
| 1,424 | 1,351 |
| 1,475 | 1,379 |
| 1,526 | 1,406 |
| 1,577 | 1,432 |
| 1,628 | 1,457 |
| 1,679 | 1,480 |
| 1,730 | 1,501 |
| 1,780 | 1,522 |
| 1,831 | 1,541 |
| 1,882 | 1,558 |
| 1,933 | 1,575 |
| 1,984 | 1,590 |
| 2,035 | 1,603 |
| 2,086 | 1,616 |
| 2,137 | 1,626 |
| 2,187 | 1,636 |
| 2,238 | 1,644 |
| 2,289 | 1,651 |
| 2,340 | 1,656 |
| 2,391 | 1,660 |
| 2,442 | 1,663 |
| 2,493 | 1,664 |
| 2,544 | 1,664 |
| 2,594 | 1,663 |
| 2,645 | 1,660 |
| 2,696 | 1,656 |
| 2,747 | 1,651 |
| 2,798 | 1,644 |
| 2,849 | 1,636 |
| 2,900 | 1,626 |
| 2,950 | 1,616 |
| 3,001 | 1,603 |
| 3,052 | 1,590 |
| 3,103 | 1,575 |
| 3,154 | 1,558 |
| 3,205 | 1,541 |
| 3,256 | 1,522 |
| 3,307 | 1,501 |
| 3,357 | 1,480 |

| | |
|-------|-------|
| 3,408 | 1,457 |
| 3,459 | 1,432 |
| 3,510 | 1,406 |
| 3,561 | 1,379 |
| 3,612 | 1,351 |
| 3,663 | 1,321 |
| 3,714 | 1,289 |
| 3,764 | 1,257 |
| 3,815 | 1,223 |
| 3,866 | 1,188 |
| 3,917 | 1,151 |
| 3,968 | 1,113 |
| 4,019 | 1,073 |
| 4,070 | 1,033 |
| 4,121 | 991 |
| 4,171 | 947 |
| 4,222 | 902 |
| 4,273 | 856 |
| 4,324 | 808 |
| 4,375 | 760 |
| 4,426 | 709 |
| 4,477 | 658 |
| 4,527 | 605 |
| 4,578 | 550 |
| 4,629 | 495 |
| 4,680 | 438 |
| 4,731 | 379 |
| 4,782 | 319 |
| 4,833 | 258 |
| 4,884 | 196 |
| 4,934 | 132 |
| 4,985 | 67 |
| 5,036 | 0 |

II.2 SHEAR DOMAIN

Table 2 wall 10 shear domain

| N [kN] | V [kN] |
|--------|--------|
| 0 | 156 |
| 51 | 179 |

| | |
|-------|-----|
| 102 | 200 |
| 153 | 219 |
| 203 | 236 |
| 254 | 252 |
| 305 | 268 |
| 356 | 282 |
| 407 | 296 |
| 458 | 309 |
| 509 | 321 |
| 560 | 333 |
| 610 | 345 |
| 661 | 356 |
| 712 | 367 |
| 763 | 378 |
| 814 | 388 |
| 865 | 398 |
| 916 | 408 |
| 967 | 418 |
| 1,017 | 427 |
| 1,068 | 436 |
| 1,119 | 445 |
| 1,170 | 454 |
| 1,221 | 463 |
| 1,272 | 471 |
| 1,323 | 479 |
| 1,374 | 488 |
| 1,424 | 496 |
| 1,475 | 504 |
| 1,526 | 511 |
| 1,577 | 519 |
| 1,628 | 527 |
| 1,679 | 534 |
| 1,730 | 541 |
| 1,780 | 549 |
| 1,831 | 556 |
| 1,882 | 563 |
| 1,933 | 570 |
| 1,984 | 577 |
| 2,035 | 584 |
| 2,086 | 590 |
| 2,137 | 597 |

| | |
|-------|-----|
| 2,187 | 604 |
| 2,238 | 610 |
| 2,289 | 617 |
| 2,340 | 623 |
| 2,391 | 629 |
| 2,442 | 636 |
| 2,493 | 642 |
| 2,544 | 648 |
| 2,594 | 654 |
| 2,645 | 660 |
| 2,696 | 666 |
| 2,747 | 672 |
| 2,798 | 678 |
| 2,849 | 684 |
| 2,900 | 689 |
| 2,950 | 695 |
| 3,001 | 701 |
| 3,052 | 706 |
| 3,103 | 712 |
| 3,154 | 717 |
| 3,205 | 723 |
| 3,256 | 728 |
| 3,307 | 734 |
| 3,357 | 739 |
| 3,408 | 745 |
| 3,459 | 750 |
| 3,510 | 755 |
| 3,561 | 760 |
| 3,612 | 765 |
| 3,663 | 771 |
| 3,714 | 776 |
| 3,764 | 781 |
| 3,815 | 786 |
| 3,866 | 791 |
| 3,917 | 796 |
| 3,968 | 801 |
| 4,019 | 806 |
| 4,070 | 811 |
| 4,121 | 816 |
| 4,171 | 820 |
| 4,222 | 825 |

| | |
|-------|-----|
| 4,273 | 830 |
| 4,324 | 835 |
| 4,375 | 839 |
| 4,426 | 844 |
| 4,477 | 849 |
| 4,527 | 853 |
| 4,578 | 858 |
| 4,629 | 863 |
| 4,680 | 867 |
| 4,731 | 872 |
| 4,782 | 876 |
| 4,833 | 881 |
| 4,884 | 885 |
| 4,934 | 890 |
| 4,985 | 894 |
| 5,036 | 899 |

| | |
|-----|-----|
| 181 | 67 |
| 193 | 71 |
| 205 | 74 |
| 217 | 78 |
| 229 | 81 |
| 241 | 84 |
| 253 | 87 |
| 265 | 90 |
| 277 | 93 |
| 289 | 96 |
| 301 | 99 |
| 314 | 101 |
| 326 | 104 |
| 338 | 106 |
| 350 | 108 |
| 362 | 110 |
| 374 | 112 |
| 386 | 114 |
| 398 | 116 |
| 410 | 118 |
| 422 | 119 |
| 434 | 121 |
| 446 | 122 |
| 458 | 124 |
| 470 | 125 |
| 482 | 126 |
| 494 | 127 |
| 506 | 128 |
| 519 | 128 |
| 531 | 129 |
| 543 | 130 |
| 555 | 130 |
| 567 | 130 |
| 579 | 131 |
| 591 | 131 |
| 603 | 131 |
| 615 | 131 |
| 627 | 130 |
| 639 | 130 |
| 651 | 130 |
| 663 | 129 |

III DOMAIN COORDINATES FROM MODEL WALL , SEISMIC ANALYSIS NO. 4 WALL 7 X DIRECTION

III.1 BENDING DOMAIN

Table 3 wall 7 bending domain

| N [kN] | V [kN] |
|--------|--------|
| 0 | 0 |
| 12 | 5 |
| 24 | 10 |
| 36 | 15 |
| 48 | 20 |
| 60 | 25 |
| 72 | 30 |
| 84 | 34 |
| 96 | 39 |
| 109 | 43 |
| 121 | 47 |
| 133 | 52 |
| 145 | 56 |
| 157 | 60 |
| 169 | 63 |

| | |
|-------|-----|
| 675 | 128 |
| 687 | 128 |
| 699 | 127 |
| 711 | 126 |
| 724 | 125 |
| 736 | 124 |
| 748 | 122 |
| 760 | 121 |
| 772 | 119 |
| 784 | 118 |
| 796 | 116 |
| 808 | 114 |
| 820 | 112 |
| 832 | 110 |
| 844 | 108 |
| 856 | 106 |
| 868 | 104 |
| 880 | 101 |
| 892 | 99 |
| 904 | 96 |
| 916 | 93 |
| 929 | 90 |
| 941 | 87 |
| 953 | 84 |
| 965 | 81 |
| 977 | 78 |
| 989 | 74 |
| 1,001 | 71 |
| 1,013 | 67 |
| 1,025 | 63 |
| 1,037 | 60 |
| 1,049 | 56 |
| 1,061 | 52 |
| 1,073 | 47 |
| 1,085 | 43 |
| 1,097 | 39 |
| 1,109 | 34 |
| 1,121 | 30 |
| 1,134 | 25 |
| 1,146 | 20 |
| 1,158 | 15 |

| | |
|-------|----|
| 1,170 | 10 |
| 1,182 | 5 |
| 1,194 | 0 |

III.2 SHEAR DOMAIN

Table 4 wall 7 shear domain

| N [kN] | V [kN] |
|--------|--------|
| 0 | 25 |
| 12 | 28 |
| 24 | 32 |
| 36 | 35 |
| 48 | 37 |
| 60 | 40 |
| 72 | 42 |
| 84 | 45 |
| 96 | 47 |
| 109 | 49 |
| 121 | 51 |
| 133 | 53 |
| 145 | 55 |
| 157 | 56 |
| 169 | 58 |
| 181 | 60 |
| 193 | 61 |
| 205 | 63 |
| 217 | 65 |
| 229 | 66 |
| 241 | 67 |
| 253 | 69 |
| 265 | 70 |
| 277 | 72 |
| 289 | 73 |
| 301 | 74 |
| 314 | 76 |
| 326 | 77 |
| 338 | 78 |
| 350 | 80 |
| 362 | 81 |
| 374 | 82 |

| | |
|-----|-----|
| 386 | 83 |
| 398 | 84 |
| 410 | 86 |
| 422 | 87 |
| 434 | 88 |
| 446 | 89 |
| 458 | 90 |
| 470 | 91 |
| 482 | 92 |
| 494 | 93 |
| 506 | 94 |
| 519 | 95 |
| 531 | 96 |
| 543 | 97 |
| 555 | 98 |
| 567 | 99 |
| 579 | 100 |
| 591 | 101 |
| 603 | 102 |
| 615 | 103 |
| 627 | 104 |
| 639 | 105 |
| 651 | 106 |
| 663 | 107 |
| 675 | 108 |
| 687 | 109 |
| 699 | 110 |
| 711 | 111 |
| 724 | 112 |
| 736 | 113 |
| 748 | 113 |
| 760 | 114 |
| 772 | 115 |
| 784 | 116 |
| 796 | 117 |
| 808 | 118 |
| 820 | 118 |
| 832 | 119 |
| 844 | 120 |
| 856 | 121 |
| 868 | 122 |

| | |
|-------|-----|
| 880 | 123 |
| 892 | 123 |
| 904 | 124 |
| 916 | 125 |
| 929 | 126 |
| 941 | 127 |
| 953 | 127 |
| 965 | 128 |
| 977 | 129 |
| 989 | 130 |
| 1,001 | 130 |
| 1,013 | 131 |
| 1,025 | 132 |
| 1,037 | 133 |
| 1,049 | 133 |
| 1,061 | 134 |
| 1,073 | 135 |
| 1,085 | 136 |
| 1,097 | 136 |
| 1,109 | 137 |
| 1,121 | 138 |
| 1,134 | 138 |
| 1,146 | 139 |
| 1,158 | 140 |
| 1,170 | 141 |
| 1,182 | 141 |
| 1,194 | 142 |

IV DOMAIN COORDINATES FROM MODEL WALL , SEISMIC ANALYSIS NO. 5 WALL 8 Y DIRECTION

IV.1 BENDING DOMAIN

Table 5 wall 8 bending domain

| N [kN] | V [kN] |
|--------|--------|
| 0 | 0 |
| 14 | 11 |
| 28 | 23 |
| 42 | 34 |

| | |
|-----|-----|
| 56 | 44 |
| 71 | 55 |
| 85 | 65 |
| 99 | 75 |
| 113 | 85 |
| 127 | 95 |
| 141 | 104 |
| 155 | 113 |
| 169 | 122 |
| 183 | 131 |
| 198 | 139 |
| 212 | 148 |
| 226 | 155 |
| 240 | 163 |
| 254 | 171 |
| 268 | 178 |
| 282 | 185 |
| 296 | 192 |
| 310 | 198 |
| 324 | 205 |
| 339 | 211 |
| 353 | 217 |
| 367 | 222 |
| 381 | 228 |
| 395 | 233 |
| 409 | 238 |
| 423 | 242 |
| 437 | 247 |
| 451 | 251 |
| 466 | 255 |
| 480 | 259 |
| 494 | 262 |
| 508 | 266 |
| 522 | 269 |
| 536 | 271 |
| 550 | 274 |
| 564 | 276 |
| 578 | 278 |
| 593 | 280 |
| 607 | 282 |
| 621 | 283 |

| | |
|-------|-----|
| 635 | 284 |
| 649 | 285 |
| 663 | 286 |
| 677 | 287 |
| 691 | 287 |
| 705 | 287 |
| 719 | 287 |
| 734 | 286 |
| 748 | 285 |
| 762 | 284 |
| 776 | 283 |
| 790 | 282 |
| 804 | 280 |
| 818 | 278 |
| 832 | 276 |
| 846 | 274 |
| 861 | 271 |
| 875 | 269 |
| 889 | 266 |
| 903 | 262 |
| 917 | 259 |
| 931 | 255 |
| 945 | 251 |
| 959 | 247 |
| 973 | 242 |
| 988 | 238 |
| 1,002 | 233 |
| 1,016 | 228 |
| 1,030 | 222 |
| 1,044 | 217 |
| 1,058 | 211 |
| 1,072 | 205 |
| 1,086 | 198 |
| 1,100 | 192 |
| 1,114 | 185 |
| 1,129 | 178 |
| 1,143 | 171 |
| 1,157 | 163 |
| 1,171 | 155 |
| 1,185 | 148 |
| 1,199 | 139 |

| | |
|-------|-----|
| 1,213 | 131 |
| 1,227 | 122 |
| 1,241 | 113 |
| 1,256 | 104 |
| 1,270 | 95 |
| 1,284 | 85 |
| 1,298 | 75 |
| 1,312 | 65 |
| 1,326 | 55 |
| 1,340 | 44 |
| 1,354 | 34 |
| 1,368 | 23 |
| 1,383 | 11 |
| 1,397 | 0 |

| | |
|-----|-----|
| 296 | 99 |
| 310 | 101 |
| 324 | 103 |
| 339 | 105 |
| 353 | 107 |
| 367 | 109 |
| 381 | 111 |
| 395 | 113 |
| 409 | 115 |
| 423 | 117 |
| 437 | 118 |
| 451 | 120 |
| 466 | 122 |
| 480 | 123 |
| 494 | 125 |
| 508 | 127 |
| 522 | 128 |
| 536 | 130 |
| 550 | 131 |
| 564 | 133 |
| 578 | 135 |
| 593 | 136 |
| 607 | 138 |
| 621 | 139 |
| 635 | 140 |
| 649 | 142 |
| 663 | 143 |
| 677 | 145 |
| 691 | 146 |
| 705 | 148 |
| 719 | 149 |
| 734 | 150 |
| 748 | 152 |
| 762 | 153 |
| 776 | 154 |
| 790 | 156 |
| 804 | 157 |
| 818 | 158 |
| 832 | 160 |
| 846 | 161 |
| 861 | 162 |

IV.2 SHEAR DOMAIN

Table 6 wall 8 shear domain

| N [kN] | V [kN] |
|--------|--------|
| 0 | 35 |
| 14 | 41 |
| 28 | 46 |
| 42 | 50 |
| 56 | 54 |
| 71 | 58 |
| 85 | 61 |
| 99 | 64 |
| 113 | 67 |
| 127 | 70 |
| 141 | 73 |
| 155 | 76 |
| 169 | 79 |
| 183 | 81 |
| 198 | 84 |
| 212 | 86 |
| 226 | 88 |
| 240 | 91 |
| 254 | 93 |
| 268 | 95 |
| 282 | 97 |

| | |
|-------|-----|
| 875 | 163 |
| 889 | 165 |
| 903 | 166 |
| 917 | 167 |
| 931 | 168 |
| 945 | 170 |
| 959 | 171 |
| 973 | 172 |
| 988 | 173 |
| 1,002 | 174 |
| 1,016 | 176 |
| 1,030 | 177 |
| 1,044 | 178 |
| 1,058 | 179 |
| 1,072 | 180 |
| 1,086 | 181 |
| 1,100 | 182 |
| 1,114 | 184 |
| 1,129 | 185 |
| 1,143 | 186 |
| 1,157 | 187 |
| 1,171 | 188 |
| 1,185 | 189 |
| 1,199 | 190 |
| 1,213 | 191 |
| 1,227 | 192 |
| 1,241 | 193 |
| 1,256 | 194 |
| 1,270 | 195 |
| 1,284 | 197 |
| 1,298 | 198 |
| 1,312 | 199 |
| 1,326 | 200 |
| 1,340 | 201 |
| 1,354 | 202 |
| 1,368 | 203 |
| 1,383 | 204 |
| 1,397 | 205 |

V ASSESSMENT OF THE PERFORMANCE FOR THE (X DIRECTION)

V.1 SDOF TO MDOF

For the conversion of forces and displacements of a system, the following equations are used to have the SDOF from the MDOF capacity curve:

$$F^* = F/\Gamma$$

$$d^* = d/\Gamma$$

Γ : participation factor

$$\Gamma = \frac{m^*}{\sum m_i \phi_i^2} \quad \text{in which } m^* = \sum m_i \phi_i$$

K : the rigidity

$$k = \frac{F(0.6Fu)}{d(0.6Fu)}$$

T : the period

$$T^* = 2\pi \sqrt{\left(\frac{m^*}{k}\right)} \quad \text{or} \quad 2\pi \sqrt{\left(\frac{m^* d^*}{F^*}\right)}$$

interpolation is made to determine the value of the displacement $d_{0.6}$ associated with the force $0.6Fu$.

| Γ_x | | | | | | | | |
|-------------|----------------|---------------|-----------------|----------|-------|-------|-------|-------|
| - | $0,6^*F_u=F_y$ | $d(0,6^*F_u)$ | dy to d^*_y | k^* | m^* | T^* | du | F_u |
| 1.74 | [KN] | [m] | [m] | [KN/m] | [ton] | [sec] | [m] | [KN] |
| | 440.00 | 0.0024 | 0.003700 | 183333.0 | 390 | 0.29 | 0.022 | 744.8 |

Table 7 The bi-linear equivalent capacity curve domain for X direction

| Bi-linear | | Note |
|-----------|------------|---------------------------------------|
| d_i [m] | F_i [KN] | |
| 0 | 0 | 0 |
| 0.0024 | 440 | Correspond to $F(0.6Fu)$, $d(0.6Fu)$ |
| 0.003700 | 661 | Correspond to F_y , dy |
| 0.0219 | 661 | horizontal plateau, F_y , du |

Table 8. transformation of the capacity curve from MDOF to SDOF

| Step | MDOF | | SDOF | |
|------|--------------|-----------|-----------------------|------------------|
| | Displacement | BaseForce | D*= Δ/Γ_x | F*= V/Γ_x |
| | m | KN | m | KN |
| 0 | 0 | 0 | 0.000000 | 0 |
| 1 | 0.00074 | 221 | 0.000425 | 127.0115 |
| 2 | 0.00146 | 392 | 0.000839 | 225.2874 |
| 3 | 0.00212 | 433 | 0.001218 | 248.8506 |
| 4 | 0.00283 | 587 | 0.001626 | 337.3563 |
| 5 | 0.00356 | 712 | 0.002046 | 409.1954 |
| 6 | 0.0043 | 817 | 0.002471 | 469.5402 |
| 7 | 0.00505 | 910 | 0.002902 | 522.9885 |
| 8 | 0.0058 | 986 | 0.003333 | 566.6667 |
| 9 | 0.00655 | 1046 | 0.003764 | 601.1494 |
| 10 | 0.00731 | 1099 | 0.004201 | 631.6092 |
| 11 | 0.00807 | 1144 | 0.004638 | 657.4713 |
| 12 | 0.00884 | 1188 | 0.005080 | 682.7586 |
| 13 | 0.00963 | 1229 | 0.005534 | 706.3218 |
| 14 | 0.01046 | 1124 | 0.006011 | 645.977 |
| 15 | 0.01135 | 1034 | 0.006523 | 594.2529 |
| 16 | 0.0122 | 1077 | 0.007011 | 618.9655 |
| 17 | 0.01313 | 1058 | 0.007546 | 608.046 |
| 18 | 0.01406 | 1068 | 0.008080 | 613.7931 |
| 19 | 0.01501 | 1083 | 0.008626 | 622.4138 |
| 20 | 0.01597 | 1100 | 0.009178 | 632.1839 |
| 21 | 0.01695 | 1119 | 0.009741 | 643.1034 |
| 22 | 0.01793 | 1138 | 0.010305 | 654.023 |
| 23 | 0.01893 | 1158 | 0.010879 | 665.5172 |
| 24 | 0.02001 | 1144 | 0.011500 | 657.4713 |
| 25 | 0.02103 | 1184 | 0.012086 | 680.4598 |
| 26 | 0.02187 | 1307 | 0.012569 | 751.1494 |
| 27 | 0.0228 | 1313 | 0.013103 | 754.5977 |
| 28 | 0.02383 | 1290 | 0.013695 | 741.3793 |
| 29 | 0.02478 | 1317 | 0.014241 | 756.8966 |

| | | | | |
|----|---------|------|----------|----------|
| 30 | 0.02582 | 1305 | 0.014839 | 750 |
| 31 | 0.02687 | 1306 | 0.015443 | 750.5747 |
| 32 | 0.02791 | 1309 | 0.016040 | 752.2989 |
| 33 | 0.02894 | 1313 | 0.016632 | 754.5977 |
| 34 | 0.03006 | 1286 | 0.017276 | 739.0805 |
| 35 | 0.03109 | 1310 | 0.017868 | 752.8736 |
| 36 | 0.03221 | 1291 | 0.018511 | 741.954 |
| 37 | 0.03325 | 1313 | 0.019109 | 754.5977 |
| 38 | 0.03488 | 1296 | 0.020046 | 744.8276 |
| 39 | 0.0363 | 1308 | 0.020862 | 751.7241 |
| 40 | 0.03818 | 1296 | 0.021943 | 744.8276 |
| 41 | 0.05173 | 1097 | 0.029730 | 630.4598 |
| 42 | 0.05767 | 1093 | 0.033144 | 628.1609 |
| 43 | 0.06336 | 1094 | 0.036414 | 628.7356 |
| 44 | 0.06917 | 1093 | 0.039753 | 628.1609 |
| 45 | 0.07499 | 1092 | 0.043098 | 627.5862 |
| 46 | 0.08082 | 1091 | 0.046448 | 627.0115 |
| 47 | 0.08664 | 1091 | 0.049793 | 627.0115 |
| 48 | 0.09247 | 1091 | 0.053144 | 627.0115 |
| 49 | 0.0983 | 1091 | 0.056494 | 627.0115 |
| 50 | 0.1086 | 919 | 0.062414 | 528.1609 |

V.2 THE BI-LINEAR EQUIVALENT CAPACITY CURVE THE SHEAR FORCES OF THE BI LINEAR TO SAG

Table 9. bi-linear capacity curve (Sd,Sag)

| | BILINEARE SDOF | | |
|----------------|----------------|--------|-------------------------------------|
| | S [cm] | V [KN] | S _{ag} [ms ⁻²] |
| Δ_0 | 0 | 0 | 0.00 |
| $\Delta_{0,6}$ | 0.24 | 440 | 1.13 |
| Δ_y | 0.37 | 661 | 1.70 |
| Δ_u | 2.2 | 661 | 1.70 |

V.3 THE SPECTRE OR THE DEMAND CURVE SHOULD BE TRANSFORMED ALSO TO THE (ADRS) FORM AS FOLLOW:

| q* | Sae(T*) | Sde (T*) =demax [cm] | Tc | d*max [cm] Performance point | u | Ru |
|-----|---------|----------------------|-----|---------------------------------|----------|----------|
| 3.6 | 6.1 | 1.39 | 0.4 | 1.68 | 4.587677 | 3.597247 |

$$q^* = \frac{Sag}{Sae(T^*)}$$

S_{ae} : the spectral acceleration correspond to (T*)

S_{ag} : max spectral acceleration of the structure

q* : the behaviour factor

$$\begin{cases} R_u = \frac{(u-1)T}{Tc} + 1 & , T > Tc \\ R_u = u & , T \leq Tc \end{cases}$$

$$u = \begin{cases} 1 + \frac{(q-1)T}{TC} & , T \leq Tc \\ q & , T > Tc \end{cases}$$

μ: The ductility capacity for the building

R_u : strength reduction factor due to ductility

$$S_a = \frac{S_{ae}}{R_u}$$

$$S_d = \frac{u}{R_u} S_{de} = \frac{uT^2}{4\pi^2} S_a$$

S_a: spectral acceleration.

S_d: spectral displacement.

Table 10. transformation of the demand curve to (ADRS) form.

| T [sec] | S _{ae} [g] | S _{ae} [ms ⁻²] | S _{de} [cm] | sae/Ru | sde/Ru |
|---------|---------------------|-------------------------------------|----------------------|----------|----------|
| 0 | 0.250 | 3.25 | 0 | 0.903469 | 0 |
| 0.05 | 0.375 | 4.875 | 0.030902623 | 1.355203 | 0.008591 |
| 0.1 | 0.500 | 6.5 | 0.164813988 | 1.806938 | 0.045817 |
| 0.15 | 0.625 | 8.125 | 0.463539342 | 2.258672 | 0.128859 |
| 0.2 | 0.625 | 8.125 | 0.824069942 | 2.258672 | 0.229084 |
| 0.25 | 0.625 | 8.125 | 1.287609284 | 2.258672 | 0.357943 |
| 0.3 | 0.625 | 8.125 | 1.854157369 | 2.258672 | 0.515438 |

| | | | | | |
|------|-------|-------------|-------------|----------|----------|
| 0.35 | 0.625 | 8.125 | 2.523714197 | 2.258672 | 0.701568 |
| 0.4 | 0.625 | 8.125 | 3.296279768 | 2.258672 | 0.916334 |
| 0.45 | 0.578 | 7.511413805 | 3.85680275 | 2.088101 | 1.072154 |
| 0.5 | 0.539 | 7.001912743 | 4.438512175 | 1.946464 | 1.233864 |
| 0.55 | 0.505 | 6.570850268 | 5.039966647 | 1.826633 | 1.401062 |
| 0.6 | 0.477 | 6.20053548 | 5.659947597 | 1.723689 | 1.573411 |
| 0.65 | 0.452 | 5.878336719 | 6.297408779 | 1.634121 | 1.750619 |
| 0.7 | 0.430 | 5.594973113 | 6.951440285 | 1.555349 | 1.932434 |
| 0.75 | 0.411 | 5.343459494 | 7.621242154 | 1.48543 | 2.118632 |
| 0.8 | 0.394 | 5.118429265 | 8.306104532 | 1.422874 | 2.309017 |
| 0.85 | 0.378 | 4.915685394 | 9.005392453 | 1.366513 | 2.503413 |
| 0.9 | 0.364 | 4.731894184 | 9.718533939 | 1.315421 | 2.701659 |
| 0.95 | 0.351 | 4.564371241 | 10.44501056 | 1.268851 | 2.903613 |
| 1 | 0.339 | 4.410928627 | 11.18434984 | 1.226196 | 3.109142 |
| 1.05 | 0.328 | 4.269763606 | 11.93611905 | 1.186953 | 3.318126 |
| 1.1 | 0.318 | 4.139376284 | 12.69992014 | 1.150707 | 3.530456 |
| 1.15 | 0.309 | 4.018507689 | 13.47538546 | 1.117107 | 3.746028 |
| 1.2 | 0.300 | 3.906092586 | 14.26217424 | 1.085856 | 3.964747 |
| 1.25 | 0.292 | 3.80122306 | 15.05996955 | 1.056703 | 4.186527 |
| 1.3 | 0.285 | 3.703120086 | 15.86847576 | 1.029432 | 4.411284 |
| 1.35 | 0.278 | 3.611111111 | 16.68741633 | 1.003854 | 4.638941 |
| 1.4 | 0.271 | 3.524612199 | 17.51653189 | 0.979808 | 4.869428 |
| 1.45 | 0.265 | 3.443113684 | 18.35557863 | 0.957153 | 5.102675 |
| 1.5 | 0.259 | 3.366168548 | 19.20432683 | 0.935763 | 5.338618 |
| 1.55 | 0.253 | 3.293382942 | 20.06255963 | 0.915529 | 5.577199 |
| 1.6 | 0.248 | 3.224408387 | 20.93007188 | 0.896355 | 5.818359 |
| 1.65 | 0.243 | 3.158935325 | 21.80666919 | 0.878154 | 6.062045 |
| 1.7 | 0.238 | 3.096687751 | 22.69216703 | 0.860849 | 6.308204 |
| 1.75 | 0.234 | 3.037418717 | 23.58638996 | 0.844373 | 6.55679 |
| 1.8 | 0.229 | 2.980906544 | 24.48917097 | 0.828663 | 6.807754 |
| 1.85 | 0.225 | 2.926951626 | 25.40035078 | 0.813664 | 7.061054 |
| 1.9 | 0.221 | 2.875373703 | 26.31977735 | 0.799326 | 7.316645 |
| 1.95 | 0.217 | 2.826009536 | 27.24730532 | 0.785604 | 7.574489 |
| 2 | 0.214 | 2.778710913 | 28.18279558 | 0.772455 | 7.834546 |
| 2.05 | 0.210 | 2.733342934 | 29.12611486 | 0.759843 | 8.09678 |
| 2.1 | 0.207 | 2.689782523 | 30.07713529 | 0.747734 | 8.361155 |

| | | | | | |
|------|-------|-------------|-------------|----------|----------|
| 2.15 | 0.204 | 2.647917139 | 31.03573414 | 0.736096 | 8.627636 |
| 2.2 | 0.201 | 2.607643657 | 32.00179343 | 0.7249 | 8.896191 |
| 2.25 | 0.198 | 2.568867387 | 32.97519966 | 0.71412 | 9.166789 |
| 2.3 | 0.195 | 2.531501213 | 33.95584359 | 0.703733 | 9.439398 |
| 2.35 | 0.192 | 2.495464843 | 34.94361991 | 0.693715 | 9.713991 |
| 2.4 | 0.189 | 2.460684136 | 35.93842708 | 0.684047 | 9.990538 |
| 2.45 | 0.187 | 2.427090522 | 36.94016709 | 0.674708 | 10.26901 |
| 2.5 | 0.184 | 2.394620474 | 37.94874529 | 0.665681 | 10.54939 |
| 2.55 | 0.182 | 2.363215049 | 38.96407019 | 0.656951 | 10.83164 |
| 2.6 | 0.179 | 2.332819473 | 39.98605328 | 0.648501 | 11.11574 |
| 2.65 | 0.177 | 2.303382774 | 41.01460893 | 0.640318 | 11.40167 |
| 2.7 | 0.175 | 2.274857451 | 42.04965419 | 0.632389 | 11.6894 |
| 2.75 | 0.173 | 2.247199181 | 43.09110869 | 0.6247 | 11.97891 |
| 2.8 | 0.171 | 2.220366551 | 44.13889449 | 0.617241 | 12.27019 |
| 2.85 | 0.169 | 2.19432082 | 45.19293598 | 0.61 | 12.5632 |
| 2.9 | 0.167 | 2.169025704 | 46.25315979 | 0.602968 | 12.85793 |
| 2.95 | 0.165 | 2.144447178 | 47.31949463 | 0.596136 | 13.15436 |
| 3 | 0.163 | 2.120553306 | 48.39187125 | 0.589493 | 13.45248 |

b) Even the bi-linear equivalent capacity curve should be transformed to spectral parameters using:

$$Sag = \frac{V}{m^*} \text{ or } \frac{F}{\Gamma \times m^*}$$

VI ASSESSMENT OF THE PERFORMANCE FOR THE (Y DIRECTION)

VI.1 SDOF TO MDOF

For the conversion of forces and displacements of a system, to have the SDOF from the MDOF capacity curve:

interpolation is made to determine the value of the displacement $d_{0.6}$ associated with the force $0.6F_u$.

| | | | | | | | | |
|------------|-----------------------|--------------------|------------------------|----------|-------|-------|--------|--------|
| Γ_x | | | | | | | | |
| - | $0,6 \cdot F_u = F_y$ | $d(0,6 \cdot F_u)$ | $dy \text{ to } d^*_y$ | k^* | m^* | T^* | du | F_u |
| 1.74 | [KN] | [m] | [m] | [KN/m] | [ton] | [sec] | [m] | [KN] |
| | 744 | 0.0013 | 0.0021 | 572196.5 | 503 | 0.186 | 0.0105 | 1239.8 |

Table 11 The bi-linear equivalent capacity curve domain for Y direction

| Bi-linear | | Note |
|-----------|------------|---|
| d_i [m] | F_i [KN] | |
| 0 | 0 | 0 |
| 0.0013 | 744 | Correspond to $F(0.6 F_u)$, $d(0.6 F_u)$ |
| 0.002100 | 1201.6 | Correspond to F_y , dy |
| 0.0105 | 1201.6 | horizontal plateau, F_y , du |

Table 12. transformation of the capacity curve from MDOF to SDOF

| Step | MDOF | | SDOF | |
|------|--------------|-----------|---------------------------|----------------------|
| | Displacement | BaseForce | $D^* = \Delta / \Gamma_x$ | $F^* = V / \Gamma_x$ |
| | m | KN | m | KN |
| 0 | 0 | 0 | 0.000000 | 0 |
| 1 | 0.00081 | 473 | 0.000488 | 284.9398 |
| 2 | 0.00162 | 947 | 0.000976 | 570.4819 |
| 3 | 0.00243 | 1399 | 0.001464 | 842.7711 |
| 4 | 0.00324 | 1825 | 0.001952 | 1099.398 |
| 5 | 0.00431 | 1950 | 0.002596 | 1174.699 |
| 6 | 0.00542 | 1995 | 0.003265 | 1201.807 |
| 7 | 0.00651 | 2036 | 0.003922 | 1226.506 |
| 8 | 0.00748 | 2050 | 0.004506 | 1234.94 |
| 9 | 0.00839 | 2057 | 0.005054 | 1239.157 |
| 10 | 0.00928 | 2058 | 0.005590 | 1239.759 |
| 11 | 0.01016 | 2055 | 0.006120 | 1237.952 |
| 12 | 0.01103 | 2052 | 0.006645 | 1236.145 |
| 13 | 0.01189 | 2048 | 0.007163 | 1233.735 |
| 14 | 0.01399 | 1826 | 0.008428 | 1100 |
| 15 | 0.01708 | 1506 | 0.010289 | 907.2289 |

VI.2 THE BI-LINEAR EQUIVALENT CAPACITY CURVE THE SHEAR FORCES OF THE BI LINEAR TO SAG

Table 13. bi-linear capacity curve (Sd,Sag)

| | BILINEARE SDOF | | |
|----------------|----------------|--------|-------------------------|
| | S [cm] | V [KN] | Sag [ms ⁻²] |
| Δ_0 | 0 | 0 | 0.00 |
| $\Delta_{0,6}$ | 0.13 | 744 | 1.48 |
| Δ_y | 0.21 | 1202 | 2.39 |
| Δ_u | 1.1 | 1202 | 2.39 |

VI.3 THE SPECTRE OR THE DEMAND CURVE SHOULD BE TRANSFORMED ALSO TO THE (ADRS) FORM AS FOLLOW:

| q* | Sae(T*) | Sde (T*) =demax [cm] | Tc | d*max [cm] Performance point | u | Ru |
|-----|---------|----------------------|-----|---------------------------------|-------|--------|
| 2.6 | 6.1 | 0.6 | 0.4 | 1 | 4.362 | 2.5643 |

Table 14. transformation of the demand curve to (ADRS) form.

| T [sec] | Sae [g] | Sae [ms ⁻²] | Sde [cm] | sae/Ru | sde/Ru |
|---------|---------|-------------------------|-------------|----------|----------|
| 0 | 0.250 | 2.4525 | 0 | 0.956412 | 0 |
| 0.05 | 0.375 | 3.67875 | 0.023319595 | 1.434619 | 0.009094 |
| 0.1 | 0.500 | 4.905 | 0.124371171 | 1.912825 | 0.048502 |
| 0.15 | 0.625 | 6.13125 | 0.349793919 | 2.391031 | 0.136411 |
| 0.2 | 0.625 | 6.13125 | 0.621855856 | 2.391031 | 0.242508 |
| 0.25 | 0.625 | 6.13125 | 0.971649775 | 2.391031 | 0.378919 |
| 0.3 | 0.625 | 6.13125 | 1.399175676 | 2.391031 | 0.545643 |
| 0.35 | 0.625 | 6.13125 | 1.90443356 | 2.391031 | 0.74268 |
| 0.4 | 0.625 | 6.13125 | 2.487423425 | 2.391031 | 0.970032 |
| 0.45 | 0.578 | 5.668228418 | 2.91040269 | 2.210464 | 1.134983 |
| 0.5 | 0.539 | 5.283751077 | 3.349369572 | 2.060528 | 1.306169 |
| 0.55 | 0.505 | 4.958464702 | 3.803236369 | 1.933675 | 1.483165 |
| 0.6 | 0.477 | 4.679019466 | 4.271083533 | 1.824698 | 1.665614 |
| 0.65 | 0.452 | 4.435883324 | 4.752121548 | 1.729881 | 1.853206 |
| 0.7 | 0.430 | 4.222052788 | 5.245663785 | 1.646493 | 2.045675 |

| | | | | | |
|------|-------|-------------|-------------|----------|----------|
| 0.75 | 0.411 | 4.032256742 | 5.751106579 | 1.572477 | 2.242785 |
| 0.8 | 0.394 | 3.862445469 | 6.267914266 | 1.506255 | 2.444327 |
| 0.85 | 0.378 | 3.709451824 | 6.795607689 | 1.446591 | 2.650113 |
| 0.9 | 0.364 | 3.57076015 | 7.333755226 | 1.392505 | 2.859977 |
| 0.95 | 0.351 | 3.44434476 | 7.881965662 | 1.343207 | 3.073765 |
| 1 | 0.339 | 3.328554602 | 8.439882456 | 1.298051 | 3.291339 |
| 1.05 | 0.328 | 3.222029306 | 9.007179069 | 1.256509 | 3.51257 |
| 1.1 | 0.318 | 3.123637027 | 9.583555119 | 1.218139 | 3.737342 |
| 1.15 | 0.309 | 3.032427725 | 10.16873318 | 1.182569 | 3.965546 |
| 1.2 | 0.300 | 2.947597559 | 10.7624561 | 1.149488 | 4.197083 |
| 1.25 | 0.292 | 2.868461401 | 11.36448471 | 1.118627 | 4.431859 |
| 1.3 | 0.285 | 2.794431388 | 11.97459594 | 1.089757 | 4.669787 |
| 1.35 | 0.278 | 2.725 | 12.59258109 | 1.06268 | 4.910785 |
| 1.4 | 0.271 | 2.659726591 | 13.21824445 | 1.037225 | 5.154778 |
| 1.45 | 0.265 | 2.598226557 | 13.85140202 | 1.013242 | 5.401693 |
| 1.5 | 0.259 | 2.540162574 | 14.49188048 | 0.990599 | 5.651463 |
| 1.55 | 0.253 | 2.485237435 | 15.13951615 | 0.969179 | 5.904025 |
| 1.6 | 0.248 | 2.433188175 | 15.79415425 | 0.948881 | 6.159317 |
| 1.65 | 0.243 | 2.383781195 | 16.45564806 | 0.929614 | 6.417283 |
| 1.7 | 0.238 | 2.336808218 | 17.12385835 | 0.911296 | 6.677868 |
| 1.75 | 0.234 | 2.292082893 | 17.79865273 | 0.893854 | 6.94102 |
| 1.8 | 0.229 | 2.249437938 | 18.47990517 | 0.877223 | 7.206691 |
| 1.85 | 0.225 | 2.208722727 | 19.16749547 | 0.861345 | 7.474834 |
| 1.9 | 0.221 | 2.169801233 | 19.8613089 | 0.846167 | 7.745403 |
| 1.95 | 0.217 | 2.132550273 | 20.56123578 | 0.83164 | 8.018357 |
| 2 | 0.214 | 2.096858005 | 21.26717113 | 0.817721 | 8.293654 |
| 2.05 | 0.210 | 2.06262263 | 21.97901437 | 0.80437 | 8.571254 |
| 2.1 | 0.207 | 2.029751273 | 22.69666902 | 0.791551 | 8.851121 |
| 2.15 | 0.204 | 1.99815901 | 23.42004246 | 0.779231 | 9.133219 |
| 2.2 | 0.201 | 1.967768021 | 24.14904566 | 0.767379 | 9.417511 |
| 2.25 | 0.198 | 1.938506851 | 24.88359298 | 0.755968 | 9.703966 |
| 2.3 | 0.195 | 1.910309762 | 25.62360197 | 0.744972 | 9.992551 |
| 2.35 | 0.192 | 1.883116162 | 26.36899318 | 0.734367 | 10.28323 |
| 2.4 | 0.189 | 1.856870106 | 27.11968997 | 0.724132 | 10.57599 |
| 2.45 | 0.187 | 1.831519848 | 27.8756184 | 0.714246 | 10.87078 |
| 2.5 | 0.184 | 1.80701745 | 28.63670702 | 0.704691 | 11.16758 |

| | | | | | |
|-------------|-------|-------------|-------------|----------|----------|
| 2.55 | 0.182 | 1.783318433 | 29.40288681 | 0.695449 | 11.46638 |
| 2.6 | 0.179 | 1.760381464 | 30.17409098 | 0.686504 | 11.76713 |
| 2.65 | 0.177 | 1.738168078 | 30.95025489 | 0.677841 | 12.06981 |
| 2.7 | 0.175 | 1.71664243 | 31.73131597 | 0.669447 | 12.3744 |
| 2.75 | 0.173 | 1.695771075 | 32.51721356 | 0.661307 | 12.68088 |
| 2.8 | 0.171 | 1.675522759 | 33.30788884 | 0.653411 | 12.98923 |
| 2.85 | 0.169 | 1.65586825 | 34.10328477 | 0.645746 | 13.29941 |
| 2.9 | 0.167 | 1.636780166 | 34.90334596 | 0.638302 | 13.61141 |
| 2.95 | 0.165 | 1.618232832 | 35.70801864 | 0.631069 | 13.92522 |
| 3 | 0.163 | 1.600202148 | 36.51725053 | 0.624038 | 14.2408 |

c) Even the bi-linear equivalent capacity curve should be transformed to spectral parameters using:

$$Sag = \frac{V}{m^*} \text{ or } \frac{F}{\Gamma \times m^*}$$

APPENDIX III

I DOMAIN COORDINATES FROM MODEL WALL, SEISMIC ANALYSIS X DIRECTION WALL 10

I.1 BENDING DOMAIN

Table 1 bending domain for wall 10 after reinforcement for X direction

| N [N] | V [N] |
|----------|----------|
| 0.00E+00 | 0.00E+00 |
| 5.09E+04 | 1.57E+04 |
| 1.02E+05 | 3.12E+04 |
| 1.53E+05 | 4.63E+04 |
| 2.03E+05 | 6.11E+04 |
| 2.54E+05 | 7.55E+04 |
| 3.05E+05 | 8.97E+04 |
| 3.56E+05 | 1.03E+05 |
| 4.07E+05 | 1.17E+05 |
| 4.58E+05 | 1.30E+05 |
| 5.09E+05 | 1.43E+05 |
| 5.60E+05 | 1.56E+05 |
| 6.10E+05 | 1.68E+05 |
| 6.61E+05 | 1.80E+05 |
| 7.12E+05 | 1.91E+05 |
| 7.63E+05 | 2.02E+05 |
| 8.14E+05 | 2.13E+05 |
| 8.65E+05 | 2.24E+05 |
| 9.16E+05 | 2.34E+05 |
| 9.67E+05 | 2.44E+05 |
| 1.02E+06 | 2.54E+05 |
| 1.07E+06 | 2.63E+05 |
| 1.12E+06 | 2.72E+05 |
| 1.17E+06 | 2.81E+05 |
| 1.22E+06 | 2.89E+05 |
| 1.27E+06 | 2.97E+05 |
| 1.32E+06 | 3.05E+05 |
| 1.37E+06 | 3.12E+05 |
| 1.42E+06 | 3.19E+05 |
| 1.48E+06 | 3.26E+05 |
| 1.53E+06 | 3.33E+05 |
| 1.58E+06 | 3.39E+05 |
| 1.63E+06 | 3.45E+05 |
| 1.68E+06 | 3.50E+05 |
| 1.73E+06 | 3.55E+05 |

| | |
|----------|----------|
| 1.78E+06 | 3.60E+05 |
| 1.83E+06 | 3.64E+05 |
| 1.88E+06 | 3.69E+05 |
| 1.93E+06 | 3.73E+05 |
| 1.98E+06 | 3.76E+05 |
| 2.03E+06 | 3.79E+05 |
| 2.09E+06 | 3.82E+05 |
| 2.14E+06 | 3.85E+05 |
| 2.19E+06 | 3.87E+05 |
| 2.24E+06 | 3.89E+05 |
| 2.29E+06 | 3.91E+05 |
| 2.34E+06 | 3.92E+05 |
| 2.39E+06 | 3.93E+05 |
| 2.44E+06 | 3.93E+05 |
| 2.49E+06 | 3.94E+05 |
| 2.54E+06 | 3.94E+05 |
| 2.59E+06 | 3.93E+05 |
| 2.65E+06 | 3.93E+05 |
| 2.70E+06 | 3.92E+05 |
| 2.75E+06 | 3.91E+05 |
| 2.80E+06 | 3.89E+05 |
| 2.85E+06 | 3.87E+05 |
| 2.90E+06 | 3.85E+05 |
| 2.95E+06 | 3.82E+05 |
| 3.00E+06 | 3.79E+05 |
| 3.05E+06 | 3.76E+05 |
| 3.10E+06 | 3.73E+05 |
| 3.15E+06 | 3.69E+05 |
| 3.20E+06 | 3.64E+05 |
| 3.26E+06 | 3.60E+05 |
| 3.31E+06 | 3.55E+05 |
| 3.36E+06 | 3.50E+05 |
| 3.41E+06 | 3.45E+05 |
| 3.46E+06 | 3.39E+05 |
| 3.51E+06 | 3.33E+05 |
| 3.56E+06 | 3.26E+05 |
| 3.61E+06 | 3.19E+05 |
| 3.66E+06 | 3.12E+05 |
| 3.71E+06 | 3.05E+05 |
| 3.76E+06 | 2.97E+05 |
| 3.82E+06 | 2.89E+05 |
| 3.87E+06 | 2.81E+05 |
| 3.92E+06 | 2.72E+05 |
| 3.97E+06 | 2.63E+05 |
| 4.02E+06 | 2.54E+05 |
| 4.07E+06 | 2.44E+05 |
| 4.12E+06 | 2.34E+05 |
| 4.17E+06 | 2.24E+05 |

| | |
|----------|----------|
| 4.22E+06 | 2.13E+05 |
| 4.27E+06 | 2.02E+05 |
| 4.32E+06 | 1.91E+05 |
| 4.37E+06 | 1.80E+05 |
| 4.43E+06 | 1.68E+05 |
| 4.48E+06 | 1.56E+05 |
| 4.53E+06 | 1.43E+05 |
| 4.58E+06 | 1.30E+05 |
| 4.63E+06 | 1.17E+05 |
| 4.68E+06 | 1.03E+05 |
| 4.73E+06 | 8.97E+04 |
| 4.78E+06 | 7.55E+04 |
| 4.83E+06 | 6.11E+04 |
| 4.88E+06 | 4.63E+04 |
| 4.93E+06 | 3.12E+04 |
| 4.99E+06 | 1.57E+04 |
| 5.04E+06 | 0.00E+00 |

| | |
|----------|----------|
| 1.17E+06 | 6.27E+05 |
| 1.22E+06 | 6.35E+05 |
| 1.27E+06 | 6.44E+05 |
| 1.32E+06 | 6.52E+05 |
| 1.37E+06 | 6.60E+05 |
| 1.42E+06 | 6.68E+05 |
| 1.48E+06 | 6.76E+05 |
| 1.53E+06 | 6.84E+05 |
| 1.58E+06 | 6.92E+05 |
| 1.63E+06 | 6.99E+05 |
| 1.68E+06 | 7.07E+05 |
| 1.73E+06 | 7.14E+05 |
| 1.78E+06 | 7.21E+05 |
| 1.83E+06 | 7.28E+05 |
| 1.88E+06 | 7.36E+05 |
| 1.93E+06 | 7.43E+05 |
| 1.98E+06 | 7.49E+05 |
| 2.03E+06 | 7.56E+05 |
| 2.09E+06 | 7.63E+05 |
| 2.14E+06 | 7.70E+05 |
| 2.19E+06 | 7.76E+05 |
| 2.24E+06 | 7.83E+05 |
| 2.29E+06 | 7.89E+05 |
| 2.34E+06 | 7.96E+05 |
| 2.39E+06 | 8.02E+05 |
| 2.44E+06 | 8.08E+05 |
| 2.49E+06 | 8.14E+05 |
| 2.54E+06 | 8.20E+05 |
| 2.59E+06 | 8.27E+05 |
| 2.65E+06 | 8.33E+05 |
| 2.70E+06 | 8.39E+05 |
| 2.75E+06 | 8.44E+05 |
| 2.80E+06 | 8.50E+05 |
| 2.85E+06 | 8.56E+05 |
| 2.90E+06 | 8.62E+05 |
| 2.95E+06 | 8.68E+05 |
| 3.00E+06 | 8.73E+05 |
| 3.05E+06 | 8.79E+05 |
| 3.10E+06 | 8.84E+05 |
| 3.15E+06 | 8.90E+05 |
| 3.20E+06 | 8.96E+05 |
| 3.26E+06 | 9.01E+05 |
| 3.31E+06 | 9.06E+05 |
| 3.36E+06 | 9.12E+05 |
| 3.41E+06 | 9.17E+05 |
| 3.46E+06 | 9.22E+05 |
| 3.51E+06 | 9.28E+05 |
| 3.56E+06 | 9.33E+05 |

I.2 SHEAR DOMAIN

Table 2 shear domain for wall 10 after reinforcement for X direction

| N [N] | V [N] |
|----------|----------|
| 0.00E+00 | 3.28E+05 |
| 5.09E+04 | 3.52E+05 |
| 1.02E+05 | 3.73E+05 |
| 1.53E+05 | 3.91E+05 |
| 2.03E+05 | 4.09E+05 |
| 2.54E+05 | 4.25E+05 |
| 3.05E+05 | 4.40E+05 |
| 3.56E+05 | 4.55E+05 |
| 4.07E+05 | 4.68E+05 |
| 4.58E+05 | 4.81E+05 |
| 5.09E+05 | 4.94E+05 |
| 5.60E+05 | 5.06E+05 |
| 6.10E+05 | 5.18E+05 |
| 6.61E+05 | 5.29E+05 |
| 7.12E+05 | 5.40E+05 |
| 7.63E+05 | 5.51E+05 |
| 8.14E+05 | 5.61E+05 |
| 8.65E+05 | 5.71E+05 |
| 9.16E+05 | 5.81E+05 |
| 9.67E+05 | 5.90E+05 |
| 1.02E+06 | 6.00E+05 |
| 1.07E+06 | 6.09E+05 |
| 1.12E+06 | 6.18E+05 |

| | |
|----------|----------|
| 3.61E+06 | 9.38E+05 |
| 3.66E+06 | 9.43E+05 |
| 3.71E+06 | 9.48E+05 |
| 3.76E+06 | 9.53E+05 |
| 3.82E+06 | 9.58E+05 |
| 3.87E+06 | 9.63E+05 |
| 3.92E+06 | 9.68E+05 |
| 3.97E+06 | 9.73E+05 |
| 4.02E+06 | 9.78E+05 |
| 4.07E+06 | 9.83E+05 |
| 4.12E+06 | 9.88E+05 |
| 4.17E+06 | 9.93E+05 |
| 4.22E+06 | 9.98E+05 |
| 4.27E+06 | 1.00E+06 |
| 4.32E+06 | 1.01E+06 |
| 4.37E+06 | 1.01E+06 |
| 4.43E+06 | 1.02E+06 |
| 4.48E+06 | 1.02E+06 |
| 4.53E+06 | 1.03E+06 |
| 4.58E+06 | 1.03E+06 |
| 4.63E+06 | 1.04E+06 |
| 4.68E+06 | 1.04E+06 |
| 4.73E+06 | 1.04E+06 |
| 4.78E+06 | 1.05E+06 |
| 4.83E+06 | 1.05E+06 |
| 4.88E+06 | 1.06E+06 |
| 4.93E+06 | 1.06E+06 |
| 4.99E+06 | 1.07E+06 |
| 5.04E+06 | 1.07E+06 |

| | |
|----------|----------|
| 9.91E+04 | 3.37E+04 |
| 1.13E+05 | 3.81E+04 |
| 1.27E+05 | 4.24E+04 |
| 1.42E+05 | 4.66E+04 |
| 1.56E+05 | 5.07E+04 |
| 1.70E+05 | 5.46E+04 |
| 1.84E+05 | 5.85E+04 |
| 1.98E+05 | 6.23E+04 |
| 2.12E+05 | 6.59E+04 |
| 2.27E+05 | 6.95E+04 |
| 2.41E+05 | 7.30E+04 |
| 2.55E+05 | 7.63E+04 |
| 2.69E+05 | 7.96E+04 |
| 2.83E+05 | 8.27E+04 |
| 2.97E+05 | 8.57E+04 |
| 3.11E+05 | 8.87E+04 |
| 3.26E+05 | 9.15E+04 |
| 3.40E+05 | 9.42E+04 |
| 3.54E+05 | 9.68E+04 |
| 3.68E+05 | 9.93E+04 |
| 3.82E+05 | 1.02E+05 |
| 3.96E+05 | 1.04E+05 |
| 4.11E+05 | 1.06E+05 |
| 4.25E+05 | 1.08E+05 |
| 4.39E+05 | 1.10E+05 |
| 4.53E+05 | 1.12E+05 |
| 4.67E+05 | 1.14E+05 |
| 4.81E+05 | 1.16E+05 |
| 4.96E+05 | 1.17E+05 |
| 5.10E+05 | 1.19E+05 |
| 5.24E+05 | 1.20E+05 |
| 5.38E+05 | 1.21E+05 |
| 5.52E+05 | 1.22E+05 |
| 5.66E+05 | 1.24E+05 |
| 5.80E+05 | 1.24E+05 |
| 5.95E+05 | 1.25E+05 |
| 6.09E+05 | 1.26E+05 |
| 6.23E+05 | 1.27E+05 |
| 6.37E+05 | 1.27E+05 |
| 6.51E+05 | 1.28E+05 |
| 6.65E+05 | 1.28E+05 |
| 6.80E+05 | 1.28E+05 |
| 6.94E+05 | 1.28E+05 |
| 7.08E+05 | 1.28E+05 |
| 7.22E+05 | 1.28E+05 |
| 7.36E+05 | 1.28E+05 |
| 7.50E+05 | 1.28E+05 |
| 7.65E+05 | 1.27E+05 |

II DOMAIN COORDINATES FROM MODEL WALL, SEISMIC ANALYSIS

X DIRECTION WALL 7

II.1 BENDING DOMAIN

Table 3 bending domain for wall 7 after reinforcement for X direction

| N [N] | V [N] |
|----------|----------|
| 0.00E+00 | 0.00E+00 |
| 1.42E+04 | 5.13E+03 |
| 2.83E+04 | 1.02E+04 |
| 4.25E+04 | 1.51E+04 |
| 5.66E+04 | 1.99E+04 |
| 7.08E+04 | 2.46E+04 |
| 8.49E+04 | 2.92E+04 |

| | |
|----------|----------|
| 7.79E+05 | 1.27E+05 |
| 7.93E+05 | 1.26E+05 |
| 8.07E+05 | 1.25E+05 |
| 8.21E+05 | 1.24E+05 |
| 8.35E+05 | 1.24E+05 |
| 8.49E+05 | 1.22E+05 |
| 8.64E+05 | 1.21E+05 |
| 8.78E+05 | 1.20E+05 |
| 8.92E+05 | 1.19E+05 |
| 9.06E+05 | 1.17E+05 |
| 9.20E+05 | 1.16E+05 |
| 9.34E+05 | 1.14E+05 |
| 9.49E+05 | 1.12E+05 |
| 9.63E+05 | 1.10E+05 |
| 9.77E+05 | 1.08E+05 |
| 9.91E+05 | 1.06E+05 |
| 1.01E+06 | 1.04E+05 |
| 1.02E+06 | 1.02E+05 |
| 1.03E+06 | 9.93E+04 |
| 1.05E+06 | 9.68E+04 |
| 1.06E+06 | 9.42E+04 |
| 1.08E+06 | 9.15E+04 |
| 1.09E+06 | 8.87E+04 |
| 1.10E+06 | 8.57E+04 |
| 1.12E+06 | 8.27E+04 |
| 1.13E+06 | 7.96E+04 |
| 1.15E+06 | 7.63E+04 |
| 1.16E+06 | 7.30E+04 |
| 1.18E+06 | 6.95E+04 |
| 1.19E+06 | 6.59E+04 |
| 1.20E+06 | 6.23E+04 |
| 1.22E+06 | 5.85E+04 |
| 1.23E+06 | 5.46E+04 |
| 1.25E+06 | 5.07E+04 |
| 1.26E+06 | 4.66E+04 |
| 1.27E+06 | 4.24E+04 |
| 1.29E+06 | 3.81E+04 |
| 1.30E+06 | 3.37E+04 |
| 1.32E+06 | 2.92E+04 |
| 1.33E+06 | 2.46E+04 |
| 1.34E+06 | 1.99E+04 |
| 1.36E+06 | 1.51E+04 |
| 1.37E+06 | 1.02E+04 |
| 1.39E+06 | 5.13E+03 |
| 1.40E+06 | 0.00E+00 |

II.2 SHEAR DOMAIN

Table 4 shear domain for wall 7 after reinforcement for X direction

| N [N] | V [N] |
|----------|----------|
| 0.00E+00 | 1.12E+05 |
| 1.42E+04 | 1.16E+05 |
| 2.83E+04 | 1.20E+05 |
| 4.25E+04 | 1.24E+05 |
| 5.66E+04 | 1.27E+05 |
| 7.08E+04 | 1.30E+05 |
| 8.49E+04 | 1.33E+05 |
| 9.91E+04 | 1.35E+05 |
| 1.13E+05 | 1.38E+05 |
| 1.27E+05 | 1.40E+05 |
| 1.42E+05 | 1.43E+05 |
| 1.56E+05 | 1.45E+05 |
| 1.70E+05 | 1.47E+05 |
| 1.84E+05 | 1.49E+05 |
| 1.98E+05 | 1.51E+05 |
| 2.12E+05 | 1.53E+05 |
| 2.27E+05 | 1.55E+05 |
| 2.41E+05 | 1.57E+05 |
| 2.55E+05 | 1.59E+05 |
| 2.69E+05 | 1.61E+05 |
| 2.83E+05 | 1.63E+05 |
| 2.97E+05 | 1.64E+05 |
| 3.11E+05 | 1.66E+05 |
| 3.26E+05 | 1.68E+05 |
| 3.40E+05 | 1.69E+05 |
| 3.54E+05 | 1.71E+05 |
| 3.68E+05 | 1.72E+05 |
| 3.82E+05 | 1.74E+05 |
| 3.96E+05 | 1.76E+05 |
| 4.11E+05 | 1.77E+05 |
| 4.25E+05 | 1.78E+05 |
| 4.39E+05 | 1.80E+05 |
| 4.53E+05 | 1.81E+05 |
| 4.67E+05 | 1.83E+05 |
| 4.81E+05 | 1.84E+05 |
| 4.96E+05 | 1.85E+05 |
| 5.10E+05 | 1.87E+05 |
| 5.24E+05 | 1.88E+05 |
| 5.38E+05 | 1.89E+05 |
| 5.52E+05 | 1.91E+05 |
| 5.66E+05 | 1.92E+05 |
| 5.80E+05 | 1.93E+05 |
| 5.95E+05 | 1.95E+05 |
| 6.09E+05 | 1.96E+05 |

| | |
|----------|----------|
| 6.23E+05 | 1.97E+05 |
| 6.37E+05 | 1.98E+05 |
| 6.51E+05 | 1.99E+05 |
| 6.65E+05 | 2.01E+05 |
| 6.80E+05 | 2.02E+05 |
| 6.94E+05 | 2.03E+05 |
| 7.08E+05 | 2.04E+05 |
| 7.22E+05 | 2.05E+05 |
| 7.36E+05 | 2.06E+05 |
| 7.50E+05 | 2.07E+05 |
| 7.65E+05 | 2.09E+05 |
| 7.79E+05 | 2.10E+05 |
| 7.93E+05 | 2.11E+05 |
| 8.07E+05 | 2.12E+05 |
| 8.21E+05 | 2.13E+05 |
| 8.35E+05 | 2.14E+05 |
| 8.49E+05 | 2.15E+05 |
| 8.64E+05 | 2.16E+05 |
| 8.78E+05 | 2.17E+05 |
| 8.92E+05 | 2.18E+05 |
| 9.06E+05 | 2.19E+05 |
| 9.20E+05 | 2.20E+05 |
| 9.34E+05 | 2.21E+05 |
| 9.49E+05 | 2.22E+05 |
| 9.63E+05 | 2.23E+05 |
| 9.77E+05 | 2.24E+05 |
| 9.91E+05 | 2.25E+05 |
| 1.01E+06 | 2.26E+05 |
| 1.02E+06 | 2.27E+05 |
| 1.03E+06 | 2.28E+05 |
| 1.05E+06 | 2.29E+05 |
| 1.06E+06 | 2.30E+05 |
| 1.08E+06 | 2.31E+05 |
| 1.09E+06 | 2.32E+05 |
| 1.10E+06 | 2.33E+05 |
| 1.12E+06 | 2.34E+05 |
| 1.13E+06 | 2.35E+05 |
| 1.15E+06 | 2.36E+05 |
| 1.16E+06 | 2.36E+05 |
| 1.18E+06 | 2.37E+05 |
| 1.19E+06 | 2.38E+05 |
| 1.20E+06 | 2.39E+05 |
| 1.22E+06 | 2.40E+05 |
| 1.23E+06 | 2.41E+05 |
| 1.25E+06 | 2.42E+05 |
| 1.26E+06 | 2.43E+05 |
| 1.27E+06 | 2.44E+05 |
| 1.29E+06 | 2.44E+05 |

| | |
|----------|----------|
| 1.30E+06 | 2.45E+05 |
| 1.32E+06 | 2.46E+05 |
| 1.33E+06 | 2.47E+05 |
| 1.34E+06 | 2.48E+05 |
| 1.36E+06 | 2.49E+05 |
| 1.37E+06 | 2.49E+05 |
| 1.39E+06 | 2.50E+05 |
| 1.40E+06 | 2.51E+05 |

III DOMAIN COORDINATES FROM MODEL WALL, SEISMIC ANALYSIS Y DIRECTION WALL 8

III.1 BENDING DOMAIN

Table 5 bending domain for wall 8 after reinforcement for Y direction

| N [N] | V [N] |
|----------|----------|
| 0.00E+00 | 0.00E+00 |
| 4.21E+03 | 1.78E+03 |
| 8.43E+03 | 3.53E+03 |
| 1.26E+04 | 5.24E+03 |
| 1.69E+04 | 6.92E+03 |
| 2.11E+04 | 8.56E+03 |
| 2.53E+04 | 1.02E+04 |
| 2.95E+04 | 1.17E+04 |
| 3.37E+04 | 1.33E+04 |
| 3.79E+04 | 1.47E+04 |
| 4.21E+04 | 1.62E+04 |
| 4.64E+04 | 1.76E+04 |
| 5.06E+04 | 1.90E+04 |
| 5.48E+04 | 2.04E+04 |
| 5.90E+04 | 2.17E+04 |
| 6.32E+04 | 2.29E+04 |
| 6.74E+04 | 2.42E+04 |
| 7.16E+04 | 2.54E+04 |
| 7.59E+04 | 2.65E+04 |
| 8.01E+04 | 2.77E+04 |
| 8.43E+04 | 2.88E+04 |
| 8.85E+04 | 2.98E+04 |
| 9.27E+04 | 3.08E+04 |
| 9.69E+04 | 3.18E+04 |
| 1.01E+05 | 3.28E+04 |
| 1.05E+05 | 3.37E+04 |
| 1.10E+05 | 3.46E+04 |
| 1.14E+05 | 3.54E+04 |

| | |
|----------|----------|
| 1.18E+05 | 3.62E+04 |
| 1.22E+05 | 3.70E+04 |
| 1.26E+05 | 3.77E+04 |
| 1.31E+05 | 3.84E+04 |
| 1.35E+05 | 3.90E+04 |
| 1.39E+05 | 3.96E+04 |
| 1.43E+05 | 4.02E+04 |
| 1.48E+05 | 4.08E+04 |
| 1.52E+05 | 4.13E+04 |
| 1.56E+05 | 4.18E+04 |
| 1.60E+05 | 4.22E+04 |
| 1.64E+05 | 4.26E+04 |
| 1.69E+05 | 4.30E+04 |
| 1.73E+05 | 4.33E+04 |
| 1.77E+05 | 4.36E+04 |
| 1.81E+05 | 4.38E+04 |
| 1.85E+05 | 4.41E+04 |
| 1.90E+05 | 4.42E+04 |
| 1.94E+05 | 4.44E+04 |
| 1.98E+05 | 4.45E+04 |
| 2.02E+05 | 4.46E+04 |
| 2.07E+05 | 4.46E+04 |
| 2.11E+05 | 4.46E+04 |
| 2.15E+05 | 4.46E+04 |
| 2.19E+05 | 4.45E+04 |
| 2.23E+05 | 4.44E+04 |
| 2.28E+05 | 4.42E+04 |
| 2.32E+05 | 4.41E+04 |
| 2.36E+05 | 4.38E+04 |
| 2.40E+05 | 4.36E+04 |
| 2.44E+05 | 4.33E+04 |
| 2.49E+05 | 4.30E+04 |
| 2.53E+05 | 4.26E+04 |
| 2.57E+05 | 4.22E+04 |
| 2.61E+05 | 4.18E+04 |
| 2.66E+05 | 4.13E+04 |
| 2.70E+05 | 4.08E+04 |
| 2.74E+05 | 4.02E+04 |
| 2.78E+05 | 3.96E+04 |
| 2.82E+05 | 3.90E+04 |
| 2.87E+05 | 3.84E+04 |
| 2.91E+05 | 3.77E+04 |
| 2.95E+05 | 3.70E+04 |
| 2.99E+05 | 3.62E+04 |
| 3.03E+05 | 3.54E+04 |
| 3.08E+05 | 3.46E+04 |
| 3.12E+05 | 3.37E+04 |
| 3.16E+05 | 3.28E+04 |

| | |
|----------|----------|
| 3.20E+05 | 3.18E+04 |
| 3.25E+05 | 3.08E+04 |
| 3.29E+05 | 2.98E+04 |
| 3.33E+05 | 2.88E+04 |
| 3.37E+05 | 2.77E+04 |
| 3.41E+05 | 2.65E+04 |
| 3.46E+05 | 2.54E+04 |
| 3.50E+05 | 2.42E+04 |
| 3.54E+05 | 2.29E+04 |
| 3.58E+05 | 2.17E+04 |
| 3.62E+05 | 2.04E+04 |
| 3.67E+05 | 1.90E+04 |
| 3.71E+05 | 1.76E+04 |
| 3.75E+05 | 1.62E+04 |
| 3.79E+05 | 1.47E+04 |
| 3.84E+05 | 1.33E+04 |
| 3.88E+05 | 1.17E+04 |
| 3.92E+05 | 1.02E+04 |
| 3.96E+05 | 8.56E+03 |
| 4.00E+05 | 6.92E+03 |
| 4.05E+05 | 5.24E+03 |
| 4.09E+05 | 3.53E+03 |
| 4.13E+05 | 1.78E+03 |
| 4.17E+05 | 0.00E+00 |

III.2 SHEAR DOMAIN

Table 6 shear domain for wall 8 after reinforcement for Y direction

| N [N] | V [N] |
|----------|----------|
| 0.00E+00 | 9.44E+03 |
| 4.21E+03 | 1.08E+04 |
| 8.43E+03 | 1.19E+04 |
| 1.26E+04 | 1.30E+04 |
| 1.69E+04 | 1.40E+04 |
| 2.11E+04 | 1.49E+04 |
| 2.53E+04 | 1.58E+04 |
| 2.95E+04 | 1.66E+04 |
| 3.37E+04 | 1.74E+04 |
| 3.79E+04 | 1.81E+04 |
| 4.21E+04 | 1.88E+04 |
| 4.64E+04 | 1.95E+04 |
| 5.06E+04 | 2.02E+04 |
| 5.48E+04 | 2.08E+04 |
| 5.90E+04 | 2.15E+04 |
| 6.32E+04 | 2.21E+04 |
| 6.74E+04 | 2.27E+04 |

| | |
|----------|----------|
| 7.16E+04 | 2.32E+04 |
| 7.59E+04 | 2.38E+04 |
| 8.01E+04 | 2.44E+04 |
| 8.43E+04 | 2.49E+04 |
| 8.85E+04 | 2.54E+04 |
| 9.27E+04 | 2.59E+04 |
| 9.69E+04 | 2.64E+04 |
| 1.01E+05 | 2.69E+04 |
| 1.05E+05 | 2.74E+04 |
| 1.10E+05 | 2.79E+04 |
| 1.14E+05 | 2.84E+04 |
| 1.18E+05 | 2.88E+04 |
| 1.22E+05 | 2.93E+04 |
| 1.26E+05 | 2.97E+04 |
| 1.31E+05 | 3.02E+04 |
| 1.35E+05 | 3.06E+04 |
| 1.39E+05 | 3.11E+04 |
| 1.43E+05 | 3.15E+04 |
| 1.48E+05 | 3.19E+04 |
| 1.52E+05 | 3.23E+04 |
| 1.56E+05 | 3.27E+04 |
| 1.60E+05 | 3.31E+04 |
| 1.64E+05 | 3.35E+04 |
| 1.69E+05 | 3.39E+04 |
| 1.73E+05 | 3.43E+04 |
| 1.77E+05 | 3.47E+04 |
| 1.81E+05 | 3.51E+04 |
| 1.85E+05 | 3.54E+04 |
| 1.90E+05 | 3.58E+04 |
| 1.94E+05 | 3.62E+04 |
| 1.98E+05 | 3.65E+04 |
| 2.02E+05 | 3.69E+04 |
| 2.07E+05 | 3.73E+04 |
| 2.11E+05 | 3.76E+04 |
| 2.15E+05 | 3.80E+04 |
| 2.19E+05 | 3.83E+04 |
| 2.23E+05 | 3.87E+04 |
| 2.28E+05 | 3.90E+04 |
| 2.32E+05 | 3.93E+04 |
| 2.36E+05 | 3.97E+04 |
| 2.40E+05 | 4.00E+04 |
| 2.44E+05 | 4.03E+04 |
| 2.49E+05 | 4.07E+04 |
| 2.53E+05 | 4.10E+04 |
| 2.57E+05 | 4.13E+04 |
| 2.61E+05 | 4.16E+04 |
| 2.66E+05 | 4.20E+04 |
| 2.70E+05 | 4.23E+04 |

| | |
|----------|----------|
| 2.74E+05 | 4.26E+04 |
| 2.78E+05 | 4.29E+04 |
| 2.82E+05 | 4.32E+04 |
| 2.87E+05 | 4.35E+04 |
| 2.91E+05 | 4.38E+04 |
| 2.95E+05 | 4.41E+04 |
| 2.99E+05 | 4.44E+04 |
| 3.03E+05 | 4.47E+04 |
| 3.08E+05 | 4.50E+04 |
| 3.12E+05 | 4.53E+04 |
| 3.16E+05 | 4.56E+04 |
| 3.20E+05 | 4.59E+04 |
| 3.25E+05 | 4.62E+04 |
| 3.29E+05 | 4.65E+04 |
| 3.33E+05 | 4.67E+04 |
| 3.37E+05 | 4.70E+04 |
| 3.41E+05 | 4.73E+04 |
| 3.46E+05 | 4.76E+04 |
| 3.50E+05 | 4.79E+04 |
| 3.54E+05 | 4.81E+04 |
| 3.58E+05 | 4.84E+04 |
| 3.62E+05 | 4.87E+04 |
| 3.67E+05 | 4.90E+04 |
| 3.71E+05 | 4.92E+04 |
| 3.75E+05 | 4.95E+04 |
| 3.79E+05 | 4.98E+04 |
| 3.84E+05 | 5.00E+04 |
| 3.88E+05 | 5.03E+04 |
| 3.92E+05 | 5.06E+04 |
| 3.96E+05 | 5.08E+04 |
| 4.00E+05 | 5.11E+04 |
| 4.05E+05 | 5.13E+04 |
| 4.09E+05 | 5.16E+04 |
| 4.13E+05 | 5.18E+04 |
| 4.17E+05 | 5.21E+04 |

IV ASSESSMENT OF THE PERFORMANCE FOR THE (X DIRECTION)

IV.1 SDOF to MDOF

For the conversion of forces and displacements of a system, the following equations are used to have the **SDOF** from the **MDOF** capacity curve:

$$F^* = F/\Gamma$$

$$d^* = d/\Gamma$$

Γ : participation factor

$$\Gamma = \frac{m^*}{\sum m_i \varphi_i^2} \quad \text{in wick} \quad m^* = \sum m_i \varphi_i$$

K: the rigidity

$$k = \frac{F(0.6Fu)}{d(0.6Fu)}$$

T: the period

$$T^* = 2\pi \sqrt{\left(\frac{m^*}{k}\right)} \quad \text{or} \quad 2\pi \sqrt{\left(\frac{m^* d^*}{F^*}\right)}$$

interpolation is made to determine the value of the displacement $d_{0.6}$ associated with the force $0.6Fu$.

| Γ_x | | | | | | | | |
|------------|---------------|--------------|---------------|----------|-------|-------|-------|-------------|
| - | $0,6*F_u=F_y$ | $d(0,6*F_u)$ | dy to d^*_y | k^* | m^* | T^* | du | Fu |
| 1.37 | [KN] | [m] | [m] | [KN/m] | [ton] | [sec] | [m] | [KN] |
| | 521.17 | 0.00110 | 0.001970 | 473789.0 | 180 | 0.122 | 0.224 | 868.6131387 |

Table 7. transformation of the capacity curve from MDOF to SDOF

| Step | MDOF | | SDOF | |
|------|-------------------|-----------------|----------------------------|------------------------|
| | Displacement m | BaseForce KN | $D^*=\Delta/\Gamma_x$ m | $F^*=V/\Gamma_x$ KN |
| 0 | 0 | 0.00E+00 | 0.000000 | 0 |
| 1 | 1.17E-03 | 7.00E+02 | 0.000854 | 510.9489 |
| 2 | 2.32E-03 | 8.50E+02 | 0.001693 | 620.438 |
| 3 | 3.39E-03 | 8.48E+02 | 0.002474 | 618.9781 |
| 4 | 4.46E-03 | 8.66E+02 | 0.003255 | 632.1168 |
| 5 | 5.56E-03 | 9.01E+02 | 0.004058 | 657.6642 |
| 6 | 6.68E-03 | 9.51E+02 | 0.004876 | 694.1606 |
| 7 | 7.86E-03 | 9.17E+02 | 0.005737 | 669.3431 |
| 8 | 9.05E-03 | 9.35E+02 | 0.006606 | 682.4818 |
| 9 | 1.03E-02 | 9.65E+02 | 0.007518 | 704.3796 |
| 10 | 1.15E-02 | 9.97E+02 | 0.008394 | 727.7372 |
| 11 | 1.26E-02 | 1.12E+03 | 0.009197 | 817.5182 |
| 12 | 1.37E-02 | 1.19E+03 | 0.010000 | 868.6131 |
| 13 | 1.48E-02 | 1.12E+03 | 0.010803 | 817.5182 |

| | | | | |
|----|----------|----------|----------|----------|
| 14 | 1.59E-02 | 1.11E+03 | 0.011606 | 810.219 |
| 15 | 1.71E-02 | 1.13E+03 | 0.012482 | 824.8175 |
| 16 | 1.83E-02 | 1.14E+03 | 0.013358 | 832.1168 |
| 17 | 1.94E-02 | 1.16E+03 | 0.014161 | 846.7153 |
| 18 | 2.06E-02 | 1.17E+03 | 0.015036 | 854.0146 |
| 19 | 2.17E-02 | 1.17E+03 | 0.015839 | 854.0146 |
| 20 | 2.29E-02 | 1.18E+03 | 0.016715 | 861.3139 |
| 21 | 2.40E-02 | 1.18E+03 | 0.017518 | 861.3139 |
| 22 | 2.52E-02 | 1.18E+03 | 0.018394 | 861.3139 |
| 23 | 2.63E-02 | 1.19E+03 | 0.019197 | 868.6131 |
| 24 | 2.75E-02 | 1.19E+03 | 0.020073 | 868.6131 |
| 25 | 2.87E-02 | 1.19E+03 | 0.020949 | 868.6131 |
| 26 | 2.98E-02 | 1.19E+03 | 0.021752 | 868.6131 |
| 27 | 3.13E-02 | 1.19E+03 | 0.022847 | 868.6131 |
| 28 | 5.37E-02 | 1.07E+03 | 0.039197 | 781.0219 |
| 29 | 1.32E-01 | 1.01E+03 | 0.096350 | 737.2263 |
| 30 | 1.72E-01 | 9.99E+02 | 0.125547 | 729.1971 |
| 31 | 3.08E-01 | 9.96E+02 | 0.224818 | 727.0073 |
| 32 | 3.13E-01 | 8.09E+02 | 0.228467 | 590.5109 |

IV.2 THE BI-LINEAR EQUIVALENT CAPACITY CURVE

Table 8 BI-LINEAR EQUIVALENT CAPACITY CURVE domain X direction

| Bi-linear | | Note |
|-----------|-------------|--------------------------------------|
| d_i [m] | F_i [KN] | |
| 0 | 0 | 0 |
| 0.00110 | 521.17 | Correspond to F (0.6 Fu), d (0.6 Fu) |
| 0.001970 | 933.3642999 | Correspond to F_y , d_y |
| 0.0100 | 933.3642999 | horizontal plateau, F_y , d_u |

IV.3 THE SPECTRE OR THE DEMAND CURVE SHOULD BE TRANSFORMED ALSO TO THE (ADRS) FORM AS FOLLOW:

| q^* | Sae(T^*) | Sde (T^*) =demax [cm] | T_c | d^*_{max} [cm] Performance point | u | R_u |
|-------|--------------|---------------------------|-------|---------------------------------------|-----|-------|
|-------|--------------|---------------------------|-------|---------------------------------------|-----|-------|

| | | | | | | |
|-----|-----|------|-----|-----|--------|-------|
| 1.4 | 7.5 | 0.25 | 0.4 | 0.4 | 2.4587 | 1.446 |
|-----|-----|------|-----|-----|--------|-------|

$$q^* = \frac{S_{ag}}{S_{ae}(T^*)}$$

S_{ae} : the spectral acceleration correspond to (T^*)

S_{ag} : max spectral acceleration of the structure

q^* : the behaviour factor

$$\begin{cases} R_u = \frac{(u-1)T}{T_c} + 1 & , T > T_c \\ R_u = u & , T \leq T_c \end{cases}$$

$$u = \begin{cases} 1 + \frac{(q-1)T}{T_c} & , T \leq T_c \\ q & , T > T_c \end{cases}$$

μ : The ductility capacity for the building

R_u : strength reduction factor due to ductility

$$S_a = \frac{S_{ae}}{R_u}$$

$$S_d = \frac{u}{R_u} S_{de} = \frac{uT^2}{4\pi^2} S_a$$

S_a : spectral acceleration.

S_d : spectral displacement.

b) Table 9. transformation of the demand curve to (ADRS) form.

| T [sec] | S_{ae} [g] | S_{ae} [ms ⁻²] | S_{de} [cm] | sae/Ru | sde/Ru |
|---------|--------------|------------------------------|---------------|----------|----------|
| 0 | 0.250 | 3.25 | 0 | 2.246988 | 0 |
| 0.05 | 0.375 | 4.875 | 0.030902623 | 3.370482 | 0.021365 |
| 0.1 | 0.500 | 6.5 | 0.164813988 | 4.493976 | 0.113949 |
| 0.15 | 0.625 | 8.125 | 0.463539342 | 5.61747 | 0.320482 |
| 0.2 | 0.625 | 8.125 | 0.824069942 | 5.61747 | 0.569746 |
| 0.25 | 0.625 | 8.125 | 1.287609284 | 5.61747 | 0.890229 |
| 0.3 | 0.625 | 8.125 | 1.854157369 | 5.61747 | 1.281929 |
| 0.35 | 0.625 | 8.125 | 2.523714197 | 5.61747 | 1.744848 |
| 0.4 | 0.625 | 8.125 | 3.296279768 | 5.61747 | 2.278985 |
| 0.45 | 0.578 | 7.511413805 | 3.85680275 | 5.193249 | 2.66652 |
| 0.5 | 0.539 | 7.001912743 | 4.438512175 | 4.840989 | 3.068703 |
| 0.55 | 0.505 | 6.570850268 | 5.039966647 | 4.542961 | 3.484537 |
| 0.6 | 0.477 | 6.20053548 | 5.659947597 | 4.286932 | 3.91318 |

| | | | | | |
|------|-------|-------------|-------------|----------|----------|
| 0.65 | 0.452 | 5.878336719 | 6.297408779 | 4.06417 | 4.353909 |
| 0.7 | 0.430 | 5.594973113 | 6.951440285 | 3.868258 | 4.806093 |
| 0.75 | 0.411 | 5.343459494 | 7.621242154 | 3.694366 | 5.269182 |
| 0.8 | 0.394 | 5.118429265 | 8.306104532 | 3.538785 | 5.742683 |
| 0.85 | 0.378 | 4.915685394 | 9.005392453 | 3.398611 | 6.226157 |
| 0.9 | 0.364 | 4.731894184 | 9.718533939 | 3.271542 | 6.719209 |
| 0.95 | 0.351 | 4.564371241 | 10.44501056 | 3.155719 | 7.221481 |
| 1 | 0.339 | 4.410928627 | 11.18434984 | 3.049632 | 7.732647 |
| 1.05 | 0.328 | 4.269763606 | 11.93611905 | 2.952033 | 8.252405 |
| 1.1 | 0.318 | 4.139376284 | 12.69992014 | 2.861886 | 8.780483 |
| 1.15 | 0.309 | 4.018507689 | 13.47538546 | 2.77832 | 9.316625 |
| 1.2 | 0.300 | 3.906092586 | 14.26217424 | 2.700598 | 9.860596 |
| 1.25 | 0.292 | 3.80122306 | 15.05996955 | 2.628093 | 10.41218 |
| 1.3 | 0.285 | 3.703120086 | 15.86847576 | 2.560267 | 10.97116 |
| 1.35 | 0.278 | 3.611111111 | 16.68741633 | 2.496653 | 11.53736 |
| 1.4 | 0.271 | 3.524612199 | 17.51653189 | 2.43685 | 12.1106 |
| 1.45 | 0.265 | 3.443113684 | 18.35557863 | 2.380503 | 12.6907 |
| 1.5 | 0.259 | 3.366168548 | 19.20432683 | 2.327305 | 13.27751 |
| 1.55 | 0.253 | 3.293382942 | 20.06255963 | 2.276982 | 13.87087 |
| 1.6 | 0.248 | 3.224408387 | 20.93007188 | 2.229295 | 14.47065 |
| 1.65 | 0.243 | 3.158935325 | 21.80666919 | 2.184028 | 15.07672 |
| 1.7 | 0.238 | 3.096687751 | 22.69216703 | 2.140991 | 15.68893 |
| 1.75 | 0.234 | 3.037418717 | 23.58638996 | 2.100013 | 16.30718 |
| 1.8 | 0.229 | 2.980906544 | 24.48917097 | 2.060942 | 16.93135 |
| 1.85 | 0.225 | 2.926951626 | 25.40035078 | 2.023639 | 17.56132 |
| 1.9 | 0.221 | 2.875373703 | 26.31977735 | 1.987979 | 18.19699 |
| 1.95 | 0.217 | 2.826009536 | 27.24730532 | 1.953849 | 18.83827 |
| 2 | 0.214 | 2.778710913 | 28.18279558 | 1.921148 | 19.48505 |
| 2.05 | 0.210 | 2.733342934 | 29.12611486 | 1.889781 | 20.13724 |
| 2.1 | 0.207 | 2.689782523 | 30.07713529 | 1.859664 | 20.79476 |
| 2.15 | 0.204 | 2.647917139 | 31.03573414 | 1.83072 | 21.45752 |
| 2.2 | 0.201 | 2.607643657 | 32.00179343 | 1.802875 | 22.12543 |
| 2.25 | 0.198 | 2.568867387 | 32.97519966 | 1.776066 | 22.79843 |
| 2.3 | 0.195 | 2.531501213 | 33.95584359 | 1.750232 | 23.47642 |
| 2.35 | 0.192 | 2.495464843 | 34.94361991 | 1.725317 | 24.15935 |
| 2.4 | 0.189 | 2.460684136 | 35.93842708 | 1.70127 | 24.84714 |

| | | | | | |
|------|-------|-------------|-------------|----------|----------|
| 2.45 | 0.187 | 2.427090522 | 36.94016709 | 1.678044 | 25.53973 |
| 2.5 | 0.184 | 2.394620474 | 37.94874529 | 1.655595 | 26.23704 |
| 2.55 | 0.182 | 2.363215049 | 38.96407019 | 1.633882 | 26.93902 |
| 2.6 | 0.179 | 2.332819473 | 39.98605328 | 1.612867 | 27.6456 |
| 2.65 | 0.177 | 2.303382774 | 41.01460893 | 1.592515 | 28.35672 |
| 2.7 | 0.175 | 2.274857451 | 42.04965419 | 1.572793 | 29.07233 |
| 2.75 | 0.173 | 2.247199181 | 43.09110869 | 1.553671 | 29.79237 |
| 2.8 | 0.171 | 2.220366551 | 44.13889449 | 1.535119 | 30.51679 |
| 2.85 | 0.169 | 2.19432082 | 45.19293598 | 1.517112 | 31.24554 |
| 2.9 | 0.167 | 2.169025704 | 46.25315979 | 1.499623 | 31.97855 |
| 2.95 | 0.165 | 2.144447178 | 47.31949463 | 1.48263 | 32.7158 |
| 3 | 0.163 | 2.120553306 | 48.39187125 | 1.46611 | 33.45722 |

b) Even the bi-linear equivalent capacity curve should be transformed to spectral parameters using:

$$\text{Sag} = \frac{V}{m^*} \text{ or } \frac{F}{\Gamma x m^*}$$

V ASSESSMENT OF THE PERFORMANCE FOR THE (Y DIRECTION)

V.1 SDOF TO MDOF

For the conversion of forces and displacements of a system, the following equations are used to have the **SDOF** from the **MDOF** capacity curve:

$$F^* = F/\Gamma$$

$$d^* = d/\Gamma$$

Γ : participation factor

$$\Gamma = \frac{m^*}{\sum m_i \varphi^2} \text{ in wick } m^* = \sum m_i \varphi_i^2$$

K: the rigidity

$$k = \frac{F(0.6Fu)}{d(0.6Fu)}$$

T: the period

$$T^* = 2\pi \sqrt{\left(\frac{m^*}{k}\right)} \text{ or } 2\pi \sqrt{\left(\frac{m^* d^*}{F^*}\right)}$$

interpolation is made to determine the value of the displacement $d_{0.6}$ associated with the force $0.6Fu$.

| | | | | | | | | |
|------------|---------------|--------------------|-----------------|----------|-------|-------|----------|-------------|
| Γ_x | | | | | | | | |
| - | $0,6*F_u=F_y$ | d $(0,6*F_u)$ | dy to d^*_y | k^* | m^* | T^* | du | F_u |
| 1.74 | [KN] | [m] | [m] | [KN/m] | [ton] | [sec] | [m] | [KN] |
| | 1340.94 | 0.00185 | 0.002850 | 724832.2 | 248 | 0.116 | 0.005007 | 2234.899329 |

Table 10. transformation of the capacity curve from MDOF to SDOF

| Step | MDOF | | SDOF | |
|------|--------------|-----------|-----------------------|------------------|
| | Displacement | BaseForce | $D^*=\Delta/\Gamma x$ | $F^*=V/\Gamma x$ |
| | m | KN | m | KN |
| 0 | 0 | 0.00E+00 | 0.000000 | 0 |
| 1 | 9.52E-04 | 6.84E+02 | 0.000639 | 459.0604 |
| 2 | 1.90E-03 | 1.37E+03 | 0.001275 | 919.4631 |
| 3 | 2.86E-03 | 2.04E+03 | 0.001919 | 1369.128 |
| 4 | 3.81E-03 | 2.77E+03 | 0.002557 | 1859.06 |
| 5 | 4.65E-03 | 3.08E+03 | 0.003121 | 2067.114 |
| 6 | 5.58E-03 | 3.29E+03 | 0.003745 | 2208.054 |
| 7 | 6.52E-03 | 3.33E+03 | 0.004376 | 2234.899 |
| 8 | 7.46E-03 | 3.33E+03 | 0.005007 | 2234.899 |
| 9 | 8.40E-03 | 3.31E+03 | 0.005638 | 2221.477 |
| 10 | 9.33E-03 | 3.29E+03 | 0.006262 | 2208.054 |
| 11 | 1.03E-02 | 3.27E+03 | 0.006913 | 2194.631 |
| 12 | 1.12E-02 | 3.26E+03 | 0.007517 | 2187.919 |
| 13 | 1.21E-02 | 3.25E+03 | 0.008121 | 2181.208 |
| 14 | 1.30E-02 | 3.24E+03 | 0.008725 | 2174.497 |
| 15 | 1.40E-02 | 3.23E+03 | 0.009396 | 2167.785 |
| 16 | 1.49E-02 | 3.22E+03 | 0.010000 | 2161.074 |
| 17 | 1.58E-02 | 3.15E+03 | 0.010604 | 2114.094 |
| 18 | 1.67E-02 | 3.08E+03 | 0.011208 | 2067.114 |
| 19 | 1.75E-02 | 3.03E+03 | 0.011745 | 2033.557 |
| 20 | 1.83E-02 | 2.99E+03 | 0.012282 | 2006.711 |
| 21 | 1.92E-02 | 2.97E+03 | 0.012886 | 1993.289 |
| 22 | 2.00E-02 | 2.95E+03 | 0.013423 | 1979.866 |
| 23 | 2.08E-02 | 2.94E+03 | 0.013960 | 1973.154 |
| 24 | 2.16E-02 | 2.94E+03 | 0.014497 | 1973.154 |
| 25 | 2.24E-02 | 2.93E+03 | 0.015034 | 1966.443 |

| | | | | |
|----|----------|----------|----------|----------|
| 26 | 2.32E-02 | 2.93E+03 | 0.015570 | 1966.443 |
| 27 | 2.40E-02 | 2.93E+03 | 0.016107 | 1966.443 |
| 28 | 2.48E-02 | 2.93E+03 | 0.016644 | 1966.443 |
| 29 | 2.56E-02 | 2.93E+03 | 0.017181 | 1966.443 |
| 30 | 2.64E-02 | 2.93E+03 | 0.017718 | 1966.443 |
| 31 | 2.72E-02 | 2.93E+03 | 0.018255 | 1966.443 |
| 32 | 2.80E-02 | 2.93E+03 | 0.018792 | 1966.443 |

V.2 THE BI-LINEAR EQUIVALENT CAPACITY CURVE

Table 11 BI-LINEAR EQUIVALENT CAPACITY CURVE domain Y direction

| Bi-linear | | Note |
|--------------------|---------------------|---|
| d _i [m] | F _i [KN] | |
| 0 | 0 | 0 |
| 0.00185 | 1340.94 | Correspond to F (0.6 Fu), d (0.6 Fu) |
| 0.002850 | 2065.771812 | Correspond to F _y , d _y |
| 0.0258 | 2065.771812 | horizontal plateau, F _y , d _u |

V.3 THE SPECTRE OR THE DEMAND CURVE SHOULD BE TRANSFORMED ALSO TO THE (ADRS) FORM AS FOLLOW:

| q* | S _{ae} (T*) | S _{de} (T*) = demax [cm] | T _c | d*max [cm] Performance point | u | R _u |
|-----|----------------------|-----------------------------------|----------------|---------------------------------|-------|----------------|
| 0.9 | 7.5 | 0.116 | 0.4 | 0.2 | 0.657 | 0.9 |

$$q^* = \frac{S_{ag}}{S_{ae}(T^*)}$$

S_{ae} : the spectral acceleration correspond to (T*)

S_{ag} : max spectral acceleration of the structure

q* : the behaviour factor

$$\begin{cases} R_u = \frac{(u-1)T}{T_c} + 1 & , T > T_c \\ R_u = u & , T \leq T_c \end{cases}$$

$$u = \begin{cases} 1 + \frac{(q-1)T}{T_c} & , T \leq T_c \\ q & , T > T_c \end{cases}$$

μ: The ductility capacity for the building

R_u : strength reduction factor due to ductility

$$S_a = \frac{S_{ae}}{R_u}$$

$$S_d = \frac{u}{R_u} S_{de} = \frac{uT^2}{4\pi^2} S_a$$

S_a: spectral acceleration.

S_d: spectral displacement.

c) Table 12. transformation of the demand curve to (ADRS) form.

| T [sec] | S _{ae} [g] | S _{ae} [ms ⁻²] | S _{de} [cm] | sae/R _u | sde/R _u |
|---------|---------------------|-------------------------------------|----------------------|--------------------|--------------------|
| 0 | 0.250 | 3.25 | 0 | 3.609548 | 0 |
| 0.05 | 0.375 | 4.875 | 0.030902623 | 5.414321 | 0.034321 |
| 0.1 | 0.500 | 6.5 | 0.164813988 | 7.219095 | 0.183047 |
| 0.15 | 0.625 | 8.125 | 0.463539342 | 9.023869 | 0.514821 |
| 0.2 | 0.625 | 8.125 | 0.824069942 | 9.023869 | 0.915237 |
| 0.25 | 0.625 | 8.125 | 1.287609284 | 9.023869 | 1.430058 |
| 0.3 | 0.625 | 8.125 | 1.854157369 | 9.023869 | 2.059283 |
| 0.35 | 0.625 | 8.125 | 2.523714197 | 9.023869 | 2.802913 |
| 0.4 | 0.625 | 8.125 | 3.296279768 | 9.023869 | 3.660947 |
| 0.45 | 0.578 | 7.511413805 | 3.85680275 | 8.342402 | 4.283481 |
| 0.5 | 0.539 | 7.001912743 | 4.438512175 | 7.776534 | 4.929545 |
| 0.55 | 0.505 | 6.570850268 | 5.039966647 | 7.297783 | 5.597538 |
| 0.6 | 0.477 | 6.20053548 | 5.659947597 | 6.886501 | 6.286108 |
| 0.65 | 0.452 | 5.878336719 | 6.297408779 | 6.528657 | 6.994091 |
| 0.7 | 0.430 | 5.594973113 | 6.951440285 | 6.213945 | 7.720478 |
| 0.75 | 0.411 | 5.343459494 | 7.621242154 | 5.934606 | 8.46438 |
| 0.8 | 0.394 | 5.118429265 | 8.306104532 | 5.684681 | 9.225009 |
| 0.85 | 0.378 | 4.915685394 | 9.005392453 | 5.459508 | 10.00166 |
| 0.9 | 0.364 | 4.731894184 | 9.718533939 | 5.255384 | 10.7937 |
| 0.95 | 0.351 | 4.564371241 | 10.44501056 | 5.069328 | 11.60054 |
| 1 | 0.339 | 4.410928627 | 11.18434984 | 4.89891 | 12.42167 |
| 1.05 | 0.328 | 4.269763606 | 11.93611905 | 4.742128 | 13.25661 |
| 1.1 | 0.318 | 4.139376284 | 12.69992014 | 4.597316 | 14.10491 |

| | | | | | |
|------|-------|-------------|-------------|----------|----------|
| 1.15 | 0.309 | 4.018507689 | 13.47538546 | 4.463075 | 14.96617 |
| 1.2 | 0.300 | 3.906092586 | 14.26217424 | 4.338224 | 15.84 |
| 1.25 | 0.292 | 3.80122306 | 15.05996955 | 4.221752 | 16.72605 |
| 1.3 | 0.285 | 3.703120086 | 15.86847576 | 4.112796 | 17.62401 |
| 1.35 | 0.278 | 3.611111111 | 16.68741633 | 4.010608 | 18.53355 |
| 1.4 | 0.271 | 3.524612199 | 17.51653189 | 3.91454 | 19.45439 |
| 1.45 | 0.265 | 3.443113684 | 18.35557863 | 3.824025 | 20.38626 |
| 1.5 | 0.259 | 3.366168548 | 19.20432683 | 3.738568 | 21.3289 |
| 1.55 | 0.253 | 3.293382942 | 20.06255963 | 3.65773 | 22.28208 |
| 1.6 | 0.248 | 3.224408387 | 20.93007188 | 3.581125 | 23.24557 |
| 1.65 | 0.243 | 3.158935325 | 21.80666919 | 3.508408 | 24.21914 |
| 1.7 | 0.238 | 3.096687751 | 22.69216703 | 3.439274 | 25.2026 |
| 1.75 | 0.234 | 3.037418717 | 23.58638996 | 3.373448 | 26.19575 |
| 1.8 | 0.229 | 2.980906544 | 24.48917097 | 3.310684 | 27.19841 |
| 1.85 | 0.225 | 2.926951626 | 25.40035078 | 3.25076 | 28.21039 |
| 1.9 | 0.221 | 2.875373703 | 26.31977735 | 3.193476 | 29.23153 |
| 1.95 | 0.217 | 2.826009536 | 27.24730532 | 3.138651 | 30.26167 |
| 2 | 0.214 | 2.778710913 | 28.18279558 | 3.08612 | 31.30066 |
| 2.05 | 0.210 | 2.733342934 | 29.12611486 | 3.035733 | 32.34834 |
| 2.1 | 0.207 | 2.689782523 | 30.07713529 | 2.987353 | 33.40457 |
| 2.15 | 0.204 | 2.647917139 | 31.03573414 | 2.940856 | 34.46922 |
| 2.2 | 0.201 | 2.607643657 | 32.00179343 | 2.896127 | 35.54215 |
| 2.25 | 0.198 | 2.568867387 | 32.97519966 | 2.853061 | 36.62325 |
| 2.3 | 0.195 | 2.531501213 | 33.95584359 | 2.811561 | 37.71238 |
| 2.35 | 0.192 | 2.495464843 | 34.94361991 | 2.771538 | 38.80943 |
| 2.4 | 0.189 | 2.460684136 | 35.93842708 | 2.73291 | 39.9143 |
| 2.45 | 0.187 | 2.427090522 | 36.94016709 | 2.6956 | 41.02686 |
| 2.5 | 0.184 | 2.394620474 | 37.94874529 | 2.659537 | 42.14702 |
| 2.55 | 0.182 | 2.363215049 | 38.96407019 | 2.624658 | 43.27467 |
| 2.6 | 0.179 | 2.332819473 | 39.98605328 | 2.590899 | 44.40971 |
| 2.65 | 0.177 | 2.303382774 | 41.01460893 | 2.558206 | 45.55206 |
| 2.7 | 0.175 | 2.274857451 | 42.04965419 | 2.526525 | 46.70161 |
| 2.75 | 0.173 | 2.247199181 | 43.09110869 | 2.495807 | 47.85828 |
| 2.8 | 0.171 | 2.220366551 | 44.13889449 | 2.466006 | 49.02198 |
| 2.85 | 0.169 | 2.19432082 | 45.19293598 | 2.437079 | 50.19263 |
| 2.9 | 0.167 | 2.169025704 | 46.25315979 | 2.408985 | 51.37015 |

| | | | | | |
|------|-------|-------------|-------------|----------|----------|
| 2.95 | 0.165 | 2.144447178 | 47.31949463 | 2.381687 | 52.55445 |
| 3 | 0.163 | 2.120553306 | 48.39187125 | 2.35515 | 53.74546 |

c) Even the bi-linear equivalent capacity curve should be transformed to spectral parameters using:

$$\text{Sag} = \frac{V}{m * } \text{ or } \frac{F}{\Gamma \times m * }$$